

THE UNIVERSITY OF HULL  
United Kingdom

POLYMER FIBRE COMPOSITES:  
INVESTIGATION INTO PERFORMANCE ENHANCEMENT  
THROUGH VISCOELASTICALLY GENERATED PRE-STRESS

being a Thesis submitted for the Degree of

Doctor of Philosophy

in the

University of Hull

by

Adnan Fazal  
B.Eng (Hons) Mechanical Engineering

August, 2014



*Dedicated to my parents*

*Whose blessings and prayers*

*Brought me this far*

*Without their prayers*

*I would not be where I am now*

# ABSTRACT

---

In this research, the performance and further development of viscoelastically pre-stressed polymer matrix composites (VPPMCs) was investigated. Pre-stressed composite samples with continuous unidirectional fibres are produced by applying a tensile load to polymeric fibres to induce tensile creep. After removing the load, the fibres are moulded in a polyester resin. Following resin curing, compressive stresses are imparted by the viscoelastically strained fibres as they attempt to recover their strain against the surrounding solid matrix material. Prior to this study, VPPMCs using nylon 6,6 fibres increased impact energy absorption and flexural modulus by 30-50% relative to control (un-stressed) counterparts. The current work contributes to ongoing efforts in VPPMC research by expanding the knowledge of existing VPPMC materials and identifying the potential for an alternative, mechanically superior polymeric fibre.

For nylon 6,6 fibre-based VPPMCs, the effects of Charpy impact span settings and fibre volume fraction (3-17%  $V_f$ ) were investigated. The effects of commingling nylon pre-stressing fibres with Kevlar fibres to produce hybrid VPPMCs was also evaluated. Moreover, as an alternative to nylon fibre, the viscoelastic characteristics and subsequent VPPMC performance of polyethylene (UHMWPE) fibre was investigated. Charpy impact and three-point bend tests were used to evaluate VPPMC samples against control (un-stressed) counterparts. In addition, microscopy techniques were applied to impact-tested samples, to analyse fracture behaviour.

For the nylon fibre-based VPPMCs, it was found that improvements in impact energy absorption from pre-stress depended principally on shear stresses activating fibre-matrix debonding during the impact process. Scanning electron microscopy of impact-tested samples revealed visual evidence of pre-stress impeding crack propagation. A short span setting (24 mm) showed greater increases in energy absorption of 25-40%, compared with samples tested at a larger span (60 mm) which gave increases of 0-13%. The results suggest that there is an increasing contribution to energy absorption from elastic deflection at larger span settings; this causes lower energy absorption as well as reducing any improvements from pre-stress effects. However, this effect was suppressed by the addition of Kevlar fibres (to produce hybrid VPPMCs), which promoted more effective energy absorption at the larger span. Moreover, bend tests on the hybrid composites demonstrated that pre-stressing further enhanced flexural modulus by ~35%.

The viscoelastic characteristics of UHMWPE fibres indicated that these fibres could release stored energy for pre-stressing over a long time period. This was effectively demonstrated with UHMWPE fibre-based VPPMCs using three-point bend tests, i.e. flexural modulus increased by 25-35% from pre-stressing with no deterioration observed over the time scale investigated (~2 years). Also, these VPPMCs absorbed ~20% more impact energy than their control counterparts, with some batches reaching 30-40%. Although fibre-matrix debonding is known to be a major energy absorption mechanism, this was not evident in the UHMWPE fibre-based VPPMCs. Instead, evidence of debonding at the skin-core interface within the UHMWPE fibres was found. This is believed to be a previously unrecognised energy absorption mechanism.

This work contributes to a further understanding of the viscoelastic properties of polymeric fibres and insight into the field of pre-stressed composite materials. The findings support the view that VPPMCs can provide a means to improve impact toughness and other mechanical characteristics for composite applications.

# ACKNOWLEDGMENT

---

I wish to express my deepest gratitude and thanks to Dr. Kevin Fancey (principal supervisor) for providing me the opportunity to pursue my research in the field of viscoelastically pre-stressed polymer matrix composites and for his understanding, continued guidance, encouragement and friendly attitude. Great appreciation for extensive support, constructive criticism and his patience throughout this study is also expressed. I was extremely fortunate to have Dr. Fancey as my principal supervisor; without him, I would not have been able to pursue this work. His wisdom and kindness have had a positive influence on me.

I would like thank my second supervisor Dr. Catherine Dobson for valuable guidance, support and encouragement throughout my studies.

I gratefully acknowledge departmental support (fee waiver) for my PhD studies, which has opened the door to a new world for me. Knowledge and experience gained during my studies at the University of Hull will always be remembered.

I would also like thank to the School of Engineering and Graduate School staff for their support and assistance throughout my studies. Special thanks go to Garry Robinson (technical staff) for his additional support and assistance with microscopic analysis. His helpful discussions are greatly appreciated. I also wish to thank the Mechanical Engineering workshop staff for their assistance. Technical support for XRD and EDX analysis from Ronnie Hewer and Tony Sinclair is gratefully acknowledged.

I would like thank Dr. Sergei Lukaschuk for providing the high speed digital camera for impact testing.

I wish to show my gratitude to all friends I met at the University of Hull, who accompanied me all the way. I have learned a lot and enjoyed being a student at the University of Hull.

Special thanks go to the anonymous reviewers for making useful comments on manuscripts generated from this research work and for the recommendation for publication in journals.

Last but not least, I am eternally grateful to my family for their encouragement and continuous prayers.

# LIST OF CONTENTS

---

<b>CHAPTER-1</b> .....	<b>1</b>
<b>INTRODUCTION</b>	
Summary .....	1
1.1 Aims and objectives .....	2
1.2 Introduction.....	2
1.3 Motivation.....	5
1.4 Background to the objectives.....	6
1.4.1 Nylon fibre-based VPPMCs.....	6
1.4.2 Hybrid commingled nylon/Kevlar fibre-based VPPMCs .....	6
1.4.3 Polyethylene fibre-based VPPMCs .....	7
1.5 Thesis structure.....	8
1.6 Work dissemination.....	11
<b>CHAPTER-2</b> .....	<b>12</b>
<b>BACKGROUND STUDIES</b>	
Summary .....	12
2.1 Introduction.....	13
2.2 Composite materials .....	14
2.2.1 Polymeric matrix materials .....	14
2.2.2 Thermosets .....	15
2.2.3 Thermoplastics .....	16
2.2.4 Processing of composite materials.....	16
2.3 Failure in composite materials .....	17
2.3.1 Failure mechanisms .....	17
2.3.2 Interface/interphase regions in composite materials .....	20
2.4 Pre-stressed composites .....	22
2.5 Types of pre-stressed composites .....	27
2.5.1 Elastically pre-stressed polymer matrix composites .....	27
2.5.1.1 Disadvantages of elastically pre-stressed composites .....	30

---

2.5.2	Viscoelastically pre-stressed polymer matrix composites .....	32
2.5.2.1	Nylon fibre-based VPPMC performance .....	33
2.5.2.2	Viscoelastic behaviour of polymeric fibres .....	36
2.6	Mechanical properties associated with pre-stressed composites .....	40
2.6.1	Mechanism-I .....	41
2.6.2	Mechanism-II .....	42
2.6.3	Mechanism-III.....	42
2.6.4	Mechanism-IV .....	43
2.6.5	Benefits of pre-stressed composites .....	45
2.7	Fibre stretching methods for pre-stressed composites .....	46
2.8	Overview on pre-stressed composites .....	57
<b>CHAPTER-3</b>	.....	<b>64</b>
<b>MATERIAL PREPARATION, GENERAL EXPERIMENTAL PROCEDURES AND EQUIPMENT FACILITIES</b>		
Summary	.....	64
3.1	Reinforcing materials .....	65
3.1.1	Nylon fibre .....	66
3.1.2	Kevlar fibre .....	67
3.1.3	Polyethylene fibre .....	67
3.2	Composite processing, procedures and equipment .....	69
3.2.1	Annealing process.....	69
3.2.2	Fibre stretching process.....	70
3.2.3	Evaluation of fibre volume fraction.....	73
3.2.4	Production of composite samples .....	75
3.3	Mechanical testing.....	77
3.3.1	Charpy impact testing.....	78
3.3.2	Three-point bend tests .....	79
3.3.3	Tensile testing .....	82
3.4	Microscopy.....	84
3.4.1	Scanning electron microscopy .....	84

---

3.4.2	Optical microscopy.....	85
3.4.3	Profile projector .....	86
3.4.4	X-ray diffraction .....	88
<b>CHAPTER-4</b>	.....	<b>90</b>
<b>PRELIMINARY WORK</b>		
	Summary .....	90
4.1	Stretching rigs evaluation.....	91
4.2	Resin selection for composite sample production .....	93
4.2.1	Investigation of exothermic characteristics (resin curing cycle) .....	93
4.2.2	Impact tests on samples produced from CC and GP polyester resins .....	96
4.2.3	Final resin selection .....	98
4.3	Evaluation of the annealing process effects on sample performance.....	99
4.3.1	Annealing of fibres in muffle and fan-assisted ovens .....	99
4.3.2	Analysis of nylon fibres through X-ray diffraction .....	100
4.3.3	Evaluation on annealing effects (composites impact testing).....	102
4.4	Conclusions.....	105
<b>CHAPTER-5</b>	.....	<b>106</b>
<b>NYLON FIBRE-BASED VPPMC IMPACT CHARACTERISTICS ON FIBRE VOLUME FRACTION AND THEIR EFFECTS ON CHARPY SPAN SETTINGS</b>		
	Summary .....	106
5.1	Background .....	107
5.1.1	Charpy impact testing standards for composite materials.....	108
5.1.2	Literature review on pre-stressed composite subject to impact load.....	111
5.2	Experimental procedure .....	112
5.3	Results and discussions .....	115
5.3.1	Fibre spatial distribution in composite samples.....	115
5.3.2	Initial observations on impact energy absorption .....	117
5.3.3	Impact testing span effects .....	122
5.3.4	Pre-stress effects and fracture observations .....	123

---

5.3.5	Effects of span and fibre volume fraction on energy absorption .....	127
5.3.6	Effects of span and fibre volume fraction on energy per unit volume ..	131
5.3.7	Effects of debonding area on energy .....	132
5.3.8	Influence of shear stress on impact performance.....	134
5.4	Conclusions.....	136
<b>CHAPTER-6 .....</b>		<b>138</b>
<b>PERFORMANCE ENHANCEMENT OF HYBRID COMPOSITES (NYLON/KEVLAR FIBRE) THROUGH VISCOELASTICALLY GENERATED PRE-STRESS</b>		
	Summary .....	138
6.1	Introduction.....	139
6.2	Background .....	140
6.2.1	Hybrid composites .....	140
6.2.2	Potential benefits from hybrid VPPMCs.....	143
6.3	Experimental procedures.....	144
6.3.1	Production of composite samples .....	144
6.3.2	Mechanical evaluation of composite samples.....	145
6.4	Results and discussions .....	147
6.4.1	Fibre spatial distribution in composite samples.....	147
6.4.2	Charpy impact tests .....	149
6.4.3	Impact energy absorption.....	153
6.4.4	Analysis on fracture behaviour of impact tested samples .....	154
6.4.5	Flexural stiffness.....	159
6.4.6	Commingled hybrid VPPMCs as practical composite structures.....	162
6.5	Conclusions.....	163
<b>CHAPTER-7 .....</b>		<b>165</b>
<b>VISCOELASTICALLY GENERATED PRE-STRESS FROM UHMWPE FIBRES AND THEIR PERFORMANCE ENHANCEMENT IN COMPOSITES</b>		
	Summary .....	165
7.1	Introduction.....	166
7.2	Background .....	170

7.2.1	UHMWPE fibre treatment and viscoelastic characteristics .....	170
7.2.2	Composite production and evaluation .....	173
7.3	Experimental procedure .....	174
7.3.1	Assessment of creep and recovery strain .....	174
7.3.2	Recovery force from polyethylene fibres .....	175
7.3.3	Mechanical evaluation of fibres.....	176
7.3.4	Composite sample production.....	178
7.3.5	Mechanical evaluation of composite samples.....	179
7.4	Results and discussions .....	180
7.4.1	Fibre-based microscopic analysis .....	180
7.4.2	Feasibility study on viscoelastic behaviour of UHMWPE fibres .....	184
7.4.3	Creep and long-term recovery strain .....	186
7.4.4	Recovery force .....	188
7.4.5	Polyethylene fibres recovery force and time-dependent behaviour .....	189
7.4.6	Comparison of test and control polyethylene fibres .....	191
7.4.7	Charpy impact tests .....	195
	7.4.7.1 Impact data and macroscopic examination.....	195
	7.4.7.2 Fibre spatial distribution in composite samples .....	198
	7.4.7.3 Fibre inspection and analysis .....	199
7.4.8	Flexural tests .....	205
7.4.9	Influence of pre-stress mechanisms on flexural modulus .....	209
7.4.10	Viscoelastic recovery force from UHMWPE fibres .....	210
7.4.11	Implications for polyethylene fibre-based VPPMCs.....	211
7.5	Conclusions.....	213
<b>CHAPTER-8 .....</b>		<b>216</b>
<b>GENERAL SUMMARY, POTENTIAL APPLICATIONS AND DIRECTIONS FOR FUTURE WORK</b>		
	Summary .....	216
8.1	Overall findings .....	217
	8.1.1 Material processing.....	217
	8.1.2 Nylon fibre-based VPPMCs.....	218

---

8.1.3	Polyethylene fibre-based VPPMCs .....	221
8.2	Potential applications .....	224
8.2.1	Ballistic protection.....	224
8.2.2	Crashworthy structures.....	225
8.2.3	Fibre reinforcement for crack resistance in concrete structures .....	227
8.2.4	Biaxial morphing structures .....	227
8.3	Directions for future work.....	228
<b>CHAPTER-9 .....</b>		<b>230</b>
<b>CONCLUSIONS</b>		
	Summary .....	230
9.1	Materials-related findings .....	231
9.2	Nylon fibre-based VPPMCs .....	231
9.3	UHMWPE fibre-based VPPMCs .....	232
9.4	Pre-stress effects on crack propagation .....	232
<b>REFERENCES .....</b>		<b>233</b>
<b>APPENDICES.....</b>		<b>252</b>
	Summary .....	252
	Appendix-A .....	253
	Chapter – 4 (experimental data) .....	253
	Appendix-B.....	259
	Chapter – 5 (experimental data) .....	259
	Appendix-C.....	263
	Chapter – 6 (experimental data) .....	263
	Appendix-D .....	266
	Chapter – 7 (experimental data) .....	266

# LIST OF FIGURES

---

Figure 2-1.	Schematic illustration of fracture in a fibre reinforced composite material.....	18
Figure 2-2	Schematic illustration of pre-stressed composites.....	23
Figure 2-3.	Schematic representation of a freely supported beam subjected to a bending load.....	24
Figure 2-4.	Polarised image of nylon 6,6 monofilament moulded in 150×30×2 mm polyester resin. The stress pattern from viscoelastic recovery in the pre-stressed samples in contrast with non pre-stress.....	33
Figure 2-5.	Effect of fibre volume fraction on the tensile properties of nylon 6,6 fibre-based viscoelastically pre-stressed composites.....	34
Figure 2-6.	Nylon 6,6 fibre-based VPPMC life as a function of ambient temperature.....	35
Figure 2-7.	Spring and dashpot model of creep and recovery strain from a polymeric material. (a) Creep strain from the applied constant load, (b) Recovery strain on the removal of load. Note, the spring represents elastic behaviour and the dashpot represents viscous behaviour of the material.....	37
Figure 2-8.	Recovery strain data of nylon 6,6 fibre after 24 hours creep at 342 MPa. Grey data-points represent real time measurement up to 4 years and the black data points are from the samples subjected to accelerated ageing up to an equivalent of 100 years. The solid line (curve) shows Equation.2-1, fitted to the black data points.....	39
Figure 2-9.	Mechanisms proposed by various authors, as being responsible for enhancing the mechanical properties of pre-stressed composites...	40
Figure 2-10.	Schematic illustration of the fracture behaviour of a pre-stressed and non pre-stressed composite material subjected to impact loading.....	44
Figure 2-11.	Dead-weight pre-stressing method adopted by Jorge <i>et al</i> [61] for composites plates.....	47
Figure 2-12.	Method used by Schulte and Marissen [62] for pre-stressed prepreg laminates using V-groove pressure bars.....	48
Figure 2-13.	Schematic diagram of the filament winding pre-stressing method...	49

Figure 2-14.	Schematic illustration of the hydraulic cylinder pre-stress rig used by Tuttle <i>et al</i> [64] for pre-stressed laminates.....	50
Figure 2-15.	Stretching setup employed by Motahhari and Cameron [68, 81] for pre-stressed composites. (a) wound fibres around grips are transferred to the stretching rig (b) tensometer machine for pre-stressing. The fibres were kept in tension during the curing process .....	51
Figure 2-16.	Fibre stretching frame employed by Zhao and Cameron [65] for a pre-stressed composite, in which fibres are wound onto the steel frame and then transferred to the tensile machine for pre-stressing. The fibres were kept in tension during the curing process.....	52
Figure 2-17.	Biaxial loading frame for pre-stressed laminates used by Jevons [67]. The laminates were attached to the clamp and load was applied by tightening locking bolts. The fibres were kept in a state of tension during the curing process.....	53
Figure 2-18.	Schematic diagram of the flat-bed rig used by Krishnamurthy [55] for pre-stressed composites. Pre-fabrication prior to clamping the prepreg laminate onto the stretching rig is shown in (a), while the stretching rig is shown in (b) by which the load on the composite is applied by the rotatable screw and maintained until the resin sets.....	54
Figure 2-19.	Fibre misalignment near end-tab region by using flat-bed pre-stressing method.....	56
Figure 3-1.	Chemical structure (mers) of polymers: (a) nylon, (b) Kevlar, and (c) polyethylene.....	68
Figure 3-2.	Ovens utilised for the annealing process. Yarns were placed in an aluminium tray to ensure uniform temperature and to prevent unwanted movement from air flow in the fan-assisted oven.....	70
Figure 3-3.	Schematics of the vertical stretching rigs for pre-stressing. Rig-(a) was mainly used for creep and recovery strain tests; strain measurement was recorded by the attached digital displacement gauge. Rig-(b) was designated to stretch nylon and UHMWPE fibres for pre-stressed composite samples; this provided the flexibility to stretch multiple yarns for high $V_f$ composite samples. Load equivalents for 340 MPa (nylon) and 0.8-1.5 GPa (UHMWPE) were applied on yarns. Note. for confidentiality, specific details of rig-(b) are not shown.....	72

---

Figure 3-4.	Process involved in the production of composite samples for both test and control samples. Pre-stressing fibres were stretched for 24 hours prior to moulding. Both test and control mouldings were prepared simultaneously from the same resin mix and completed within 30 minutes.....	75
Figure 3-5.	Production of the composite samples (a) pre-stressed (test) and unstressed (control) fibres are cut to the appropriate length and brushed to separate filaments, (b) fibres are brushed and ready for moulding, (c) fibres are mounted in the thermoset polyester resin. Both test and control mouldings were prepared simultaneously from the same resin mix and completed within 30 minutes.....	76
Figure 3-6.	Schematic diagram of the Charpy impact tester and end-view of the composite sample configuration for impact tests.....	78
Figure 3-7.	Schematic diagram of the three-point bend test arrangement with a freely suspended load for the evaluation of flexural modulus. Composite sample orientation is also shown. A load of 10 N was applied for UHMWPE fibre composites and 4.2 N for hybrid composites (commingled nylon/Kevlar fibres) and resin-only samples.....	80
Figure 3-8.	Tensile testing setup (a) and jig assembly (b) for UHMWPE fibres.....	83
Figure 3-9.	Scanning electron microscope used for microscopic analysis, left side image shows SEM specimen chamber with mounted (impact tested) sample.....	84
Figure 3-10.	Sputter Coater used for gold coating to improve sample conductivity for SEM analysis.....	85
Figure 3-11.	Stereo microscope with attached digital camera.....	86
Figure 3-12.	Profile projector for visual inspection of impact tested samples. Measurements of debonded regions were taken using the micrometre x-y stage.....	87
Figure 3-13.	X-ray diffraction of nylon 6,6 fibres. Note sample prepared for XRD analysis is also shown.....	89
Figure 4-1.	Calibration setup of the two stretching rigs used for pre-stressing and creep-recovery experiments.....	91

Figure 4-2.	Mean calibration data of the stretching rigs from the applied load. Individual data are presented in Appendix-A.....	92
Figure 4-3.	Schematic illustration of polyester resin exothermic tests.....	94
Figure 4-4.	Exothermic test from the curing of polyester general purpose resin mixed with 2% catalyst. Note, various curing stages are indicated by arrows. Subjectively, these are stated as <i>A</i> (viscous), <i>B</i> (gel) and <i>C</i> (hard gel).....	94
Figure 4-5.	Exothermic tests from the curing of polyester clear-casting resin, (a) mixed with 2% catalyst and (b) mixed with 1% catalyst. Note, various curing stages are indicated by arrows. Subjectively, these are stated as <i>A</i> (viscous), <i>B</i> (gel) and <i>C</i> (hard gel).....	95
Figure 4-6.	Mean increases in impact energy of batches produced from general purpose and clear-casting resins. (data from Table 4-1)....	97
Figure 4-7.	X-ray diffraction analysis of nylon 6,6 fibres annealed in fan-assisted and muffle oven at 150°C for 0.5 hour. Note, FWHM method is highlighted in (a <sup>1</sup> ), similar approach applied for all samples.....	101
Figure 4-8.	Mean increases in impact energy (test samples relative to their control counterparts) with standard errors, (data from Table 4-3)...	104
Figure 5-1.	Schematic illustration of Charpy impact tests setup.....	114
Figure 5-2.	Representative optical micrograph (polished) sections of nylon 6,6 fibre spatial distribution of composite samples evaluated from open-casting with polyester resin.....	116
Figure 5-3.	Mean increases in impact energy (test samples relative to identical control counterparts) with standard error, as a function of fibre volume fraction $V_f$ (data from Table 5-2).....	119
Figure 5-4.	Representative fracture and debonding characteristics observed from test (pre-stressed) and control (un-stressed) samples for each $V_f$ value and span setting. Note photos are taken from the fibre-rich side (away from the impact point).....	120
Figure 5-5.	Representative micrograph of the nylon fibre sample tested at 60 mm Charpy span settings. Local debonding between matrix cracks is clearly visible, indicated by the circled region. Note photo taken from fibre-rich side of sample (away from impact point).....	121

Figure 5-6.	High speed camera footage ( $3.8 \text{ ms}^{-1}$ ) highlighting impact event from a nylon-fibre composite sample tested at 60 mm span setting.....	122
Figure 5-7.	Representative SEM micrograph cross-sections of impact tested nylon fibre composite sample showing pre-stress affecting crack propagation. The crack width in pre-stressed sample is narrow in comparison with the un-stressed counterpart.....	124
Figure 5-8.	Representative SEM micrograph cross-sections of nylon fibre composite samples (low $V_f$ 3.3%) subjected to Charpy impact tests at span settings of 24 and 60 mm (similar features are observed in all samples).....	125
Figure 5-9.	Representative SEM micrograph cross-sections of nylon fibre (high $V_f$ 16.6%) composite samples subjected to Charpy impact tests at the span settings of 24 and 60 mm (similar features are observed in all samples).....	126
Figure 5-10.	Mean impact energies from test (pre-stressed) and control (no pre-stress) nylon fibre composite as a function of Charpy span setting. Data points with standard error bars are the means from three batches (data from Table 5-2).....	128
Figure 5-11.	Schematic illustration of the fracture processes at 24 and 60 mm Charpy span settings.....	129
Figure 5-12.	Dependence of impact energy/unit volume ( $u$ ), on span to thickness ratio ( $L/h$ ) for test (pre-stressed) and control (un-stressed) samples at 3.3% and 16.6% $V_f$ . Also shown are CFRP data at comparable $h$ values from Ref [131].....	131
Figure 5-13.	Mean impact energies (from Figure 5-10) at 24, 40 and 60 mm span setting plotted against the product of estimated debonding area ( $A$ ), and fibre volume fraction ( $V_f$ ). Solid lines and equations are from linear regression, $r$ is the correlation of coefficient.....	133
Figure 6-1.	Schematic illustration of hybrid (commingled nylon/Kevlar fibres) composite sample showing fibre dispersion.....	145
Figure 6-2.	Representative optical micrograph (polished) sections of the hybrid (nylon/Kevlar) and Kevlar fibre-only composite sample spatial distribution evaluated from open-casting with polyester resin. Note $V_f$ values are nominal .....	148
Figure 6-3.	Mean impact energy data at (a) 24 mm and (b) 60 mm spans from test (pre-stressed) and control (un-stressed) hybrid composite	

	batches of (3.3% $V_f$ nylon, 1.2% $V_f$ Kevlar commingled) from Table 6-1. Also shown for comparison are data from nylon fibre-only (3.3% $V_f$ ) from Table 5-2, Kevlar fibre-only (3.6% $V_f$ ) and matrix resin-only batches from Table 6-2. All samples were tested at 336 hours (2 weeks) after moulding.....	151
Figure 6-4.	Typical hybrid and Kevlar fibre composite samples after Charpy impact testing at 24 and 60 mm span settings. Note photos are taken from the fibre-rich side (away from the impact point).....	152
Figure 6-5.	Representative SEM micrograph cross-sections of commingled 4.5% nominal $V_f$ (nylon 3.3% $V_f$ and Kevlar 1.2% $V_f$ ) samples tested by Charpy impact testing at 24 mm span (similar features are observed in all samples).....	156
Figure 6-6.	Representative SEM micrograph cross-sections of commingled 4.5% nominal $V_f$ (nylon 3.3% $V_f$ and Kevlar 1.2% $V_f$ ) samples tested by Charpy impact testing at 60 mm span (similar features are observed in all samples).....	157
Figure 6-7.	Representative SEM micrograph cross-sections from both sides of the fracture surface of Kevlar fibre-only composite samples (3.6% nominal $V_f$ ), subjected to Charpy impact tests at 24 and 60 mm spans. Area reduction at the fibre ends indicates tensile type failure, clearly visible in higher magnified micrographs. Similar features are observed in all Kevlar fibre samples tested at 24 and 60 mm span settings.....	158
Figure 6-8.	Flexural modulus values for test (pre-stressed) and control (un-stressed) hybrid composites determined from three-point bend tests; samples with 4.5% $V_f$ (commingled nylon 3.3% $V_f$ and Kevlar 1.2% $V_f$ ). Each value represents the mean of three samples with their corresponding standard error, from Table 6-3.....	161
Figure 7-1.	Schematic illustration of the solution gel spinning process for producing UHMWPE fibres.....	167
Figure 7-2.	Fibrillar structure of gel spun UHMWPE fibres, showing filaments are connected by bundles of very thin fibrils; also macro fibrillar structures on the surface of the filaments are clearly visible in both micrographs.....	168
Figure 7-3.	Schematic diagram of the creep-recovery test cycle to investigate force-time characteristics of viscoelastically recovering UHMWPE fibres.....	172

Figure 7-4.	Schematic diagram of the viscoelastic recovery force measurement rig. The adjustable lower bobbin allows the yarn (fibres) to contract to a fixed strain from a loose state. The cradle, suspending the upper bobbin, allows the contraction forces to exert compression on the sensor.....	176
Figure 7-5.	Schematic diagram of the tensile testing setup and jig assembly for UHMWPE fibres.....	177
Figure 7-6.	Representative SEM micrograph of annealed test (previously loaded) and control (un-stressed) UHMWPE fibres. The test fibres were subjected to creep conditions adopted for composite samples. Both fibre groups were previously annealed at 120°C ....	181
Figure 7-7.	UHMWPE annealed and as-received fibres are mounted on graphite rod sections, ready for EDX analysis.....	182
Figure 7-8.	EDX tests on UHMWPE fibres show no evidence of oxidation in the annealed fibres. Carbon is clearly visible in both samples with no indication of other elements, such as oxygen, from the annealing process.....	183
Figure 7-9.	Recovery strain behaviour of UHMWPE (Dyneema SK60) fibres subjected to various creep stress (real time ~3 years). Creep stress is determined from the applied load on a single yarn (24 hours) and unloaded yarn cross-sectional area. For comparison, data derived from Ref [10] is also shown for nylon 6,6 yarn. Note changes in Creep stress from (a) to (d).....	185
Figure 7-10.	Creep and recovery strain results for annealed and non-annealed (as-received) UHMWPE (Dyneema SK60) fibres. (a) Strain from 24 hour, 1.36 GPa creep stress, in (b) recovery strain results corresponding to the creep data in (a). The solid curves represent the Weibull model fit using Equation 2-1, with listed parameters and coefficient of correlation.....	187
Figure 7-11.	UHMWPE viscoelastic recovery force in terms of axial stress output (force relative to the total cross-sectional area of the fibres) for yarn subjected to a 24 hour creep stress of 1.36 GPa. For comparison, data derived from Ref [91] is also shown, in which nylon 6,6 yarn was subjected to a 24 hour creep stress of 0.32 GPa. Equation 7-1 is fitted to the first 8 hours for UHMWPE fibres; parameters are shown for both yarns.....	189
Figure 7-12.	Stress-strain plots from tensile tests performed on UHMWPE yarn. (a) control (annealed) and as-received (non-annealed) fibres. (b) test (previously stressed) and control (annealed) fibres. The test yarn in (b) was evaluated at 168 hours after releasing the 24 hours creep stress of 1.3 GPa.....	193

---

Figure 7-13.	Representative SEM micrographs of tensile tested UHMWPE fractured fibres. From left to right, annealed test (previously stressed), control (un-stressed) and non-annealed (as-received) samples show similar characteristics.....	194
Figure 7-14.	Typical UHMWPE fibre-based composites, showing test (pre-stressed) and control (un-stressed) samples after impact testing. For comparison, equivalent nylon 6,6 fibre-based samples are also shown from Figure 5-4.....	196
Figure 7-15.	Representative optical micrograph (polished) sections of UHMWPE fibre spatial distributions in composite samples produced by open-casting with polyester resin.....	198
Figure 7-16.	Representative SEM micrographs of impact tested UHMWPE fibre composites showing typical fracture surfaces in test, control and as-received (non-annealed) samples.....	200
Figure 7-17.	SEM image from the fracture surface of a control (un-stressed) sample, showing clear evidence of the skin-core structure in a UHMWPE fibre.....	201
Figure 7-18.	Representative SEM micrographs of UHMWPE fibre based composites subjected to Charpy impact tests. In the test (pre-stressed) samples, the stored energy from pre-stressing appears to be released in the form of fibre bending (recoiling) following fracture; in contrast with control (un-stressed) fibres which exhibit tensile type failure.....	202
Figure 7-19.	Representative SEM micrographs of typical fractured cross-sections of a UHMWPE fibre based composite sample from Charpy impact testing. All samples fractured into two halves. The two mating fracture surfaces show pull-out of fibres and corresponding cavities in (a) and (b).....	203
Figure 7-20.	Representative SEM images of typical fractured cross-sections of UHMWPE a fibre-based composite sample from Charpy impact testing shows fibre pull-out and their corresponding void formation in close detail.....	203
Figure 7-21.	Representative SEM micrograph of an impact tested UHMWPE fibre-based composite sample showing crack and river marks in the matrix.....	204
Figure 7-22.	UHMWPE fibre-based composites: test (pre-stressed) and control (un-stressed) flexural modulus values, determined from the three-point bend tests. Each value represents the mean of three samples with corresponding standard error. (data from Table 7-3 and 7-4)..	206

# LIST OF TABLES

---

Table 2-1.	Literature review on pre-stressed composites.....	58
Table 3-1.	Properties of the fibres (supplier specification) investigated and used in reinforced composite samples.....	65
Table 3-2.	High performance fibres properties for comparison with polymeric fibres shown in Table 3-1.....	66
Table 3-3.	Nominal fibre volume fraction values in the composite samples. These were evaluated from Equation 3.1, where the cross-sectional area of the sample was $3 \times 10 \text{ mm}^2$ . The radius values for nylon, UHMWPE and Kevlar fibres were 13.75, 6.0 and 9.0 $\mu\text{m}$ respectively. The fibre radius is based on supplier specification from Table 3-1.....	74
Table 3-4.	Summary of the materials used for the production of composite samples and testing setup.....	77
Table 3-5.	Standards for flexural modulus testing.....	79
Table 4-1.	Charpy impact test data from nylon fibre composite batches: 5 test (pre-stressed) and 5 control (un-stressed) samples per batch tested at 24 mm span setting. Data is normalised by dividing impact absorbed energy (J) by the cross-sectional area of the sample. S.E is the standard error of the mean. (Individual tested sample data are presented in Appendix-A).....	97
Table 4-2.	FWHM results from the XRD peaks shown in Figure 4-7.....	101
Table 4-3.	Charpy impact test data from nylon fibre composite batches: 5 test (pre-stressed) and 5 control (un-stressed) samples per batch tested at 24 mm span setting. Data are normalised by dividing impact absorbed energy (J) by the cross-sectional area of the sample. S.E is the standard error of the mean.....	103

Table 5-1.	Summary of published Charpy (flatwise) impact tests on fibre-reinforced polymeric composites.....	109
Table 5-2.	Charpy impact test data from nylon fibre composite batches: 5 test (pre-stressed) and 5 control (un-stressed) samples per batch tested at 24, 40 and 60 mm span settings. Data is normalised by dividing impact absorbed energy (J) by the cross-sectional area of the sample. S.E is the standard error of the mean. (Individual tested sample data are presented in Appendix-B).....	118
Table 6-1.	Charpy impact test data from hybrid (nylon and Kevlar commingled) fibre composite samples tested at 24 and 60 mm span. Each batch includes 5 test (pre-stressed) and 5 control (un-stressed) samples of nominal 4.5% $V_f$ (3.3% nylon and 1.2% Kevlar). Data is normalised by dividing impact absorbed energy (J) by the sample cross-sectional area. S.E is the standard error of the mean. (Individual tested sample data are presented in Appendix-C).....	149
Table 6-2.	Charpy impact tests results from batches of Kevlar fibre-only composite (3.6% $V_f$ ) and resin-only samples tested at 24 and 60 mm span (5 samples per batch). Data is normalised by dividing impact absorbed energy (J) by the sample cross-sectional area. S.E is the standard error of the mean. (Individual sample data are presented in Appendix-C).....	150
Table 6-3.	Flexural modulus results from three-point bend tests on individual hybrid composite samples of 4.5% nominal $V_f$ (commingled nylon 3.3% $V_f$ and Kevlar 1.2% $V_f$ ) and polyester resin-only samples. S.E is the standard error of the mean.....	160
Table 7-1.	Summary of the tensile test results of annealed test (previously stressed), control (un-stressed) and non-annealed (as-received) UHMWPE fibres. S.E is the standard error of the mean.....	192
Table 7-2.	Charpy impact tests data of UHMWPE fibre composite samples tested at 24 and 60 mm spans. For each span, a total of 15 batches	

	were tested, each batch consisting of 5 test and 5 control samples. Data is normalised by dividing impact absorbed energy (J) by the sample cross-sectional area. S.E is the standard error of the mean. (Individual tested sample data are presented in Appendix-D).....	197
Table 7-3.	UHMWPE fibre-based composites: flexural modulus results data from samples with 3.6% $V_f$ using the three-point bend tests. S.E is the standard error of the mean.....	207
Table 7-4.	UHMWPE fibre-based composites: flexural modulus results data from samples with 7.2% $V_f$ using the three-point bend tests. S.E is the standard error of the mean.....	208
Table A-1.	Stretching rig calibration data (Figure 4-2a). S.E is the standard error.....	254
Table A-2.	Stretching rig calibration data (Figure 4-2b). S.E is the standard error.....	255
Table A-3	Charpy impact test data from nylon fibre composites (2-4% $V_f$ ) produced from clear-casting (C-C) and general purpose (GP) polyester resins (data are shown in Figure 4-6, Chapter-4). Batches of test (pre-stressed) and control (un-stressed) samples tested at 24 mm span setting. Data are normalised by dividing impact energy (J) by the cross-sectional area of the sample. S.E is the standard error of the mean.....	256
Table A-4.	Charpy impact data from nylon fibre composites (2-4% $V_f$ ) produced from fibre annealed in fan-assisted oven (data are shown in Figure 4-8, Chapter-4). Batches of test (pre-stressed) and control (un-stressed) samples tested at 24 mm span setting. Data are normalised by dividing impact energy (J) by the cross-sectional area of the sample. S.E is the standard error of the mean.....	257
Table A-5.	Charpy impact data from nylon fibre composites (2-4% $V_f$ ) produced from fibre annealed in muffle oven (data are shown in Figure 4-8). Batches of test (pre-stressed) and control (un-stressed) samples tested at 24 mm span setting. S.E is the standard error of the mean.....	258

Table B-1.	Charpy impact data from nylon fibre composites (data are shown in Figure 5-3, Chapter-5). Batches of test (pre-stressed) and control (un-stressed) samples (3.3% $V_f$ ) tested at 24, 40 and 60 mm span settings. Data are normalised by dividing impact energy (J) by the cross-sectional area of the sample. S.E is the standard error of the mean.....	260
Table B-2.	Charpy impact data from nylon fibre composites (data are shown in Figure 5-3, Chapter-5). Batches of test (pre-stressed) and control (un-stressed) samples (10% $V_f$ ) tested at 24, 40 and 60 mm span settings. Data are normalised by dividing impact energy (J) by the cross-sectional area of the sample. S.E is the standard error of the mean.....	261
Table B-3.	Charpy impact data from nylon fibre composites (data are shown in Figure 5-3, Chapter 5). Batches of test (pre-stressed) and control (un-stressed) samples (16.6 % $V_f$ ) tested at 24, 40 and 60 mm span settings. Data are normalised by dividing impact energy (J) by the cross-sectional area of the sample. S.E is the standard error of the mean.....	262
Table C-1.	Charpy impact data from hybrid (nylon and Kevlar commingled) fibre composite samples tested at 24 and 60 mm span (data are shown in Figure 6-3, Chapter-6). Each batch comprises 5 test (pre-stressed) and 5 control (un-stressed) samples of 4.5% $V_f$ (3.3% nylon and 1.2% Kevlar). Data are normalised by dividing impact energy (J) by the sample cross-sectional area. S.E is the standard error of the mean.....	264
Table C-2.	Charpy impact results from batches of Kevlar fibre-only composites (3.6% $V_f$ ) and resin-only samples tested at 24 and 60 mm span (data are shown in Figure 6-3, Chapter-6). Data are normalised by dividing impact energy (J) by the sample cross-sectional area. S.E is the standard error of the mean.....	265

---

Table D-1.	Charpy impact data of UHMWPE fibre composite samples (3.6% $V_f$ ) tested (24 hours after moulding) at 24 and 60 mm span. Each batch comprises 5 test (pre-stressed) and 5 control (un-stressed) samples. Data are normalised by dividing impact energy (J) by the sample cross-sectional area. S.E is the standard error of the mean.....	267
Table D-2.	Charpy impact data of UHMWPE fibre composite samples (3.6% $V_f$ ) tested (96 hours after moulding) at 24 and 60 mm span. Each batch comprises 5 test (pre-stressed) and 5 control (un-stressed) samples. Data are normalised by dividing impact energy (J) by the sample cross-sectional area. S.E is the standard error of the mean.....	268
Table D-3.	Charpy impact data of UHMWPE fibre composite samples (3.6% $V_f$ ) tested (168 hours after moulding) at 24 and 60 mm span. Each batch comprises 5 test (pre-stressed) and 5 control (un-stressed) samples. Data are normalised by dividing impact energy (J) by the sample cross-sectional area. S.E is the standard error of the mean.....	269
Table D-4.	Charpy impact data of UHMWPE fibre composite samples (3.6% $V_f$ ) tested (336 hours after moulding) at 24 and 60 mm span. Each batch comprises 5 test (pre-stressed) and 5 control (un-stressed) samples. Data are normalised by dividing impact energy (J) by the sample cross-sectional area. S.E is the standard error of the mean.....	270
Table D-5.	Charpy impact data of UHMWPE fibre composite samples (3.6% $V_f$ ) tested (1008 hours after moulding) at 24 and 60 mm span. Each batch comprises 5 test (pre-stressed) and 5 control (un-stressed) samples. Data are normalised by dividing impact energy (J) by the sample cross-sectional area. S.E is the standard error of the mean.....	271

# ABBREVIATIONS

---

A	Area
ASTM	American Society for Testing and Materials
BSI	British Standards Institution
CC	Clear-casting Polyester Resin
CFRP	Carbon Fibre Reinforced Polymer
CRAG	Composite Research Advisory Group
EDX	Energy Dispersive X-ray
EPPMC	Elastically Pre-stressed Polymer Matrix Composite
FRC	Fibre Reinforced Concrete
FRP	Fibre Reinforced Polymer
FWHM	Full Width Half Maximum
GFRP	Glass Fibre Reinforced Polymer
GP	General-purpose Polyester Resin
HDPE	High Density Polyethylene
ISO	International Standard Organisation
KWW	Kohrausch-Williams-Watts
LDPE	Low Density Polyethylene
PEEK	Polyether-ether-ketone
PMC	Polymer Matrix Composite
PP	Polypropylene
PPTA	poly-paraphenylene Terephthalamide
SEM	Scanning Electron Microscopy
UHMWPE	Ultra High Molecular Weight Polyethylene
$V_f$	Fibre Volume Fraction
VPPMC	Viscoelastically Pre-stressed Polymer Matrix Composite
XRD	X-ray Diffraction

# SYMBOLS

---

$\sigma(t)$	Stress (time dependent)
$\varepsilon_{rvis}(t)$	Viscoelastic and viscous flow strain on recovery at time
$\varepsilon_r$	Viscoelastic strain recovery
$\varepsilon_f$	Viscous flow effects
$\eta$	Characteristic life parameter
$\beta$	Weibull shape parameter
$\delta$	Deflection
$I$	Second moment of area

# CHAPTER-1

## INTRODUCTION

---

### SUMMARY

In this study, investigations into viscoelastically pre-stressed polymer matrix composites (VPPMCs) are performed. This work produced the first PhD thesis in the field of VPPMC technology and it has been driven mainly by comprehensive experimental investigations. The VPPMC production process involves applying tension to polymeric fibres; the tensile load is then released (prior to moulding) and the fibres are embedded into a polyester resin. Following matrix solidification, compressive stresses are imparted in the matrix by the viscoelastically strained fibres which improve mechanical properties.

This chapter highlights the aims and objectives of the work, these being to provide a further understanding through the evaluation of fibre volume fraction effects, fibre commingling and the use of polyethylene fibre as an alternative to (established) nylon 6,6 fibre. A brief introduction to VPPMC technology and a background to the objectives together with thesis structure details are also presented.

## **1.1 AIMS AND OBJECTIVES**

The aim of this research study is to provide further knowledge and insight of viscoelastically pre-stressed polymer matrix composite (VPPMC) technology.

By focusing on Charpy impact testing and three-point bend tests, the objectives are:

- Production and evaluation of nylon 6,6 fibre-based VPPMC samples, to understand the role of fibre volume fraction.
- Evaluate the effects of commingling (tough) nylon 6,6 pre-stressing fibres with (strong and stiff) Kevlar fibres to produce hybrid VPPMCs.
- Investigate the viscoelastic characteristics and VPPMC performance of (potentially superior) polyethylene fibre as an alternative to nylon 6,6 fibre.
- Investigate VPPMC fibre-matrix interface interactions from above through the use of optical and scanning electron microscopy.

## **1.2 INTRODUCTION**

The desire for lightweight and stiffer materials encourages the development of high performance strength fibre reinforced composites; consequently, composite materials become more prevalent in engineering applications. In the last few decades, significant progress has been made in the development of the high strength advanced composite materials in terms of material behaviour under impact and other load conditions. In recent years, broad technological efforts have led to thermosetting and thermoplastic composites being used in many sectors. These include aerospace (aircraft structures and satellites), automotive (crashworthiness, fuel tanks and other moulded parts), defence

(impact/blast protection), medical (dental materials and prosthetic devices) and energy (wind turbine blades) [1]. Over the past 20 years, the aircraft industry has driven the development of advanced composite materials and extensively exploited their use in the latest commercial aircraft [1]. Aircraft structures, made of composite materials, have demonstrated weight saving of up to 50% over conventional metals [2]. Similar trends have been followed by the automotive industry, in which the structural components must be lighter, stiffer and strong enough to withstand loads and to resist impact damage. These requirements are achieved by optimising the properties of reinforcing fibres and their appropriate selection in terms of strength, stiffness, strain-to-failure, fibre volume fraction and their orientation. Nowadays, technological advances in the field of composite materials have produced cars that are lighter, faster and safer than ever before [1]. By using polymer composite materials, the manufacturer has the flexibility in design and fabrication, selecting different types of fibres for various applications. This can be done by mixing various types of fibres with different properties in the same resin mix to produce a hybrid composite.

The response of composite materials to impact by a foreign object has further increased the need for a better understanding of their behaviour under various load conditions. Despite the tremendous benefits of advanced composite materials have over metals where high strength/stiffness and low weight are essential, further understanding for the development and improvement in terms of high energy absorption capability is required. Pre-stressing could be one of the possibilities for improving composite material properties without increasing section dimensions or mass. So far, enhancement in the mechanical properties of composite materials by using pre-stressing is not (currently) an established method. Nevertheless, some researchers have successfully demonstrated the benefits of pre-stressed composites. Pre-stressed polymeric matrix composites were probably first introduced by Zhigun in 1968 [3]; this work was followed by others, such as Manders and Chou in 1983 [4] and Tuttle in 1988 [5].

Pre-stressed composites can be produced by applying a load to the fibres which is then released after matrix curing. After removal of the load, these strained fibres attempt to

recover to their original state, while the solid matrix around the fibres restricts fibre recovery and this results in the fibres imparting compressive stresses to the surrounding matrix. For commercial applications, composite components can vary in size ranging from a few millimetres to several meters. Representative examples here would be materials for dental restoration to the wind turbine blades and aircraft structures. The question arises here, how it can be possible to ensure that the recovery force generated from pre-strained fibres (in composites) can be achievable on a large scale. In elastically pre-stressed polymer matrix composites (EPPMCs), the pre-strain load is applied to the fibres during the moulding process and maintained until the resin is cured. Therefore, applying load to the fibres on a large scale to produce EPPMCs may be unrealistic.

In the literature, a solution to the above issue was made by Fancey in the late 1990s [6]. Fancey published the first findings on viscoelastically pre-stressed polymer matrix composites (VPPMCs) at the University of Hull in 2000 [7], and since then Fancey's work has made major contributions towards VPPMC technology [7-10]. Fancey's method is unique, in which the pre-stressed composites exploit viscoelastic recovery force by using polymeric (nylon 6,6) fibres. Here these fibres were stretched under a load prior to moulding; on releasing the load, elastic strain was instantaneously recovered, while the viscoelastic strain would recover with time (slow process). These pre-strained fibres were then embedded into a polyester resin mix; on solidification of the resin, compressive stresses were produced in the matrix as these pre-strained fibres attempted recovery, while the solid matrix would not allow fibre movement [7-10].

It is noteworthy that Fancey, subsequently with Pang, have been the only authors working in VPPMC technology [7-13]. In the recent years, however, Cui *et al* [14] have performed investigations on the viscoelastic behaviour of natural fibres, in which they demonstrated VPPMCs based on bamboo fibre and have shown that the flexural moduli and toughness were increased. Although potential alternatives may be emerging, VPPMCs based on nylon 6,6 fibres remain (currently) the most established route, the pre-stress being demonstrated to last at least 20 years at a constant 40°C [10].

Although, working in the field of pre-stressed composites is an interesting area of research, it has received a very little attention and as a consequence, it is far away from potential commercialisation. Relatively, few workers have performed research in EPPMCs and VPPMCs. For this study, Fancey's previous work on VPPMCs is of particular interest and has provided the major contribution to the literature sections of this thesis.

### **1.3 MOTIVATION**

This research intends to contribute to the ongoing efforts in viscoelastically pre-stressed polymer matrix composites research through curiosity-driven investigations, as highlighted in Section 1.1(objectives). Motivation is enhanced by the fact that this is a unique area of research pioneered at the University of Hull. These investigations are intended to expand knowledge of existing VPPMC technology (based on nylon 6,6 fibres) and to identify the potential of an alternative, mechanically superior polymeric fibre (e.g. polyethylene).

## **1.4 BACKGROUND TO THE OBJECTIVES**

### **1.4.1 NYLON FIBRE-BASED VISCOELASTICALLY PRE-STRESSED COMPOSITES**

The failure of a composite material is often mixed mode, involving matrix cracking, fibre fracture, fibre pull-out and debonding. The material behaviour and response to impact conditions plays an important role in considering their performance in energy absorption, e.g. critical stresses may arise simultaneously at several points in the material during impact testing. In a low velocity impact test such as Charpy or Izod, the contact time of the pendulum is long enough for the sample to respond back to the impact; in consequence absorbed energy can occur by (i) elastic deformation through deflection and (ii) plastic deformation through matrix and fibre fracture. Cantwell and Morton [15] classified low velocity as being up to  $10 \text{ ms}^{-1}$ , and identified the ability of the fibres resistance to a low velocity impact from elastic energy storage, based on the modulus and failure strain of the fibres. This work has confirmed that the response of the composite sample subjected to low velocity impact is mainly dependent on the nature of reinforcing fibre, testing setup and fibre volume fraction, so the effects from viscoelastically generated pre-stress can also be expected to be dependent on these conditions.

### **1.4.2 VISCOELASTICALLY PRE-STRESSED COMPOSITES BASED ON COMMINGLED NYLON/KEVLAR FIBRES**

In many applications, where energy absorption under impact conditions combined with various loading situations, is of major concern, then a possible solution would be to produce hybrid composites by commingling two or more types of fibre in the same resin mix. This approach may improve the mechanical properties of the material by combining the benefits available from each fibre type.

It is well known that material toughness (energy absorption) is generally associated with a combination of high ductility and high strength. In this work, the effects of hybridisation by using Kevlar-29 and nylon 6,6 fibres are investigated. Kevlar fibre exhibits high strength and substantially less strain-to-failure (i.e. ~4%) [16], whilst nylon 6,6 fibres have high strain-to-failure values of 14-22% and high ductility [17]. Thus by commingling these two fibres, the resulting hybrid composite may provide greater property improvement capabilities over the corresponding single fibre type composites. The contribution of viscoelastically generated pre-stress via the commingled nylon fibres may add further enhancement in terms of the composite material impact toughness. Similarly, the stiffer Kevlar fibres should be expected to produce stiffer composites, as the tensile region in bending will depend on Young's modulus  $E$  of the fibres. Although  $E$  for nylon 6,6 fibres is substantially lower (3.3 GPa) than Kevlar-29 (58 GPa) [16, 17], the effect of pre-stress generated by nylon 6,6 fibres commingled with Kevlar-29 fibres may also provide an increase in flexural modulus.

### **1.4.3 POLYETHYLENE FIBRE-BASED VISCOELASTICALLY PRE-STRESSED COMPOSITES**

In the last three decades, substantial progress has been made in exploiting the fundamental properties of strong and tough fibres. Significant developments in strong fibres includes polyamides (aramid) [18] and Zylon [19]. However, VPPMCs requires fibres to possess appropriate viscoelastic characteristics; for this reason, common structural fibres (e.g. glass, carbon) and some high performance polymeric fibres may be unsuitable for generating viscoelastic pre-stress. Therefore, selecting a suitable polymeric fibre, that is superior to nylon 6,6 requires careful consideration, if it can enable VPPMC technology to be exploited for load-bearing applications.

In this work, the motivation to use UHMWPE fibres was their high strength and stiffness, high energy absorption capability for impact/blast protection (bullet proof vests, helmets, car panels, cut-resistant gloves) and medical applications such as prosthetics and dental restoratives [20-23]. To develop UHMWPE fibre-based VPPMCs

would require the establishment of appropriate conditions for obtaining suitable viscoelastic recovery from the fibres (i.e. annealing and creep loading) followed by mechanical evaluation and analysis of the resulting VPPMCs. This would provide answers to the following questions: (a) how long can viscoelastic recovery (creep induced strain recovery) last in UHMWPE fibres, (b) how much force can the fibres provide in pre-stressed composites and (c) ultimately, are UHMWPE fibre-based VPPMCs viable?. For (c), the aim is to demonstrate viability by performing Charpy impact and three-point bend tests.

## **1.5 THESIS STRUCTURE**

### **CHAPTER-2**

Chapter-2 provides a review of fibre reinforced composite materials, focused on relevance to this research. This includes history, background and failure mechanisms of polymer composite materials. This is followed by a detailed overview on pre-stressed composites. The concepts and differences between elastically and viscoelastically pre-stressed polymer matrix composites are evaluated. The methodology of fibre pre-stressing is also presented to highlight the potential complexities involved in the processing of elastically pre-stressed composites; this gives the opportunity to compare the advantages and disadvantages of various pre-stressing methods which have been adopted by other researchers working in this field. Chronological summary of pre-stressed composites (from the literature) is presented in a table to provide the reader with a coherent list of the progress made in this field.

### **CHAPTER-3**

Chapter-3 provides a general overview of the materials used and equipment facilities employed in this study. The selection of reinforcing material (fibre) and comparison with other commercial fibres in terms of mechanical properties such as strength and stiffness is also discussed. This is followed by the experimental methodology and the

processes involved for the production of composite samples. A brief description on the procedure of fibre pre-stressing, preparation prior moulding and equipment used for mechanical testing is also discussed.

#### **CHAPTER-4**

Chapter-4 focuses on the preliminary studies undertaken during this work to minimise the risk of any uncertainties generated from the processing of material for the production and testing of VPPMC samples. In addition, investigations were performed to acquire information needed for performing this research work, such as calibration of the stretching rigs to evaluate pre-stress levels in fibres for VPPMC production. The selection of the matrix material and possible effects of the oven to be used for the annealing process are covered.

#### **CHAPTER-5**

Chapter-5 investigates the mechanisms considered responsible for VPPMCs improving impact toughness by performing Charpy impact tests on unidirectional nylon 6,6 fibre/polyester resin samples. Here, a range of span settings (24-60mm) and composite fibre volume fractions are evaluated. In addition, visual evidence from impact-tested samples on the influence of pre-stressing on crack propagation is presented.

#### **CHAPTER-6**

Chapter-6 investigates an approach to further enhance material properties by commingling pre-stressing nylon fibres with other mechanical superior fibres (Kevlar) in the same resin mix. Kevlar fibres have high strength and stiffness, whilst nylon fibres have high ductility; thus, by commingling these fibres prior to moulding, the resulting hybrid composite would be expected to be mechanically superior to the corresponding single fibre-type composites. The contribution made by viscoelastically generated pre-stress, via the commingled nylon fibres should add further enhancement. These composites are evaluated in terms of impact toughness and flexural stiffness.

## **CHAPTER-7**

Chapter-7 reports the first findings on the viscoelastic characteristics of polyethylene (UHMWPE) fibres under load-time conditions suitable for VPPMC production. This involved fibre creep-recovery strain studies to determine the appropriate conditions for producing UHMWPE fibre-based VPPMC samples. The viability of these VPPMCs are demonstrated through Charpy impact and three-point bend tests.

## **CHAPTER-8**

In Chapter-8, a detailed general summary based on the findings of this work are presented, which leads to highlighting some potential applications for future exploitation. Also, suggestions for the direction of future work in the field of VPPMCs are discussed.

## **CHAPTER-9**

The overall findings and conclusions of this research work are presented in Chapter-9.

## 1.6 WORK DISSEMINATION

Research findings from this thesis are presented in the following publications.

### JOURNALS (PEER-REVIEWED)

1. **Adnan Fazal** and Kevin Fancey. Viscoelastically prestressed polymeric matrix composites – Effects of test span and fibre volume fraction on Charpy impact characteristics. *Composites Part B*, 2013. 44(1): p. 472-479.
2. **Adnan Fazal** and Kevin Fancey. Viscoelastically generated prestress from ultra-high molecular weight polyethylene fibres. *Journal of Materials Science*, 2013. 48(16): p. 5559-5570.
3. **Adnan Fazal** and Kevin Fancey. Performance enhancement of Nylon/Kevlar fiber composites through viscoelastically generated pre-stress. *Polymer Composites*, 2014. 35(5): p. 931-938.
4. **Adnan Fazal** and Kevin Fancey. UHMWPE fibre-based composites: prestress-induced enhancement of impact properties. *Composites Part B*, 2014. 66: p. 1-6.

### CONFERENCE PROCEEDINGS

5. **Adnan Fazal** and Kevin Fancey. Performance enhancement of Kevlar fibre composites through viscoelastically generated prestress. *17<sup>th</sup> International Conference on Composite Structures*. 17-21 June, 2013 (Porto, Portugal).
6. **Adnan Fazal** and Kevin Fancey. Polymer Matrix Composites: Performance enhancement through viscoelastically generated pre-stress. *22<sup>nd</sup> International Conference on Composites/Nano Engineering*. 13-19 July, 2014 (Malta).

During the course of PhD studies, following publications on the long-term behaviour on VPPMC were also generated.

7. Kevin Fancey and **Adnan Fazal**. The long-term performance of viscoelastically prestressed polymeric matrix composites. *17<sup>th</sup> International Conference on Composite Structures*. 17-21 June, 2013 (Porto, Portugal).
8. Kevin Fancey and **Adnan Fazal**. Pre-stressed polymeric matrix composites: longevity aspects. *Polymer Composites*, 2014 (In press).

# CHAPTER-2

## BACKGROUND STUDIES

---

### SUMMARY

This chapter provides a review of fibre reinforced composite materials appropriate to this research. The first section covers history, background and failure mechanisms of polymer composite materials. This is followed by a detailed account of pre-stressed composites.

The concept and differences between elastically and viscoelastically pre-stressed composites are clarified by providing evidence from the literature. These include the benefits of viscoelastically pre-stressed composites over elastically pre-stressed composites. The methodology of fibre pre-stressing is also presented to highlight the potential complexities involved in the processing of pre-stressed composites; this also gives the opportunity to compare the advantages and disadvantages of various pre-stressing methods which have been adopted by other researchers working in this field.

Finally, at the end of this chapter, an overview on pre-stressed composites is presented in a table in which further detail of the materials, pre-stressing methodology and main findings are provided. Information in the table is presented in chronological order to provide a coherent summary to the reader of the progress made in this field.

## 2.1 INTRODUCTION

The history of composite materials dates back as far as 7000 years, when ancient artisans used pitch to bind reeds for composite boats [24]. The use of fibres as a structural material can be traced back to 4000 years such as the old arch in China constructed from fibre reinforced clay [25]. A similar approach was followed by Egyptians about 3000 years ago in which they used straw to reinforce clay to build walls [26] and it can also be seen in the Great wall of China, which was built 2000 years ago [25].

With the passage of time, interest in fibres waned and other durable materials were introduced. The use of glass fibre reinforced composites was first introduced by Ellis and Rust in the late 1930s [24] and used in the aircraft industry in the 1940s [27]. In the early 1950s, it was introduced into the automobile industry [28]. Composite materials are becoming an essential part of today's life such as electronic packaging to medical equipment and space vehicles to home building materials [29]. In recent years, composite materials are used extensively in aircraft structures because of their advantages, such as light weight, corrosion resistance and high strength/stiffness characteristics. A potential for weight saving exists in many applications within the aerospace and automotive industries [30].

A major breakthrough can be observed in the aircraft industry in which the main structure of fuselages are made of composite materials, such as the Boeing 787 Dreamliner, Airbus A380 and A350 XWB [31]. The Airbus A350 XWB is expected to enter into service in the coming years and is projected to have more than 50% of its structure made of composite materials [32, 33], while the Boeing 787 Dreamliner is unique in its utilisation of composite materials, which is approximately 50% of the weight of the aircraft [1]. The wings of the Dreamliner are composed of up to 80% composite material and 20% aluminium, in comparison with the previous Boeing 777, in which only 12% composite material was used [34]. The current generation of civil aircraft have successfully demonstrated the replacement of secondary structures by

reinforced composite such as glass, carbon and Kevlar fibres. An advantage of the reinforced composites over traditional materials such as aluminium includes high stiffness, better fatigue life and also reduced stress levels on metallic components. Composites reinforced with glass, carbon, Kevlar and other tough fibres with high strength to weight ratio make an attractive material for many applications. The next section highlights the different types of composite material and the processes involved in their production.

## **2.2 COMPOSITE MATERIALS**

### **2.2.1 POLYMERIC MATRIX MATERIALS**

Composites are the combination of two or more materials which are differing in their composition and the individual constituents retain their separate identities. These separate constituents act together to give the necessary mechanical strength and stiffness to the composite material. Reinforced concrete is a good example of composites, in which steel and concrete retain their individual identities in the finished structure and both constituents act together resulting in improving the load capability of the finished structure. In a reinforced concrete structure, steel rods are capable of carrying tensile loads while the concrete carries compression loads.

Similarly, fibre reinforced polymer composites can be produced by embedding fibres into a polymer matrix. The fibres are usually stiffer and stronger than the matrix resin and the primary role of the fibres is to provide strength and stiffness to the composite, while the matrix resin transfers load to the fibres and maintains the fibres in their desired position. The matrix also protects fibres from external environmental damage such as chemicals and moisture. Embedding fibres into a resin matrix produces fibre reinforced composite material which improves overall properties of the material, which

cannot be achieved with any of the constituents acting alone; also both fibres and matrix retain their physical and chemical identities in the composite. The mechanical strength of polymer matrix composites mainly depends on the properties of their constituent materials, such as types of fibre, their quantity, distribution and orientation. Composite structures for commercial applications such as aerospace adopts the highest fibre volume fraction which can be up to 60% [30]. It is worthy to note that the matrix also plays an important role in the composite material.

Most commonly, composite materials produced on a commercial scale use polymer matrix materials (resins). Polymers are well-suited as matrix materials due to their low densities and processing temperatures. The matrix in fibre reinforced composites is the binding material; it also integrates the whole structure to form a required shape. Another function of the matrix is providing protection against an adverse environment. Without a good understanding of the matrix material (associated with their physical and chemical properties) it may not be an easy decision to select the best matrix material for the desired application. Matrix materials are widespread and varied in properties; common polymeric matrix materials include polyester, epoxy, polyethylene and Polyether-ether-ketone (PEEK). These can be categorised into two groups i.e. thermoset or thermoplastic which are summarised below.

### **2.2.2 THERMOSETS**

The composites industry is dominated by thermosetting resins because of lower cost, relative ease of processing and availability. Thermoset composites have been used in the aircraft industry since the 1940s [27]. A thermoset usually consists of low molecular weight resin and a compatible curing agent known as a hardener, which is typically used to increase the curing rate. Mixing hardener with a polymer resin forms a low viscosity liquid which undergoes a chemical reaction and generates three-dimensional cross-linked structures, resulting in an infusible and insoluble solid phase that cannot be re-processed [35]. The process of converting liquid viscous resin to the solid state by polymerisation is called the cure cycle [36]. Common thermosetting resins used as a

composites matrices are epoxies, unsaturated polyesters, vinyl esters, bismaleimides, polyimides and phenolics [35].

### **2.2.3 THERMOPLASTICS**

Thermoplastic composites can be distinguished from thermosets in that no chemical reaction occurs during the processing stage; these can be formed by heating (processing temperature) thermoplastic matrix materials. Injection moulding, extrusion and compression moulding are the typical methods to produce thermoplastic composites with high production rates; also products with complex geometries with good dimensional accuracy can be produced by these methods [31]. Thermoplastics consist of linear or branched chain molecules with strong intra-molecular bonds and weak intermolecular bonds, these are high-molecular weight polymers either semi-crystalline or amorphous in structure, which can be reprocessed [29, 37]. Processing of thermoplastics involves higher temperature and pressure; therefore the cost of processing and manufacturing of thermoplastic composites are relatively higher than thermosets. Typically, thermoplastics used as a matrix material are PEEK, Poly phenylene sulphide (PPS), Polyether imide (PEI) and Polyimide (PI) [35].

### **2.2.4 PROCESSING OF COMPOSITE MATERIALS**

Manufacturing of the composite material can be mainly categorised into two phases, i.e. pre-forming and processing. In the pre-forming phase, fibres and resin are placed in a mould or shaped into a structural form. The next phase is the processing, in which temperature and pressure is applied to consolidate the desired structure. For thermoset resins, chemical cross-linking reactions solidify the structures, whilst thermoplastic resins become hard after cooling from the processing temperature. Composites can be produced by using a wide variety of processing the techniques such as hand lay-up, hot pressing, vacuum bagging, pressure bagging, resin transfer moulding, filament winding, pultrusion and autoclave moulding. Autoclave-based processing is a widely used

method of producing high-quality composites in the aerospace industry [38]. Typically, an autoclave consists on control system such as pressure vessel, gas compressor, heating system and vacuum pump. The final composite product is not only determined by the function of individual properties of resin and fibre, but also on the processing method and parameters such as ratio of the constituent materials.

## **2.3 FAILURE IN COMPOSITE MATERIALS**

### **2.3.1 FAILURE MECHANISMS**

In general, material subjected to loads (static or impact) mainly absorb energy by two basic mechanisms (i) deformation and (ii) creation of new surface area through crack propagation. The failure of composite materials is one of the most challenging and important areas to be understood. Fracture mechanisms of composite materials are very different from homogenous/isotropic materials. In Ref [39], it is suggested that the energy absorption or toughness of homogenous materials can be measured by various methods and be correlated with fracture mechanics theory such as Griffith theory (for brittle type fracture). However, theories developed for a single phase material cannot be implemented to predict the fracture behaviour of a non-homogeneous composite material. The unique properties of a composite material are their failure characteristics; i.e. microstructure inhomogeneity provides numerous paths in which the load can be redistributed. Nevertheless, fracture mechanisms introduced by others [40, 41] suggest that the fracture modes of composite materials involves matrix cracking, interface fracture and the work done by the fibre crack or debonding.

The fracture mechanisms in unidirectional composites such as fibre/matrix debonding, fibre fracture, fibre pull-out, matrix cracks and stress redistribution due to the fibre fracture can result in synergy in work of fracture, i.e. work of fracture in the composite

can be more than the sum of fracture energies of its constituents [27]. Research by others [27, 42, 43] have shown that the damage mechanisms in a unidirectional composite may be divided into three types. These are matrix cracking, fibre breakage and interfacial shear failure, schematically these are shown in Figure 2-1 and are summarised here.

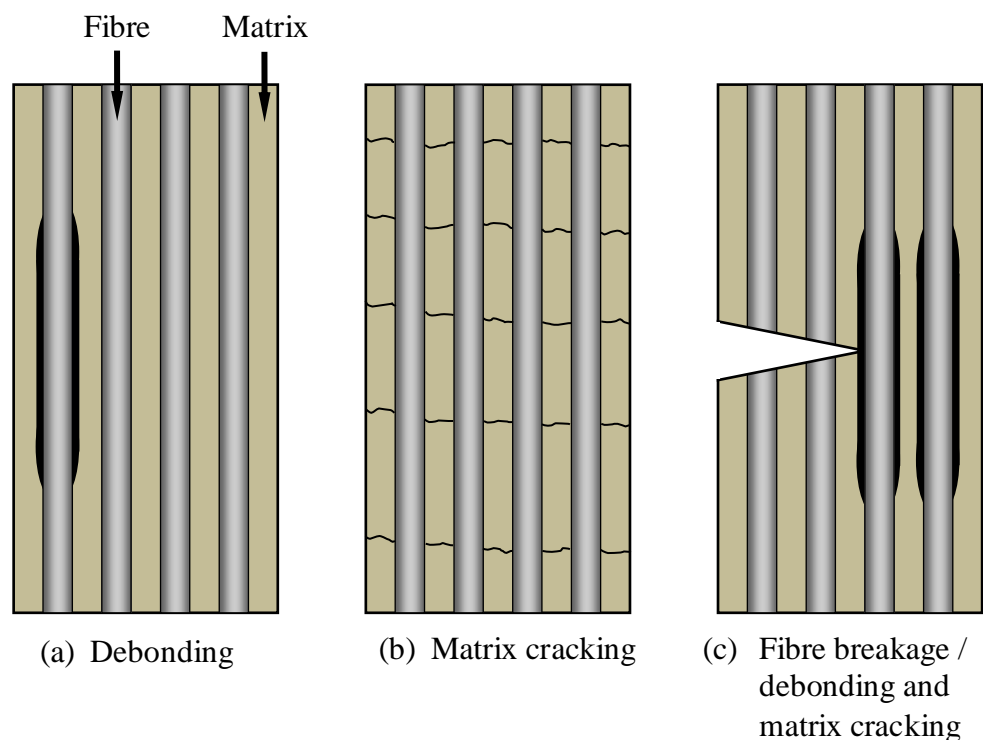


**Figure 2-1. Schematic illustration of fracture in a fibre reinforced composite material.**

**(a) Debonding/delamination**

When a composite is subjected to an impact load, it generates high localised deformation, this causes transverse shear stresses. These stresses can cause damage in the form of debonding of the fibre from the surrounding matrix at the interface region; it grows along the fibre/matrix interface and as a result absorbs more energy than transverse fracture. If the stress concentration on the

fibres at the debonding region exceeds their failure strength then fibres will fracture which can lead to transverse cracking.

**(b) Matrix cracking**

Because of the brittle nature of matrix materials, cracks usually appear at lower loads in comparison with fibre fracture. If lower loads are applied to the composite, the cracks in the matrix may be arrested at the interface regions, where the surface of the fibre bonds with the matrix. However, at greater loads, the higher stresses at the crack tip might lead to fibre failure.

**(c) Fibre fracture/interfacial shear failure**

A crack in the matrix may propagate under a continuing load until it hits an interface region, in which a fibre can be fractured if the shear stress exceeds the strength of the weakest fibre in the composite.

The two possible failure mechanisms in fibre reinforced composites are to be expected. These are described by Fuwa *et al* [44] and are summarised below.

- (i) If the adhesion between fibres and matrix is weak, failure of the composite is expected to occur along the interface, which leads to longitudinal splitting with fibre fracture and interface debonding. These types of failure are observed in glass/epoxy composites.
- (ii) If adhesion at the fibre/matrix interface is strong, then failure may occur in the form of matrix cracks and fibre fracture. This will lead to separation of the sample into two or more pieces. These types of failure are typically observed in carbon fibre/epoxy composites.

Studies by others [45] have shown that a composite material subjected to low velocity impact can result in significant internal damage in the form of matrix cracks and debonding (delamination). In general, the crack propagates through the matrix until it reaches a fibre. The impact toughness increases from the fibre withstanding the applied stress and by the diversion of crack propagation at the fibre/matrix interface region i.e.

detachment of the fibres from matrix. By this, a crack can propagate along the fibre without fracturing it and the creation of a new surface around the fibre consumes energy, resulting in absorbing great amounts of energy during the failure process [39]. Thus, fracture toughness of the material can be increased through debonding. The interphase region in a composite material plays an important role; their effects on the performance of composite material are explained in the next section.

### **2.3.2 INTERFACE/INTERPHASE REGIONS IN COMPOSITE MATERIALS**

The performance of any reinforced composite not only depends on the individual constituents and their arrangement of reinforcing material but also the interactions between fibres and matrix. In general, it is assumed that a composite material contains fibre and matrix (at macro level). However, on a micro scale, additional regions exist between fibre and matrix called the interface and interphase [46-48]. These local regions form during the processing of the composite material, where the matrix and fibres bond together. The physical properties of interphase regions usually depend on the chemical and mechanical properties of the matrix and fibres. The interphase region mainly determines mechanical properties of the composite material because of its role in transferring sufficient stress (load) from the matrix to fibre [28, 49-53]. In other words, the stress acting on the matrix is transferred to the fibres through interphase region, thus it is the source of communication between the fibres and matrix. The adhesion between fibre/matrix and the load transfer at the interphase region play an important role in the performance of composite materials [27]. Therefore, adequate adhesion between the fibres and matrix can improve the load transfer capability of the composite constituents. Optimal interfacial adhesion between the fibre and matrix is necessary for a proper transfer of load. Therefore, interfacial bonding must be strong enough for an efficient transfer of the applied load but not excessive, since it could also promote crack propagation across the fibres and consequently reduce the toughness of the composite material [54]. Interfacial fibre/matrix bonding in a composite material can be divided into three levels i.e. weak, ideal and strong.

The attainment of good mechanical properties in composite materials depends significantly on the efficiency of stress transfer from matrix to fibre. In terms of improving fibre and matrix adhesion, many modification techniques can be used depending on the type of fibre and matrix. Many researchers have shown interest in the enhancement of interphase regions, for example, coupling agents can be used to establish chemical bonding between fibres and matrix due to their chemical composition [27]. In Ref [55], it is suggested that the properties and type of the coupling agents have to be optimised for different fibre and matrix materials. Other researchers [47] have shown from numerical modelling that the interphase region has a significant effect on the local interfacial thermal residual stresses and transverse failure stress and strain. Their work has demonstrated that increasing the interphase region to more than 10% of the fibre radius would reduce mechanical performance of the composites.

Based on the above discussion, the realistic approach for adequate transfer of load to the fibres would be an ideal adhesion level i.e. neither strong nor weak interfacial bonding. During the fracturing process, cracks are usually formed in the matrix; if the interfacial adhesion is strong then the crack propagation in the matrix would be expected to pass through the fibres by breaking them resulting in a lower fracture toughness. However, if the interfacial adhesion is weak, then cracks in the matrix would be arrested by the fibres, resulting in higher fracture toughness by absorbing more energy through debonding. This is explained by Cook *et al* [56] and is summarised as follows. The tensile stresses exist parallel to the running crack and they are one fifth of the normal stress concentration at the crack tip. The adhesion between fibre/matrix can be manipulated to improve the impact toughness of a composite material. In order to arrest these crack, if weak interface introduce in the path of crack then debonding must occur and the crack will be arrested at fibre matrix interphase region.

## 2.4 PRE-STRESSED COMPOSITES

In many aspects of engineering materials, concrete is the simplest form of reinforced material. The tensile and compressive strength of concrete is about 4 MPa and 30 MPa respectively [30], because of the good compressive strength, it is mainly used for applications where compressive loads exist. However, most engineering structures are subjected to both tensile and compressive forces. In order to improve tensile strength, this can be achieved by using steel rod to reinforce the concrete matrix. Also, further enhancement can be achieved by intentionally introducing compressive stresses in reinforced concrete structures. This can be done by tensioning high strength reinforcing steel rods to induce pre-strain (within the steel elastic limit) during the manufacturing process. Once the concrete matrix solidifies, the pre-strain load can be released. These pre-tensioned steel rods tend to retract to their original length. However, the adhesion between steel rod and concrete prevents these pre-strained rods to recover to their original length and as a result, the concrete is in a state of compression [57]. This produces pre-stressed reinforced concrete. The development of the pre-stressing concept was introduced for structural materials to enhance their mechanical performance (strength and stiffness). The application of pre-stressing for a concrete structural material is a well-known concept, whilst the potential benefits for fibre reinforced pre-stressed composites seems to be comparatively recent. However, other researchers have demonstrated the benefit of pre-stressing by using carbon [58-60] and aramid [59] fibres in concrete structures.

Similar to reinforced concrete materials, polymer matrix materials tend to be more resistant to compressive loads than tensile loads. Therefore, reinforcement can be used to improve both compression and tensile properties by adding stronger and stiffer fibres. The most common fibre reinforced materials are glass, carbon, aramid and polyethylene [30]. Pre-stressed concrete manufacturing principles may be applied to the composite by applying tension to the fibres as the matrix material cures resulting in elastically pre-stressed polymer matrix composites (EPPMCs). Zhigun [3] and Tuttle [5] were amongst the earliest investigators to evaluate this elastic pre-stressing principle. Fancey [7, 8] is the only researcher who has investigated viscoelastic behaviour of polymeric fibres and

successfully demonstrated their benefits in the form of viscoelastically pre-stressed polymer matrix composites (VPPMCs).

Pre-stressed composites can be produced by applying load to the fibres and then these stretched fibres are embedded into a liquid resin. On solidification of the resin, these fibres are bonded to the matrix in their tension state. As these stretched fibres are locked in a solid matrix, they cannot return to their free state. Therefore, the cured matrix maintains fibre tension, which imparts compressive stresses to the surrounding matrix. The principles and benefits of pre-stressing are schematically illustrated in Figures 2-2 and 2-3. An overview of pre-stressed composites from the literature is presented in chronological order in Table 2-1(Section 2.8).

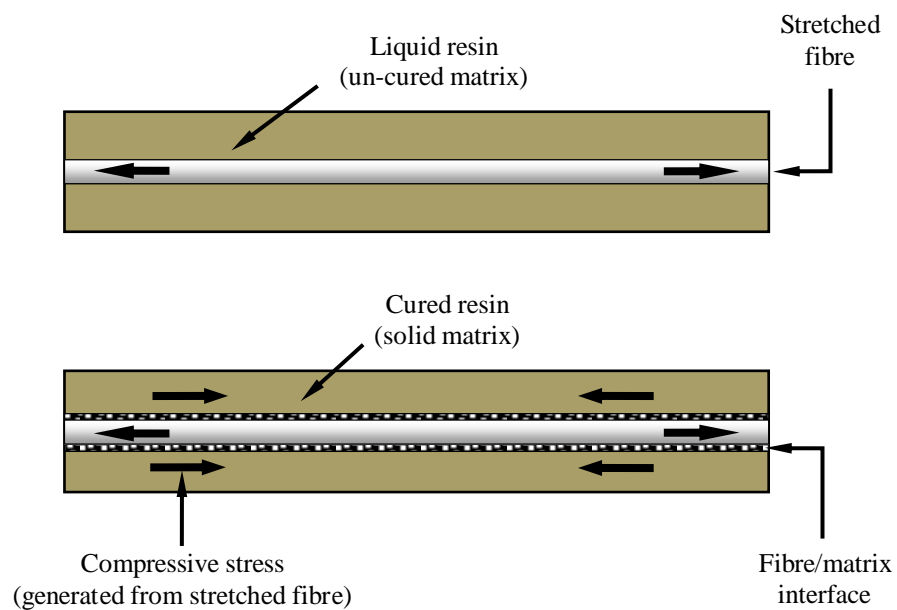


**Figure 2-2. Schematic illustration of pre-stressed composites.**

Referring to Figure 2-3(a), if a mid-span load is applied to a freely supported non pre-stressed beam, then the half cross-section of the beam (above neutral axis) would be subjected to a compressive stresses while the other half (below neutral axis) would be subjected to tensile stresses. This causes high deflection at the loading point (mid-

point). Many researchers have investigated the effects of compressive stresses in the composite material, which can be intentionally introduced from fibre pre-stressing methods. As a result, the pre-stress would be expected to enhance material properties such as tensile strength and stiffness [12, 61-66], impact toughness [8, 10, 67-69] and flexural stiffness [3, 13, 65, 70, 71]. As illustrated in Figure 2-3(b), deflection of the pre-stressed beam is reduced by neutralising (shifting) the load distribution. This effect has been previously proposed in Refs [13, 70, 72], in which authors suggested that residual compressive stresses within the matrix reduces the tensile stress magnitude from bending. This reduction in tensile stress has been previously suggested in Ref [70], for increasing flexural strength. Moreover, it is further explained in Ref [13], in which authors suggested that the neutral axis in a pre-stressed composite will be moved closer to the lower surface, as a greater proportion of the matrix remains in residual compression. This compression will reduce the magnitude of tensile forces below the neutral axis, thereby increasing flexural stiffness [13]. In addition, the modulus of the polymer is known to be increased when compressed (due to lower molecular mobility) [73], thus overall flexural stiffness may be increased.

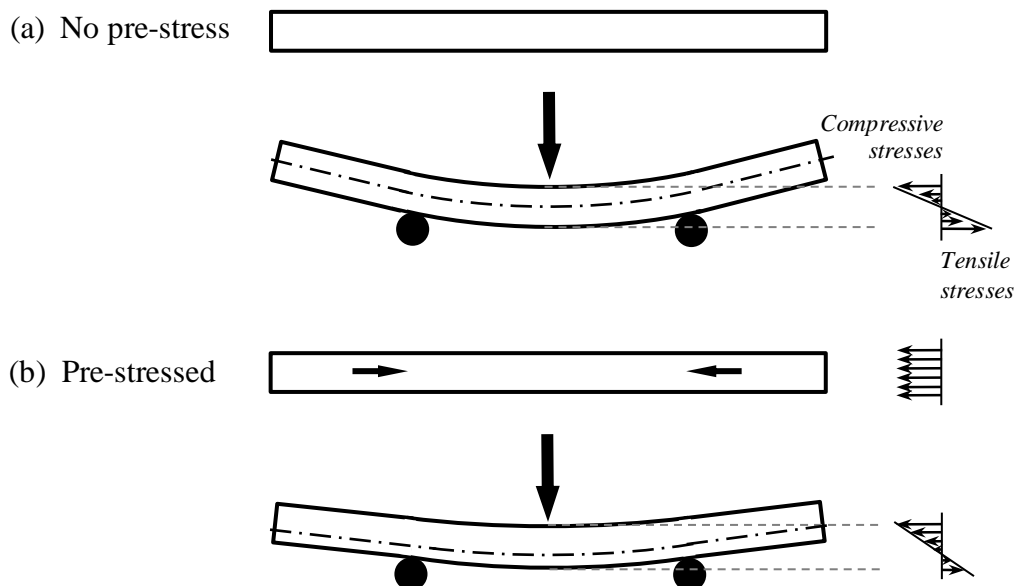


**Figure 2-3. Schematic representation of a freely supported beam subjected to a bending load. Arrows in the beam indicate compressive stresses generated from pre-stressing. Note, bending stiffness of beam (b) is exaggerated for clarity.**

In addition to increased flexural stiffness, pre-stress can improve flexural strength. For example, when a non-pre-stressed sample is subjected to a bending force, the outer layer of the sample is subjected to the greatest tensile stresses. Once these stresses from the applied load gain enough energy to initiate cracks, then failure occurs in the tensile region of the sample. However, for a pre-stressed sample, the formation of compressive residual stresses in the matrix provides more resistance to crack propagation, resulting in higher flexural strength. The presence of these compressive stresses in the matrix reduces tensile stresses generated by the bending force; thereby more bending force is required to propagate cracks.

It is well known that residual stresses exist in conventional fibre reinforced composites. These can be formed (i) as a result of chemical shrinkage of the matrix during curing cycle (ii) the differences in coefficient of thermal expansion between the constituents of the composite material i.e. fibre and matrix. In the literature, many researchers have reported the presence of residual stresses (in a composite material), and explained their benefits and disadvantages [74-79]. In terms of benefits, residual stresses can be introduced from pre-stressing to enhance composite material properties. This can be achieved by the attempted relaxation (recovery strain) of pre-strained fibres, while constrained by the matrix. These pre-stressed composites have been demonstrated by many researchers to show fibre pre-stressing can reduce manufacturing-induced residual stresses in composite materials [5, 13, 55, 80, 81].

The earliest approach to fibre pre-stressing for the improvement of flexural properties was conducted by Zhigun in 1968 [3] and the 'previously stressed fibre' term was introduced by Manders and Chou in 1983 [4], in which they provided a theoretical analysis for the enhancement of composite materials in terms of strength by using previously stressed fibres before embedding them into the resin. This was on the basis that failure of fibres in a composite causes a stress wave to propagate which subjects the neighbouring fibres to a dynamic overstress. These dynamic stress concentrations are generally greater than static stress concentrations, which increases the probability of adjacent fibres to fail [4]. Their analysis indicates that any weak fibres may be pre-

fractured by applying a load prior moulding to reduce the risk of dynamic overstress problems. Manders and Chou [4] have also discussed strength enhancement in terms of pre-stress level, fibre variability and stress concentration. The ‘previously stressed fibre’ approach was first introduced in the form of viscoelastically pre-stressed fibre composites by Fancey in 2000 [8], in which the load was applied to polymeric fibres prior to moulding. On the release of the load these strained fibres were embedded into a resin to impose compressive stresses in the matrix, which consequently enhanced the mechanical properties of the composite material. Manders and Chou [4] used a ‘previously stressed fibre’ approach to fracture weak fibres before moulding, whereas Fancey [8] adopted ‘previously strained fibres’ to exploit viscoelastic recovery to produce a pre-stressed composite.

Krishnamurthy [55] suggested fibre pre-stressing is the only possible method which can counteract both process-induced residual stresses and fibre waviness. He also suggested the compressive stresses would impede crack propagation in the matrix resulting in delaying/preventing the formation of matrix cracks in the composite material. Dvorak and Alexander [80] also demonstrated similar effects i.e. minimising residual stresses in the matrix, this could improve the strength of the composite. They also suggested that the fibre pre-stressing could minimise fibre waviness as the fibres are subjected to pre-stress during the curing process, which results in minimising fibre movement and improves the strength of composite material. In Ref [80], the authors suggested that the impact, flexural and low stress level fatigue properties could be also improved by pre-stressing.

## **2.5 TYPES OF PRE-STRESSED COMPOSITES**

To date, pre-stressed composites are produced by (i) by the conventional method i.e. elastically pre-stressed polymer matrix composites (EPPMCs) in which stretching in the fibres is achieved within their elastic limit and the load is maintained throughout the curing cycle and (ii) a novel approach in which polymeric fibres are used for pre-stressing to produce viscoelastically pre-stressed polymer matrix composites (VPPMCs), in which the load is applied but released prior to moulding.

Although, this study focuses on viscoelastically pre-stressed polymer matrix composites, for comparison, both pre-stressed composites (EPPMCs and VPPMCs) are discussed in detail below.

### **2.5.1 ELASTICALLY PRE-STRESSED POLYMER MATRIX COMPOSITES**

Studies with elastically pre-stressed unidirectional fibre composites have been demonstrated within the last 15 years. In the manufacturing process, predefined loads are applied to the fibres prior to matrix curing and the loads are maintained throughout the curing cycle. Once the matrix is cured and the composite cooled down to room temperature the loads are removed. The elastic contraction of strained fibres on removal of the loads induces compressive stresses in the matrix regions of the composite. Many researchers have demonstrated improvements in mechanical properties from (conventional) elastic pre-stressing methods [5, 55, 60-63, 65, 68, 70, 81, 82].

Schulte and Marissen [62] investigated the effect of fibre pre-stress on hybrid Kevlar and carbon/epoxy cross-ply composites under tensile loads. Their study has shown that pre-stressing improves tensile strength of the composites and also minimises transverse matrix cracking. A study by Hadi and Ashton [66] on their fibre pre-stressed composites shows improvements in tensile strength of 25% and elastic modulus of 50%. For beam-

shaped geometries, Motahhari and Cameron investigated flexural strength/modulus [70] and impact strength [68] of pre-stressed glass fibre reinforced composites, in which an improvement of up to 33% from pre-stressing was reported. In Refs [66, 68, 70], studies on pre-stressed composites are of particular interest in terms of suggesting proposed mechanisms responsible for the performance enhancement in composite materials. Their explanations for the improvement in pre-stressed composites are based on the matrix compressive stresses divert and impeding crack propagation and reducing composite strain resulting from external loads. The improvements in pre-stressed composite material properties based on the above proposed mechanisms are summarised in detail below.

Pre-stressed fibres create compressive stresses in the matrix and consequently this provides more resistance to crack initiation and propagation. Therefore, in a pre-stressed composite, more loads would be required to initiate cracks and more energy would be expected to be consumed in crack propagation. Investigation into different pre-stressing levels on glass fibre/epoxy composites were performed in Ref [68]. Their study on impact performance has shown that increasing the level of pre-stressing promotes fibre/matrix debonding and this is more dominant than transverse fracture. For low level fibre pre-stressing, however, transverse fracture becomes more dominant over fibre/matrix debonding [68]. The effect of debonding results in the formation of a new large surface area between fibres and matrix which absorbs more energy in comparison with non pre-stress and low level pre-stressed composites. To simulate the actual impact by a foreign object, many test procedures have been suggested by other researchers. Nevertheless, damage in pre-stressed composite follow mechanisms which were discussed previously in Section 2.3: these are fibre/matrix deformation, fibre tensile failure and debonding/delamination.

If a composite is subjected to an impact load, kinetic energy of a projectile is an important parameter but several other factors also affect the response of the material. For example, a large mass with low velocity may cause global damage and high energy absorption than a lower mass projectile with high velocity. Experimental studies on

impact performance of elastically pre-stressed composites (glass fibre/epoxy) laminates investigated by Jevons [67] have shown that the effect of pre-stressing is more pronounced at high mass low velocity impact than for low mass high velocity impact. The reason for the different behaviour is provided in Ref [67] and summarised here. For a low velocity high mass projectile, the impacting bodies remain in contact during penetration. This means, impact loading contact is long enough for the stress wave to propagate globally in the composite sample, which in turn causes damage by means of the maximum allowable strain in the fibre direction. This results in more energy absorbed in the form of delamination. For a high velocity low mass projectile, there would be less time to transfer all of its energy to the composite sample because the impact event would be very short. Therefore the contact ceases before the stress wave reaches the sample boundaries resulting in the deforming only locally (crushed) at the impact region [27]. Jevons study on EPPMCs (glass fibre/epoxy) has shown the high local shear stresses from high velocity impact override pre-stressing benefits. Therefore, no noticeable changes in delamination area or energy absorption are observed as a result of pre-stress [67].

In Refs [68, 70] studies on pre-stressed composites have shown that the improvement in impact and flexural strength continues up to a certain level i.e. there is an optimum level in which maximum benefits from pre-stressing can be achieved; beyond this, increasing the pre-stressing level shows a reduction in the material performance. Zhao and Camron [65] have also observed a similar phenomenon of an optimum pre-stress level in their studies on pre-stressed glass fibre/polypropylene matrix composites. They have shown pre-stressing improves tensile strength and modulus up to an optimum pre-stress level (85 MPa); above this limit the material performance declined. In Ref [55], similar findings in the reduction of tensile strength were observed in which an optimum pre-stressing level of 108 MPa was obtained.

From the above review, it can be concluded that an optimum level of pre-stressing exists and it plays an important role in the performance of pre-stressed composites. Similarly, an optimum level of fibre volume fraction also plays a major role in the

properties of reinforced composites. For example, as suggested in Ref [12], in a pre-stressed fibre reinforced composite, an optimum spacing between adjacent fibres must be maintained to achieve the maximum benefit. In terms of pre-stressed composites, too few fibres will result in less compressive stress within the matrix; conversely, too many fibres will reduce the cross-sectional area over which the compressive stress can function [12]. Therefore, high level pre-stressing and  $V_f$  would be expected to impart more compressive stresses to the surrounding matrix; as a result matrix capacity may not be enough to accommodate such large compressive stresses, which therefore results in reducing the benefits of pre-stressing.

Dvorak and Suvorov [80] predicted the effects of fibre pre-stressing on symmetrical glass fibre/epoxy laminates. Their analysis has shown that fibre pre-stressing increases the resistance to first ply failure by reducing the tensile residual stresses in the matrix. They have also suggested that the pre-tensioning applied in the fibre could minimise fibre waviness in a composite material. Similar studies on symmetrical laminates were conducted by Daynes *et al* [83] to create morphing structures based on bi-stable pre-stressed buckled laminates. They produced  $(0^\circ/90^\circ/90^\circ/0^\circ)$  pre-stressed carbon and glass fibre laminates, in which the load was applied to both fibres in the outer layer of zero degree plies and maintained during the curing process. On releasing the load, residual stresses generated from fibre pre-stress enabled the laminates to buckle in the centre regions. This buckling process caused the laminates to become bi-stable in that the state of buckling could be “flipped” into either one of two states.

### **2.5.1.1 DISADVANTAGES OF ELASTICALLY PRE-STRESSED COMPOSITES**

Clearly, the elastic pre-stressing method offers opportunities for improving the mechanical properties of fibre reinforced polymer composites. There are however potential drawbacks, which are highlighted in Fancey’s previous studies on viscoelastically pre-stressed composites [9] and are summarised here. The main drawbacks in elastically pre-stressed composites are the fibres have to be in a state of

tension during the curing process. This means the applied load must be maintained during the curing cycle. Therefore, this imposes restrictions on fibre orientation and product geometry. Secondly, the polymeric matrix material may undergo creep in an attempt to counteract the compressive stresses. In particular, localised matrix creep effects near the fibre-matrix interface would be expected to cause the pre-stress effect to deteriorate with time. To date, there appears to be no publications on possible changes in the long-term behaviour of elastically pre-stressed composites. Some of the disadvantages related to the production of EPPMCs are summarised in detail below.

Motahhari's [84] studies on glass and carbon fibre/epoxy pre-stressed composites reported the difficulties involved to maintain fibres in tension during the curing process. To overcome this problem, he designed a special oven, in which both ends were open to provide space for stretching facilities. However, this created another problem of not achieving a uniform temperature during the curing process. Therefore, the middle section of the pre-stressed composite sample was selected for testing; this was achieved by cutting both ends of the sample. During the curing process, temperature plays an important role in composite curing and resulting mechanical properties; producing a pre-stressed composite with a non-uniform temperature during curing is questionable.

Krishnamurthy [55] produced glass fibre/epoxy pre-stressed composite laminates, in which a dead load was applied during the curing process to the glass fibres by tightening screws (bolts). He observed during microscopic examination of the resulting composite samples that some fibres breakage occurred from pre-stressing. His explanation for this cause was that the weak fibres failed from the applied load; as a result, strong (un-broken) fibres withstood the pre-stressing load and produced the compressive stresses in the composite. However, no further details are given, such as the percentage of fibre breakage in these samples.

## 2.5.2 VISCOELASTICALLY PRE-STRESSED POLYMER MATRIX COMPOSITES

This section covers the development of viscoelastically pre-stressed polymer composites (VPPMCs) based on an alternative pre-stressing principle developed at Hull University by Fancey and patented in 1997 [6]. This method prevents the potential drawbacks highlighted for elastically pre-stressed composites in the previous section. The principle involves the use of polymeric fibres to impart compressive stresses through viscoelastic recovery. The polymeric fibres are stretched under a load for a period of time to induce creep. On removal of the load, these polymeric fibres initially undergo elastic recovery, but a proportion of the total fibre deformation is viscoelastic. This remains in the strained fibres, giving further time-dependent recovery. These strained fibres are embedded into a resin matrix. When the matrix is cured, compressive stresses are imparted by the viscoelastically strained fibres as they continue to attempt strain recovery against the surrounding solid matrix material. This viscoelastically generated compressive pre-stress improves the mechanical properties of the composite material. The processes involved in the production of VPPMCs are presented in Chapter-3 (Section 3.2).

The benefits of viscoelastic pre-stressing over elastic pre-stressing in composites are reported in Ref [12] and are summarised below.

- (i) Fibre stretching and moulding are two separate operations, enabling more flexibility in the production of composite material and facilitating complex component geometries. Also, the stretching process imposes no constraints on fibre length, distribution and orientation.
- (ii) The pre-stress effect would be expected to deteriorate gradually, due to localised matrix creep effects near the fibre matrix interface. However, this will be expected to be counteracted by active responses from the long term recovery mechanisms of the polymeric fibres.

Fancey's [7-9], earlier investigations were focussed on the fibre load-time conditions for suitable creep and recovery, evidence of viscoelastically induced pre-stress and its benefits to the mechanical properties. Direct evidence of viscoelastically induced pre-stress is shown in Figure 2-4 using photoelasticity principles. Here, nylon 6,6 monofilaments were moulded into an optically transparent resin and mounted on a Polariscope under cross-polarised monochromatic (sodium) light. The result shows clear evidence of residual stresses around the filament in the pre-stressed sample.

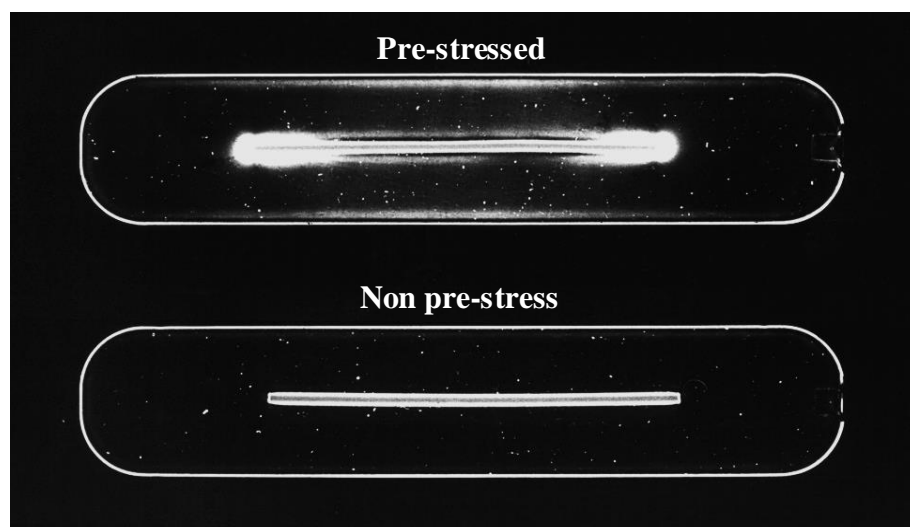


**Figure 2-4. Polarised image of nylon 6,6 monofilament moulded in 150×30×2 mm polyester resin. The stress pattern from viscoelastic recovery in the pre-stressed samples in contrast with non pre-stress. After [8].**

### 2.5.2.1 NYLON FIBRE-BASED VPPMC PERFORMANCE

The main findings of viscoelastically pre-stressed polymer matrix composites based on unidirectional nylon 6,6 fibres are summarised here. Compared with un-stressed (control) counterparts, Fancey's studies have shown increases in flexural modulus by ~50% from three point bend tests [13], also energy absorption enhancement from the low velocity impact improved by 30%, while some batches showed up to 50% increase in energy absorption [7-10].

In another study using tensile testing, these VPPMCs have demonstrated increases in tensile strength, modulus and strain-limited toughness of 15%, 30% and 40% respectively [12]. Here, batches of composite samples with  $V_f$  values of 16%, 28%, 41%, 53% were tested and the results in Ref [12] showed there was an optimum  $V_f$  value of ~35-40% at which the maximum benefits from pre-stressing could be achieved. The results are summarised in Figure 2-5 below. In Ref [12], the authors suggest this effect can be attributed to the competing roles between the fibres and matrix in the composite which are determined by their respective cross-sectional areas. For example, at lower  $V_f$  values, less compressive stress will be produced due to the fact that there are fewer fibres in the matrix; while, at higher  $V_f$ , too many fibres will reduce the matrix cross-sectional area available for compressive stresses generated from pre-stressing.

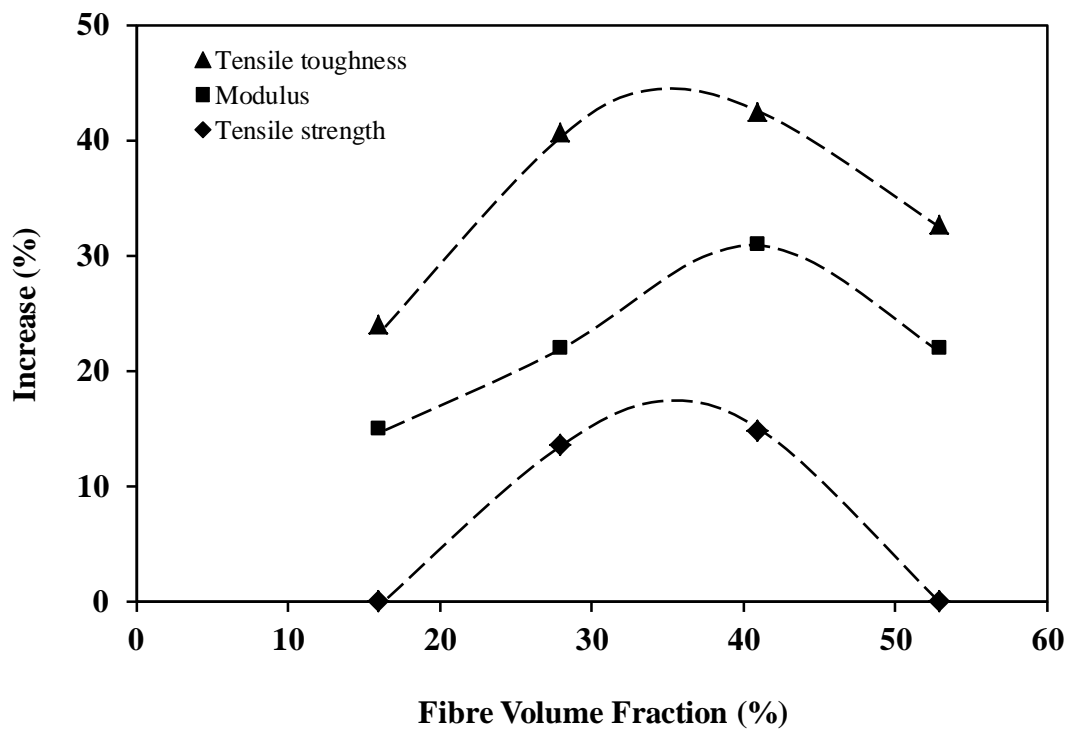


Figure 2-5. Effect of fibre volume fraction on the tensile properties of nylon 6,6 fibre-based viscoelastically pre-stressed composites. After [12].

Fancey's studies on accelerated ageing (time-temperature superposition) of nylon 6,6 fibre-based VPPMCs, have shown no deterioration in impact performance over a duration equivalent to 1000 years at a constant 20°C [10], the results are shown in Figure 2-6 below. However, it is important to note that viscoelastic activity increases with temperature, thus a higher temperature will reduce the life span; for example, 1000 years at 20°C reduces to 20 years at a constant temperature of 40°C [85]. Nevertheless, 20 years life span would still make VPPMC technology a realistic option for many practical applications. This suggests that viscoelastic activity and the benefits associated with compressive stresses in composites generated from pre-stressing will function over the long time periods. Recent unpublished data have indicated that these boundaries can be further increased so that the life span of nylon fibre-based VPPMCs is expected to last at least 25 years at a constant 50 °C [86].

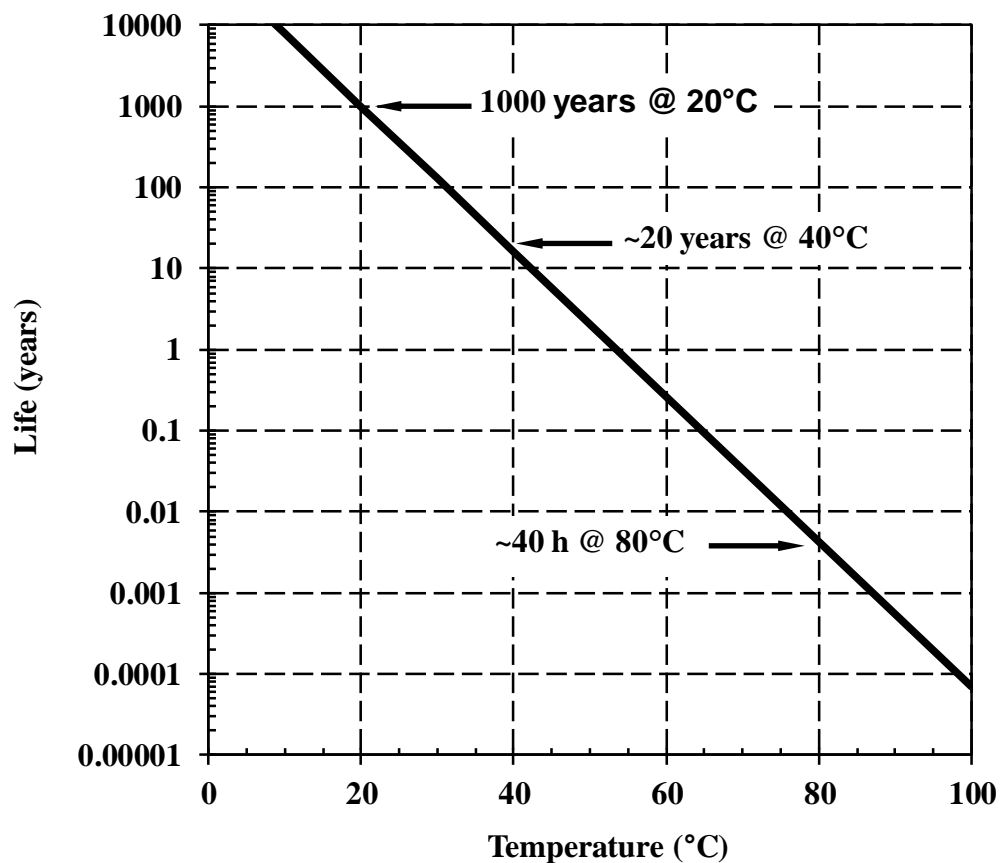


Figure 2-6. Nylon 6,6 fibre-based VPPMC life as a function of ambient temperature. After [10].

Similar investigation were also performed for the flexural properties of nylon fibre-based VPPMCs, in which the modulus values of test (pre-stressed) samples were higher than their corresponding control (un-stressed) counterparts [13]. These samples were aged up to 100 years at 20 °C by using the time temperature superposition principles; more details on time temperature superposition can be found in Refs [8-11].

### **2.5.2.2 VISCOELASTIC BEHAVIOUR OF POLYMERIC FIBRES**

In general, mechanical models are commonly used to present the polymeric deformation of materials, which can be Maxwell (spring and dashpot in series) or Voigt (spring and dashpot in parallel) [87]. Complex models can be generated to show overall behaviour of the material by adding more elements and these include Zener, which is a combination of Maxwell and Voigt models [85]. A well-known (simple) mechanical spring and dashpot model is presented in Figure 2-7, in which time dependent viscoelastic behaviour of the material is described by the spring and dashpot in parallel (Voigt element) [30, 88]. In Figure 2-7(a), the applied load initially increases strain by elastic strain from the spring and then further increases with time from the Voigt element and dashpot. The dashpot element provides resistance to the strain i.e. causing the strain to increase slowly. The time dependent recovery strain is shown in Figure 2-7 (b); it can be seen on removal of the load, the elastic strain disappears instantaneously, while the remaining viscoelastic strain (Voigt element) recovers slowly with time. The dashpot (for viscous flow) remains the same.

Although from a mechanical viewpoint, the model in Figure 2-7 explains the basic forms of polymeric deformation, it does not represent behaviour of most polymers accurately. For example, viscoelastic deformation in Figure 2-7 would occur smoothly, i.e. material undergoing creep, recovery or stress relaxation changes continuously with time, which may not necessarily be true for polymeric materials. In response to this, Fancey has followed an alternative approach, in which he has referred to a latch-based spring dashpot model to show the viscoelastic behaviour of polymeric materials [89, 90]. Further details on the latch-based model and the viscoelastic behaviour of nylon 6,6

can be found in Ref [90], which are incorporated with his experimental based findings from semi-crystalline nylon 6,6 fibre in Ref [89]. In his latch-based spring-dashpot model, changes in the material occur through incremental jumps, which represent the action of creep, recovery and stress relaxation on a molecular level; these jumps occur by the action of time-dependent latch elements [89, 90]. Although, this might be more relevant for the amorphous regions, the relative contribution of viscoelastic recovery forces from the crystalline regions of polymeric materials is unknown [91]. However, in Ref [92] jumping of line segments or kinks through the crystalline regions of nylon 6,6 fibres in response to the applied stress has been briefly discussed.

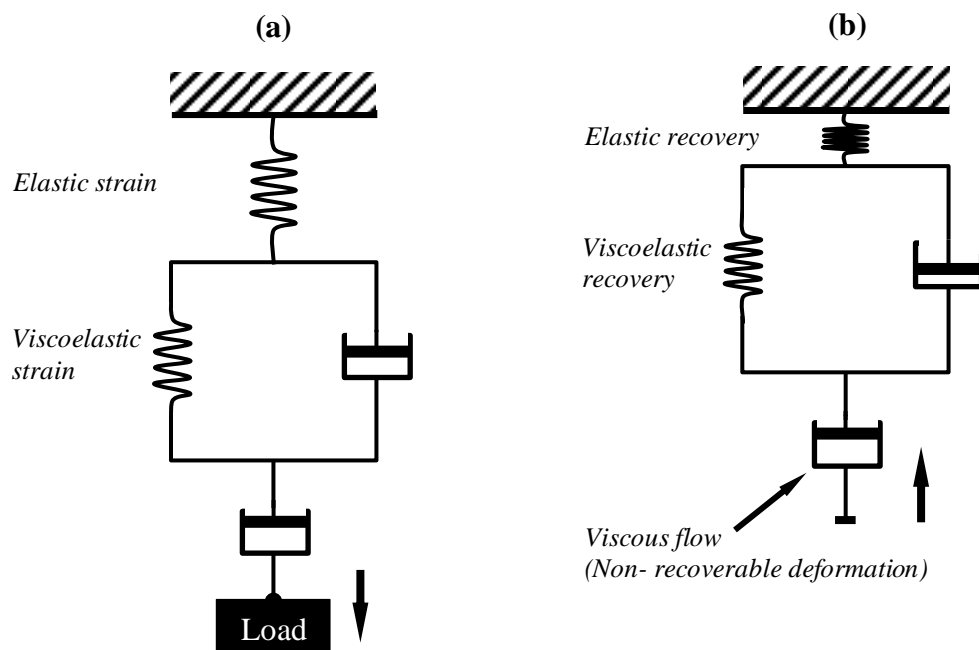


**Figure 2-7. Spring and dashpot model of creep and recovery strain from a polymeric material. (a) Creep strain from the applied constant load, (b) Recovery strain on the removal of load. Note, the spring represents elastic behaviour and the dashpot represents viscous behaviour of the material.**

In Ref [89], Fancey has suggested that recovery strain of viscoelastic materials such as polymeric fibres could be accurately represented by Equation 2-1, based on Weibull distribution function; in which the time dependent recovery strain  $\varepsilon_{rvis}(t)$ , as a function of time is given by:

$$\varepsilon_{rvis}(t) = \varepsilon_r \left[ \exp \left( - \left( \frac{t}{\eta_r} \right)^{\beta_r} \right) \right] + \varepsilon_f \quad (2-1)$$

Equation 2-1 is based on Weibull or Kohlrausch-Williams-Watts (KWW) relationship, in which polymeric deformation can be represented by a model consisting of time-dependent mechanical latch elements [89, 90]. In the above Equation, viscoelastic strain recovery is represented by  $\varepsilon_r$  function, which depends on the Weibull shape parameter  $\beta_r$  and characteristic life  $\eta_r$ . The permanent strain from viscous flow effects  $\varepsilon_f$  is the residual strain as time  $t$  approaches  $\infty$ . The Weibull function is used in reliability engineering to represent the time-dependent failure of elements in a population [93]. This is synonymous with polymeric deformation being represented by a population of time-dependent latches in Fancey's modelling [89, 90]. For stress relaxation, the Kohlrausch-Williams-Watts (KWW) function is considered to be the approximation to the Eyring relationship [94] which is supported by experimental evidence provided in Ref [90].

As stated in Section 2.5.1.1, localised matrix creep effects near the fibre/matrix interface in elastically pre-stressed composites would be expected to deteriorate with time. Whilst in contrast with viscoelastically pre-stressed composites, the long-term viscoelastic activity of polymeric fibres remains active for a long time, and this would be expected to respond to any changes occurring in the matrix [9]. Previous studies on nylon 6,6 fibre recovery strain [8, 9, 11] are presented in Figure 2-8. It is important to note that the annealed and non-annealed (as-received) fibres, after being subjected to identical creep conditions (342 MPa for 24 hours), have shown different behaviour. The recovery strain data for non-annealed fibres approaches zero within 1000 hours after releasing the creep

stress; whilst, the viscoelastic recovery rate of the annealed fibres is much slower. Therefore, recovery strain activity would be expected to last over a much longer time scale. Since, impact testing of samples subjected to accelerated ageing demonstrates that the viscoelastic recovery mechanisms remain active at least up to 1000 years at 20 °C [10] (shown in Figure 2-6), this also supports the extrapolated recovery strain curve in Figure 2-8 below.

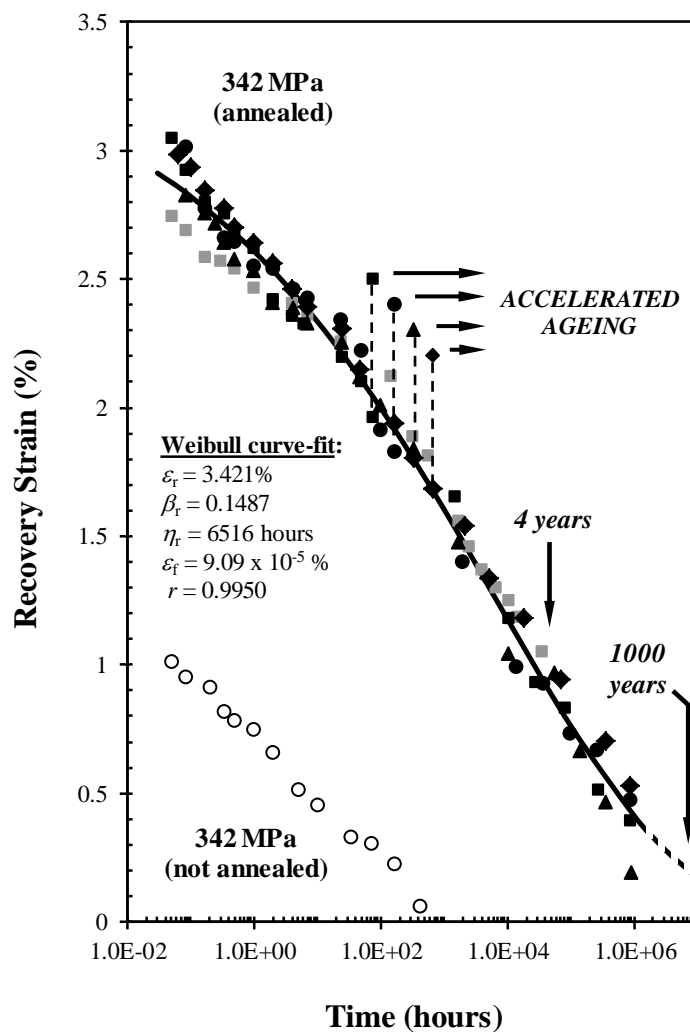


**Figure 2-8. Recovery strain data of nylon 6,6 fibre after 24 hours creep at 342 MPa. Grey data-points represent real time measurement up to 4 years and the black data points are from the samples (yarns) subjected to accelerated ageing up to an equivalent of 100 years. The solid line (curve) shows Equation.2-1, fitted to the black data points. After [10].**

## 2.6 MECHANICAL PROPERTIES ASSOCIATED WITH PRE-STRESSED COMPOSITES

To-date, research on EPPMCs and VPPMCs has demonstrated enhanced mechanical performance in terms of flexural, tensile and impact properties. These improvements were explained through mechanisms previously suggested by authors during their investigations based on EPPMC and VPPMC materials. In this study, these proposed mechanisms are reviewed and integrated, to provide a more coherent picture to show the benefits of pre-stressing in terms of enhancing material properties. These are shown in Figure 2-9, and summarised as follows.

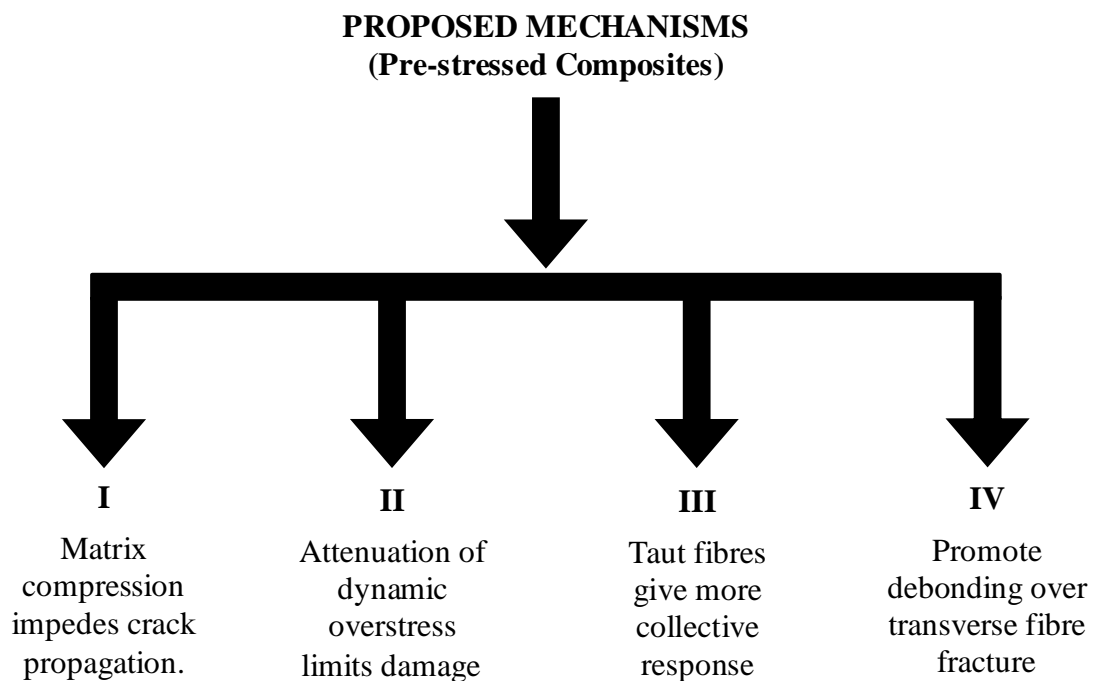


**Figure 2-9. Mechanisms proposed by various authors [4, 10, 12, 68, 70, 72], as being responsible for enhancing the mechanical properties of pre-stressed composites.**

### **2.6.1 MECHANISM-I: MATRIX COMPRESSION IMPEDES CRACK PROPAGATION FROM EXTERNAL TENSILE LOADS**

As described in previous sections, fibre pre-stressing imparts compressive stresses to the surrounding matrix. These compressive stresses impede crack propagation, thereby delaying and preventing the formation of cracks in a composite material, which results in improving mechanical properties. These effects have been observed by many researchers [8, 10, 12, 55, 68, 70, 84] and are summarised below.

An improvement of tensile strength in viscoelastically pre-stressed composites is demonstrated in Ref [12], and summarised here. A tensile load is needed to overcome compressive forces with the matrix. This compressive force from pre-stressing thereby impedes crack formation within the matrix and reduces fibre fractures. These effects are attributed to the proposed Mechanism-I.

Similarly, improvements in flexural stiffness is observed in both EPPMCs and nylon fibre-based VPPMCs, these improvements are attributed to deflection-dependent forces resisting the applied bending load [70] and collective response of the pre-stressed fibres [72]. Pang and Fancey [13] have proposed a further explanation for the improvement in flexural stiffness from pre-stressing, in which the compressive stresses from pre-stressing shifts the neutral axis of the beam sample, resulting in reduced tensile forces acting on the beam from the applied load. This is shown schematically in Figure 2-3 (Section 2.4). Also as the matrix would be in a compressive state, the matrix modulus may be greater [73], and this might also contribute to the improvement in bending stiffness. Based on the above, potential contributions from the proposed explanations for flexural stiffness improvement may originate from both Mechanisms-I and III. Finally, Fancey's study on nylon fibre-based VPPMCs has shown improvements in impact toughness, which is also partially attributed to Mechanism-I. Here, matrix compression impedes crack propagation in a pre-stressed composite, which increases the fracture energy required, resulting in enhancement of impact toughness [7, 8].

### **2.6.2 MECHANISM-II: MATRIX COMPRESSION ATTENUATES DYNAMIC OVERSTRESS EFFECTS, REDUCING THE PROBABILITY OF COLLECTIVE FIBRE FAILURE**

Mechanism-II was derived by considering the dynamic overstress effect described by Manders and Chou in 1983 [4], and was proposed by Pang and Fancey in 2008 [12], for their investigation on tensile behaviour of viscoelastically pre-stressed composites. Pang and Fancey explained that viscoelastic or elastic pre-stressing would be expected to attenuate dynamic overstress effects because compressive stresses in the matrix imparted by the pre-stressed fibres would be expected to reduce collective fibre failure [12]. Further details can be found in Refs [10, 12] and are summarised here. When a fibre fractures in a composite material from the applied load, a stress wave propagates outwards and subjects the neighbouring fibres to a dynamic (oscillatory) overstress. Therefore, the probability of failure amongst neighbouring fibres increases, thereby causing the composite material to be further weakened.

### **2.6.3 MECHANISM-III: RESIDUAL FIBRE TENSION CAUSES FIBRES TO RESPOND MORE COLLECTIVELY AND EFFECTIVELY TO EXTERNAL LOADS**

Mechanism-III originated from studies by Motahhari and Cameron, on elastically pre-stressed composites, in which they showed improvements in flexural modulus from pre-stressing. Their explanation for the improvement was based on the pre-stressed fibres being taut and straightened; therefore their response to applied loads can be expected to be instantaneous and should occur more collectively [70]. If these fibres deform as the load increases, then pre-stressed fibres in the composites would be expected to contribute more effectively so the occurrence of a subsequent fibre fracture will be less progressive. Fancey's studies on nylon fibre-based viscoelastically pre-stressed composites has suggested Mechanism-III in Refs [10, 12], in which the strain-to-failure

of pre-stressed composite samples was consistently 10-20% lower than their control (non pre-stress) counterparts. Here, the taut fibres with their faster and more collective response should increase tensile strength and also reduce composite displacement during fibre fracture.

#### **2.6.4 MECHANISM-IV: RESIDUAL SHEAR STRESSES AT THE FIBRE-MATRIX INTERFACE REGIONS PROMOTE (ENERGY ABSORBING) DEBONDING OVER TRANSVERSE FRACTURE.**

Mechanism-IV was originally proposed by Motahhari and Cameron in their impact studies on elastically pre-stressed composites [68], in which residual stresses generated from pre-stressing promote energy absorption through debonding in preference to transverse fracture. Similar effects have been reported by Fancey for his studies on nylon fibre-based viscoelastic pre-stressed composites [7, 8, 10], where improved impact toughness was observed in test (pre-stressed) samples, compared with control (non pre-stressed) counterparts. It is well known that the formation of a new surface requires expenditure of energy, as the surface area available for debonding is relatively larger than the cross-sectional area of the fibres; therefore, energy absorption would be expected to be higher in debonding compared with transverse fracture, thereby improving composite material toughness.

The above mechanism is schematically illustrated in Figure 2-10. Here, a composite sample is subjected to impact, at the event of crack propagation; two possibilities can be imagined (i) crack progressively fractures matrix and fibres (transverse fracture) and (ii) crack changes direction at the fibre matrix interface region and moves parallel in fibre direction (debonding). In general, it is well known that a crack will follow the easiest path to propagate. From Figure 2-10(a), it can be seen, in a non pre-stressed composite sample, the crack grows towards the fibres and fractures them. Therefore, breaking of fibres is the easiest path for the crack propagation, thereby resulting in lower energy absorption. However, in a pre-stressed composite (Figure 2-10b), longitudinal

debonding in the fibre direction is the easiest path and the main source of energy absorption with few fibre fractures at the tension side. This suggests the crack prefers to move parallel in the fibre direction instead of breaking through the fibres.

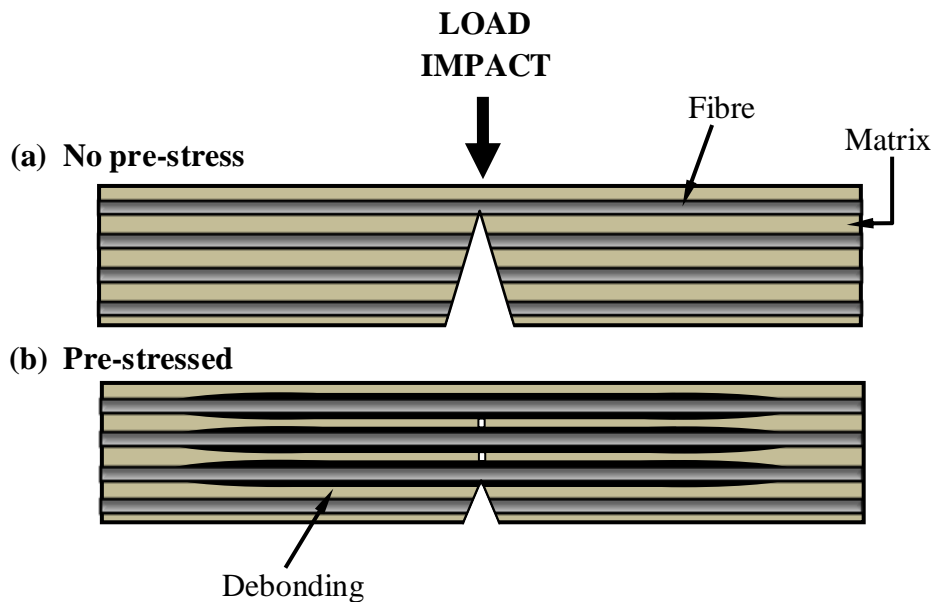


**Figure 2-10. Schematic illustration of the fracture behaviour of a pre-stressed and non pre-stressed composite material subjected to impact loading.**

The energy absorption in a fibre-reinforced composite subjected to an impact load is further summarised as follows, prior to a detail explanation:

- (a) Crack propagation in a non pre-stressed composite absorbing energy through transverse fracture e.g. matrix cracks and breakage of fibres; which results in lower energy absorption.
- (b) Crack propagation in a pre-stressed composite, absorbing energy mainly through debonding at fibre matrix interface region resulting in high energy absorption. Improvement in the absorption of energy is the sum of overall fracture mechanisms i.e. debonding, matrix cracking and fibre breakage at the highest stress region.

The general energy absorption (from debonding) in a pre-stressed composite can be attributed to the residual stresses at the fibre matrix interface. These residual stresses, generated from pre-stressing, make the interface region vulnerable to external impact loads. Therefore, at the event of impact, when a crack approaches an interface region, fibre-matrix separation occurs at a lower energy compared to the energy needed for breaking the fibres. This causes the crack to divert from its route and move along the interface regions, resulting fibre-matrix debonding.

Fancey's [7, 8, 10] investigations into nylon fibre-based viscoelastically pre-stressed composites showed increased fibre-matrix debonding with fewer fibre fractures in the test (pre-stressed) samples, compared with control (non pre-stressed) samples. Here, these effects are further explained; in which the shear stresses responsible for matrix compression from pre-stressing also reduce the forces required for initiating debonding. Therefore, in the pre-stressed composite samples, crack propagation through fibre-matrix debonding tends to be promoted over transverse fracture, and these effects are attributed to the proposed Mechanism-IV.

### **2.6.5 BENEFITS OF THE PRE-STRESSED COMPOSITES FROM THE PROPOSED MECHANISMS**

The proposed mechanisms believed to be responsible for the improvements in fibre pre-stressed composite materials are discussed in Ref [10] and are summarised here. Mechanisms-I and III would be expected to increase the energy absorption from fibre-matrix deformation, since external impact loads would need to work (i) against compressive stresses generated from pre-stressing and (ii) the collective response from the fibres. The dynamic overstress effect in Mechanism-II will reduce collective fibre failure. Therefore, the corresponding region of impact penetration damage to the fibres may be smaller. Pre-stressing promotes the formation of fibre-matrix debonding over transverse fracture resulting in increased energy absorption, which is associated with Mechanism-IV.

By considering these Mechanisms, pre-stressing may enhance the effectiveness of composite materials and increasing their usefulness for light-weight protection from impacts. Especially for VPPMCs, polymeric fibres (exploiting VPPMC mechanisms) commingled with other high strength fibre structures could be developed to maximise energy absorption with optimum post-structural integrity [10]. Moreover in VPPMCs, fibre parameters may be optimised for specific uses and may be exploited for applications requiring non-planar geometries, e.g. body armour protection such as helmets and footwear. Other applications could include ceramic/polymer composite materials, which employ a ceramic plate to spread the impact load over a relatively ductile composite (backing layer) used in armour vehicle for protection [95]. VPPMC technology may provide opportunities for enhancing the backing layer (load resistance) properties of the structures by the proposed Mechanisms.

## **2.7 FIBRE STRETCHING METHODS FOR PRE-STRESSED COMPOSITES**

The production of pre-stressed composites entails the need of a facility to induce pre-strain in the fibres (i.e. a stretching rig). In the literature, various methods have been developed by researchers for the production of pre-stressed composites. Pre-stressing in a composite is achieved by applying a load to the fibres during the curing process and is maintained until the resin solidifies. But this restricts fibre orientation and limits sample production to simple geometries. However, Fancey's method [7-10] for fibre stretching is quite unique from all other methods found in the literature. He applied a dead load (pre-strain) to nylon 6,6 fibre by using a vertically mounted stretching rig. Details of the stretching rig are not given in his publications; however, the preparation and production of composite samples can be found in Refs [7, 8, 10-13], in which pre-stressed composite sample procedures were completed in two steps: (i) a stretching load was applied to the nylon 6,6 fibres for 24 hours and, (ii) the load was released prior to moulding and the strained fibres were embedded in a polyester resin. These fibre exhibits viscoelastic properties, as elastic strain in the fibres would disappear on load

removal, while the viscoelastic strain would tend to recover with time (slow recovery). On the solidification of resin, the remaining viscoelastic strain in the fibres imparts compressive stresses to the matrix producing a viscoelastically pre-stressed composite.

As reported earlier, in elastically pre-stressed composites, the load has to be maintained during the curing process, so that fibre orientation and moulding geometries are restricted. The fibre stretching techniques for EPPMCs are briefly discussed below.

Jorge *et al* [61] produced elastically pre-stressed composites by using E-glass fibre/polyester resin in which fibres were stretched by applying a dead load up to 100N to the fibre ends with a flatbed stretching device; see Figure 2-11. They have claimed that the overall tensile strength and modulus of the pre-stressed composite are increased. By using this method, it may not be possible (in the author's opinion) to obtain a uniform fibre distribution in the composite and also bending of the (brittle) glass fibres by steel pins in the setup may cause fibre fracture.

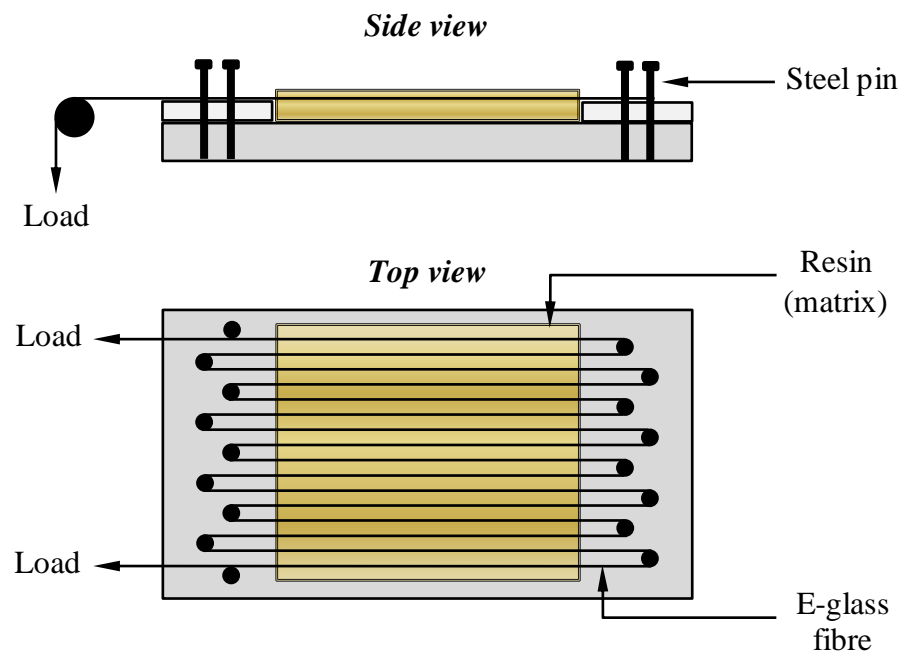


**Figure 2-11. Dead-weight pre-stressing method adopted by Jorge *et al* for composite plates. After [61] (re-drawn).**

Schulte and Marissen [62] performed an investigation into the effect of matrix cracking in elastically pre-stressed composites. They produced hybrid composite cross ply epoxy laminates ( $0^\circ/90^\circ/90^\circ/0^\circ$ ) with Kevlar and carbon fibre reinforcement. Composites with fibre pre-stress levels of 0 MPa (no pre-stress) and 341 MPa (1.1% pre-strain) were produced by using V-shaped grooves, as shown in Figure 2-12 below. Both ends of the outer plies i.e. Kevlar fibres ( $0^\circ$ ) were mechanically fastened with the V-shaped bar because the carbon fibres were more brittle and would be expected to be damaged by the V-shaped slot. In author's opinion, the main disadvantage of these type of setup for pre-stressing is that brittle types of fibre such as glass or carbon cannot be processed as kinking of the fibres in the V-slot can result in fibres fractures during the pre-stress process. Also, a further possibility of uneven load distribution through the laminate thickness can be expected, as the top plies would experience more pre-stressing load than lower plies.

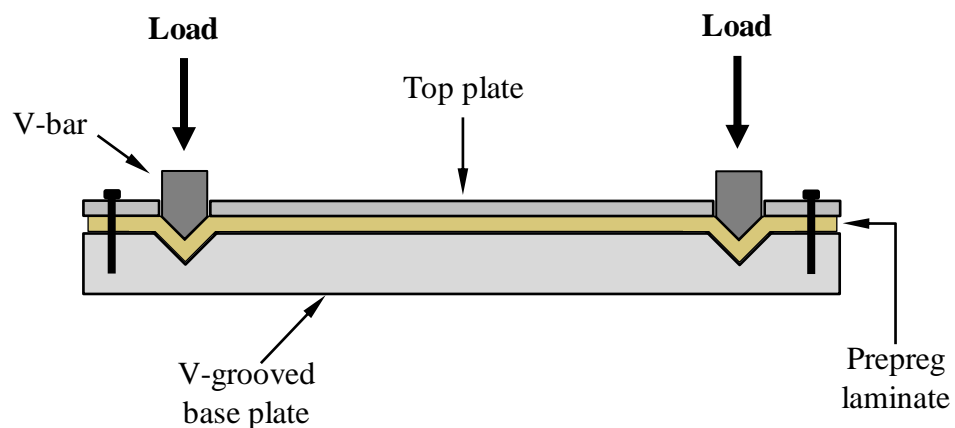


**Figure 2-12. Method used by Schulte and Marissen for pre-stressed prepreg laminates using V-groove pressure bars for pre-stressing. After [62] (re-drawn).**

Hadi and Ashton [66] have produced unidirectional pre-stressed composites by using a flat plate filament winding method. This method was also adopted by Rose and Whitney [96] for their carbon fibre/epoxy cross ply laminate pre-stressed composites. In this method, different pre-stress loads can be applied to the fibres for pre-stressing. In the

filament winding, continuous resin-impregnated fibres were laid onto a revolving mandrel to produce elastically pre-stressed composites. As shown in Figure 2-13 below, fibres are pulled with a known load, passed into a liquid resin bath, and then wrapped tightly over the mandrel and finally cured in an autoclave. This is a particularly suitable method for producing elastically pre-stressed composites on a high production scale. The main disadvantage of this filament winding method is to maintain and monitor the required pre-stress level during the curing process; this drawback was highlighted in Ref [55].

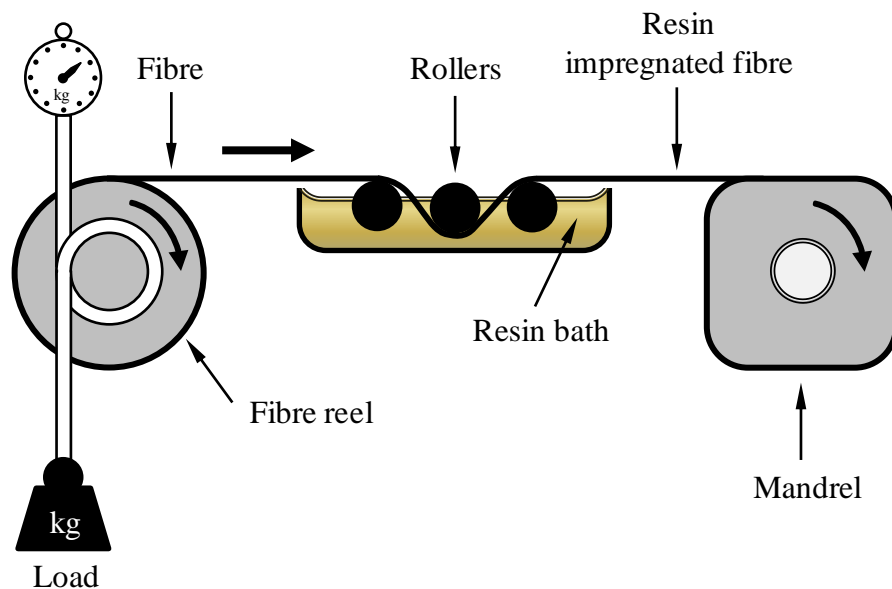


**Figure 2-13. Schematic diagram of the filament winding pre-stressing method. After [66] (re-drawn).**

Tuttle *et al* [64] employed a hydraulic cylinder to produce various pre-stressing levels to carbon fibre/epoxy laminates, as shown in Figure 2-14. Here, the prepreg plies were wrapped around the movable loading rod. Pre-tension to the laminates was applied and controlled by a hydraulic pump. The pressure gauge was used to maintain the appropriate level of pre-stressing. The frame was attached to a hot press for curing purposes. By using this method, elastically pre-stressed panels were produced with pre-

stress levels from 0 to 621 MPa. However, ply slippage was reported, which occurred at the higher pre-stress levels, though this was eliminated by using a modified loading rod. By using this method, tension to the laminates could be applied only in one direction and was limited to the hot-press method only.

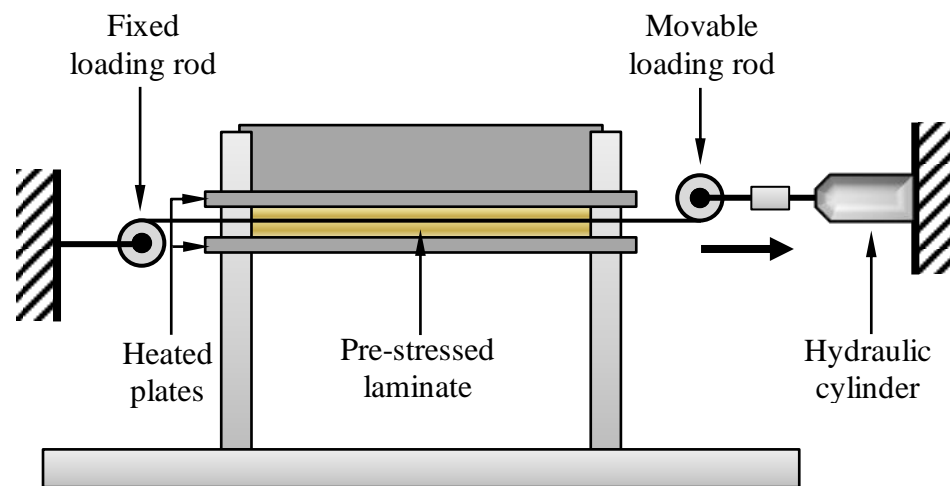


**Figure 2-14. Schematic illustration of the hydraulic cylinder pre-stress rig used by Tuttle *et al* for pre-stressed laminates. After [64] (re-drawn).**

Motahhari and Cameron [68, 81, 84] adopted a horizontal tensometer machine for producing their pre-stressed composites. Pre-tension in glass fibres was achieved by an electric motor to rotate a drum, which pulled a cable, place the fibres in a state of tension, as shown in Figure 2-15. The pre-stressed fibres were impregnated with an epoxy resin and oven cured, while a constant load was maintained on the fibres until the end of the curing process. This is the simplest form of pre-stressing, which enabled the pre-stress level to be measured from the load cell attached within the cable. However, the combined stretching and curing process presented challenges. It is reported in Ref [68] that a specially designed (open-ended) oven was used for the curing process, which allowed the fibres to pass through. However, this created another problem of not achieving a uniform temperature needed for curing. It is reported in Ref [84], that the

temperature dropped at both ends, thus only the middle sections of the samples were appropriately cured.

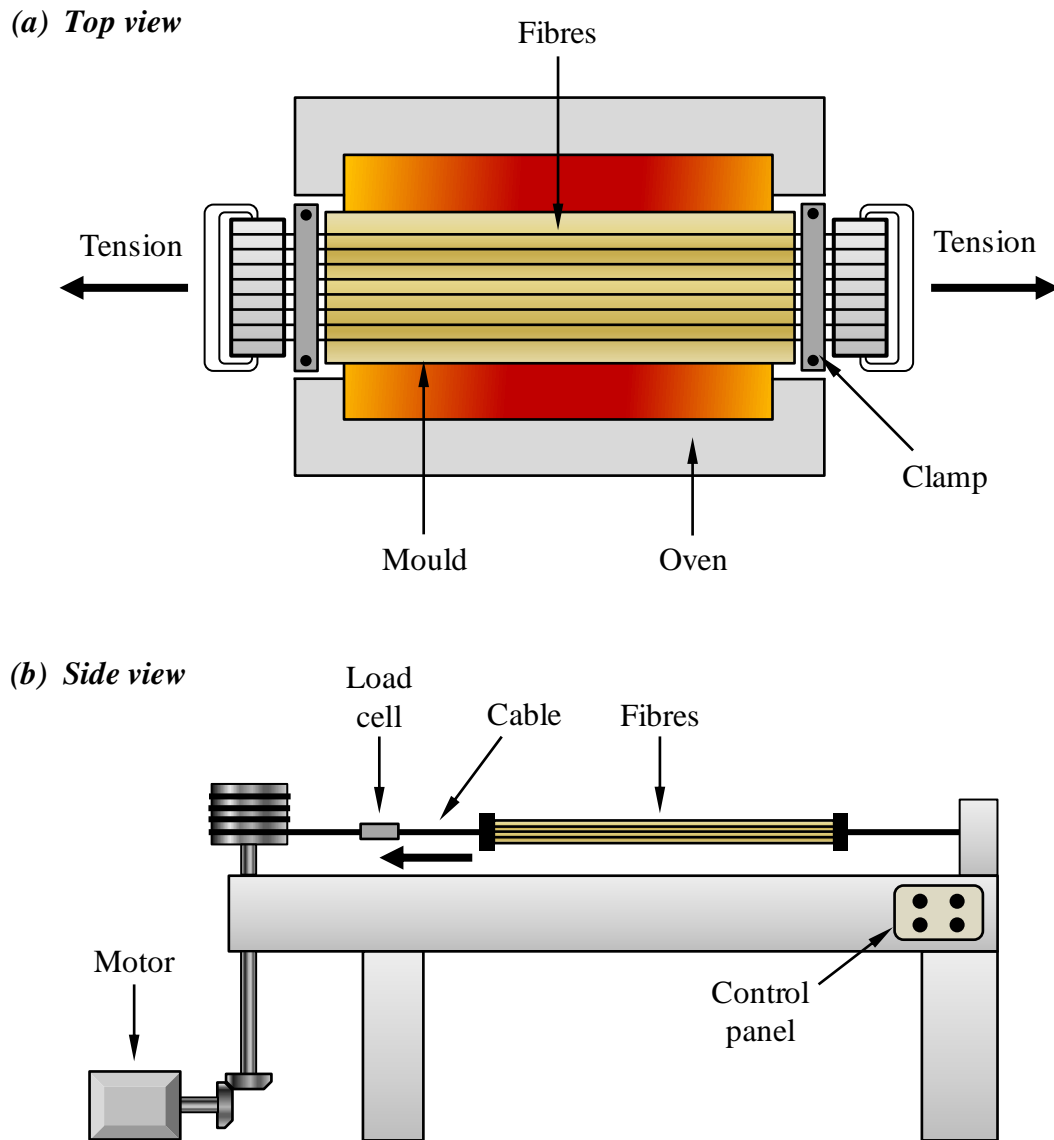


**Figure 2-15.** Stretching setup employed by Motahhari and Cameron for pre-stressed composites. (a) wound fibres around grips are transferred to the stretching rig (b) tensometer machine for pre-stressing. The fibres were kept in tension during the curing process. After [68, 81] (re-drawn).

Zhao and Cameron [65] produced glass fibre/polypropylene thermoplastic pre-stressed composites by using a fibre stretching frame attached to a tensile tester for pre-stressing, as shown in Figure 2-16 below. The hybrid yarns of matrix (polypropylene) and reinforcing filaments (glass fibres) were first wound onto the steel frame and then transferred to the tensile test machine to be stretched at the required level. As the fibres had to be stretched during curing process, the locking mechanism in the stretching frame held fibres in their desired place after releasing the load from the tensile tester. The stretched fibres on the frame were then placed between the upper and lower parts of a heated compression mould, in which the polypropylene fibres melted from the applied heat to form the matrix. From this, it can be seen that although the fixed load was initially applied to both glass and polypropylene fibres, the glass fibres would carry the total load after the polypropylene fibres had been melted. Therefore, the pre-stress level of glass fibres would expect to be higher due to the re-distributed extra load from the melted polypropylene fibres.

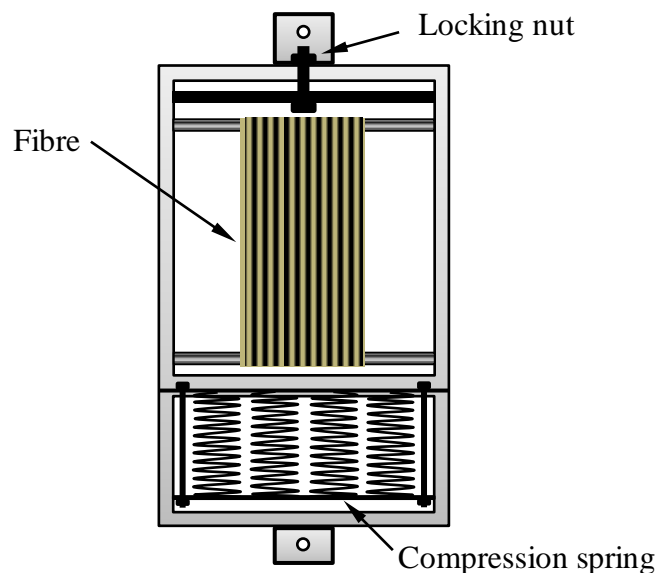


**Figure 2-16. Fibre stretching frame employed by Zhao and Cameron for a pre-stressed composite, in which fibres are wound onto the steel frame and then transferred to the tensile machine for pre-stressing. The fibres were kept in tension during the curing process. After [65] (re-drawn).**

Jevons [67] produced glass fibre/epoxy cross-ply laminates by using a biaxial loading frame. Pre-stressing was achieved in two stages. The first stage involved laying up cross-ply laminates and curing the ends of the prepreg with aluminium tabs; on completion of the curing process, holes were drilled in the end regions of the prepreg to be attached to the loading frame. For the second stage, pre-stress loads on the composite were applied by tightening locking bolts in the biaxial frame, as shown in Figure 2-17 below. After achieving the desired pre-stress level, the frame was processed in an autoclave. The loads were maintained during the curing process and released once the composite had cured.

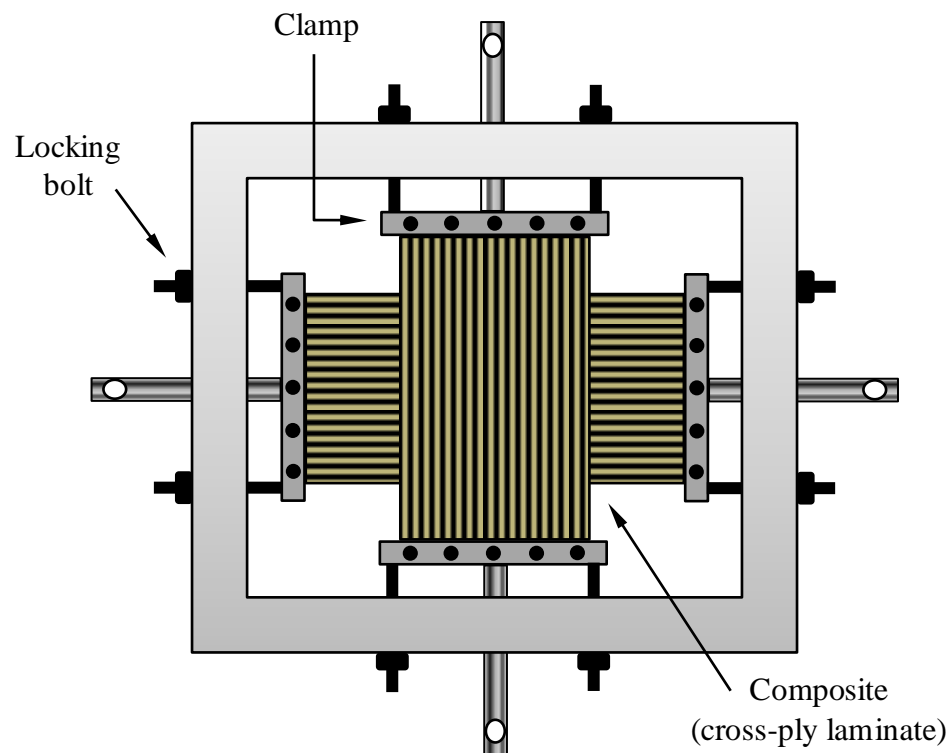


**Figure 2-17. Biaxial loading frame for pre-stressed laminates used by Jevons. The laminates were attached to the clamp and load was applied by tightening locking bolts. The fibres were kept in a state of tension during the curing process. After [67] (re-drawn).**

Similar to Jevons [67], a biaxial loading frame setup for pre-stressing has been used by Krishnamurthy and Daynes *et al* [55, 83] with minor modifications. They used a flat-bed pre-stress method for the production of glass and carbon fibre prepreg laminates. The ends of the prepreg were cured in order to clamp onto the pre-stress rig, as shown in Figure 2-18 below. In Ref [55], it is shown that a loading stress up to 100 MPa could be applied to the flat-bed stretching rig.

In Figure 2-18 below, two blocks were used in which one was fixed while the other was movable for applying the fibre pre-stress load. By tightening the load screw, the movable block moved in the tensile loading direction. Once the desired load was applied to the laminates, the block was locked in its tension state. In total, composite samples with four different levels of pre-stress (51, 80, 108 and 105 MPa) were produced and tested. The results were compared with an un-stressed (0 MPa) composite.

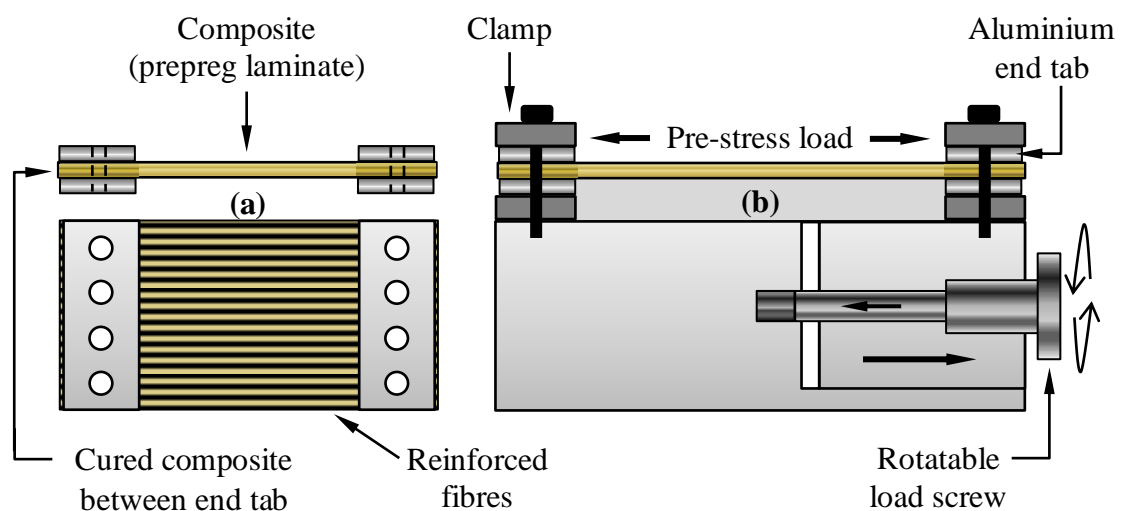


**Figure 2-18. Schematic diagram of the flat-bed rig used by Krishnamurthy for pre-stressed composites. Pre-fabrication prior to clamping the prepreg laminate onto the stretching rig is shown in (a), while the stretching rig is shown in (b) by which the load on the composite is applied by the rotatable screw and maintained until the resin sets. After [55] (re-drawn).**

As previously stated, Daynes *et al* [83] used a similar method for their studies on glass and carbon fibre bi-stable pre-stressed buckled laminates. In their studies, pre-strain on laminates was mechanically applied by using a load screw in which 0.15% pre-strain was achieved for CFRP and 0.40% for GFRP with curing temperatures of 180°C and 125°C respectively.

Disadvantages of using the flat-bed pre-stress method:

- (1) The difference in thickness between the hot-press cured prepreg ends and the autoclave-cured laminate, misalignment of fibre near at the end tab region and bending of the composite after removing the load are reported in Ref [55] and are shown in Figure 2-19.

Stretching fibres by using this method is a two-step process. The first step involves curing the prepreg laminate ends by applying high temperature and pressure to the end-tab region (hot-press cured). High pressure and temperature instigate fibre movement; subsequently as the resin near the end-tab region cures, this freezes the fibre misalignment near the end-tab region. Secondly, the prepreg laminate must be clamped to the rig and the load must be applied until the composite is cured. Once this load is released (after cooling to room temperature); the misaligned fibre in the previously cured end tab regions can result in composite bending (distortion).

There are many challenges associated with the flat-bed pre-stressing method. Many attempts for improving the flat-bed stretching rig design have been made to reduce fibre misalignment, but fibre must be protected by epoxy resin to reduce premature fibre failure [55, 83].

- (2) The desired pre-stress level may not be achievable by using the flat-bed pre-stressing technique. Here, the load is applied to the cured end-tab region instead of conventionally applying the load directly to the uncured laminate or

fibres. The misalignment fibres between the cured end tab region and uncured laminate is clearly visible in Figure 2-19 below. This indicates that the pre-stress level in the composite would be lower due to the greater cross-sectional thickness in the misaligned fibre region.

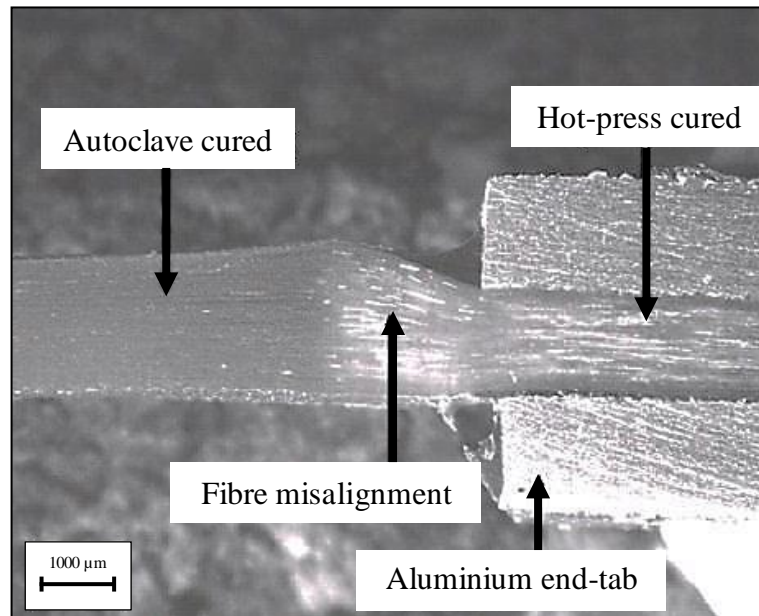


**Figure 2-19. Fibre misalignment near end-tab region by using flat-bed pre-stressing method. After [55].**

## 2.8 OVERVIEW ON PRE-STRESSED COMPOSITES

In Sections 2.4 to 2.7, the background to pre-stressed composites is discussed, which covers various aspects of pre-stressing methods, material behaviour and their performance. Many researchers have investigated the effects of compressive stresses in the composite material; these compressive stresses are intentionally introduced through fibre pre-stressing to enhance mechanical properties which have been evaluated by impact, tensile and bending tests. It can be seen in Section 2.7, researchers working in the field of pre-stressed composites has adopted a wide range of complex methods for creating elastically generated pre-stress. VPPMC technology provide a much simpler alternative and this approach was adopted by Fancey. Since this study investigates further development in the performance of viscoelastically pre-stressed composites, the research of Fancey and Pang is of direct relevance.

In the literature, the earliest approach to fibre pre-stressing (for the improvement of flexural properties) was performed by Zhigun in 1968 [3] and later by Manders and Chou in 1983 [4], investigated the enhancement of composite materials. Here, fibres were stretched to enable the weaker fibres to fracture (and be removed) prior to moulding into composite samples. Although, the resulting stronger fibres improved composite strength, however these composites were not in a state of pre-stress from this method. In 2000, Fancey [8] introduced ‘previously stressed fibre’ in the form of unidirectional viscoelastically pre-stressed composites. Here, the load was applied to polymeric fibres prior to moulding, and on releasing the load; these strained fibres were embedded into a resin to create pre-stressed composites from viscoelastically recovery mechanisms.

From the literature, an overview of pre-stressed composites is presented in chronological order in Table 2-1, to provide a coherent summary of the published work; this covers pre-stressing methods, material details, composite evaluation and the main findings.

**Table 2-1. Literature review on pre-stressed composites.**

Reference	Research area	Pre-stress method	Material	Main findings
1968 Zhigun [3]	Tension and compression test	Applied tension to the rods by tightening nuts	Woven glass fibre Phenol-formaldehyde resin Flat plate sheet	<ul style="list-style-type: none"> <li>Elastic characteristics of woven glass fibre composites were improved.</li> <li>Straightening warp fibres by pre-stressing increased overall stiffness.</li> </ul>
1988 Tuttle [5]	Mechanical/thermal analysis of pre-stressed composites laminates	Not specified	Carbon fibre Epoxy unidirectional composite 60% $V_f$	<ul style="list-style-type: none"> <li>Predicted 24 MPa tensile residual stresses in the matrix.</li> <li>Pre-stress reduced matrix residual stresses.</li> </ul>
1990 Jorge <i>et al</i> [61]	Tensile properties (EPPMC)	Dead weight (Flat plate)	E-glass fibre Epoxy unidirectional composite 56% $V_f$	<ul style="list-style-type: none"> <li>Tensile strength and modulus increased with pre-stressing, up to a certain pre-stress level.</li> </ul>
1992 Schulte and Marrison [62]	Tensile properties and transverse cracking (EPPMC)	V-slot mechanical fastening	Epoxy hybrid cross-ply laminate composite (0°/90°/90°/0°) Aramid fibre (0°) Carbon fibre (90°)	<ul style="list-style-type: none"> <li>Pre-stressing increased average fracture stress and strain by 2.8% and 3.3% respectively.</li> <li>341 MPa pre-stress increased the strain to transverse crack initiation by 0.2%.</li> </ul>
1993 Rose and Whitney [96]	Mathematical modelling and experimental measurement of ply failure (EPPMC)	Filament winding flat panel	Carbon fibre Epoxy cross-ply composite (0°/90°/90°/0°) 70 % $V_f$	<ul style="list-style-type: none"> <li>690 MPa pre-stressing increased the failure strength of first ply.</li> <li>Model did not correlate with the experimental results.</li> </ul>

**Table 2-1. Literature review on pre-stressed composites (continued).**

Reference	Research area	Pre-stress method	Material	Main findings
1995 Sui <i>et al</i> [63]	Tensile properties	Not specified	Vynylon (poly-vinyl alcohol) fibre Epoxy-aluminium laminate (VIRALL) Fibre: 32 % $V_f$ Aluminium: 56.5 % $V_f$	<ul style="list-style-type: none"> <li>• Pre-stressing increased initial modulus, elastic limit strain, yield strength and failure strength.</li> </ul>
1996 Tuttle <i>et al</i> [64]	Tensile properties and transverse cracking (EPPMC)	Hydraulic rig (Flat plate)	Carbon fibre Epoxy un-symmetrical cross ply composite 70 % $V_f$	<ul style="list-style-type: none"> <li>• Curvature of un-symmetrical laminates decreased by increasing the levels of fibre pre-stressing.</li> <li>• Transverse cracks were reduced by pre-stressing.</li> <li>• Composites showed no difference in ultimate tensile strength from pre-stressing.</li> </ul>
1997 Motahhari and Cameron [81]	Measurement of applied pre-stress and mathematical modelling of residual stress (EPPMC)	Horizontal tensile testing machine	E-glass fibre Epoxy unidirectional composite 62±2 % $V_f$	<ul style="list-style-type: none"> <li>• Pre-stressing reduced residual stresses in the matrix.</li> </ul>

**Table 2-1. Literature review on pre-stressed composites (continued).**

Reference	Research area	Pre-stress method	Material	Main findings
1998 Motahhari and Cameron [68]	Impact properties (EPPMC)	Horizontal tensile testing machine	E-glass fibre Epoxy unidirectional composite $62 \pm 2 \% V_f$	<ul style="list-style-type: none"> <li>• Increase in impact strength by 33% for 60 MPa pre-stressed composite. Above this level a reduction in impact strength was observed.</li> <li>• Pre-stressed composites showed more splitting and delamination compared to un-stressed samples.</li> </ul>
1998 Zhao and Cameron [65]	Tensile, flexural and interlaminar shear strength (EPPMC)	Fibre stretching frame (alignment rig)	Commingled E-glass fibre polypropylene unidirectional composite $34.2 \% V_f$	<ul style="list-style-type: none"> <li>• Fibre pre-stressing enhanced composite tensile strength, flexural strength and ILSS by 20%, 21% and 10% respectively.</li> <li>• Above an optimum pre-stress level, composite properties stabilised.</li> </ul>
1998 Hadi and Ashton [66]	Tensile properties in fibre direction (EPPMC)	Filament winding	E-glass fibre Epoxy unidirectional composite 30%, 45% and 60 % $V_f$	<ul style="list-style-type: none"> <li>• Pre-stressing improved tensile strength and modulus of the composite samples.</li> </ul>
1999 Motahhari and Cameron [70]	Flexural properties (EPPMC)	Horizontal tensile testing machine	E-glass fibre Epoxy unidirectional composite 60% $V_f$	<ul style="list-style-type: none"> <li>• Flexural strength and modulus increased by 33% by pre-stressing.</li> <li>• An optimum pre-stress level for improved flexural stiffness and strength.</li> </ul>

**Table 2-1. Literature review on pre-stressed composites (continued).**

Reference	Research area	Pre-stress method	Material	Main findings
2000 Fancey [8]	Impact properties (VPPMC)	Bespoke vertical stretching rig	Nylon 6,6 fibre Polyester unidirectional composite 2-3% $V_f$	<ul style="list-style-type: none"> <li>Compressive stresses induced into the matrix through the viscoelastic recovery mechanisms of nylon fibres.</li> <li>Pre-stressed samples absorbed 25% more impact energy than their control counterparts.</li> </ul>
(2000) Dvorak <i>et al</i> [80]	Mathematical modelling effect of the residual stresses on pre-stress.	Not specified	S-glass fibre Epoxy cross-ply and quasi-isotropic laminates 50 % $V_f$	<ul style="list-style-type: none"> <li>Model showed the fibre pre-stress reduced tensile residual stresses in the matrix and increased resistance to matrix damage.</li> </ul>
2002 Jevons <i>et al</i> [69]	Low velocity impact (EPPMC)	Biaxial loading frame	E-glass fibre Epoxy cross-ply laminates (0°/90° <sub>2</sub> /0° <sub>2</sub> /90°/0°/90°) 56% $V_f$	<ul style="list-style-type: none"> <li>Composite samples subjected to low velocity impact tests showed improvement in impact properties from pre-stressing.</li> </ul>

**Table 2-1. Literature review on pre-stressed composites (continued).**

Reference	Research area	Pre-stress method	Material	Main findings
2004 Jevons [67]	Low and high velocity impact performance, experimental and modelling (EPPMC)	Biaxial loading frame	E-glass fibre Epoxy cross-ply laminates (0°/90° <sub>2</sub> /0° <sub>2</sub> /90°/0°/90°) 56% $V_f$	<ul style="list-style-type: none"> <li>• In a low velocity impact, benefits of pre-stressing were observed in terms of energy absorption through delamination, while no such benefits were observed from high velocity impact tests.</li> <li>• FEA modelling on pre-stressed composite was not capable of taking pre-stressing into account, or for pre-stressing composite failure mechanisms. Thus, modelling did not correlate with the experimental data.</li> </ul>
2006 Krishnamurthy [55]	Tensile, compressive and fatigue properties, experimental and analytical model (EPPMC)	Flat-bed pre-stressing machine	Glass fibre Epoxy cross-ply laminates (0°/90°/0°/90°/90°/0°/90°/0°) 58% $V_f$	<ul style="list-style-type: none"> <li>• Composite properties improved through pre-stressing.</li> <li>• Maximum benefit from pre-stressing achieved at optimum level of pre-stressing.</li> </ul>
2008 Pang and Fancey [12]	Tensile properties (VPPMC)	Bespoke vertical stretching rig	Nylon 6,6 fibre Epoxy unidirectional composite 16, 28, 41 and 53% $V_f$	<ul style="list-style-type: none"> <li>• Tensile modulus and strength increased by 30% and 15% respectively.</li> <li>• Optimum values for <math>V_f</math> was 35 to 40%.</li> </ul>

**Table 2-1. Literature review on pre-stressed composites (continued).**

Reference	Research area	Pre-stress method	Material	Main findings
2008 Daynes <i>et al</i> [83]	Analytical and FEA modelling on bi-stable pre-stressed buckled laminates (EPPMC)	Flat-bed pre-stressing machine	Carbon and glass fibre Hexcel cross-ply laminates (0°/90°/90°/0°), Pre-strain applied on 0° fibres. 57% and 58% $V_f$	<ul style="list-style-type: none"> <li>Residual stresses generated from pre-stressing were used to produce bi-stable symmetric laminates i.e. buckling (two bi-stable bowing geometries).</li> </ul>
2009 Pang and Fancey [13]	Flexural properties (VPPMC)	Bespoke vertical stretching rig	Nylon 6,6 fibre Epoxy and polyester unidirectional composite 8%, 12% and 16% $V_f$	<ul style="list-style-type: none"> <li>Flexural modulus of viscoelastic pre-stressed composites increased by ~50% compared to non pre-stressed samples.</li> </ul>
2010 Schlichting <i>et al</i> [71]	Flexural properties (EPPMC)	Horizontal stretching rig	Glass fibre (unidirectional) Adoro and Quixfil 12% $V_f$	<ul style="list-style-type: none"> <li>Flexural strength improved by 28% (Adoro resin) and 33% (Quixfil resin).</li> </ul>
2012 Cui <i>et al</i> [14]	Flexural properties (VPPMC)	Not specified	Bamboo reinforced composite PSL (Parallel Strand Lumber)	<ul style="list-style-type: none"> <li>Flexural modulus of pre-stressed composites increased by ~27% compared to non pre-stressed samples.</li> </ul>
2014 Nishi <i>et al</i> [82]	Impact properties (EPPMC)	Dead weight	Carbon fibre (CFRP) Epoxy 50% $V_f$	<ul style="list-style-type: none"> <li>Compressive stresses to the matrix were imparted from 0° fibres through pre-stressing, which increased the strength of composite samples.</li> </ul>

# CHAPTER-3

## MATERIAL PREPARATION, GENERAL EXPERIMENTAL PROCEDURES AND EQUIPMENT FACILITIES

---

### SUMMARY

This Chapter presents a general overview on materials and equipment used in this study. The selection of reinforcing fibre and their comparison with other commercial fibres in terms of mechanical properties such as strength and stiffness is also discussed. This is followed by experimental methodology and processing for the production of composite samples.

A brief description on the procedure of fibre pre-stressing and preparation prior moulding is discussed. The production of composite samples and the equipment used for mechanical testing are described. Finally, details of the equipment used for investigation in this research is briefly discussed (e.g. microscopy).

For clarity, where appropriate, sections for experimental procedures are included in other chapters, where specific testing methods and sample preparation are relevant to those individual chapters.

### 3.1 REINFORCING MATERIALS

It is well known that fibres play an important role in the performance of composite materials. Fibres are the main load-bearing constituents, providing strength and stiffness to the composite material. The mechanical properties of a polymeric material such as tensile strength and modulus are strongly dependent on its micro-structure and crystallinity. In addition to investigating VPPMCs using nylon 6,6 fibre and also Kevlar fibre (for commingling), the viscoelastic behaviour of UHMWPE fibre is investigated in this study. Semi-crystalline polymers consist of crystalline and amorphous regions, in which the polymer chains are closely and randomly packed respectively [97]. In order to establish appropriate conditions for the processing of UHMWPE fibre based VPPMCs, the objective was to determine whether UHMWPE fibre would exhibit suitable viscoelastic properties. To address this issue, methods employed for pre-stressing is briefly discussed in this Chapter.

All fibres used in this study were continuous multi-filament untwisted yarns supplied by Goodfellow Cambridge Ltd, UK; their properties are shown in Table 3-1 and a short summary of these fibres is also provided. For comparison, the properties of other commercial high performance fibres such as glass and carbon are shown in Table 3-2.

**Table 3-1. Properties of the fibres (supplier specification) investigated and used in reinforced composite samples [16, 17, 98].**

<b>Fibre (filament in yarn)</b>	<b>Filament diameter (<math>\mu\text{m}</math>)</b>	<b>Density (<math>\text{g}\cdot\text{cm}^{-3}</math>)</b>	<b>Strain to failure (%)</b>	<b>Tensile strength (MPa)</b>	<b>Tensile modulus (GPa)</b>
<b>Nylon 6,6</b> (140 filaments)	27.5	1.14	14 - 22	82	3.3
<b>Kevlar 29</b> (120 filaments)	18	1.44	3.7	2760	58
<b>UHMWPE Dyneema SK60</b> (1600 filaments)	12	0.97	3.5	2560	87

It can be seen from Table 3-2 below that S-glass fibre exhibits high strength but lower modulus compared with carbon fibre; thus glass fibre cannot be stiffer than carbon fibre. Nevertheless, glass fibre can be a good candidate in a composite material where strength is the main criterion, but clearly less useful for applications where very high stiffness is required. In general, carbon fibres are characterised by high strength and stiffness. However, both parameters cannot be maximised simultaneously, and these effects are shown in Ref [30]. Here, by plotting the tensile strength and modulus of various carbon fibres, their results indicated that the high strength carbon fibres have the lower modulus while fibres with high stiffness have the lower tensile strength.

**Table 3-2. High performance fibres properties for comparison with polymeric fibres shown in Table 3-1.**

<b>Ref</b>	<b>Fibre</b>	<b>Density (g.cm<sup>-3</sup>)</b>	<b>Strain to Failure (%)</b>	<b>Tensile Strength (GPa)</b>	<b>Tensile Modulus (GPa)</b>
[99]	Carbon	1.86	0.8	2.5 - 2.7	350-370
[100, 101]	E-glass	2.55	3.0	1.7 - 2.4	70
[18, 100]	S-glass	2.50	5.4	3.5	85

### 3.1.1 NYLON FIBRE

The first nylon (or polyamide) material was developed in the 1930s and commercialisation was started in 1939 [102]. It is a very attractive material because of properties such as high strain-to-failure, low density and durability. However, the high polar nature of the amide groups favour absorption of moisture from the atmosphere; therefore, strict attention is required during processing [102]. Although, inferior in mechanical performance with respect to glass and carbon fibres, nylon is an attractive material in terms of balancing cost-advantages, remarkable high strain-to-failure properties, easy processing and handling. Thus nylon can be a convenient reinforcing

material for composites. The nylon chemical structure (as the mer) is shown in Figure 3-1(a), and it contains hydrogen, nitrogen, carbon and oxygen elements [30]. It may be noted that the low modulus (3.3 GPa) and tensile strength (82 MPa) given in Table 3.1 can be compared with the typical matrix materials such as polyester resins, i.e. 2.7 GPa modulus and ~ 47 MPa tensile strength [103].

### **3.1.2 KEVLAR FIBRE**

In 1965, Stephanie Kwolek and Herbert Blades at DuPont discovered a new method of producing polymer chain extensions [104]. Poly-p-benzamide (polymer) was found to form a liquid crystalline solution due to the simple receptiveness of its molecular backbone [104]. The key structural requirement for the backbone was the para orientation on the benzene ring, which allows the formation of rod like structures; the crystalline chains are interconnected by hydrogen bonds that make these fibres extremely strong (mer is shown in Figure 3-1b). This development led to the formation of poly-para-phenylene terephthalamide (PPTA). An aramid known as Kevlar, which is a registered trade name of DuPont [18, 104]. Kevlar is a highly crystalline synthetic fibre and it possesses a unique combination of high strength/modulus, toughness and thermal stability [18, 104]. These properties of Kevlar fibre made it as a good candidate for applications requiring high strength and toughness such as ballistic resistance. In comparison with glass and carbon fibres, the properties of Kevlar fibres are superior in terms of lower density, highest strength and stiffness [16]. Kevlar reinforced composites are mainly used for applications where stiffness, strength and damage resistance are important criteria as well as for saving weight. The Kevlar chemical structure contains hydrogen, nitrogen, carbon and oxygen elements [30], shown in Figure 3-1(b).

### **3.1.3 POLYETHYLENE FIBRE**

The most common fibres used in composites for structural applications are Kevlar, carbon and glass fibre. Owing to their high strength and stiffness properties, glass and

carbon fibres are widely used in the aircraft industry, but they are brittle in nature and carbon fibre in particular has very low strain-to-failure values [43]. In polymeric fibres, the density of carbon bonds can never be as high as that in carbon fibres because of the molecular side groups. Nevertheless, it can be seen from Table 3-1, that UHMWPE fibre exhibits unique mechanical properties in terms of high strength and stiffness, relative to density. Moreover, polyethylene fibres possess a relatively high strain-to-failure in comparison with carbon fibres. Due to these properties, polyethylene fibres have a high potential for use in a composite structures.

UHMWPE fibres are mostly used to produce ballistic vest covers, safety helmets, cut-resistant gloves, climbing ropes and many other structural applications where stiffer, stronger and tougher properties are required [105]. In addition, polyethylene based materials have received wider attention because of their biocompatibility, excellent stability in body fluids, inertness and easy formability [1]. These fibres can be produced from dilute polymer solutions through the gel spinning method, in which chain molecules can be drawn in the fibre direction. Peterlin, Ward, Peijs, Govaert, Lemstra and their co-workers have made a major contribution to the development of gel-spun polyethylene fibres [106-115]. Their work underpinned the foundation of UHMWPE fibres under the trade names of Dyneema and Spectra [116]. The polyethylene fibre chemical structure is shown in Figure 3-1(c); the material contains hydrogen and carbon elements [30]. Further details of the processing involved in the production of polyethylene fibres are provided in Chapter-7 (Section 7.1).

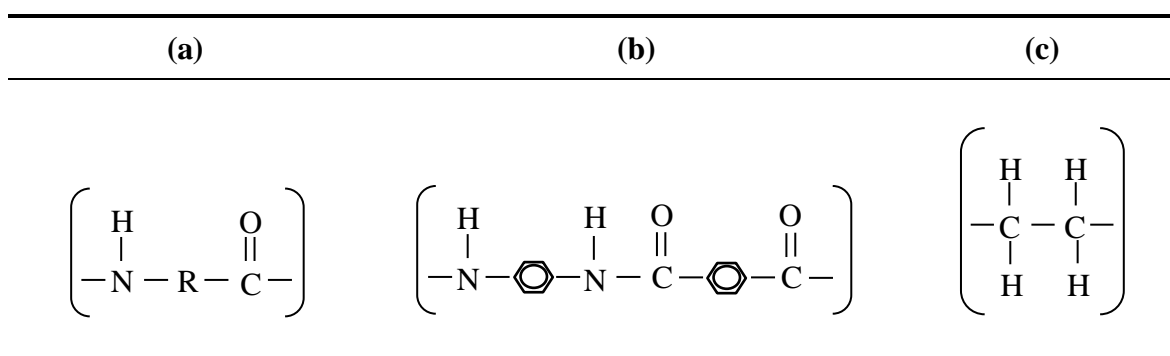


**Figure 3-1. Chemical structure (mers) of polymers: (a) nylon, (b) Kevlar, and (c) polyethylene.**

## **3.2 COMPOSITE PROCESSING, PROCEDURES AND EQUIPMENT**

### **3.2.1 ANNEALING PROCESS**

In common with previous nylon fibre-based VPPMC processing [7-13], fibres in this work required annealing to remove manufacturing-induced residual stresses and to provide suitable viscoelastic creep-recovery characteristics. Previous studies have shown that annealing of nylon 6,6 fibres at 150°C for 0.5 hour (prior to the stretching process) plays an important role in their viscoelastic behaviour [7-13]. Viscoelastically generated pre-stress requires fibres to store mechanical energy so that it can be released over a very long timescale. Thus, after removing a tensile creep load and undergoing instantaneous (elastic) recovery, potentially suitable fibres should exhibit a significant proportion of long-term viscoelastic recovery strain, followed by zero (or almost zero) steady-state strain from viscous flow effects. In Refs [8-10], investigation into viscoelastic recovery showed that for the nylon 6,6 yarn, a significantly higher residual strain was obtained in contrast with 'as-received' fibres; the latter exhibited notably lower strains under both creep and recovery conditions.

In accordance with previous nylon fibre-based VPPMC studies [7-13], the annealing process had to follow the same procedure, so that the findings would allow comparison. In this work, however, a fan-assisted (Carbolite) oven was utilised for the annealing process instead of the muffle furnace used in previous work [7-13]. This was based on two reasons (i) it offers a uniform temperature distribution ( $\pm 0.5^\circ\text{C}$ ) and (ii) provided greater capacity, a high volume of fibres could be annealed in one run. Both muffle and fan-assisted ovens are shown in Figure 3-2, and these had been previously calibrated [10]. The annealing condition for nylon 6,6 fibres were maintained similar to those reported in Refs [7-13]; however, for UHMWPE fibres a different temperature was required. More detail on UHMWPE annealing processing is provided in Chapter-7 (Section 7.2). For the annealing process, a suitable length of yarn was placed

(unconstrained) in an aluminium tray and maintained at 150°C (nylon 6,6) and 120°C (UHMWPE) for 0.5 hour in the fan-assisted oven, shown in Figure 3-2(b) below.

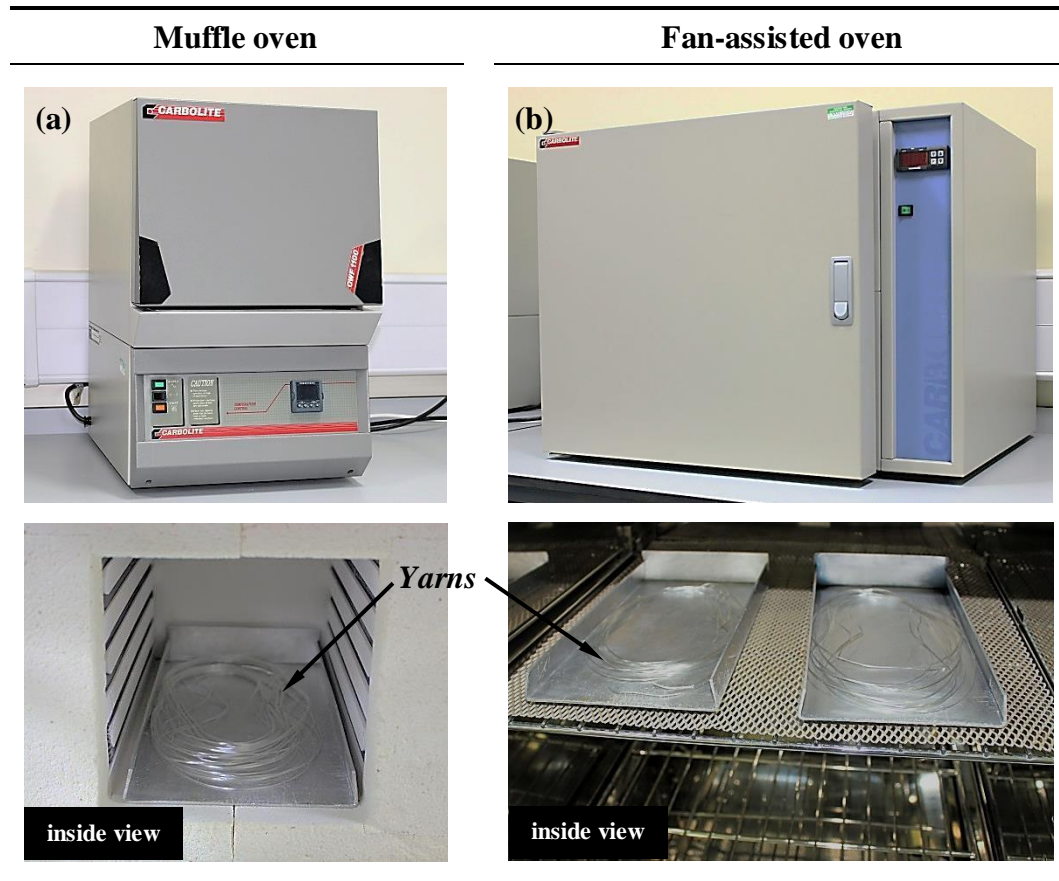


Figure 3-2. Ovens utilised for the annealing process. Yarns were placed in an aluminium tray to ensure uniform temperature and to prevent unwanted movement from air flow in the fan-assisted oven.

### 3.2.2 FIBRE STRETCHING PROCESS

For the production of pre-stressed composite samples, a pre-determined fixed load was applied to nylon 6,6 and UHMWPE fibres for 24 hours (prior to moulding) to induce creep strain. This section provides information on the stretching process and the stretching rigs used in this work for pre-stressing.

Applying an adequate level of pre-stressing to the fibres is a challenging task. As reported in Chapter-2 (Section 2.7), various methods have been adopted to produce elastically pre-stressed composites [55, 62, 64-68, 81, 83, 84, 96]. The main disadvantages of elastically pre-stressed composites are that the stretching of fibres for pre-stressing must be performed during the moulding process i.e. the load has to be maintained until the resin has cured, which restricts fibre orientation. In addition, this method can only be implemented for composite samples, which require a simple geometry. Relative to elastically pre-stressed composites, Fancy's [7-10], approach for fibre stretching in the production of viscoelastically pre-stressed composites is quite different from all other methods found in the literature, in which a dead load (pre-strain) to the nylon 6,6 fibre was applied for 24 hours by using a bespoke stretching rig and the same method is adopted for this work, the procedure being discussed in detail below:

In this work, pre-stressing was achieved by using the vertically mounted stretching rigs, shown in Figure 3-3. To allow comparison with previous work, the pre-stress level for nylon 6,6 fibre was maintained similar to Fancy's previous investigations on nylon fibre-based VPPMCs in which fibres were subjected to ~340 MPa stress [9-13]. However, for UHMWPE fibres, the first practical requirement was to establish suitable load conditions. As shown in Table 3-1, UHMWPE fibres are stronger and stiffer than nylon 6,6 fibres, therefore the principal aim was to establish the condition necessary for UHMWPE fibres to retain a usable level of residual viscoelastic strain after releasing the applied load. This was achieved through strain-time recovery measurements from the applied creep load by using Rig-(a), shown in Figure 3-3.

Rig-(a), commonly employed in previously published VPPMC studies, was used to determine the time-dependent creep properties of UHMWPE fibres by applying a 24 hour load on the counter-balanced platform [9-13]. Strain from creep and the resulting recovery were measured by the distance between two inked marks on the yarn (typically 300-400 mm apart), using a digital displacement gauge with a precision level of  $\pm 0.01$  mm attached to the rig.

Rig-(b) shown in Figure 3.3 was previously employed for investigations by Pang and Fancey on higher  $V_f$  nylon fibre-based VPPMCs [12, 13]. It was specifically designed to stretch multiple yarns, thereby offering the opportunity to produce high fibre volume pre-stressed composites. Both stretching rigs have the capability to facilitate various ranges of load needed for pre-stressing. It can be seen from Figure 3-3 below, that the fibre stretching procedures are much simpler in comparison with other pre-stressing methods reported in Chapter-2 (Section 2.7).

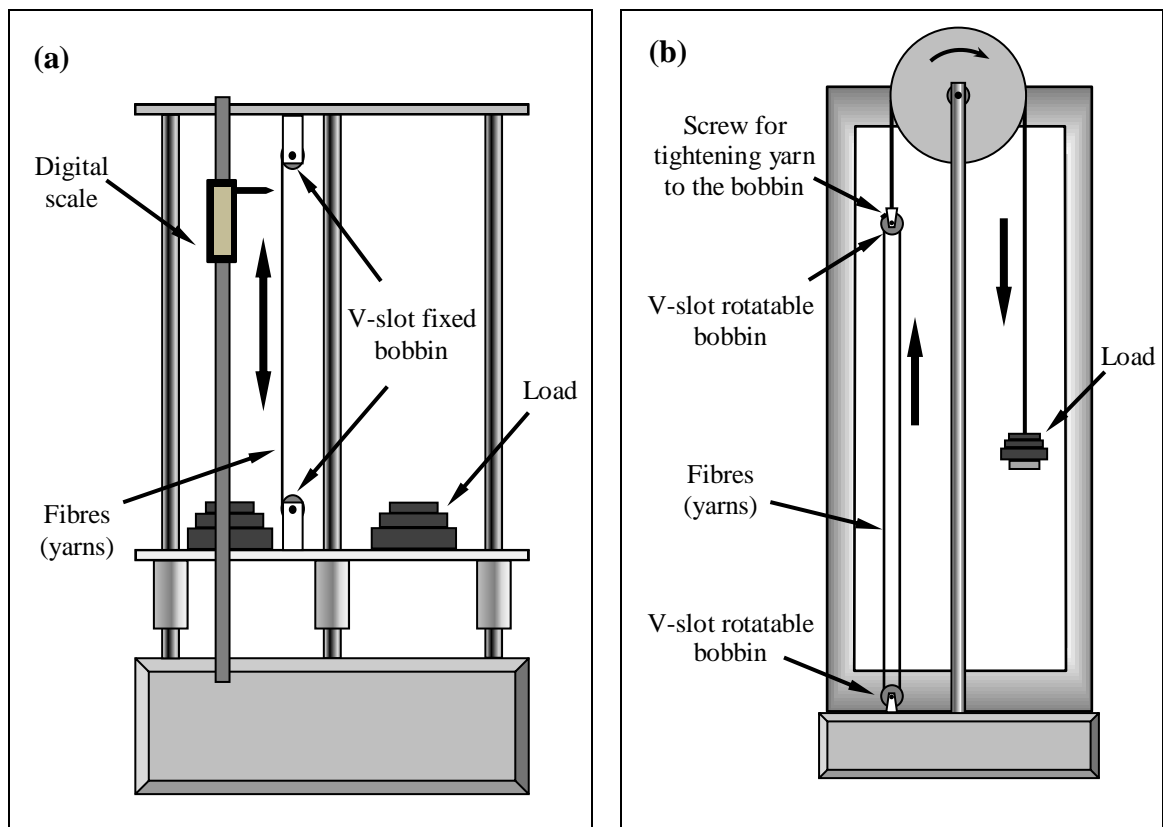


**Figure 3-3. Schematics of the vertical stretching rigs for pre-stressing. Rig-(a) was mainly used for creep and recovery strain tests; strain measurement was recorded by the attached digital displacement gauge. Rig-(b) was designated to stretch nylon and UHMWPE fibres for pre-stressed composite samples; this provided the flexibility to stretch multiple yarns for high  $V_f$  composite samples. Load equivalents for 340 MPa (nylon) and 0.8-1.5 GPa (UHMWPE) were applied on yarns. Note. for confidentiality, specific details of rig-(b) are not shown.**

In common with earlier VPPMC based processing [7-13], a similar procedure was adopted here, in which the nylon 6,6 and UHMWPE fibres were annealed prior to the stretching process. To produce one batch, the fan-assisted oven was used, in which two

lengths of yarn (designated test and control) were simultaneously annealed (unconstrained) for 0.5 hour. Due to the change in atmospheric temperature and humidity, fibre preparation and composite production in this study was performed in a laboratory, where temperature and humidity was maintained at  $20\pm 2^\circ\text{C}$  and  $40\pm 10\%$  RH.

### 3.2.3 EVALUATION OF FIBRE VOLUME FRACTION

In this work, batches of composite samples from low to high fibre volume fraction ( $V_f$ ) were produced to evaluate their performance and general characteristics by using mechanical testing. The evaluation of  $V_f$  was determined by considering the cross-sectional area of the fibres by using Equation 3-1. However, various methods can be used for the calculation of fibre volume fraction. For example, an image analysis method has been performed elsewhere [55], in which the cross-sectional SEM images of a unidirectional composite sample were processed by Leica image analysis software; the average  $V_f$  values from 10 micro frames were considered. It is well known that the dispersion of fibres in a composite sample can be varied; therefore image analysis may not be a reliable approach. Thus, for unidirectional continuous fibres in rectangular samples, considering the sample cross-sectional area and number of fibres is the simplest method for determining  $V_f$ .

$$V_f = \left( \frac{A_f}{A_c} \right) \times 100 \quad (3-1)$$

Where,  $A_f$  and  $A_c$  are the cross-sectional area of the fibres and composite respectively. Here,  $A_f$  is determined from fibre diameter, the number of fibres in one yarn and the number of yarns within  $A_c$ .

It should be noted that any values for  $V_f$  from Equation 3.1 are nominal; thus local variation in fibre spatial distribution are not accounted for. In this work, however, as such variations are expected to be similar in both test (pre-stressed) and control (un-

stressed) samples, the effects are negligible for comparative purposes. Clearly, variations in fibre spatial distribution within sample cross-sections could affect mechanical properties such as bending stiffness and these are discussed in Section 3.3.2.

For mechanical testing, batches of composite samples were produced, using nylon, hybrid (nylon/Kevlar) and UHMWPE fibres. The nominal  $V_f$  values for nylon fibre-based composites was 3.3, 9.9 and 16.6%; hybrid samples were produced with 4.5%  $V_f$ , consisting of 3.3% nylon and 1.2% Kevlar fibres and are summarised in Table 3-3 below. UHMWPE fibre composite samples were 3.6 and 7.2%  $V_f$ . To enable a more comprehensive analysis of the results in comparison with nylon and polyethylene fibre composites, additional Kevlar fibre-only composite samples of 3.6%  $V_f$  (no pre-stress) were also produced.

**Table 3-3. Nominal fibre volume fraction values in the composite samples. These were evaluated from Equation 3.1, where the cross-sectional area of the sample was  $3 \times 10 \text{ mm}^2$ . The radius values for nylon, UHMWPE and Kevlar fibres were 13.75, 6.0 and 9.0  $\mu\text{m}$  respectively. The fibre radius is based on supplier specification from Table 3-1.**

Quantity of yarns (fibres)	Fibre cross-sectional area ( $A_f$ ) ( $\text{mm}^2$ )	Nominal fibre volume fraction ( $V_f$ ) (%)
<i>Nylon 6,6</i>		
12 yarns (1680 filaments)	1.00	$3.3 \pm 0.2$
36 yarns (5040 filaments)	2.99	$9.9 \pm 0.6$
60 yarns (8400 filaments)	4.99	$16.6 \pm 1.0$
<i>UHMWPE (Dyneema-SK60)</i>		
6 yarns (9600 filaments)	1.09	$3.6 \pm 0.2$
12 yarns (19200 filaments)	2.17	$7.2 \pm 0.5$
<i>Commingled (Nylon*/Kevlar**)</i>		
*12 yarns (1680 filaments)	1.00	$3.3 \pm 0.2$
**12 yarns (1440 filaments)	0.37	$1.2 \pm 0.1$
<i>Kevlar-only</i>		
36 yarns (4320 filaments)	1.10	$3.6 \pm 0.2$

### 3.2.4 PRODUCTION OF COMPOSITE SAMPLES

The production of composite samples for mechanical testing followed the same principles previously adopted by Fancy for his studies on viscoelastically pre-stressed composites [7-9]. The process involved in the production of composite samples is shown in Figure 3-4 below. To produce one batch, two lengths of yarn (designated test and control) were simultaneously annealed (unconstrained) for 0.5 hour at 150°C (nylon 6,6 fibre) and 120°C (UHMWPE fibre) in the fan-assisted oven. Stretching rig-(b) was then used to subject the test yarn to a 24 hour creep stress (shown in Figure 3.3), whilst the control yarn was positioned (unconstrained) in close proximity for exposure to the same ambient conditions ( $20\pm 2^\circ\text{C}$ ). On releasing the creep load, both yarns were folded, cut to appropriate lengths and brushed into flat ribbons ready for moulding (shown in Figure 3.5). From viscoelastic recovery force data [91], the pre-stained fibres would be expected to produce an axial stress (across the fibres) of  $\sim 10$  MPa within a VPPMC.

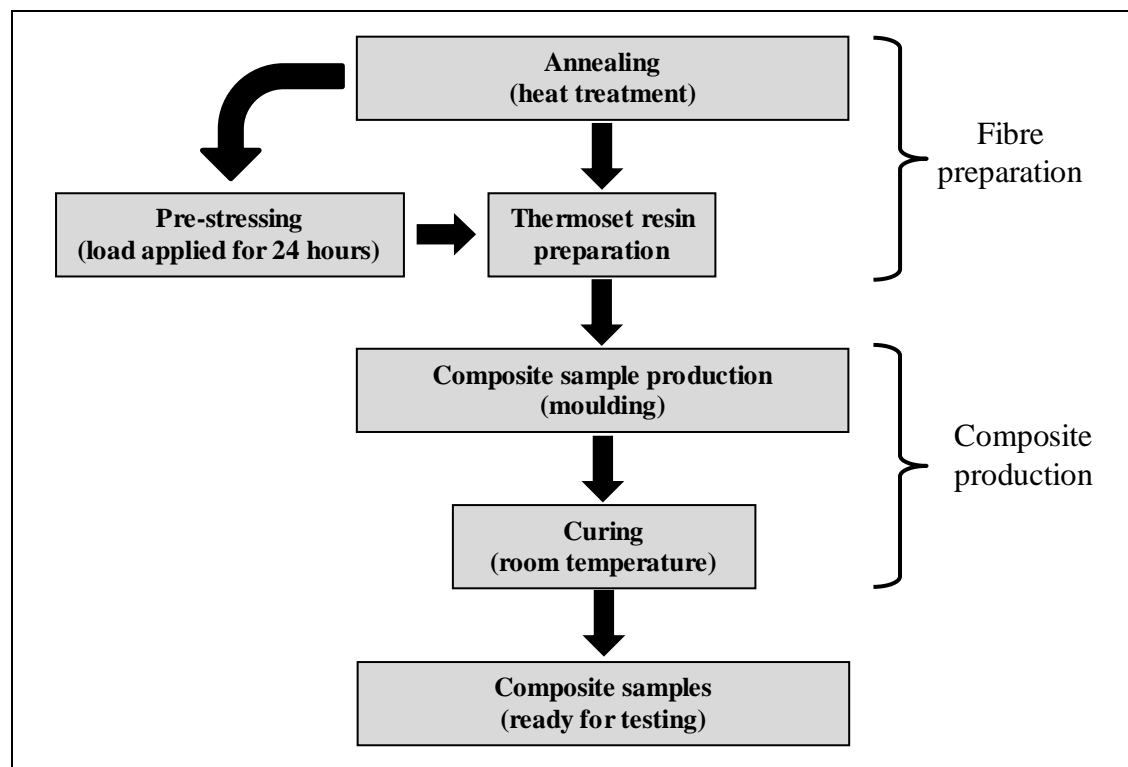


**Figure 3-4.** Process involved in the production of composite samples for both test and control samples. Pre-stressing fibres were stretched for 24 hours prior to moulding. Both test and control mouldings were prepared simultaneously from the same resin mix and completed within 30 minutes.

Unidirectional continuous fibres composite samples were prepared by an open-casting method; two aluminium moulds were used each with a 10 mm wide polished channel, 3 mm in depth and 450 mm long, enabling a strip of test and control materials to be cast simultaneously from the same resin mix, as shown in Figure 3-5(c) below. The matrix material was a clear-casting polyester resin, Cray Valley Norsodyne E9252, mixed with 1% MEKP catalyst, supplied by CFS Fibre-glass supplies, UK. Preparation of the resin was performed by dispensing portions of the resin and hardener into a mixing cup and then stirring them together thoroughly with a wooden mixing stick for two minutes. The curing time had three stages i.e. wet lay-up time (liquid state), initial cure (gel state) and final cure (solid state); the time required for the resin to change from liquid to gel states was ~0.25 hour, whilst cure time (solid state) was ~2 hours at room temperature, by which de-moulding could be performed.

Following de-moulding, the resulting composite strips were cut into five samples per mould for Charpy impact testing and two samples each for bend tests, with sample sizes being 80×10×3.1 mm and 200×10×3.1 mm. Tolerance on sample thickness was ±0.1 mm. The samples were then held under a weighted steel strip for 24 hours to prevent potential bending effects from internal stresses and then sealed in polythene bags and stored at room temperature (20±2°C).

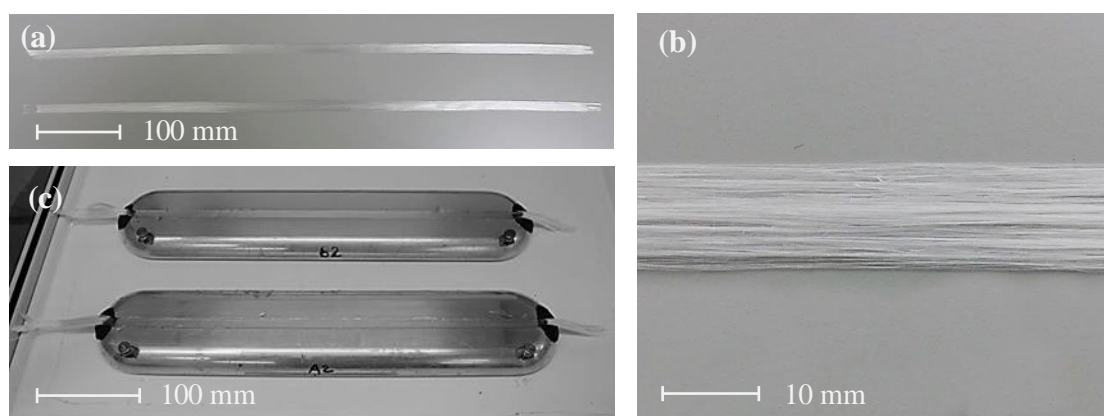


**Figure 3-5. Production of the composite samples (a) pre-stressed (test) and unstressed (control) fibres are cut to the appropriate length and brushed to separate filaments, (b) fibres are brushed and ready for moulding, (c) fibres are mounted in the thermoset polyester resin. Both test and control mouldings were prepared simultaneously from the same resin mix and completed within 30 minutes.**

### 3.3 MECHANICAL TESTING

Performance of the composite samples was mainly evaluated by Charpy impact testing and three-point bend tests. Results of the pre-stressed (test) samples were compared with their identical un-stressed (control) counterparts. In addition, tensile testing was performed for polyethylene fibres to evaluate their mechanical properties. Details of the composite sample and testing setups are provided in Table 3-4, and are further explained in the following sections. The percentage improvements in increased energy absorption from impact tests and flexural modulus from three-point bend tests were calculated by Equation 3-2, where  $T$  and  $C$  represent test and control samples.

$$\text{Increase (\%)} = \frac{T-C}{C} \times 100 \quad (3-2)$$

**Table 3-4. Summary of the materials used for the production of composite samples and testing setup.**

<b>Fibre types</b>	<b>Resin</b>	<b>Mechanical testing</b>
<ul style="list-style-type: none"> <li>Nylon 6,6 (3.3, 10.0 and 16.6% <math>V_f</math>)</li> </ul>	<ul style="list-style-type: none"> <li>Polyester (thermoset)</li> </ul>	<ul style="list-style-type: none"> <li>Charpy impact tests <u>span settings</u> 24, 40 and 60 mm</li> </ul>
<ul style="list-style-type: none"> <li>UHMWPE <i>Dyneema-SK60</i> (3.6 and 7.2% <math>V_f</math>)</li> </ul>		<ul style="list-style-type: none"> <li><u>sample dimensions</u> <math>80(l) \times 10(w) \times 3(t)</math> mm</li> </ul>
<ul style="list-style-type: none"> <li>Kevlar 29 (1.2 and 3.6% <math>V_f</math>)</li> </ul>		<ul style="list-style-type: none"> <li>Three-point bend tests <u>span setting</u> 100 mm</li> <li><u>sample dimensions</u> <math>200(l) \times 10(w) \times 3(t)</math> mm</li> </ul>

### 3.3.1 CHARPY IMPACT TESTING

In aircraft structures, dropping tools and bird strikes are possible examples of low velocity impact damage. The internal damage from impact may have catastrophic consequences on the subsequent load carrying capability of the composite structure. In recent years, composite material damage from low velocity impact has received greatest attention. Composite material behaviour in terms of energy absorption has been recognised as an important research area of interest for many industries. For example, the sensitivity of the constituents in composite materials to impact damage and their specific energy absorbing capabilities are key factors in F1 racing car development [117].

In this work, impact tests were performed on a Ceast Resil-25 Charpy machine (non-instrumented) using 7.5 and 15 Joule hammers at a velocity of  $3.8 \text{ ms}^{-1}$  with a span setting range of 24-60 mm; this operated in accordance with BSI standards (BS EN ISO-179) [118]. Investigations from Charpy-based studies on open-cast nylon fibre-based VPPMCs, the fibres tended to settle towards the bottom of the mould prior to curing [7-11]. This effect is also observed in this study. Therefore, similar to the earlier approach, samples were mounted with the fibre-rich side facing away from the pendulum hammer, as schematically illustrated in Figure 3-6 below.

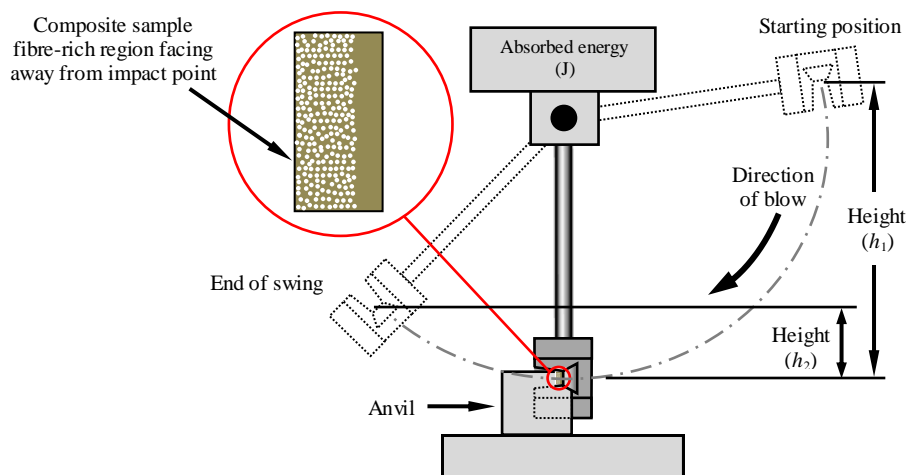


**Figure 3-6. Schematic diagram of the Charpy impact tester and end-view of the composite sample configuration for impact tests.**

### 3.3.2 THREE-POINT BEND TESTS

Flexural deformation is a popular technique for modulus measurement because it requires simple apparatus and specimen geometry (rectangular cross-sectional beam). In this study, three-point bend tests were performed for the evaluation of flexural modulus according to the ASTM D-790M recommendation, with a span to thickness ratio ( $L/h$ ) of  $\sim 30$ . For flexural tests, ASTM and BSI allow a wide freedom of choice in terms of sample dimensions and span to thickness ratios, provided the samples have rectangular cross-sections. International standards for flexural modulus testing are summarised in Table 3-5 below.

**Table 3-5. Standards for flexural modulus testing [119].**

Specification	Sample thickness (mm)	Sample width (mm)	Sample length (mm)	Span to thickness ratio	Supporting pin radius (mm)	Loading pin radius (mm)
<b>ASTM D-790M</b>	1 - 25	10 - 25	50 - 1800	16, 32, 40, 60	3 - $15h$	3 - $4h$
<b>BSI 2782</b>	1 - 50	15 - 80	$20h$	16	2	5
<b>CRAIG</b>	2	10	100	16, 20, 25, 40	3	5, 12.5

Sample testing was performed with a freely suspended load applied at the centre of the sample by using a simple bend test rig, shown in Figure 3-7. The flexural modulus of the composite sample was obtained by measuring the displacement (deflection) at the centre of the sample. To improve measurement accuracy, a video recording of each deflection in progress was made; for repeatability, three batches were evaluated. The test set-up and procedures were identical to those performed previously for nylon fibre-based VPPMCs [13]; i.e. each sample was mounted horizontally with the moulded bottom surface facing downwards and a deflection reading was taken at 5 seconds after

applying the load to obtain (as close as possible) the elasticity modulus. Although small deflections restricted measurement precision and accuracy, a low load was used in Ref [13] (~4 N) to minimise opportunities for specimen damage. In this study, to achieve comparable deflections from the samples, a load of 4.2 N was used for hybrid (commingled nylon/Kevlar) fibre composite samples (including resin-only samples) and 10 N for polyethylene fibre-based composite samples.

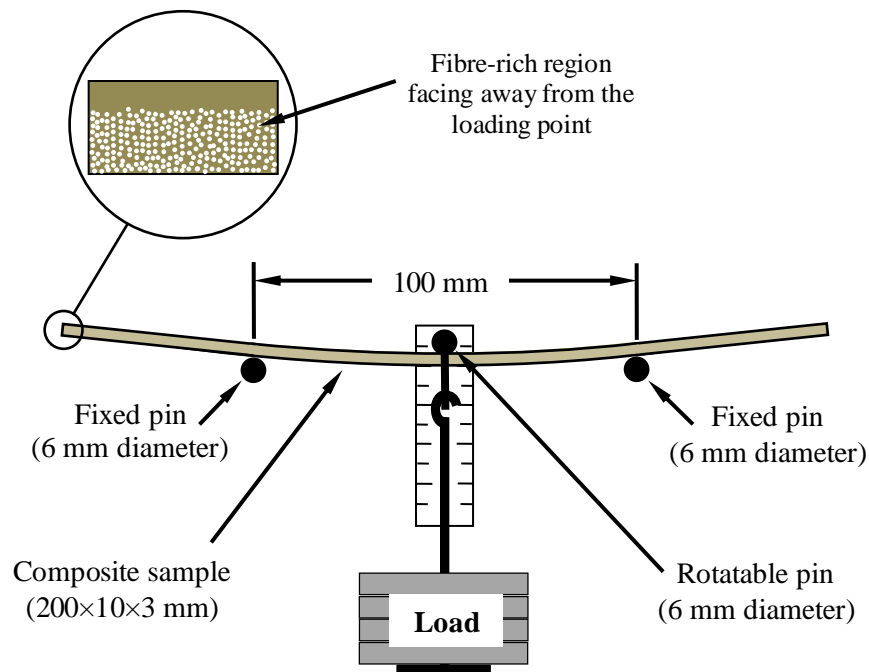


**Figure 3-7. Schematic diagram of the three-point bend test arrangement with a freely suspended load for the evaluation of flexural modulus. Composite sample orientation is also shown. A load of 10 N was applied for UHMWPE fibre composites and 4.2 N for hybrid composites (commingled nylon/Kevlar fibres) and resin-only samples.**

From the conventional three-point beam-bending relationship [120], the flexural modulus  $E(t)$  can be determined from deflection  $\delta(t)$  at the centre of the beam at time  $t$  (i.e. 5 seconds) by using Equation 3-3 below. Here,  $P$  is the applied load,  $L$  is the span and  $I$  is the second moment of area  $\left(\frac{bh^3}{12}\right)$  for a rectangular sample of width  $b$  and thickness  $h$ .

$$E(t) = \frac{PL^3}{48\delta(t)I} \quad (3-3)$$

As reported in Section 3.3.1, fibres tended to sink to the bottom of the mould during open casting, resulting in a greater fibre concentration at one side of the composite samples. Even though the density of the fibres and resin (in liquid state) are very similar, this effect was also observed in previous nylon fibre-based VPPMCs with polyester resin samples used for flexural studies [13] and Charpy impact testing [7-11]. Thus, as with the previous work, all samples for three-point bend tests were mounted with the fibre-rich side facing away from the loading point, as illustrated in Figure 3-7.

By considering the effects of non-uniform fibre spatial distribution in a composite sample, it can be assumed that there is a fibre-rich and a resin-rich zone. As reported, the fibre-rich region faced away from the loading point, so that the fibre-rich area in a composite sample would face more tensile stresses in contrast with the resin-rich region (i.e. the compression side). Therefore, the following two aspects can be considered in terms of withstanding the applied load:

- (i) The fibre-rich region withstands tensile stresses generated from the applied load at the outer surface of the composite sample consequently reducing the risk of sample damage.
- (ii) It can be assumed that these samples are based on two layers, i.e. the matrix-only region and fibre reinforced region. Therefore, the fibre and resin regions response to the applied load can be considered individually.

In Ref [121], Turner described that if the material constituents vary throughout the beam thickness then the flexural response to transverse forces cannot be translated into a single modulus i.e. stiffness of the beam is dominated by the outer layer (tension side), and is generally known as stacking sequence dependence. For example, in tensile testing on composite laminates, the individual layers contribute in parallel to the applied load; whilst in a bend test, the force-deflection relationship defines a notional modulus which reflects the fibre alignment in the individual lamellae irrespective of the stacking sequence. Therefore, in flexural tests, the contribution of each lamella depends on its

position with respect to the neutral axis. Thus, these statements validate the assumption considered for the evaluation of flexural modulus investigated in this work; i.e. bend tests performed on the composite samples are comparable to laminates, in the form of fibre-rich and resin-rich layers. In Chapter-2 (Figure 2-3, Section 2.4), the role of pre-stressing and their effects on the neutral axis were briefly discussed.

### **3.3.3 TENSILE TESTING**

The tensile properties of UHMWPE fibres were evaluated to determine whether the stretching process for pre-stressing affect their mechanical behaviour. If such changes, e.g. work hardening occur, then direct comparison between test (pre-stressed) and control (un-stressed) composite samples would be inappropriate. Previous SEM studies on nylon fibres have shown no significant changes in the fibre diameter from the stretching process [7], suggesting that pre-stressing does not affect fibre size. However, this was not possible with the UHMWPE fibres investigated in this work, due to dimensional (cross-sectional) variations between individual filaments, shown in Chapter-7 (Figure 7-15). Although these filaments have a supplier-specified mean diameter (12  $\mu\text{m}$ ), unlike other fibres, polyethylene fibres are not circular. Instead their cross-sectional geometries are bean or kidney-shaped, as described by others [122-124]. This causes difficulties in determining cross-sectional area; also test and control filament cross-sectional geometries would (ideally) need to be matched to enable direct comparison. Thus macroscopic tensile testing of test and control yarns (fibre bundles) had to be performed.

For the above reason, the principal aim was to determine possible differences between test and control fibres. Therefore, individual lengths of yarn (4 pre-stretched and 4 control) were tested in succession by using specially designed capstan jiggling attached to a Lloyd LR100K machine, shown in Figure 3-8. A gauge length of 130 mm was adopted for all samples and the loading rate was 200 mm/min. The tensile tests were performed at  $20\pm 1^\circ\text{C}$ , 168 hours (1 week) following stretching procedures. The resulting

stress-strain curves provided information (via analysis software) on tensile strength ( $\sigma_f$ ), modulus  $E$  and strain-to-failure ( $\epsilon_f$ ).

Compared with most materials, fibres are more sensitive to stress concentrations when clamped and stretched during tensile testing, though the capstan method can be an effective technique [125]. Therefore, specially designed capstan jigs were manufactured to reduce stress concentrations on the fibre ends, as shown in Figure 3-8(b) below. The capstan design and dimensions were comparable to those used elsewhere for UHMWPE fibre evaluation [126]. Further details on UHMWPE fibre tensile tests are provided in Chapter-7 (Section 7.3.3).



**Figure 3-8. Tensile testing setup (a) and jig assembly (b) for UHMWPE fibres.**

## 3.4 MICROSCOPY

As reported earlier, previous studies on nylon fibre-based VPPMCs have shown no evidence of differences in either fibre topography from the stretching process, or fibre spatial distribution between test and control samples [7, 12]. However, these effects are relatively unknown for the hybrid and UHMWPE fibre-based composites studied in this work. As reported in Chapter-1, polyethylene fibres are introduced into VPPMC technology for the first time. Of particular concern is whether the stretching process could change the size or surface characteristics of the UHMWPE fibres, which in turn could influence findings from the subsequent evaluation of the composite samples. For similar reasons, geometrical aspects of fibre spatial distribution in the composite samples had to be known. Therefore, a comprehensive investigation has been undertaken by utilising microscopy techniques in order to answer these questions.

### 3.4.1 SCANNING ELECTRON MICROSCOPY

Scanning electron microscopy (SEM) was employed in order to examine fibre topography and impact-tested sample fracture characteristics. The SEM used in this study was a Stereoscan 360, supplied by Cambridge Instruments (Carl Zeiss SMT Ltd), shown in Figure 3-9. Samples for SEM analysis were mounted on aluminium pin stubs by using a colloidal silver adhesive. To alleviate effects of sample charging, samples were gold coated using an Edwards S150B sputter coating unit, shown in Figure 3-10.

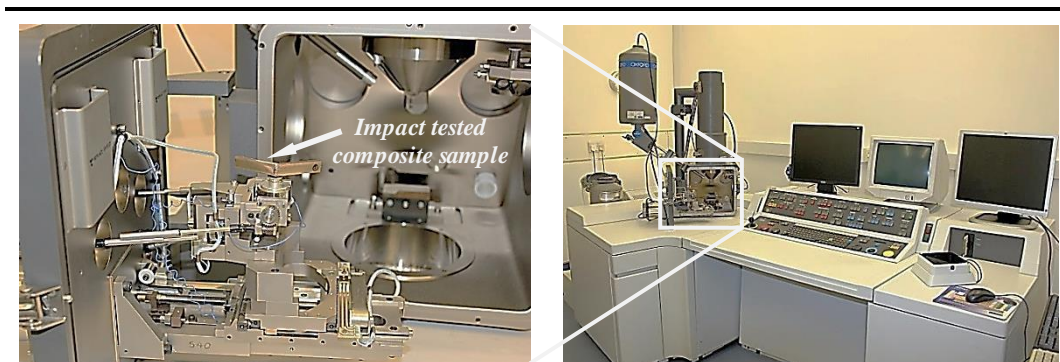


**Figure 3-9.** Scanning electron microscope used for microscopic analysis, left side image shows SEM specimen chamber with mounted (impact tested) sample.

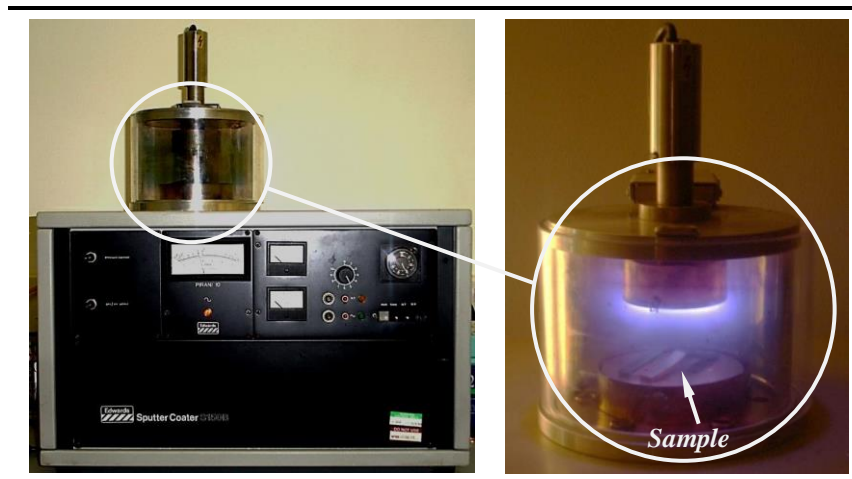


**Figure 3-10. Sputter Coater used for gold coating to improve sample conductivity for SEM analysis.**

### **3.4.2 OPTICAL MICROSCOPY**

Fibre spatial distribution in the composite samples was evaluated using a Nikon SMZ-2T stereo microscope, shown in Figure 3-11. Micrographs were acquired with a Q-imaging MicroPublisher 3.3 RTV digital camera (also shown in Figure 3-11) and Media Cybernetics Image Pro-Plus software. Transverse sections from the composite samples were cut by using a diamond cutter, which were then mounted in epoxy resin. The specimens were ground by using 240 and 1200 grit silicon carbide (SiC) abrasive paper. Sample polishing was carried out by using abrasive diamond compounds of 6 micron followed by 1 micron grades. For the final polishing stage, 0.05 micron colloidal silica was utilised. The polished samples were dried and placed in a desiccator and stored in a temperature/humidity controlled laboratory, ready for microscopic analysis.

For enhancement of image contrast between fibre and surrounding matrix material, samples were sputter coated in gold (coating thickness 10 nm approximately) by using the Edwards S150B sputter coating unit, shown in Figure 3-10.

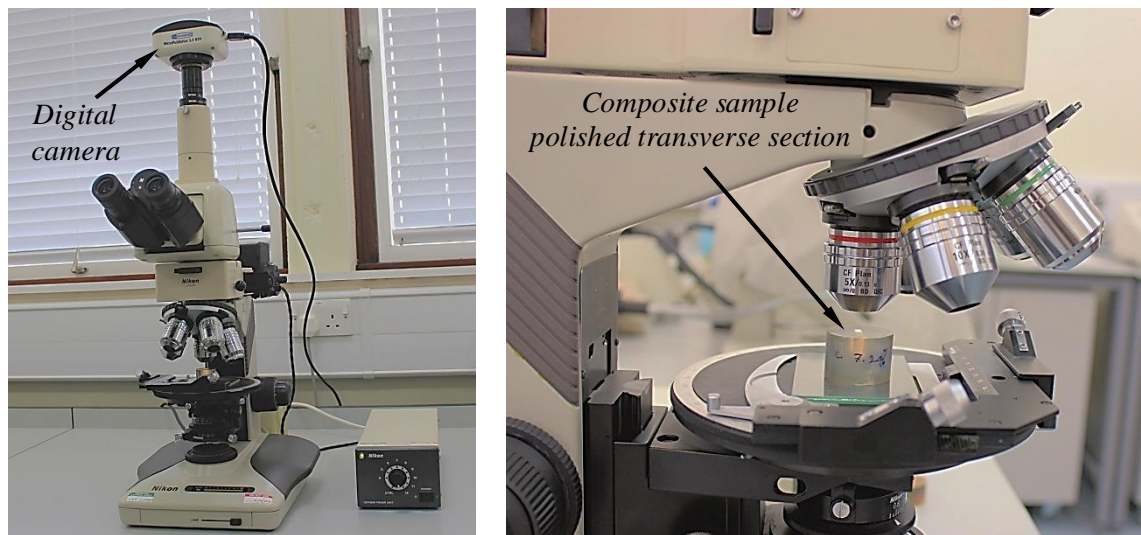


**Figure 3-11. Stereo microscope with attached digital camera.**

### 3.4.3 PROFILE PROJECTOR

As reviewed in Chapter-2, the principal mechanism responsible for improved impact energy absorption in pre-stressed composite materials is impact-induced fibre matrix interfacial debonding in preference to transverse fibre fracture [68]. Thus, as also reported in Chapter-2, the effects of this are observed through an increased area of debonding (or delamination) within a pre-stressed sample.

The energy absorption of impact tested composite samples in this study was not conclusive in characterising material behaviour, particularly, for samples tested at 60 mm span settings. Therefore, further visual inspection of impact-tested samples was carried out using a Shinko profile projector (model VSF-300), shown in Figure 3-12(a).

This utilises sub-stage (transmitted) illumination through the composite sample placed upon on x-y stage, which renders the fibre/matrix debonded regions more visible. A series of objective lenses (10x, 20x and 50x) were used, in order to magnify areas showing features such as localised debonding and matrix cracking on a viewing screen as shown in Figure 3-12(b). Measurements of debonded regions were carried out via the x-y micrometre stage, shown in Figure 3-12(c) below.

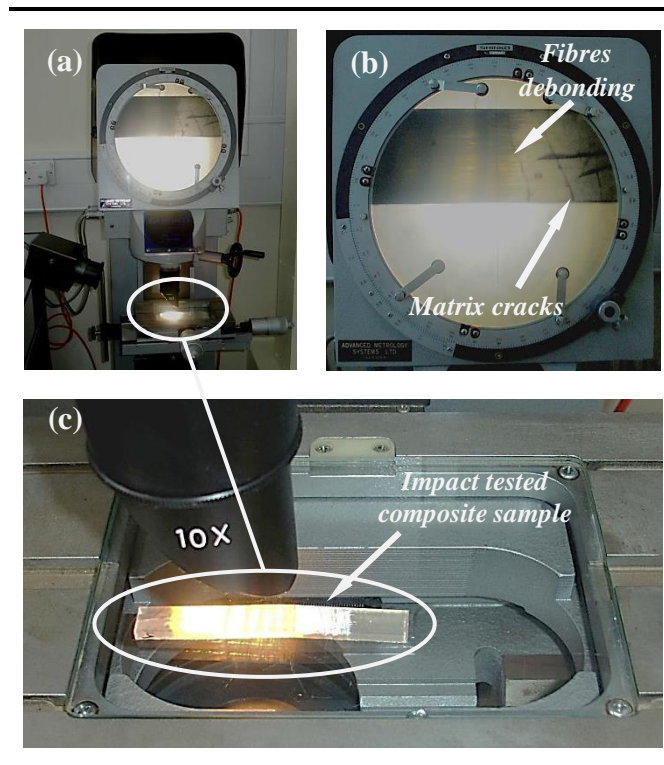


**Figure 3-12. Profile projector for visual inspection of impact tested samples. Measurements of debonded regions were taken using the micrometre x-y stage.**

### 3.4.4 X-RAY DIFFRACTION

In order to compare nylon 6,6 fibre-based VPPMC performance with previous studies [7-13], the fibre annealing process must follow the same procedure so that the findings would be comparable. In the previous nylon fibre-based VPPMC studies, the muffle furnace (shown in Figure 3-2a) was utilised for the annealing process, which was designed to run at higher temperatures (up to 1100°C) than the lower temperatures needed for VPPMC research. From calibration data, it was found that a uniform temperature at 150°C required for fibre annealing was not possible with the muffle furnace. However, the non-uniform temperature distribution was improved through the use of an aluminium tray (Figure 3-2) in earlier work [10]. Clearly, the potential for non-uniform heating of the fibres could have affected annealing characteristics. In addition, the limited space available in the muffle furnace restricted the annealing of large fibre quantities needed for this work. Therefore, an alternative oven was required.

As reported in Section 3.2.1, in this work the fan-assisted oven (Figure 3-2b), was utilised for annealing of nylon 6,6 fibres, using the same temperature conditions reported in Refs [8-10], i.e. 150 °C for 0.5 hour. After careful calibration, it was essential to further verify any crystalline changes, which may have occurred from the annealing process by using the fan-assisted oven instead of the muffle furnace. If any effects in these (semi-crystalline) nylon 6,6 fibres had occurred from the heat treatment process, then direct comparison with previous nylon fibre-based VPPMCs would be invalid.

In Ref [127], it is reported that crystalline substances can provide an X-ray diffraction (XRD) pattern; that the same substance gives the same pattern. Also, if the material has a mixture of substances, then each will produce its own pattern independently. Therefore, XRD would be an appropriate analysis method to assess the crystalline peaks from nylon 6,6 fibres. Thus, samples of nylon 6,6 fibre were annealed in both fan-assisted and muffle ovens (Figure 3-2) at 150°C for 0.5 hours and examined by an XRD Siemens D5000 X-Ray Diffractometer, shown in Figure 3-13. The crystalline peaks

were plotted from XRD data and processed by using the full-width half-maximum (FWHM) method. Details of the XRD analysis are provided in Chapter-4 (Section 4.3).

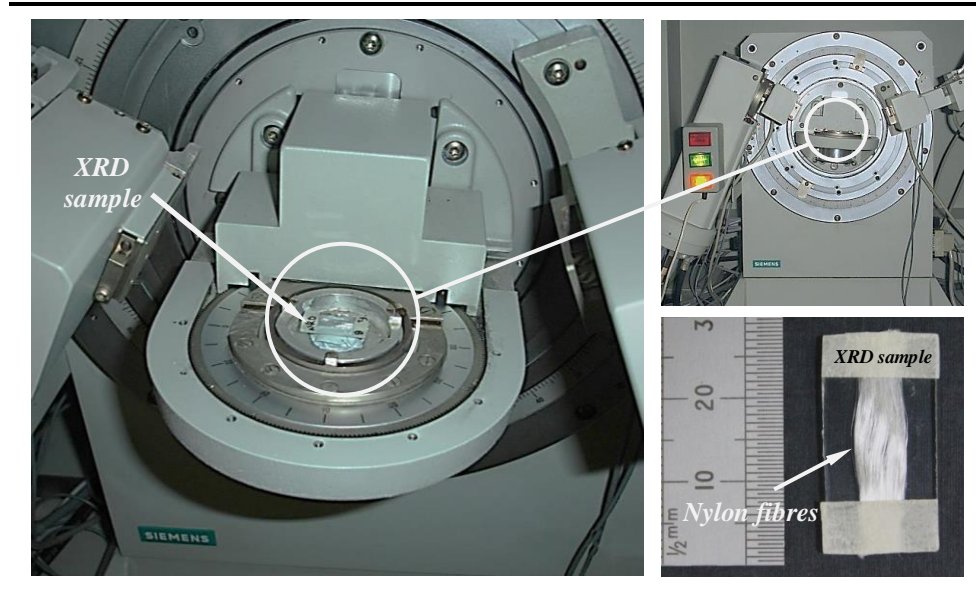


**Figure 3-13.** X-ray diffraction of nylon 6,6 fibres. Note sample prepared for XRD analysis is also shown.

# CHAPTER-4

## PRELIMINARY WORK

---

### SUMMARY

This Chapter focuses on preliminary studies undertaken during this project to minimise the risks of any uncertainty generated from the processing of material and for testing of pre-stressed composite samples. These studies involved evaluation and selection of appropriate matrix material and effects of the annealing process. In addition, preliminary work, such as calibration of the stretching rigs was performed for applying known pre-stress levels in fibres needed for the composites.

This chapter shows that the matrix material plays an important role in the performance of pre-stressed composite materials. This is demonstrated by comparing impact energy absorption of the composite samples produced from general purpose and clear-casting polyester resins. In addition, it was found that the annealing process required to remove manufacturing-induced residual stresses and to provide suitable viscoelastic creep-recovery characteristics was not affected by using different types of ovens, i.e. fan-assisted or muffle ovens (subject to similar temperature conditions).

From this preliminary work, a clear-casting polyester resin was selected to be used as the matrix material for the production of composite samples. This was on the basis of the following: (i) benefit of pre-stressing demonstrated from impact tests, (ii) optical transparency, (iii) low viscosity, and (iv) moderate curing temperature.

## 4.1 STRETCHING RIGS EVALUATION

Calibration of both stretching rigs was required to evaluate pre-stress levels. This was achieved by applying a dead load on the yarn. Force from the applied creep load was recorded from the attached digital scale, shown in Figure 4-1 below. For accuracy, eight readings of each load were taken and the mean values are shown in Figure 4-2. The pre-stress level was evaluated by using Equation 4-1 below; where,  $F$  is the force (linear equation from Figure 4-2) and  $A_f$  is the cross-sectional area of the yarn (fibres).

$$\sigma_{\text{prestress}}^f = \frac{F}{A_f} \quad (4-1)$$

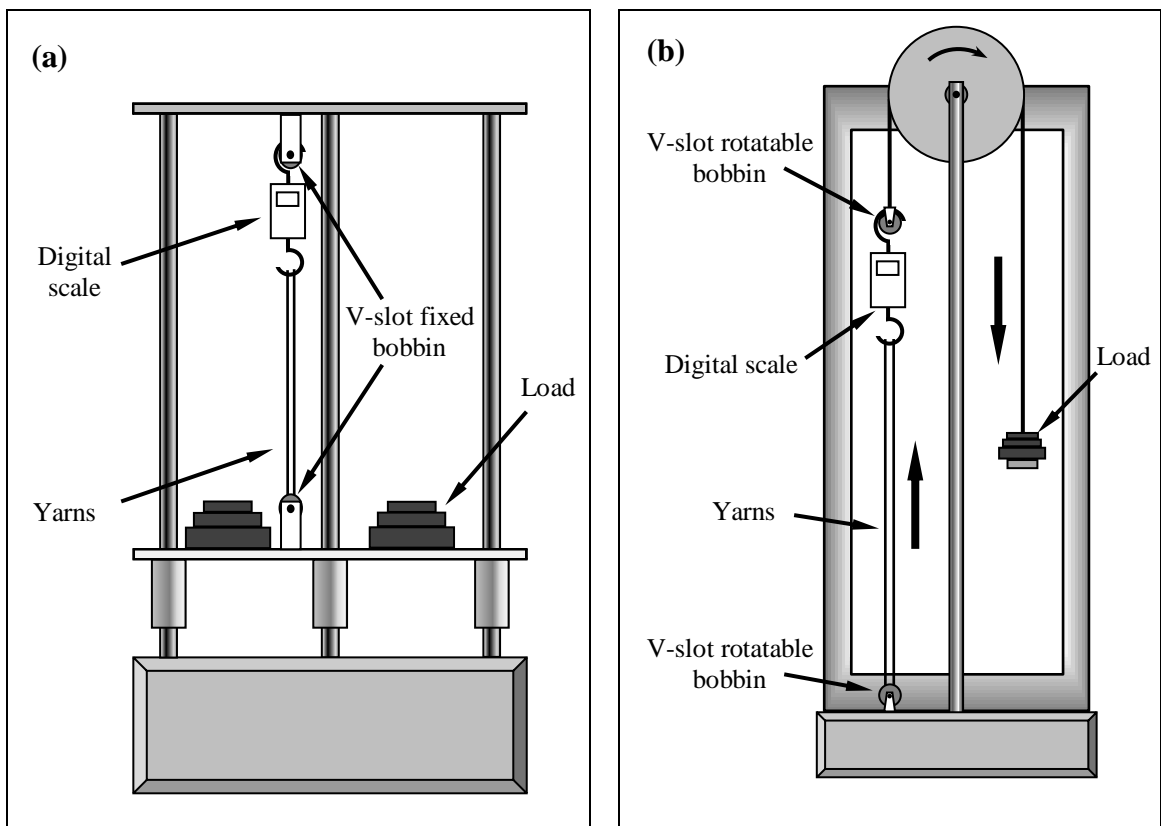


Figure 4-1. Calibration setup of the two stretching rigs used for pre-stressing and creep-recovery experiments.

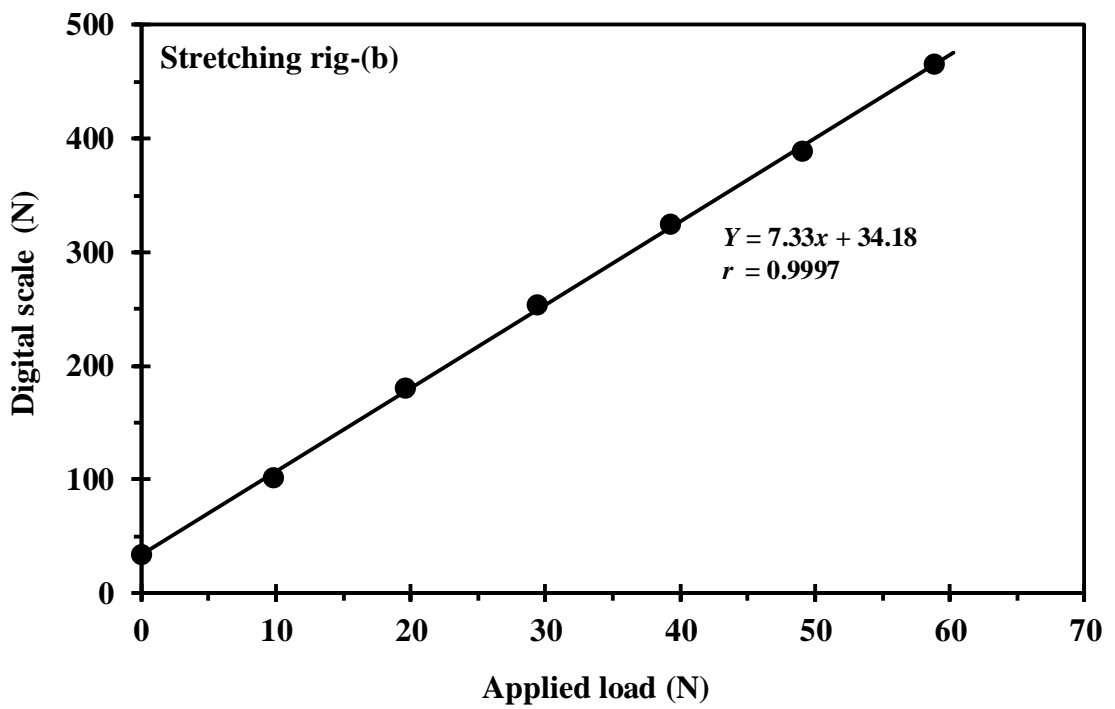
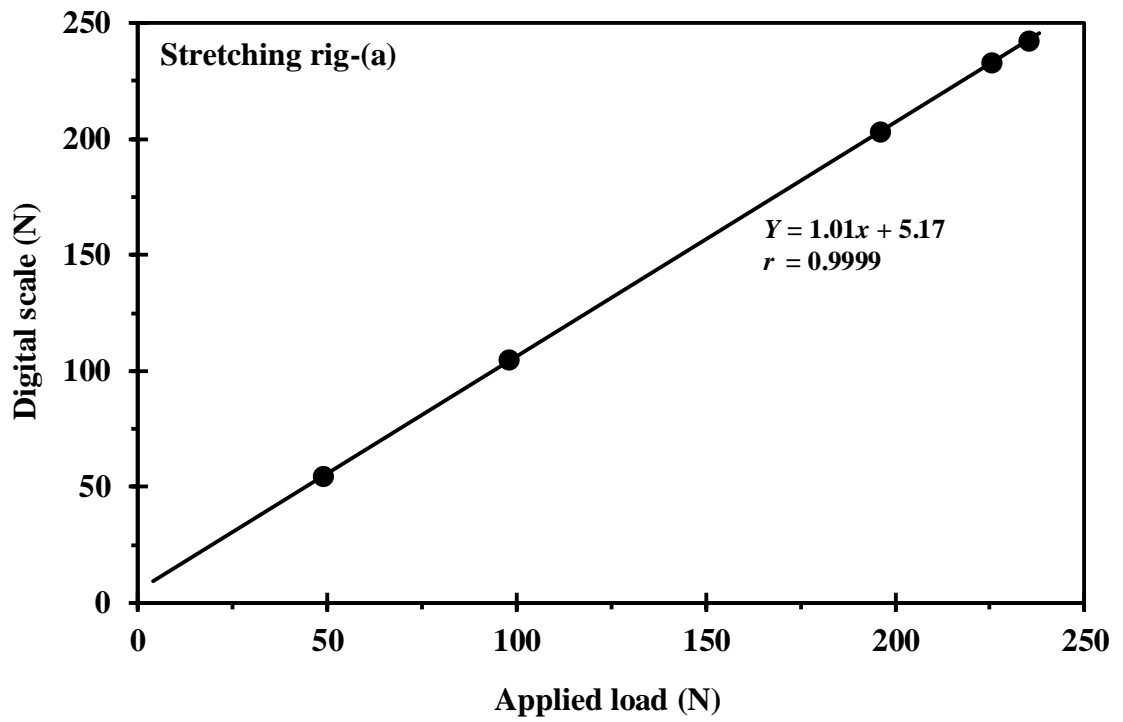


Figure 4-2. Mean calibration data of the stretching rigs from the applied load. Individual data are presented in Appendix-A.

## **4.2 RESIN SELECTION FOR COMPOSITE SAMPLE PRODUCTION**

### **4.2.1 INVESTIGATION OF EXOTHERMIC CHARACTERISTICS DURING THE RESIN CURING CYCLE**

In this study, process and production of the samples followed the same principles previously adopted by Fancey for his investigations on viscoelastically pre-stressed composites [7-10, 13]. The matrix materials used in Fancey's work for the production of composite samples were polyester (semi-transparent) [128], clear casting [10, 11, 13], general purpose [10, 11] and epoxy resins [13]. However, in this work, it was not possible to use the same matrix materials adopted previously; this was caused by resin supply problems, which resulted in the need to find alternative sources.

The resin used for the production of composite samples in this study was a polyester resin, supplied by CFS Fibre-glass supplies (UK). It is well known that the properties of polyester resins such as curing time and temperature can differ considerably. Therefore, it was essential to check the viability of any new polyester resins supplied by CFS. To evaluate this, the first approach was to perform exothermic tests on polyester general-purpose (GP) and clear-casting (CC) resins. Here, GP resin was Encore-30 and CC resin was Cray Valley Norsodyne-E9252. Experimental setup of the exothermic test is schematically illustrated in Figure 4-3. Following supplier specification, CC resin was mixed with 1 and 2% hardener, and GP resin was mixed with 2% hardener and cast in a high density polyethylene (HDPE) mould. The experiment was performed at ambient temperature and was monitored by digital thermohygrometer. The resin temperature was monitored by a thermocouple inserted through a hole in the bottom of the mould, the thermocouple protruding 5 mm into the resin. This was connected to a TES-303 thermometer until the resin cured. The data obtained from the exothermic tests are plotted in Figures 4-4 and 4-5.

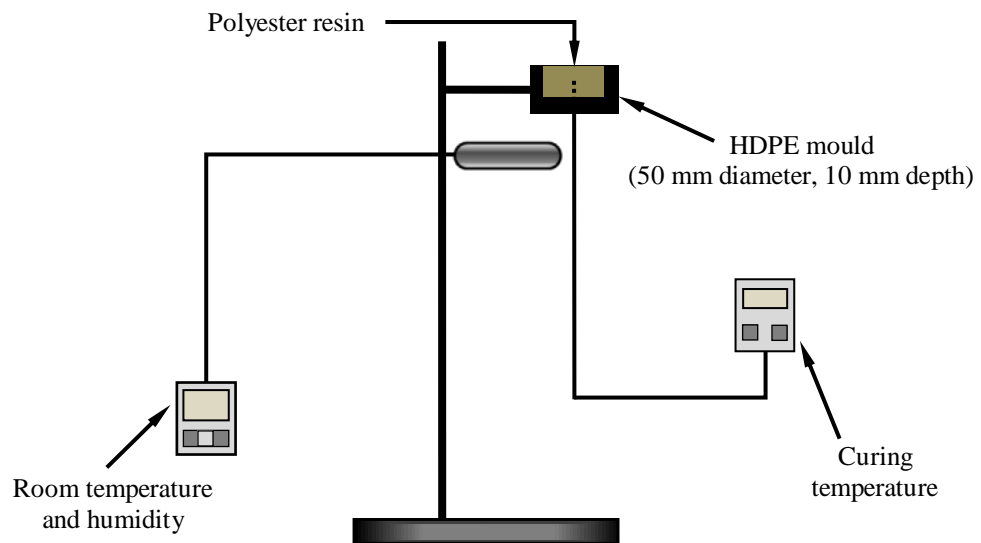


Figure 4-3. Schematic illustration of polyester resin exothermic tests.

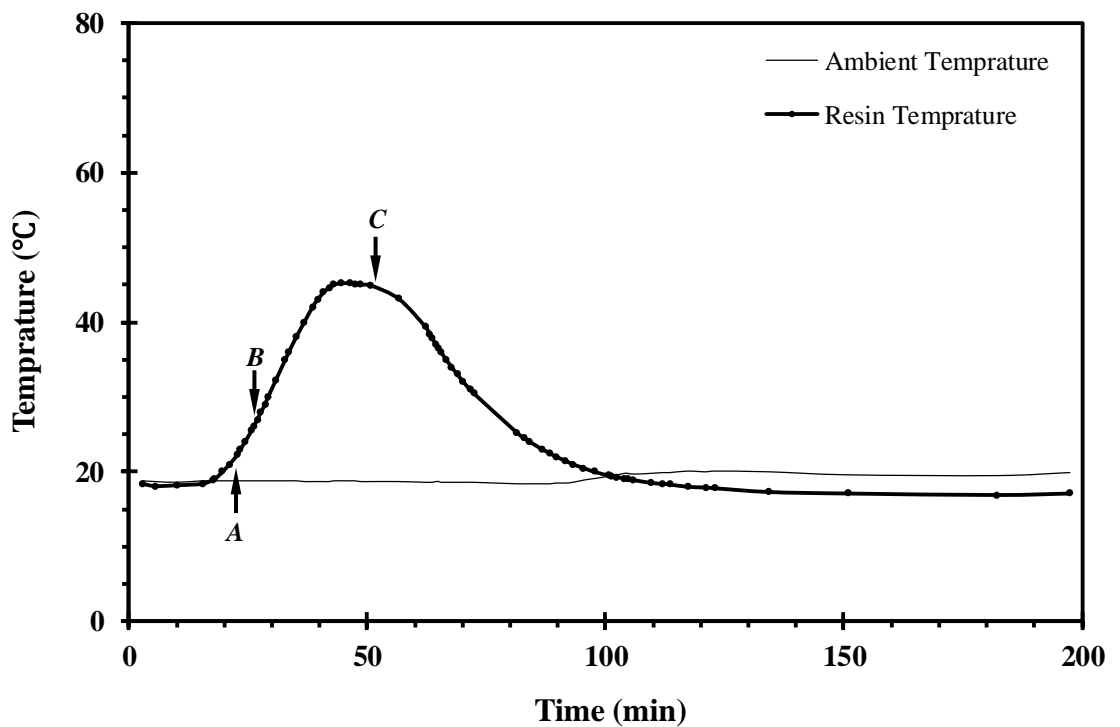


Figure 4-4. Exothermic test from the curing of polyester general purpose resin mixed with 2% catalyst. Note, various curing stages are indicated by arrows. Subjectively, these are stated as A (viscous), B (gel) and C (hard gel).

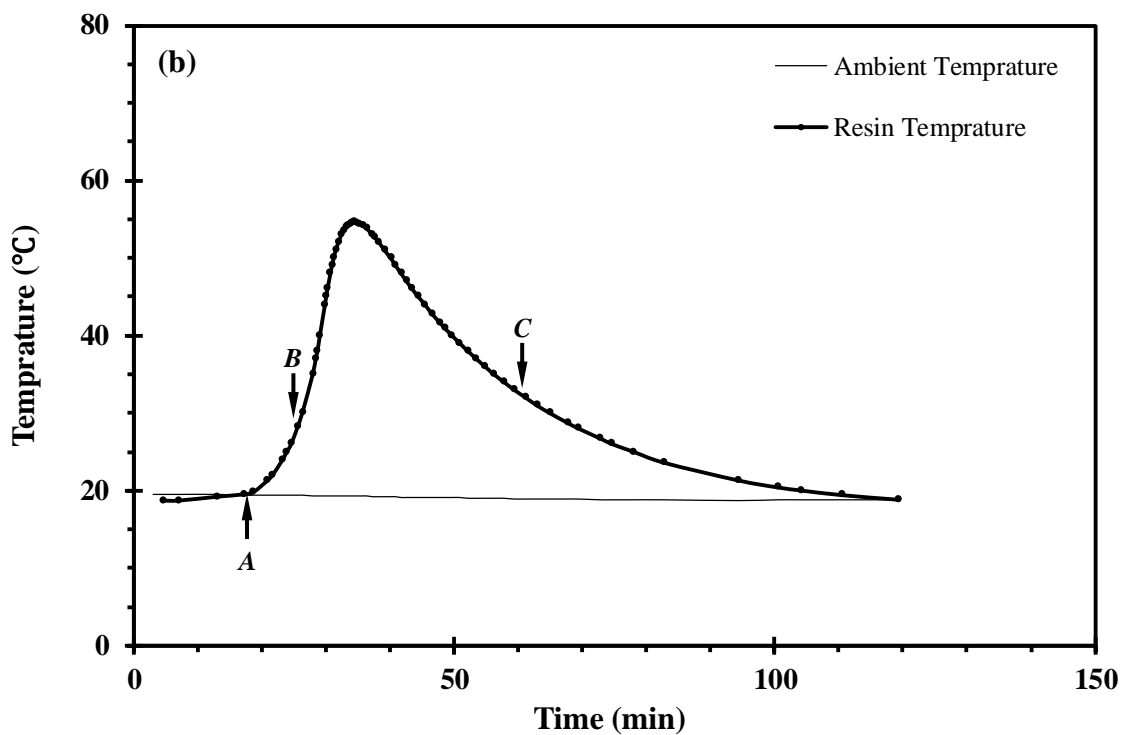
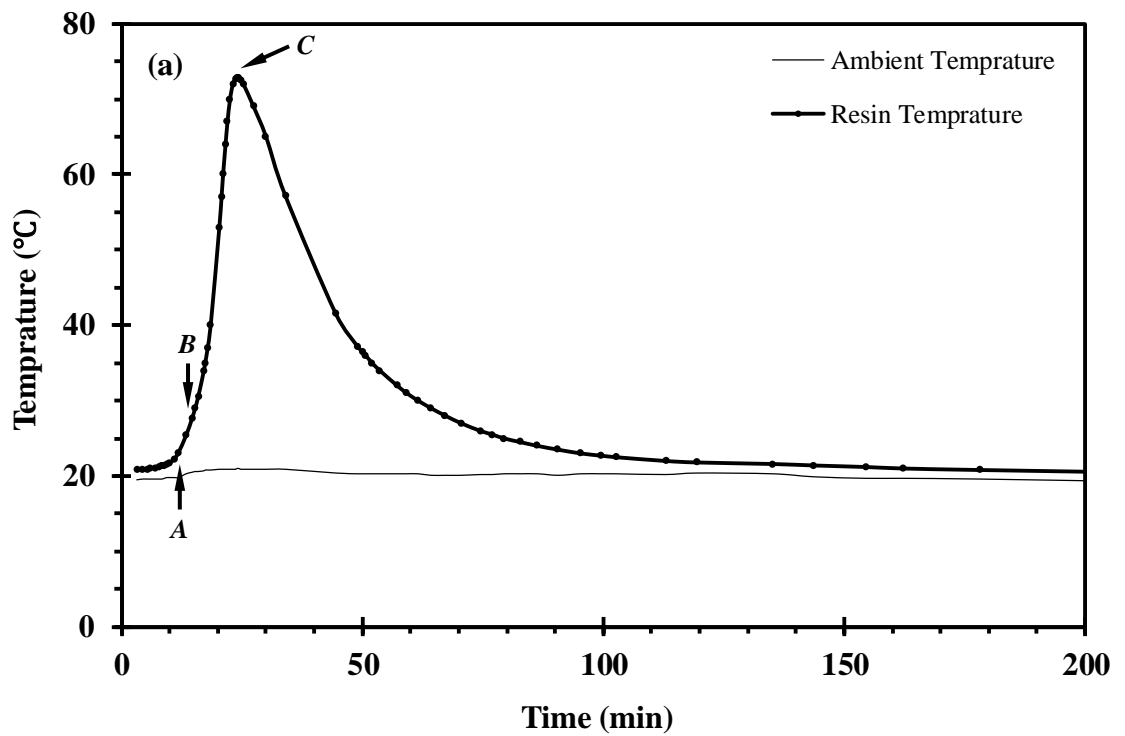


Figure 4-5. Exothermic tests from the curing of polyester clear-casting resin, (a) mixed with 2% catalyst and (b) mixed with 1% catalyst. Note, various curing stages are indicated by arrows. Subjectively, these are stated as *A* (viscous), *B* (gel) and *C* (hard gel).

From Figure 4-4 (GP resin) and Figure 4-5 (CC resin), differences in curing time and temperature are visible. In addition, on completion of the curing cycle, sample widths and thicknesses were measured to evaluate shrinkage effects. It was found that the resin with 2% catalyst exhibited the greatest shrinkage. This could be related to variances in resin curing cycle times and temperatures. However, these findings were not conclusive; therefore, further investigations were required, which are discussed in the next section.

## **4.2.2 IMPACT TESTS ON COMPOSITE SAMPLES PRODUCED FROM CLEAR CASTING AND GENERAL PURPOSE POLYESTER RESINS**

As reported in Section 4.2.1, differences in exothermic and shrinkage characteristics between the GP and CC resins were observed. It was decided to produce three batches of nylon fibre-based VPPMCs from both resins and evaluate on the Charpy impact tester to compare their impact toughness values. The production of composite samples and testing procedures followed those adopted in Refs [7-9], so the findings would be comparable. Thus samples with 2-3%  $V_f$  were produced, using stretching rig-(a), in accordance with the procedure in Section 3.2 (Chapter-3).

Impact test data from the composite samples are shown in Table 4-1 and Figure 4-6. It appears that batches of composite samples produced from the GP resin show no improvement in energy absorption from the pre-stress effects. However, the pre-stress effect is evident in samples produced from the CC resin, i.e. the mean increase in energy absorption from pre-stressing is ~45%, whilst one batch reached ~58%, compared with their control counterparts. Previous VPPMC studies, on impact energy absorption by Fancy have shown up to 30% improvement, from samples produced using different polyester GP and CC resins [10, 11] to those employed here. Although, findings for the new CC resin are comparable with Refs [10, 11], this is clearly not the case for the new GP resin samples.

**Table 4-1. Charpy impact test data from nylon fibre composite batches: 5 test (pre-stressed) and 5 control (un-stressed) samples per batch tested at 24 mm span setting. Data is normalised by dividing impact absorbed energy (J) by the cross-sectional area of the sample. S.E is the standard error of the mean. (Individual tested sample data are presented in Appendix-A).**

Polyester resin	Mean impact energy (kJm <sup>-2</sup> )		Increase in energy (% ± S.E)
	Test ± S.E	Control ± S.E	
<b>General-purpose</b> (with 2% Catalyst)	44.2 ± 2.5	52.4 ± 2.3	-15.7
	56.1 ± 2.6	57.3 ± 1.6	-2.2
	56.8 ± 2.1	56.5 ± 1.4	0.5
<i>Mean ± S.E</i>	<b>52.2 ± 2.4</b>	<b>55.4 ± 1.8</b>	<b>-5.8 ± 5.0</b>
<b>Clear-casting</b> (with 1% Catalyst)	56.5 ± 1.3	43.6 ± 1.6	29.8
	59.0 ± 2.3	40.5 ± 1.8	45.9
	73.0 ± 1.8	46.4 ± 1.6	57.6
<i>Mean ± S.E</i>	<b>62.9 ± 1.8</b>	<b>43.5 ± 1.7</b>	<b>44.4 ± 8.1</b>

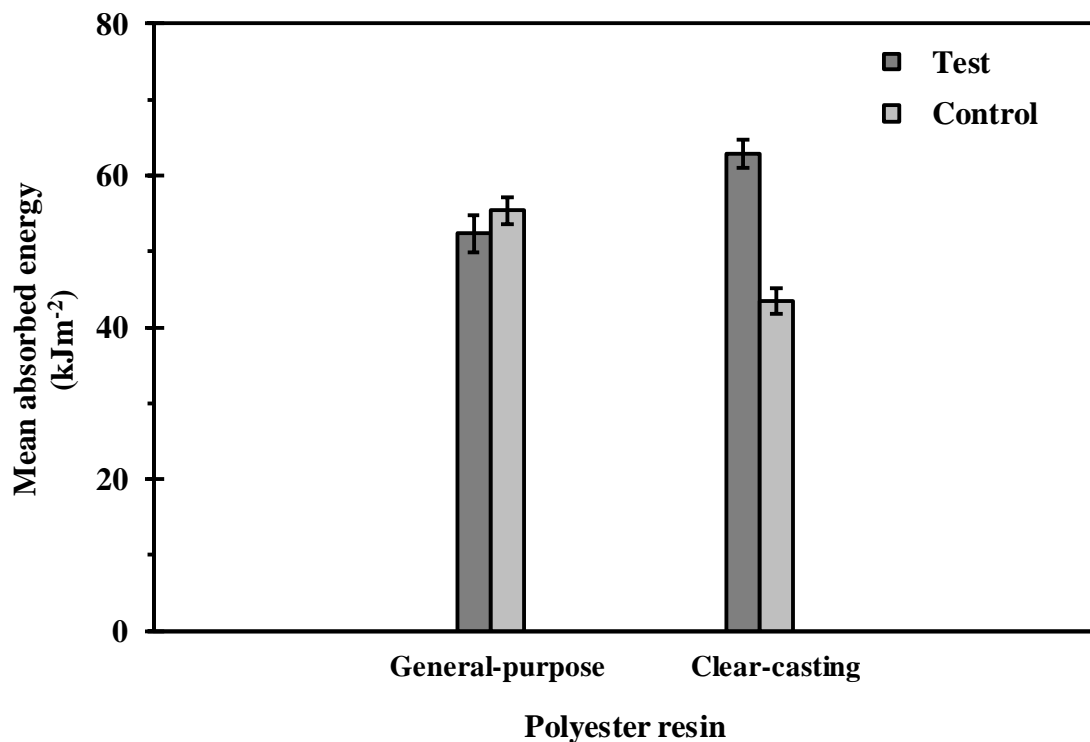


**Figure 4-6. Mean increases in impact energy of batches produced from general purpose and clear-casting resins. (data from Table 4-1).**

As reported in Chapter-2, Motahhari and Cameron [68] have shown that the principal mechanism responsible for improved energy absorption in pre-stressed composites is impact-induced fibre-matrix interfacial debonding in preference to transverse fibre fracture. This debonding mechanism is promoted by residual shear stresses at fibre-matrix interfaces caused by elastic [68] or viscoelastic [10] fibre pre-stressing, which results in increased impact energy absorption. For the new GP resin (investigated for this work), a possible explanation for no pre-stress induced improvement may be poor fibre-matrix adhesion. This view is supported by the fact that the mean energy absorption in Table 4-1 for the GP control samples ( $55.4 \text{ kJm}^{-2}$ ) is notably higher than the corresponding CC result ( $43.5 \text{ kJm}^{-2}$ ). Although this could be due to the GP resin being tougher, it may also indicate that debonding is easier in the GP resin, so that residual shear stresses at fibre-matrix interfaces from pre-stress have little effect in the test samples.

### 4.2.3 FINAL RESIN SELECTION

In the Section 4.2.2, initial investigations on the polyester general-purpose (GP) and clear-casting (CC) resins have indicated that resin plays an important role in the performance of pre-stressed composites. Batches of composite samples produced from the new GP resin (supplied by CFS) have shown no improvement from the pre-stress effect. This is in contrast with a GP resin previously used [10, 11]. Further investigations would be required to address this issue; however, it was beyond the scope of this thesis to investigate the possible causes. Therefore, in this work, it was decided to use the new CC resin for the production of composite samples. The decision was based on the following properties of CC resin:

- The benefits of pre-stressing are demonstrated successfully.
- Good transparency allows clear visibility of debonded regions after impact tests.
- Low viscosity facilitates casting of samples with high  $V_f$  values.
- Moderate curing temperature.

## **4.3 EVALUATION OF THE ANNEALING PROCESS EFFECTS ON SAMPLE PERFORMANCE**

### **4.3.1 ANNEALING OF FIBRES IN MUFFLE AND FAN- ASSISTED OVENS**

As reported in Chapter-3 (Section 3.2), the annealing of fibres for pre-stressed composites was essential for the long-term viscoelastic recovery mechanism. In Refs [7-11], Fancey's investigations on viscoelastic recovery have shown that the nylon 6,6 yarn exhibited significantly higher strains under creep and recovery conditions than as-received fibres. These were compared with fibres that had been annealed at 150°C for 0.5 hour prior to identical loading conditions. On releasing stress from the annealed fibres, elastic strain was instantaneously removed, the remaining recovery strain (viscoelastic activity) of ~3% dropped to ~2.5% after 2 hours and ~2% after 100 hours, i.e. the strain decreased very slowly with time and evidence showed it remained active beyond 1000 years at 20°C [10, 11]. In contrast, recovery strain of as-received fibres approached strain levels close to zero within 1000 hours of releasing the creep load [8-11].

In this work, the fan-assisted oven was employed for annealing because it provided a uniform temperature and facilitated the large quantities of fibres needed for the production of high  $V_f$  composite samples. In previous studies on VPPMCs, the muffle furnace was used for the annealing of nylon 6,6 fibres [7-11, 13]. The annealing conditions for nylon 6,6 fibres in this study are similar to those used for previous nylon-based studies, i.e. 150°C for 0.5 hour. However, forced air flow in the fan-assisted oven may affect the viscoelastic behaviour of nylon 6,6 fibres differently to the muffle furnace environment. Therefore, it was necessary to check this by annealing nylon 6,6 fibres in both fan-assisted and muffle ovens. If any changes in fibre properties occurred from the annealing process by using the fan-assisted oven instead of the muffle furnace, then direct comparison with previous findings on nylon fibre-based VPPMCs would be

inappropriate. X-ray diffraction (XRD) would be an appropriate approach to differentiate any crystalline structure difference in fibres annealed from each oven. However, it was also proposed that Charpy impact testing of composite samples using nylon fibres annealed from each oven might be required to provide further verification.

### **4.3.2 ANALYSIS OF NYLON FIBRES THROUGH X-RAY DIFFRACTION**

The crystalline structures of nylon 6,6 fibres annealed at 150°C for 0.5 hour in both fan-assisted and muffle ovens were examined by XRD. In previous studies, nylon fibre-based VPPMC samples were produced with 2-3%  $V_f$  [7, 9, 10]. To be consistent, the samples for XRD analysis were produced by using a representative quantity of fibres for these samples, annealed in both ovens (shown in Chapter-3, Figure 3-2). As it could be possible that the upper surface of the fibres absorb more or less heat energy than the lower surface, samples of the annealed fibres (upper and lower surface) from each oven were examined. The resulting XRD plots were processed by using Full-width-half-maximum (FWHM) method. The 2D plots and FWHM data are shown in Figure 4-7 and Table 4-2.

From Table 4-2, no difference can be observed from the XRD data. However, the XRD plots in Figure 4-7(a<sup>1</sup>-a<sup>2</sup> and b<sup>1</sup>-b<sup>2</sup>), shows some inconsistency in the crystalline peaks. It can be seen that the very narrow peak between 15° and 20° exists in Figure 4-7(a<sup>1</sup>, a<sup>2</sup> and b<sup>1</sup>), but not in Figure 4-7(b<sup>2</sup>). After careful consideration and some repeated scans, it was concluded that the inconsistency might have been caused by a technical fault in the XRD equipment, which (in turn) could have affected these results. Therefore, this raised some doubts over the reliability of the XRD equipment which reinforced the need to provide further evidence that there were no differences in annealing effects between the two ovens.

It was decided to produce low  $V_f$  (2-3%) VPPMC samples for Charpy impact tests with fibres annealed from each oven. It was expected that the impact toughness would be similar to those observed in Table 4-1 (CC resin samples) and previous nylon fibre-based VPPMC studies [7-11, 129]; thus, if any changes in composite sample performance were observed, it would be caused by fibres annealed in the fan-assisted oven affecting fibre properties.

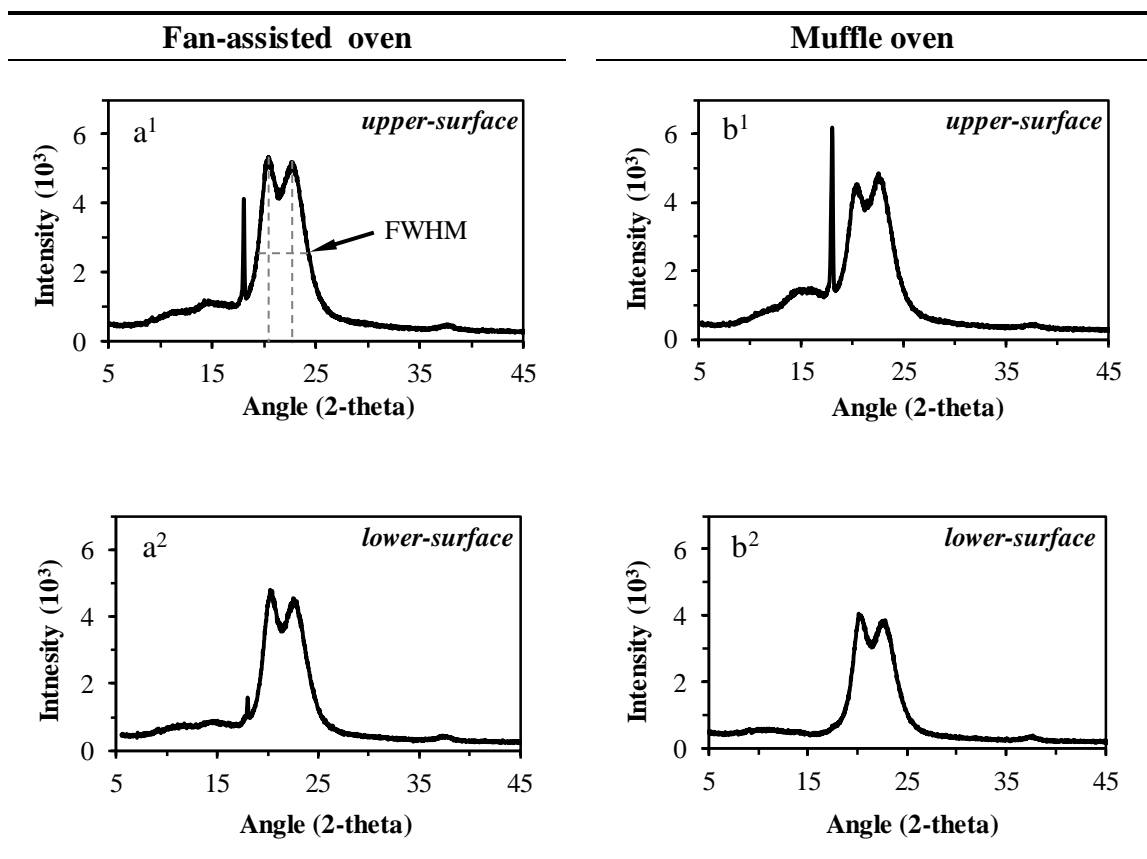


Figure 4-7. X-ray diffraction analysis of nylon 6,6 fibres annealed in fan-assisted and muffle oven at 150°C for 0.5 hour. Note, FWHM method is highlighted in (a<sup>1</sup>), similar approach applied for all samples.

Table 4-2. FWHM results from the XRD peaks shown in Figure 4-7.

	Fan-assisted oven	Muffle oven
Fibre-upper surface	5.0°	5.0°
Fibre-lower surface	4.8°	4.8°

### 4.3.3 EVALUATION ON ANNEALING EFFECTS IN COMPOSITES THROUGH IMPACT TESTING

Batches of nylon fibre composite samples (test and control) were produced with CC resin and tested using the Charpy impact tester (24 mm span setting). For each batch nylon 6,6 yarn was annealed either in the fan-assisted oven or muffle furnace at 150°C for 0.5 hour. Details for the production of composite samples are briefly covered in Chapter-3 (Section 3.2). However, for this work, fibre volume fraction and testing setup was identical to those adopted previously for impact performance of VPPMCs [7-11, 129], so that direct comparison with these findings could be made. Therefore, rig-a (Figure 4-1) was used for stretching the fibres and  $V_f$  was 2-3%.

To ensure appropriate accuracy, sixteen batches of composite samples were produced i.e. eight batches corresponding to each oven. Results are shown in Table 4-3 and Figure 4-8. It can be seen from Table 4-3, that the mean increase in energy absorption from pre-stressing (both sets) shows no real difference i.e. 40.5% (fan-assisted) and 41.6% (muffle). These findings are further confirmed by two-tailed hypothesis *t*-tests, which show no significant differences at both 5% and 2% levels in energy absorption between both sets of data. This demonstrates that using the fan-assisted oven instead of the muffle furnace has no effect on fibre annealing. In terms of the benefits from pre-stressing, as expected, it can be seen from Figure 4-8, the pre-stressed samples absorbed more impact energy than their control counterparts and it is clear that there is no observable difference between outcomes from both ovens. Moreover, these findings are comparable with Table 4-1 (CC resin samples) and previous nylon fibre-based studies reported in Refs [7-11, 129].

**Table 4-3. Charpy impact test data from nylon fibre composite batches: 5 test (pre-stressed) and 5 control (un-stressed) samples per batch tested at 24 mm span setting. Data are normalised by dividing impact absorbed energy (J) by the cross-sectional area of the sample. S.E is the standard error of the mean. (Individual tested sample data are presented in Appendix-A).**

Oven used for annealing	Mean impact energy (kJm <sup>-2</sup> )		Increase in energy (% ± S.E)
	Test ± S.E	Control ± S.E	
<b>Fan-assisted</b>	65.1 ± 3.4	45.0 ± 1.7	44.6
	65.7 ± 5.6	51.4 ± 1.8	27.9
	56.0 ± 0.7	46.6 ± 1.6	20.2
	65.2 ± 2.2	45.0 ± 1.9	44.9
	59.4 ± 1.9	43.3 ± 2.6	37.2
	62.4 ± 2.9	44.4 ± 1.0	40.6
	62.7 ± 5.5	37.4 ± 1.5	67.7
	59.4 ± 3.5	42.1 ± 1.8	41.1
	<b>Mean ± S.E</b>	<b>62.0 ± 3.2</b>	<b>44.4 ± 1.9</b>
<b>Muffle</b>	44.9 ± 1.9	37.3 ± 1.7	20.4
	56.1 ± 1.5	46.8 ± 1.6	19.9
	60.1 ± 2.1	39.9 ± 1.7	50.7
	71.9 ± 1.8	46.1 ± 1.7	55.9
	57.1 ± 3.1	44.8 ± 2.7	27.5
	65.3 ± 2.1	47.2 ± 3.2	38.3
	66.4 ± 2.1	41.2 ± 1.5	61.4
	64.5 ± 2.4	40.5 ± 1.2	59.1
	<b>Mean ± S.E</b>	<b>60.8 ± 2.1</b>	<b>43.0 ± 1.9</b>

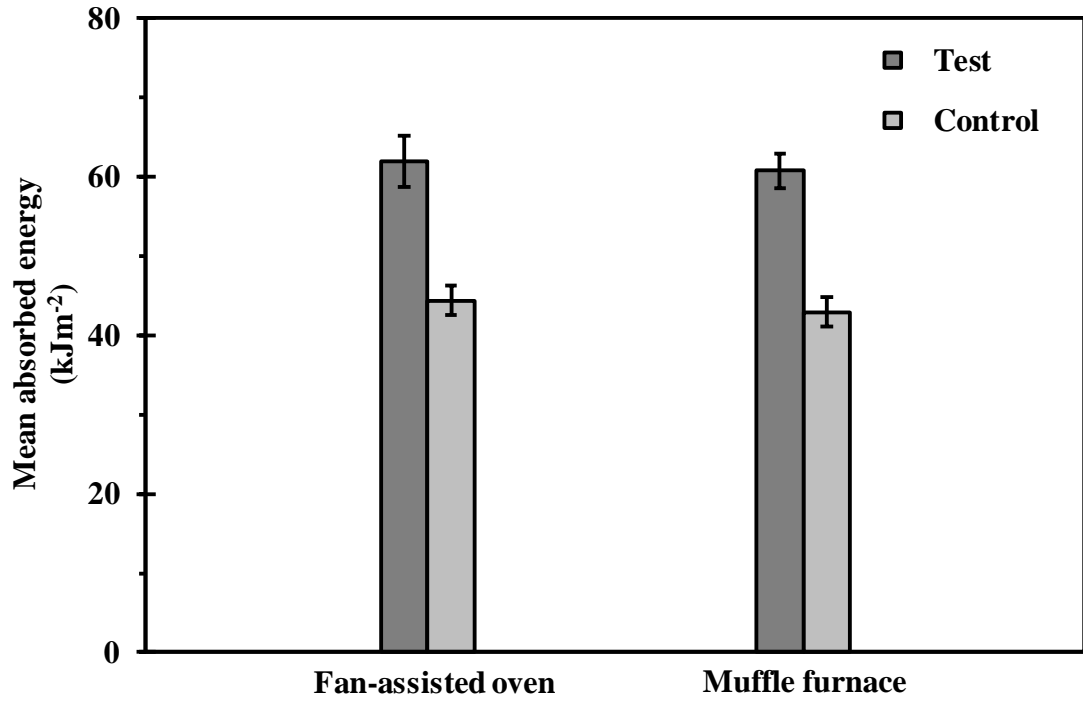


Figure 4-8. Mean increases in impact energy (test samples relative to their control counterparts) with standard errors, (data from Table 4-3).

## 4.4 CONCLUSIONS

Preliminary investigations on the processing of material have been performed to acquire information needed for this research work. These include (a) selection of the matrix material and (b) the effects of oven used for fibre annealing. For this, composite samples were produced, tested on the Charpy impact tester and the results were compared with previously published nylon fibre-based VPPMCs. The main findings (based on observations and inferences) are summarised below:

- (i) From the two resins selected for evaluation, i.e. polyester general purpose (GP) and clear casting (CC), the CC resin has been adopted. This was based on (a) pre-stressing benefits successfully demonstrated from impact tests, (b) optical transparency, (c) low viscosity, and (d) moderate curing temperature.
- (ii) For the Charpy impact testing, VPPMC samples showed a mean increase in energy absorption of at least 40% compared with control counterparts, using CC resin. However, there was no equivalent increase in energy absorption using the GP resin. This may be due to the adhesion between fibres and matrix. The GP resin investigated in this work was the only resin found (to date), that was unsuccessful in demonstrating improved performance from viscoelastically generating pre-stressing. To address this issue, further investigations would be required, e.g. fibre pull-out tests to evaluate fibre-matrix adhesion. However, it was beyond the scope of this thesis to investigate the possible reasons for not obtaining any improvement from the pre-stress effect with the new GP resin.
- (iii) By performing X-ray diffraction analysis on annealed nylon 6,6 fibres and Charpy impact testing of associated composites samples, no differences were detected between annealing fibres in the fan-assisted oven (to be used for this work) and the muffle furnace (used in previous nylon fibre-based VPPMC studies).

# CHAPTER-5

## NYLON FIBRE-BASED VPPMC IMPACT CHARACTERISTICS ON FIBRE VOLUME FRACTION AND THEIR EFFECTS ON CHARPY SPAN SETTINGS

---

### SUMMARY

In this Chapter, a novel form of pre-stressed composite is presented, in which tension is applied to nylon 6,6 fibres to induce creep strain, the applied load being removed before moulding them into a resin. After matrix curing, the viscoelastically strained fibres impart compressive stresses to the surrounding matrix, thereby improving mechanical properties without the need to increase mass or section size.

This study investigates the mechanisms considered responsible for VPPMCs improving impact toughness by performing Charpy impact tests on unidirectional nylon 6,6 fibres/polyester resin samples over a range of span settings (24-60mm) and fibre volume fractions (3-17%).

The main findings are (i) improved impact energy absorption (up to 40%) depends principally on shear stress-induced fibre matrix debonding and (ii) energy absorption improves slightly with increasing fibre volume fraction, but the relationship is statistically weak. These are in comparison with identical control (un-stressed) counterparts. Moreover, visual evidence from impact-tested samples, that pre-stressing impedes crack propagation is also demonstrated.

These findings are discussed in relation to improving the impact performance of practical structures.

## 5.1 BACKGROUND

Although, a review of pre-stressed composites is provided in Chapter-2 (Section 2.4), production techniques and specific findings from the literature (most relevant to this Chapter) are summarised here to understand the basic principles of pre-stressing responsible for the improvement in mechanical performance of fibre reinforced composite materials.

The production of VPPMCs involves applying load to the polymeric fibres to induce viscoelastic creep strain. The tensile load is then released before moulding the fibres into a resin (matrix). On solidification of the matrix, compressive stresses are imparted by the strained fibres as they attempt to recover viscoelastic strain. This matrix compression, which is balanced by residual tension within the fibres, improves the mechanical property of the composite. A similar state of matrix compression-fibre tension may also be achieved with an elastically pre-stressed composite (EPPMC), in which fibres are subjected to elastic strain during matrix curing to achieve the required pre-stress.

Results from studies of unidirectional glass fibre EPPMCs indicate that elastic pre-stressing could increase tensile strength by ~25%, elastic modulus by ~50% [66] and impact resistance, flexural stiffness and strength by up to 33% [68, 70], when compared with un-stressed (control) counterparts. Explanations for such improvements have been based on matrix compression and fibre tension effects which can impede or deflect propagating cracks and reduce composite strain resulting from external tensile or bending loads [66, 68, 70]. The long-term mechanical performance of VPPMCs was characterised through Charpy impact testing [8, 9, 11], culminating in the most recent study, which (i) demonstrates no deterioration in impact performance over a duration equivalent to 40°C ambient for ~20 years and (ii) shows that VPPMC samples absorb, on average, ~30% more impact energy than their control (un-stressed) counterparts [10].

To date, viscoelastic pre-stressed samples for Charpy impact testing have only been evaluated at a low fibre volume fraction  $V_f$  (2-3%). To further investigate fracture and energy absorption characteristics of low to high fibre volume fraction composites, this chapter reports on Charpy impact evaluation over a range of test span settings (24 to 60 mm) and  $V_f$  values from 3.3% to 16.6%.

### **5.1.1 CHARPY IMPACT TESTING STANDARDS FOR COMPOSITE MATERIALS**

Mechanical testing is usually the first stage in the process of predicting composite material performance. However, inappropriate or inaccurate test data can almost inevitably lead to questionable predictions. A survey performed in 1987 on standardised mechanical tests concluded that the existing system of test methods is deficient on the following three aspects [121].

- (i) Too many variations
- (ii) Do not fit to the intended purpose
- (iii) Important phenomena and properties are neglected by the testing community

Testing insufficiencies are common in industry, particularly when the material is novel, or the application is innovative. Thus, restrictions in the testing standards can constrain the evaluations needed to understand material performance. In this study, impact performance of nylon 6,6 fibre-based VPPMCs are investigated by (low velocity) Charpy impact testing with the EN ISO-179 standard. In Table 5-1, an overview from the literature in chronological order provided information on typical conditions used for Charpy (flatwise) impact tests on fibre-reinforced polymeric composite specimens. In most cases, a range of failure mechanisms is reported, from fibre debonding or delamination (interlaminar shear) through to tensile, i.e. cleavage-type transverse fractures from brittle specimens. Common ( $L$ ) settings are 40 and 60 mm with extensive ranges of span to thickness ratio ( $L/h$ ) and varying specimen thicknesses.

**Table 5-1. Summary of published Charpy (flatwise) impact tests on fibre-reinforced polymeric composites.**

Year	Ref	Fibre/Matrix	Specimen		Span (mm)	$L/h$	Failure Mode
			Size (mm)	Type			
1976	[130]	Carbon/Epoxy	$55 \times 10 \times 10$	--	40	4	DE
			$55 \times 10 \times 2.5E$	--	40	$16E$	--
1994	[131]	Carbon/Epoxy	$(L+20) \times 10 \times (1-5)$	--	30-100	6-40	D, T
			$(L+30) \times 10 \times 1$	--	60, 90	60, 90	T
1998	[68]	Glass/Epoxy	$81 \times 19 \times 6$	--	$50E$	$8.5E$	D
1998	[132]	Glass/Epoxy	$? \times 5 \times 2$	--	40	20	--
2008	[133]	Carbon/Epoxy	$80 \times 10 \times 3$	2	60	20	D, T
			$80 \times 10 \times 5$	--	60	12	D, T
2008	[134]	Carbon/Epoxy	$80 \times 10 \times 1.7$	--	40	23.5	D, T
2009	[135]	Jute, Cellulose/ PP	--	S	--	--	--
2010	[136]	Glass, Carbon/ Epoxy	$80 \times 15 \times 1.5$	--	$60E$	$40E$	D, T
2010	[137]	Glass/Epoxy	$80 \times 15 \times 4$	1	$62E$	$15.5E$	D, T
2010	[138]	Glass/HDPE, Wood	--	S	--	--	--
2010	[139]	Glass/Nylon	$80 \times 10 \times 4$	1	$62E$	$15.5E$	--
2012	[140]	Wood/PP	$80 \times 10 \times 4$	1	$62E$	$15.5E$	--
2013	[141]	Carbon black, Talc particles/ HDPE	$80 \times 10 \times 4$	1	$62E$	$15.5E$	--
2013	[142]	Rayon textile/ Cellulose	$80 \times 10 \times 3$	--	$62E$	$15.5E$	D
2014	[82]	Carbon/Epoxy	$80 \times 10 \times 2$	--	40	20	--

$E$  = Estimated or inferred from information provided

$S$  = ISO-179 specified with no further information

D = Failure by fibre debonding or delamination

T = Tensile (brittle, cleavage) failure

Charpy testing is a well-known method to evaluate the impact toughness of materials. For plastics, the EN ISO-179 standard [118] describes three test specimen types, detailing their dimensions and required span ( $L$ ). Un-notched Type-2 or Type-3 specimens are used for materials capable of exhibiting interlaminar shear e.g. long fibre-reinforced materials, these being tested ‘flatwise’ or ‘edgewise’ to the pendulum blow direction. Thus flatwise orientation is most appropriate for evaluation of pre-stress effects. Preferred specimen thickness ( $h$ ) is 3 mm for Types-2 and Type-3 and the standard states there are no other specified specimen sizes, the most important parameter being the ( $L/h$ ) ratio for flatwise testing. For Type-2, ( $L$ ) is  $20h$  but this is lower for Type-3, being  $6h$  or  $8h$ . The choice between Type-2 and Type-3 is determined by the nature of failure; according to the standard, these are expected to be tensile-type failures for Type-2 and interlaminar shear failures for Type-3 specimens.

It is well known that the contribution to beam deflection from shearing forces becomes increasingly significant as ( $L/h$ ) is decreased [13]. Adams and Miller [130] highlighted the effects of shear stress during beam failure and, although principally a study based on static flexural testing, they also reported findings from Charpy tests on thick (10 mm) and thinner (~2.5 mm) polymeric composite samples (Table 5-1). For the 10 mm thick sample, contributions from shear effects were increased by the small ( $L/h$ ) value (i.e. 4) and, although the thinner samples raised ( $L/h$ ) to 16, it may be inferred from Ref [130] that this caused no substantial change. In the context of ( $L/h$ ) values, the work of Nagai and Miyairi [131] in Table 5-1 is of particular interest. From Charpy tests, if impact energy is considered to be absorbed within the specimen volume defined by span size, the impact energy per unit volume,  $u$ , can be defined as:

$$u = \frac{U}{bhL} \quad (5-1)$$

Where  $U$  is the measured impact energy and  $b$  is the sample width. It was found in Ref [131], that the contribution from shear-induced delamination failure decreased with increasing ( $L/h$ ), causing  $u$  to reach an approximately constant minimum value for ( $L/h$ )

$\geq 20$  for unidirectional CFRP specimens and  $(L/h) \geq 16$  for woven CFRP samples. Thus provided that  $(L/h)$  is sufficiently large,  $u$  effectively becomes independent of  $L$  and sample dimensions, making it a potentially useful parameter for comparative purposes. By using such large  $(L/h)$  values however, these findings pre-suppose that Charpy test conditions should be set up to promote energy absorption through elastic deflection, followed by failure through transverse fracture, in preference to failure by debonding or delamination. Nevertheless, compared with bending strength, CFRPs have inferior interlaminar shear strength [131] and when subjected to general impact conditions, debonding or delamination becomes a major failure mechanism [134, 143].

### **5.1.2 LITERATURE REVIEW ON PRE-STRESSED COMPOSITE SUBJECTED TO LOW VELOCITY IMPACT LOAD**

In contrast with views supporting the use of large  $(L/h)$  values, to date, Fancey's studies for the evaluation of VPPMCs by Charpy testing has focused on using an  $(L/h)$  value of  $\sim 8$  with sample dimensions ( $80 \times 10 \times 3.2$  mm) being close to ISO-179 Specimen Type-2. Therefore, the appropriate span would have been 60 mm; however,  $L$  was set to 24 mm, in accordance with Specimen Type-3. Originally, the available nylon yarn for moulding VPPMC samples limited  $V_f$  to 2-3%, hence the shorter span prevented the possibility of some samples falling below the minimum energy readings set by the standard [7-11].

Charpy impact testing of EPPMCs by Motahhari and Cameron [68] also adopted a similar  $(L/h)$  value ( $\sim 8.5$ ). They found that the impact energy absorption of glass fibre/epoxy samples could be increased by up to 33% from elastically generated pre-stress, i.e. comparable to that achieved by viscoelastic pre-stressing  $\sim 30\%$  [10]. In Ref [68], the principal mechanism for this improvement was impact-induced fibre-matrix interfacial debonding in preference to transverse fracture of fibres. This debonding mechanism absorbs more impact energy than transverse fracture and is promoted by the

residual shear stresses at fibre-matrix interfaces caused by elastic [68] or viscoelastic [10] fibre pre-stressing.

In this chapter, following from the mechanisms proposed by Motahhari and Cameron [68], it is suggested that pre-stress-induced interfacial shear stresses (which promote debonding) are activated by externally imposed stresses from shearing forces caused by the impact. Thus shear stress-induced debonding from impact is enhanced by the presence of pre-stress. Since the contribution from impact-induced shear effects should decrease with increasing  $(L/h)$ , it is proposed that the benefits provided by pre-stress-induced interfacial shear stresses may diminish at larger span settings (for a constant  $h$ ). A further hypothesis is that samples with higher  $V_f$  values will increase opportunities for energy absorption through pre-stress-enhanced fibre debonding.

It should be noted that studies on unidirectional fibre PMCs commonly refer to failure by delamination, reflecting the use of prepregs [130, 131, 133, 136] as opposed to separate fibres in unidirectional EPPMCs [68] and VPPMCs [10]. In this study, since prepregs are not employed, the term “debonding” is used in favour of “delamination”.

## 5.2 EXPERIMENTAL PROCEDURE

VPPMC sample production and test procedures have been published previously [7-11] and experimental setups are briefly discussed in Chapter-3. However, the production method of nylon fibre-based VPPMC samples for Charpy impact tests is summarised here. Batches of composite samples were produced at three nominal  $V_f$  values, i.e. 3.3%, 10.0% and 16.6%. For each batch nylon 6,6 yarn was annealed in a fan-assisted oven for 30 minutes at 150°C. One set of yarn was attached to a stretching rig-b (shown in Chapter-3, Figure 3-3) and subjected to 340 MPa tensile creep stress for 24 hours. The annealed control yarn was positioned close to the stretching rig for exposure to the same

ambient conditions ( $20\pm 2^\circ\text{C}$ ,  $40\pm 10\%$  RH). Then both yarns were folded, cut into appropriate lengths and combed into flat ribbons ready for moulding.

Immediately prior to moulding, control yarns were observed to exhibit slightly more waviness than corresponding pre-stretched test yarns. Since  $V_f$  calculations were simply based on the fibre cross-sectional area,  $V_f$  would have tended to be higher in the resulting composite control samples. Nevertheless, the effect on  $V_f$  will have been minimal; from linear measurements of test and control yarns,  $V_f$  was calculated to be less than 1.015 times that of composite test sample counterparts.

The matrix resin for composite samples was Cray Valley Norsodyne-E9252, mixed with 1% MEKP catalyst, supplied by CFS Fibreglass Supplies, UK. This was a clear-casting polyester resin, selected for high filler loading capability. The resin gel time was  $\sim 15$  minutes and it was cured after 2 hours (at room temperature).

Unidirectional continuous fibre composite samples were prepared by open-casting. Two aluminium moulds were used each with a 10 mm wide channel of 3 mm depth, enabling a strip of test and control materials to be cast simultaneously from the same resin mix (shown in Figure 3-5). This procedure was completed within 30 minutes of the fibre stretching process. Following de-moulding, test and control composite strips were each cut into five samples, the sample size being  $80\times 10\times 3.1$  mm. Tolerance on sample thickness was  $\pm 0.1$ mm. These samples were then held under a weighted steel strip for 24 hours to prevent potential bending effects from internal stresses. Then the batch (5 test and 5 control samples) was sealed in polythene bags and stored at room temperature ( $20\pm 2^\circ\text{C}$ ) for 336 hours (two weeks) prior to impact testing.

A Ceast Resil-25 Charpy machine (non-instrumented) with a 7.5 or 15 J hammer was used for impact testing at  $3.8\text{ ms}^{-1}$ , which operated in accordance with the BSI-179 standard [118]. As reported in Chapter-3 (Section 3.3.1), it was observed that the fibres tended to settle towards the bottom of the mould prior to curing. This was previously

reported by Fancey for Charpy-based studies using open-cast polyester matrix samples [7-11]. Similar to Fancey's approach, samples were mounted with the fibre-rich side facing away from the pendulum hammer, schematically illustrated in Figure 5-1 with the three span settings investigated, i.e. 24, 40 and 60 mm.

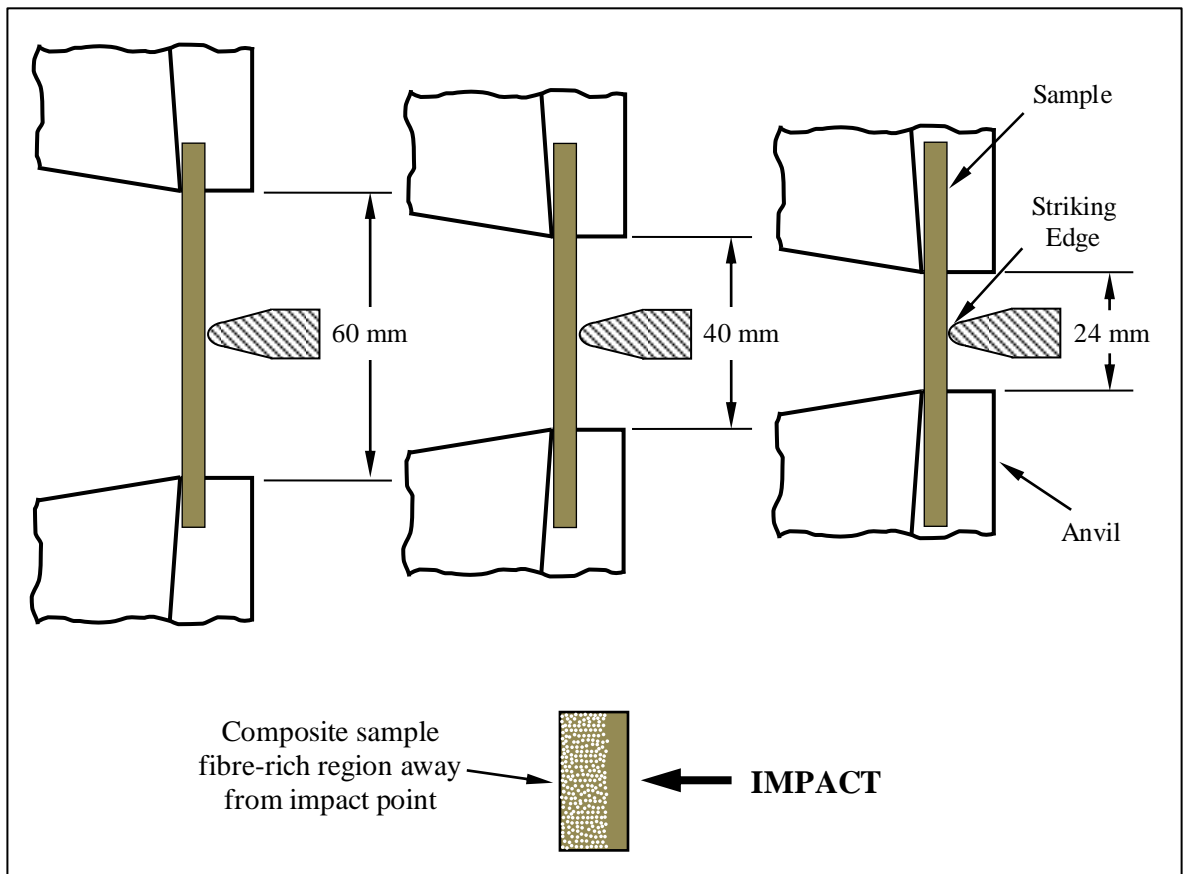


**Figure 5-1. Schematic illustration of Charpy impact tests setup.**

For each  $V_f$ , three batches were impact tested at the span settings shown in Figure 5-1. Despite meticulous set-up procedures and alignment checks, some samples at 40 and 60 mm spans were observed to be susceptible to being struck off-centre by the Charpy hammer, the effect being most significant at 60 mm span.

## 5.3 RESULTS AND DISCUSSIONS

### 5.3.1 FIBRE SPATIAL DISTRIBUTION IN COMPOSITE SAMPLES

Charpy sample fibre distributions were examined by optical microscopy. Figure 5-2 represents typical fibre spatial distributions of all samples studied. For both test (pre-stressed) and control (un-stressed) samples, fibre concentration was greatest towards the bottom of the moulding, the effect being most prominent at 3.3%  $V_f$ , where the fibre-rich region occupies only ~35–40% of the cross-sectional area. As reported in Section 5.2, this concurs with previous Charpy-based studies using open-cast polyester matrix samples; hence  $V_f$  calculations represent average values.

Of particular concern however, was whether there were any systematic differences in spatial distribution between equivalent test and control samples. Figure 5-2 shows some tendency towards the concentration gradient of fibres in control samples being more diffuse than the corresponding test samples. Although this may be attributed to control yarn waviness, it was not observed in cross-sections from a previous study [13], where a different polyester resin was used. Thus minor differences in resin curing characteristics may have exacerbated this effect. A more diffusely distributed layer of fibres might be expected to increase the total fibre-matrix interface area available for energy absorption (through debonding), thereby preferentially improving the Charpy impact toughness of the control samples. In the worst case, this combined with the marginally higher  $V_f$  in the control samples, would therefore reduce differences in impact toughness observed between test and control groups. However, although undesirable, it is suggested that the effects would be sufficiently small to be negligible.

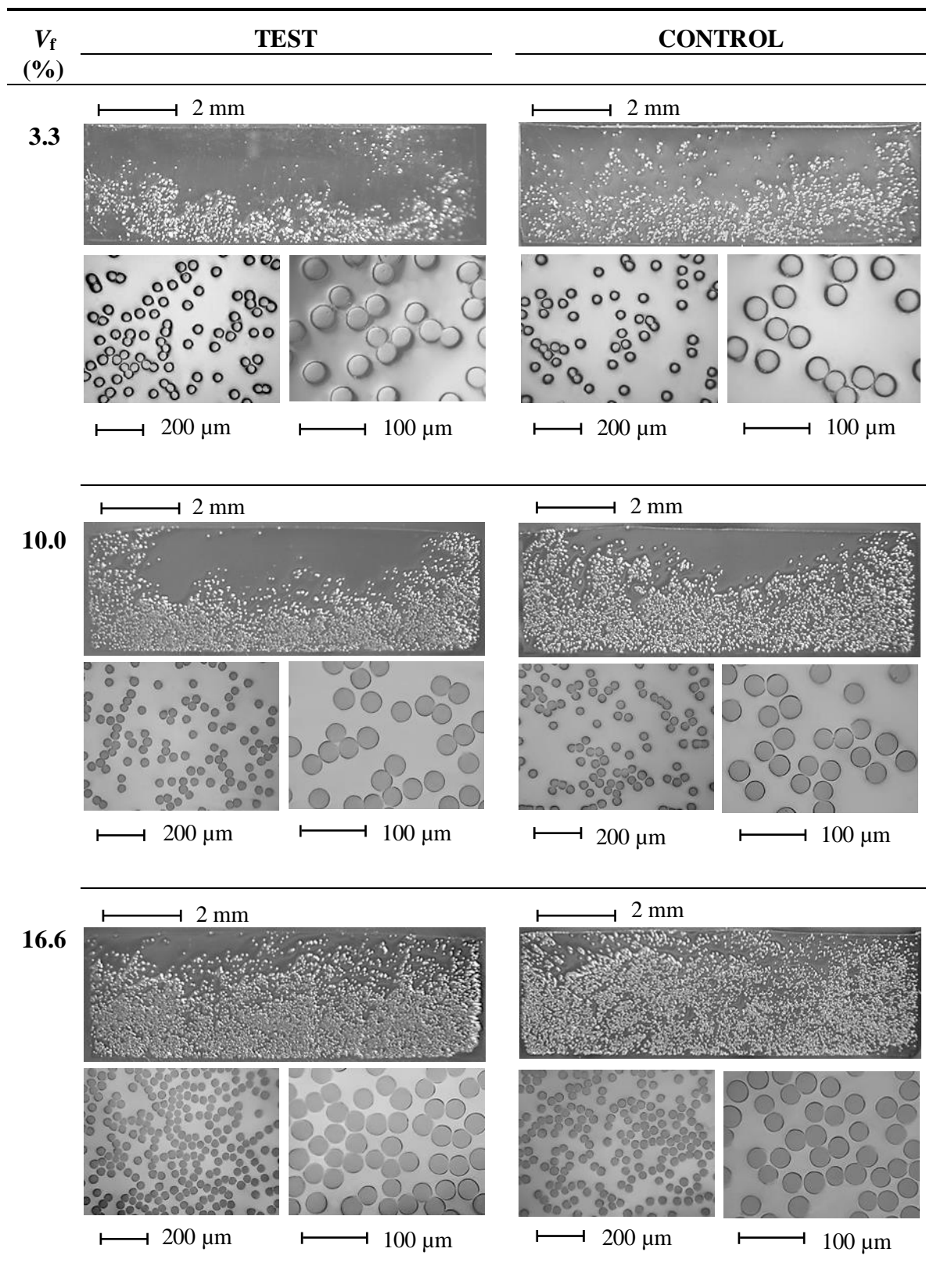


**Figure 5-2. Representative optical micrograph (polished) sections of nylon 6,6 fibre spatial distribution of composite samples evaluated from open-casting with polyester resin. Note  $V_f$  values are nominal.**

### 5.3.2 INITIAL OBSERVATIONS ON IMPACT ENERGY ABSORPTION

Table 5-2 summarises the impact test data. From this, Figure 5-3 shows the increase in impact energy absorbed (test samples relative to control counterparts) as a function of  $V_f$  for each span setting. The considerable batch-to-batch variation seen in Table 5-2 is denoted by the error bars, these representing uncertainty in the mean values (standard errors).

For data at 60 mm span, there are further concerns, because the effects of batch-to-batch variability have been exacerbated by low increases in energy. Table 5-2 shows two batches producing (small) negative increases in energy absorbed at 3.3%  $V_f$  and one batch at 16.6%  $V_f$  is effectively zero. It is observed that some samples at larger span (40 and 60 mm) were being struck off-centre by the Charpy hammer. Thus any potentially observable trend in Figure 5-3 requires caution.

In contrast, some conclusions may be drawn from data at the other span settings. At 40 mm span, the three data points in Figure 5-3 show an approximately linear trend. Each of these data points are, however, means from three batches and, when a least squares fit of the nine individual batch values for energy increase (Table 5-2) is performed, the correlation coefficient (0.540) indicates no linear correlation, statistically, at 0.05 significance level. Although a linear relationship in the 40 mm span data may be ruled out, there is still a modest increase in energy absorbed by test samples, i.e. from ~9% (3.3%  $V_f$ ) rising to ~15% (16.6%  $V_f$ ). Because of error bar magnitudes however, a one-tailed  $t$ -test is required to compare the means at 3.3% and 16.6%  $V_f$ . This demonstrates that the observed increase at 16.6%  $V_f$  is significant at 0.10 but not at the 0.05 level. Thus it suggests that there is only a weak positive trend between increase in impact energy and fibre volume fraction  $V_f$ .

**Table 5-2. Charpy impact test data from nylon fibre composite batches: 5 test (pre-stressed) and 5 control (un-stressed) samples per batch tested at 24, 40 and 60 mm span settings. Data is normalised by dividing impact absorbed energy (J) by the cross-sectional area of the sample. S.E is the standard error of the mean. Note  $V_f$  values are nominal. (Individual tested sample data are presented in Appendix-B).**

$V_f$ (%)	Span (mm)	Mean impact energy ( $\text{kJm}^{-2}$ )		Increase in energy (%)	Mean increase in energy (% $\pm$ S.E)
		Test $\pm$ S.E	Control $\pm$ S.E		
3.3	24	91.2 $\pm$ 1.0	61.8 $\pm$ 3.2	47.5	38.9 $\pm$ 4.5
		92.0 $\pm$ 2.0	69.6 $\pm$ 1.5	32.1	
		88.7 $\pm$ 4.0	64.7 $\pm$ 1.5	37.1	
	40	71.1 $\pm$ 2.5	64.9 $\pm$ 2.1	9.5	8.7 $\pm$ 4.1
		73.4 $\pm$ 3.1	63.7 $\pm$ 2.2	15.2	
		67.6 $\pm$ 2.1	66.7 $\pm$ 4.4	1.3	
	60	33.9 $\pm$ 2.5	35.4 $\pm$ 3.2	- 4.1	-1.0 $\pm$ 2.7
		41.9 $\pm$ 3.7	40.1 $\pm$ 0.8	4.3	
		38.9 $\pm$ 1.9	40.1 $\pm$ 1.7	- 3.1	
10.0	24	250.8 $\pm$ 6.1	165.6 $\pm$ 9.6	51.4	34.0 $\pm$ 9.3
		204.9 $\pm$ 12.9	156.4 $\pm$ 7.0	31.0	
		205.8 $\pm$ 13.7	171.8 $\pm$ 13.9	19.8	
	40	160.2 $\pm$ 1.8	149.1 $\pm$ 3.3	7.5	12.3 $\pm$ 3.0
		179.8 $\pm$ 2.4	152.7 $\pm$ 4.0	17.7	
		143.6 $\pm$ 2.7	128.5 $\pm$ 1.3	11.7	
	60	87.5 $\pm$ 2.7	78.1 $\pm$ 4.9	12.1	13.4 $\pm$ 1.5
		85.6 $\pm$ 2.9	76.6 $\pm$ 5.0	11.7	
		85.7 $\pm$ 3.9	73.6 $\pm$ 2.6	16.4	
16.6	24	265.8 $\pm$ 8.9	214.2 $\pm$ 9.4	24.1	25.6 $\pm$ 1.4
		300.7 $\pm$ 8.3	234.4 $\pm$ 9.9	28.3	
		282.7 $\pm$ 2.4	227.4 $\pm$ 9.1	24.3	
	40	202.5 $\pm$ 2.2	175.3 $\pm$ 5.5	15.5	15.3 $\pm$ 1.3
		212.5 $\pm$ 4.6	181.0 $\pm$ 5.7	17.4	
		217.5 $\pm$ 4.3	192.5 $\pm$ 5.1	13.0	
	60	103.9 $\pm$ 2.6	103.8 $\pm$ 4.5	0.1	9.3 $\pm$ 4.6
		99.4 $\pm$ 1.8	87.8 $\pm$ 5.4	13.3	
		111.5 $\pm$ 1.5	97.4 $\pm$ 1.7	14.5	

In Figure 5-3 below, at 24 mm span, the increase in impact energy is reduced from ~39% at 3.3%  $V_f$  to ~26% at 16.6%  $V_f$ , i.e. a 1/3 reduction. A one-tailed  $t$ -test (0.05 level) shows this reduction is statistically significant. Since this negative trend does not occur at the 40 mm span, this suggest, it can be attributed to an increase in drag caused by the greater resistance from higher  $V_f$  samples being forced through the Charpy anvil supports following impact. Higher  $V_f$  samples will have been stiffer and thus more resistant to deformation (immediately after fracture) during this event, and resistance from drag provided by test or control samples (giving additional energy absorption) would have been similar, irrespective of pre-stress effects.

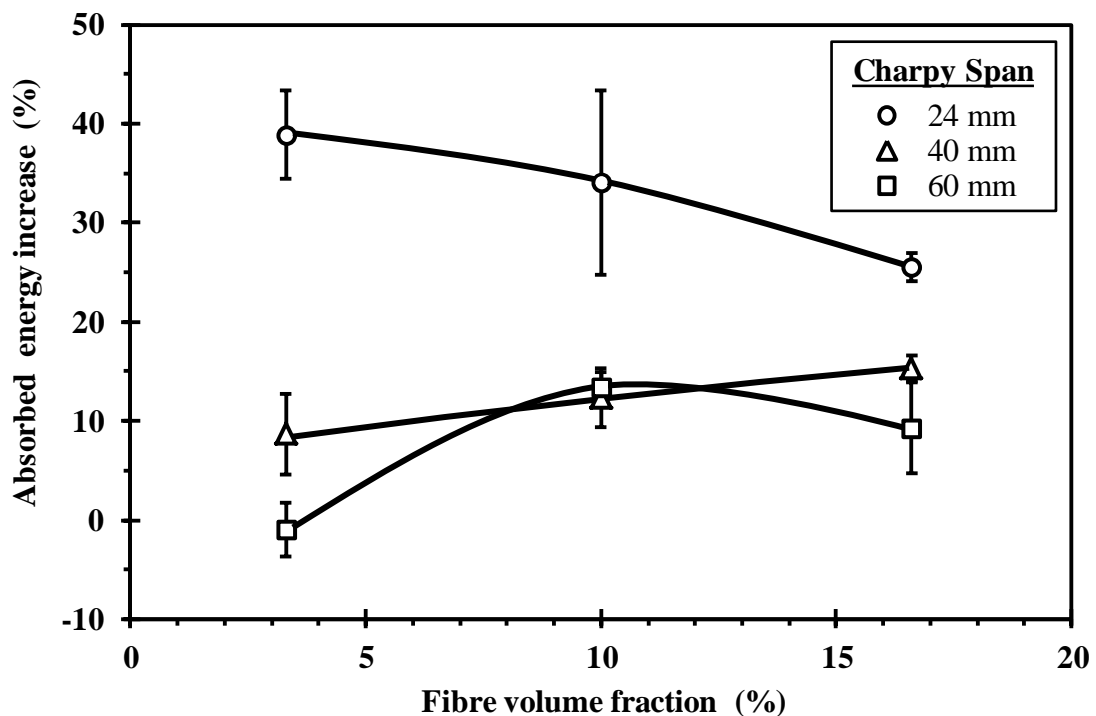


**Figure 5-3.** Mean increases in impact energy (test samples relative to identical control counterparts) with standard error, as a function of fibre volume fraction  $V_f$  (data from Table 5-2).

Figure 5-4 shows representative fractures from test (pre-stressed) and control (un-stressed) samples at the three span settings. For all  $V_f$  values at 24 mm span and all span settings at 3.3%  $V_f$ , samples generally exhibited a small cluster of fractures in the central region, sometimes with a vertical crack at either side in the vicinity of the Charpy anvil shoulders. This was consistent with samples being pushed through the anvil shoulders following impact and remaining in a deformed state with a ‘V’ shaped profile after testing. For 10% and 16.6%  $V_f$ , a wider spread of multiple (mainly) vertical cracks was observed, particularly at larger spans, concurring with a transition to fractured samples with more curved deformation profiles. Larger spans also left samples with less residual deformation after testing. It can be seen from Figure 5-4 below that the debonding region of test samples are greater than control, this can be observed in all span settings. Previously, nylon fibre-based VPPMC impact studies (at 24 mm span) have shown the same debonding effects [7, 8, 10, 11].

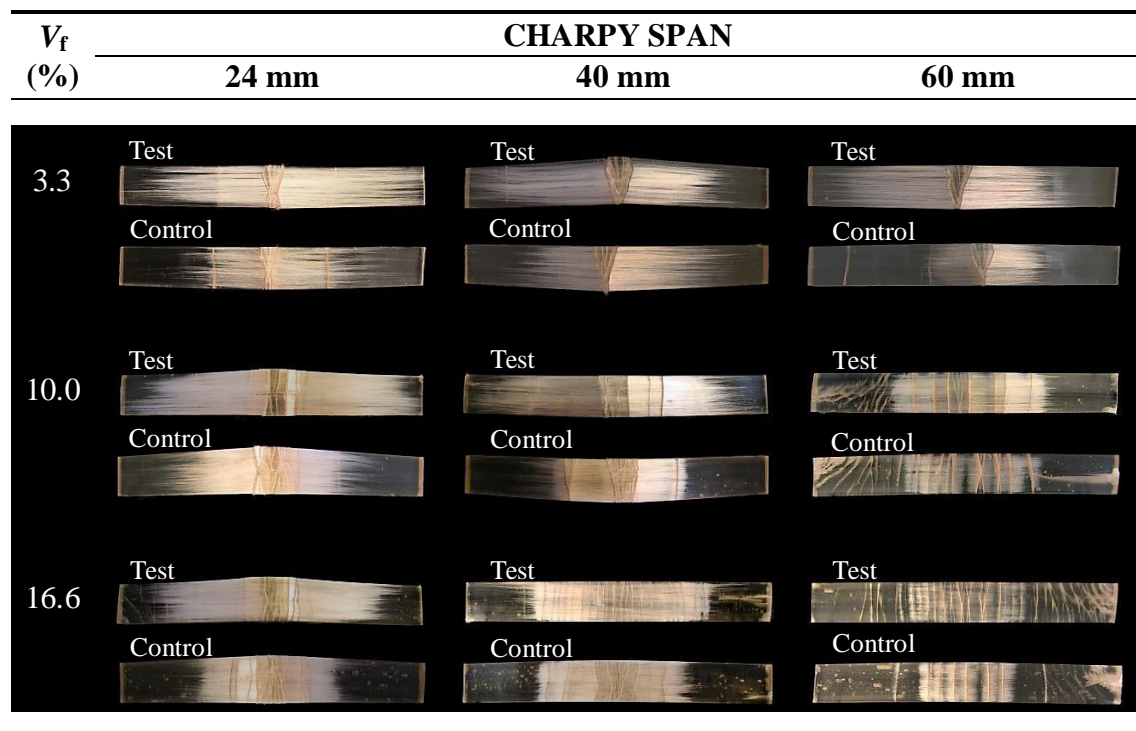


**Figure 5-4. Representative fracture and debonding characteristics observed from test (pre-stressed) and control (un-stressed) samples for each  $V_f$  value and span setting. Note photos are taken from the fibre-rich side (away from the impact point).**

As reported earlier, samples tested at larger spans were most susceptible to being struck off-centre by the Charpy hammer. Owing to the more centralised fracture pattern, this was more easily observed at 3.3%  $V_f$  (Figure 5-4). It is estimated that ~60% of all 3.3%  $V_f$  samples tested at 60 mm span were fractured 3-8 mm off-centre. At 10% and 16.6%  $V_f$ , more than half of the 60 mm span samples also showed multiple diagonal cracking at one end (visible in Figure 5-4). Unlike through-thickness damage in the main fracture region, these cracks are restricted to the matrix-rich side (facing the hammer). This suggests that the off-centre impacts and diagonal cracking are symptoms of (unwanted) lateral sample movement during testing; this can be attributed to the limited sample support at the 60 mm span setting.

In addition to the greater debonding regions in the test samples (compared with their control counterparts) at all  $V_f$  and span settings, Figure 5-4 shows the multiple vertical cracks at larger spans tending to produce debonding regions of a more discontinuous nature for higher  $V_f$  test and control samples. Therefore, further visual inspection on impact tested samples was conducted with a Shinko profile projector, in which profiles of the debonding regions were highlighted by transmitting light through the sample surface. In order to gain a better insight into the debonded regions, sample profiles were magnified (with 10x-50x optical lenses), as shown in Figure 5-5 below.

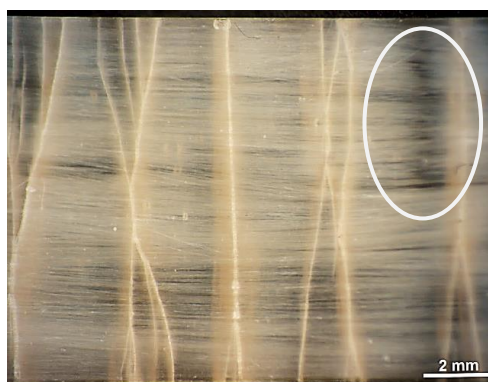


**Figure 5-5. Representative micrograph of the nylon fibre sample tested at 60 mm Charpy span settings. Local debonding between matrix cracks is clearly visible, indicated by the circled region. Note photo taken from fibre-rich side of sample (away from impact point).**

### 5.3.3 IMPACT TESTING SPAN EFFECTS

In general, when a sample is struck by a Charpy hammer, cracks are wider at the tension side and narrow towards compression side. Therefore, fibres away from the impact zone would be expected to face high tensile stresses. To further examine the failure mechanism of samples, such as bending and fracture during impact tests, high speed video photography was recorded by using Casio camera Ex-FH100 with a speed rate of 420 frames per second; a series of video stills from an impact event is shown in Figure 5-6.

It was observed, during the impact event, the freely supported sample initially bends from the impact load and in consequence cracks are initiated on the tension side (opposite to the impact point). As the load duration continues, sample deflection increases, which encourages transverse crack propagation at the highest shear-stress region (mid-point). At a shorter span setting (24 mm), cracks propagate in the brittle matrix material until they reach reinforcing fibres; the cracks then propagate parallel to the fibres due to the debonding mechanism at fibre/matrix interface. At a larger span (60 mm), samples bend excessively from the impact load because of the small support (10 mm each side), and slips between the support anvils before being fully loaded by the hammer. These effects are further discussed in the next section.

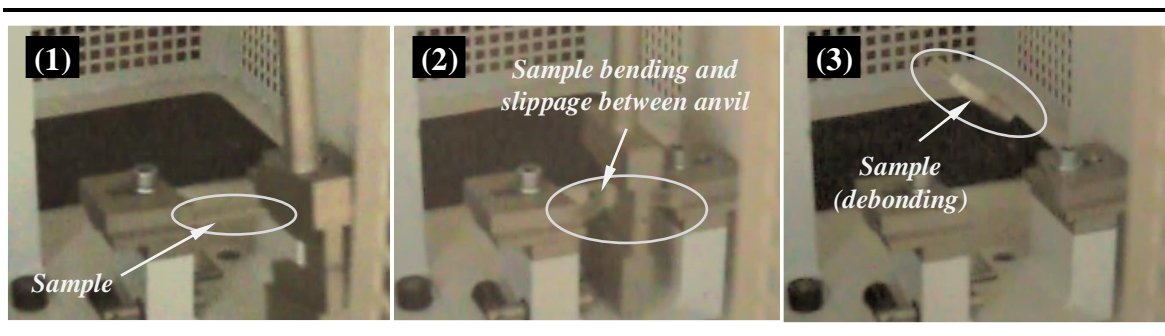


**Figure 5-6. High speed camera footage ( $3.8 \text{ ms}^{-1}$ ) highlighting impact event from a nylon-fibre composite sample tested at 60 mm span setting. It can be seen, initially the sample bends at mid-point and slips between anvils (image-2), because of the small support (10 mm each side); For clarity, sample is highlighted by arrows.**

### 5.3.4 PRE-STRESS EFFECTS AND FRACTURE OBSERVATIONS

As discussed in Chapter-2, failure mechanisms in a composite material involve matrix cracking, fibre breakage and debonding. Studies by others have shown that during the fracture process, fibres make bridges between crack surfaces which reduce crack propagation [84]. It is a well-known phenomenon that transverse shear stresses from impact loads lead to the propagation of cracks by breaking fibre bridges. Although fibre reinforcement in a matrix is known to provide significant resistance to crack propagation, previous studies have suggested that compressive pre-stressing enhances such benefits [10, 68]. This supports the observation in Figure 5-7, in which crack propagation is significantly reduced by the pre-stress effect. This validates the proposed Mechanism-I (pre-stress impeding crack propagation). Other researchers [62, 64] also reported that crack development in pre-stressed composites is reduced by pre-stressing. Similar effects were observed by Rose and Whitney [96] from studies on carbon fibre/epoxy laminates, in which failure of the first ply was delayed by pre-stressing. However, no visual evidence was provided in the literature and Figure 5-7 provides the first such evidence.

In addition, it was observed that following impact, composite samples tended to return to their original (straight) position. It can be seen from Figure 5-7, in the pre-stressed composite sample, fibres in the matrix crack appear to have undergone lateral expansion (swelling) resulting in increasing fibre diameter, in contrast with their control (un-stressed) counterparts, in which fibres bend following impact. Clearly, the underlying cause must be attributed to the active viscoelastic recovery behaviour of the fibres in the test sample. A possible explanation is that fibres on the compression side of the sample attempt to pull cracks together by long-term viscoelastic recovery behaviour, resulting in narrowing the crack width.

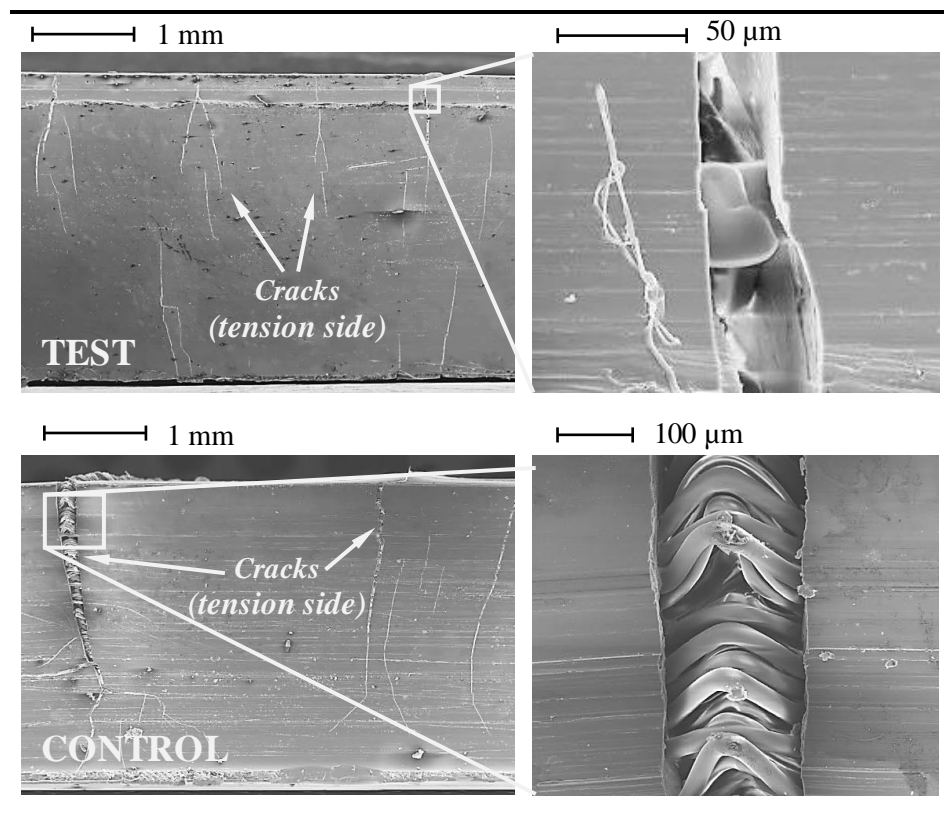


**Figure 5-7. Representative SEM micrograph cross-sections of impact tested nylon-fibre composite sample showing pre-stress affecting crack propagation. The crack width in pre-stressed sample is narrow in comparison with the un-stressed counterpart. These samples were stored in a laboratory at room temperature for 336 hours (2 weeks) prior to impact testing. SEM micrographs were taken at 3300 hours (~5 months) after test. Note differences in magnification.**

Representative SEM fracture morphologies of nylon-fibre composite samples at 3.3% and 16.6%  $V_f$ , subjected to impact tests at span settings of 24 mm and 60 mm are presented in Figure 5-8 and Figure 5-9. Selected areas at higher magnification are also shown. It is observed that the damage mechanism involves fibre fracture, fibre/matrix debonding and matrix cracks in all cases. However, fibre fracture in the control samples is more dominant, especially for the low  $V_f$  samples tested at 24 mm span. Of particular interest, high  $V_f$  samples tested at 60 mm span (Figure 5-9) show no significant difference in fracture morphologies between test and control samples, supporting findings of Table 5-2, i.e. less benefit from pre-stressing. Also, swelling of fibres in pre-stressed composites is visible, which is not observed in the control samples (similar to Figure 5-7). However, to understand this effect more thoroughly, would require further investigations which are beyond the scope of this thesis.

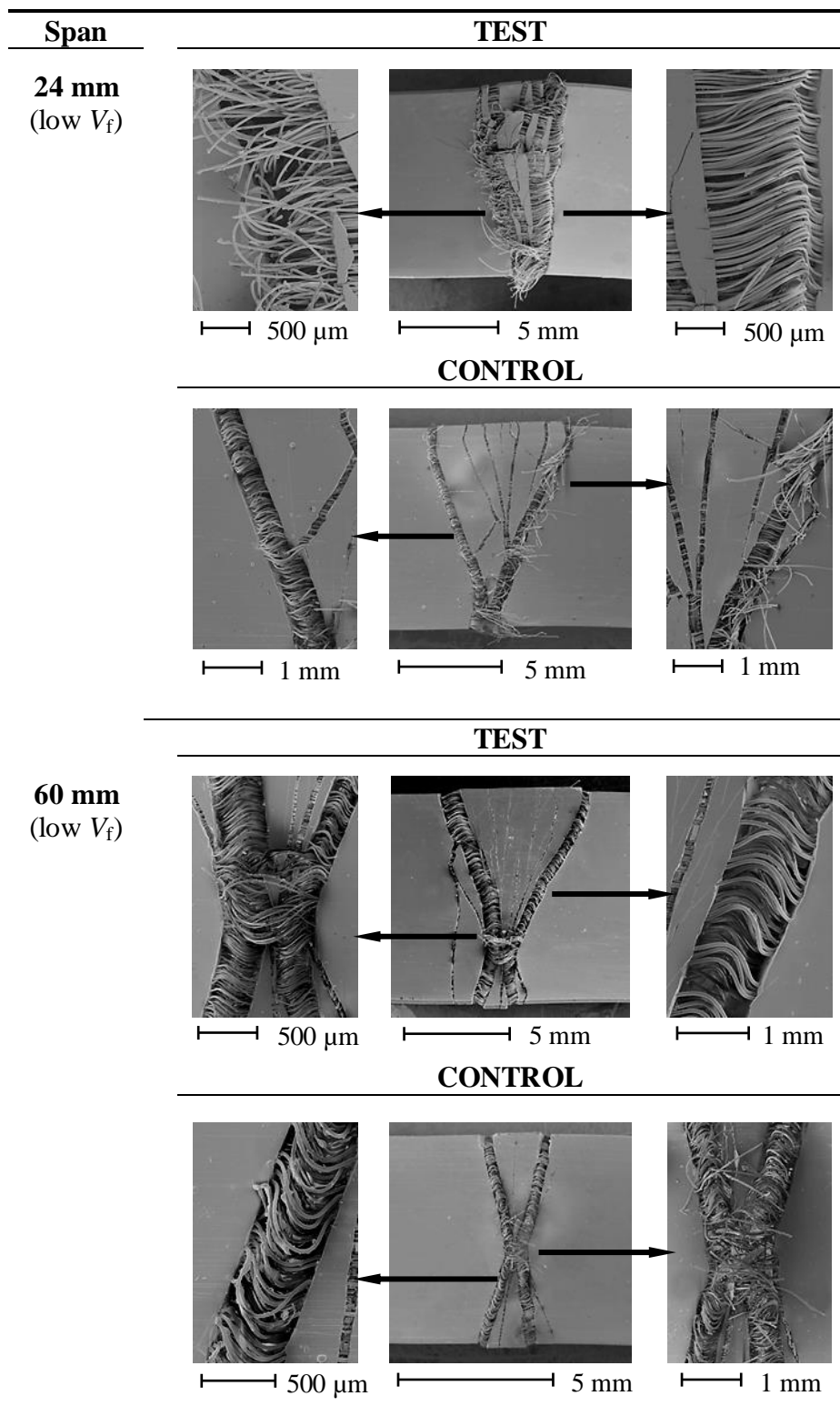


**Figure 5-8. Representative SEM micrograph cross-sections of nylon-fibre composite samples (low  $V_f$  3.3%) subjected to Charpy impact tests at span settings of 24 and 60 mm. Samples were stored at room temperature for 336 hours (2 weeks) prior to testing. SEM micrographs were taken at 3300 hours (~5 months) after impact tests. Similar features are observed in all samples; higher magnified images of the selected area are highlighted by arrows; note differences in magnification.**

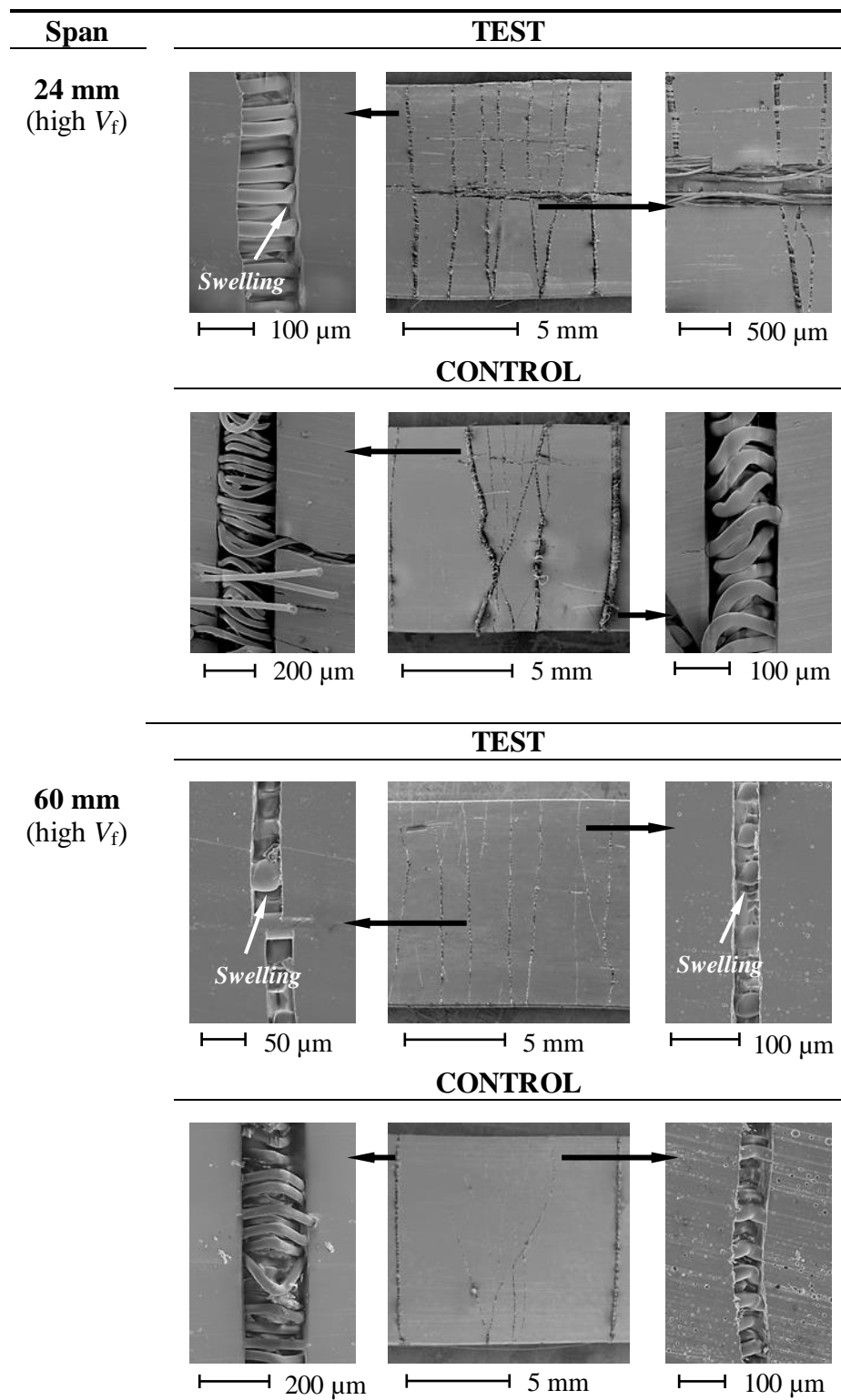


Figure 5-9. Representative SEM micrograph cross-sections of nylon-fibre composite samples (high  $V_f$  16.6%) subjected to Charpy impact tests at the span settings of 24 and 60 mm. Samples were stored at room temperature for 336 hours (2 weeks) prior to testing. SEM micrographs were taken at 3300 hours (~5 months) after impact tests. Similar features are observed in all samples; higher magnified images of the selected area are highlighted by arrows; note differences in magnification.

### 5.3.5 EFFECTS OF SPAN AND FIBRE VOLUME FRACTION ON ENERGY ABSORPTION

By plotting the mean impact energy data for test and control batches as a function of span settings, Figure 5-10 shows that with increasing span ( $L$ ), (i) energy absorption by both test and control groups decreases and (ii) the increase in energy absorbed by test samples over their control counterparts diminishes. Additionally, (iii) the change in energy absorbed by control samples is less sensitive to a change in span for  $24 < (L) < 40$  mm. These observations are discussed in detail below.

Figure 5-10 suggests that for samples tested at larger spans, energy absorption can be attributed to an increasing contribution from elastic deflection as the sample is forced through the anvil shoulders, with less contribution from fracture-inducing (plastic) deformation. Thus less energy becomes absorbed from fracture-based mechanisms during the impact process. This corresponds with the increasing prevalence of multiple vertical cracks and reduced residual deformation of samples at the larger span settings, i.e. samples retain their initial “straight” position (Figure 5-4). Secondly, increased energy absorption resulting from pre-stress must depend on the contribution from shear stress during impact, the latter decreasing as span setting ( $L$ ) is increased. Since there is no pre-stress effect in the control samples, this may also explain their energy absorption characteristics would be less sensitive to increasing contributions from shear at the shorter span settings.

Based on the data plotted in Figure 5-10, span settings have a profound effect on increase in energy absorption (from pre-stress), which also changes with  $V_f$ . For 24 mm span setting, the testing configuration was close to ISO-179 Specimen Type-3, the only difference being that the length of samples (80 mm) was greater than that recommended by the standard (33 or 39 mm for  $h = 3$  mm). Although, ISO-179 states that the most important (geometric) parameter is the span to thickness ( $L/h$ ) ratio [118]. However, current findings indicate that drag effects, especially from the higher  $V_f$  samples, have some influence on impact energy data at short span settings. As illustrated in Figure 5-

11 (24 mm span), this must be expected; if the Charpy hammer pushes the fractured sample through the anvil shoulders following impact, clearance either side of the 10 mm wide hammer will only be 4 mm for a 3 mm thick sample. Although the longer sample lengths used in this study would have worsened the effect, it is highly probable that impact energy readings from shorter (Specimen Type-3) fibre-reinforced samples, in which hinged (incomplete) breaks occur, would also be affected by drag. At 24 mm span, the increase in impact energy is reduced from  $\sim 39\%$  ( $3.3\% V_f$ ) to  $\sim 26\%$  ( $16.6\% V_f$ ) in Figure 5-3. This can be attributed to an increase in drag caused by the greater resistance from samples with higher  $V_f$  being forced through the Charpy anvil support following impact. Also, the resistance from drag would have been similar for both test and control samples, irrespective of pre-stress effects.

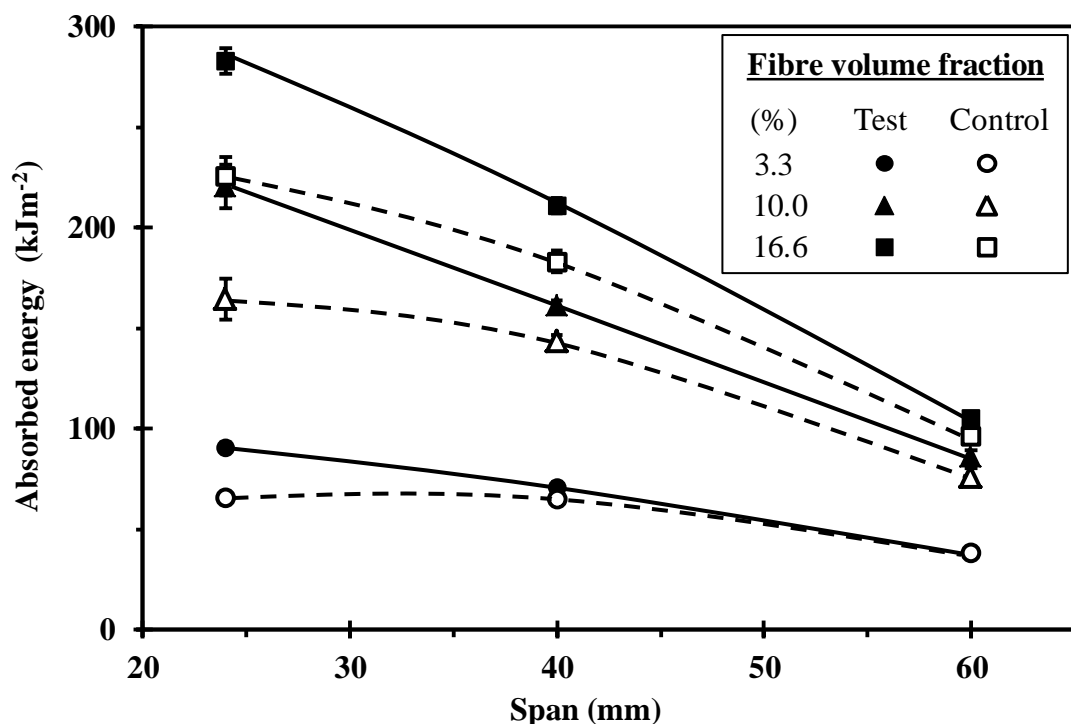
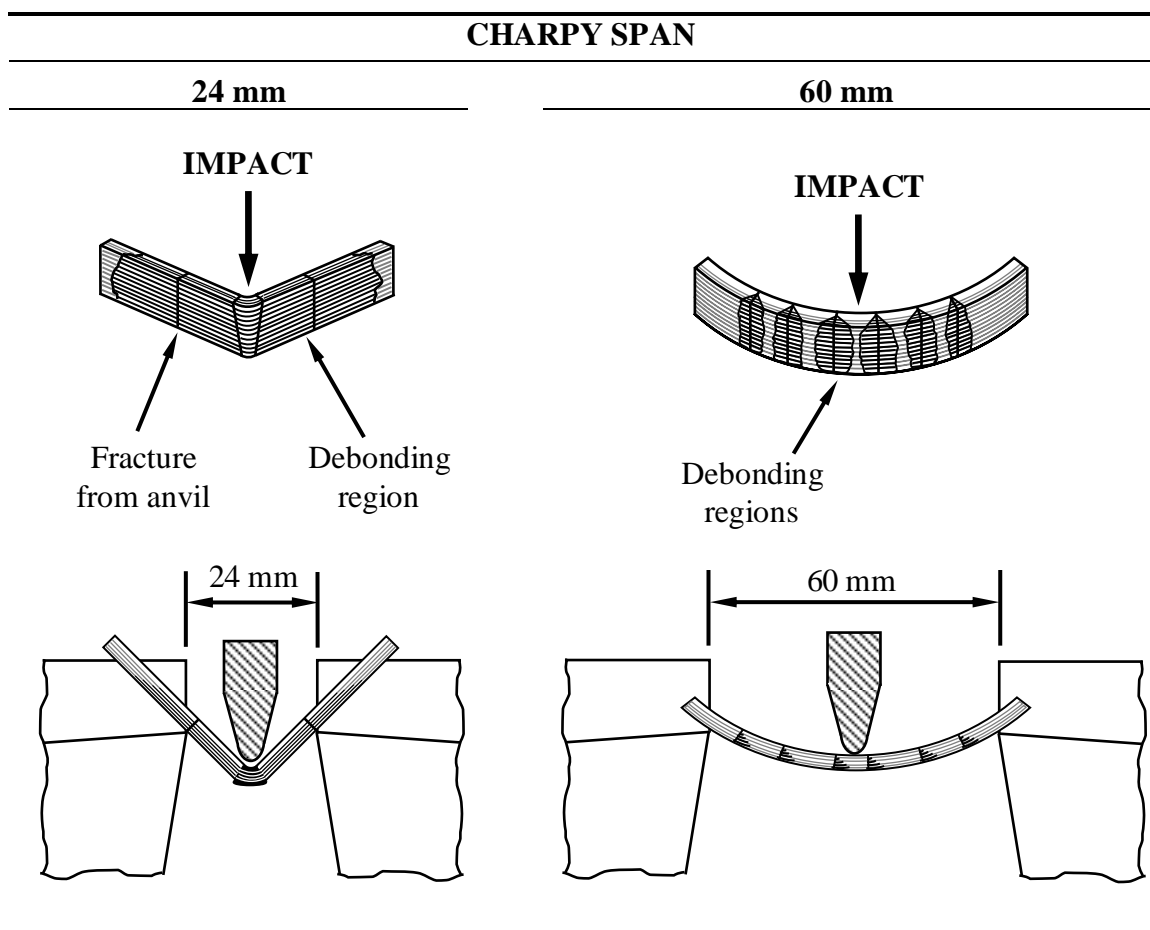


Figure 5-10. Mean impact energies from test (pre-stressed) and control (no pre-stress) nylon fibre composite as a function of Charpy span setting. Data points with standard error bars are the means from three batches (data from Table 5-2).

At 60 mm span, the impact energy absorption can be attributed to an increasing contribution from elastic deflection as the sample is forced through the anvil shoulders, with less contribution from fracture-inducing (plastic) deformation (as illustrated in Figure 5-11). Thus although drag effects could have been negligible, samples deflecting elastically (prior to the onset of fracture mechanisms) will have been significant at the 60 mm span setting. Cantwell and Morton [144-146] investigated damage in CFRP laminates induced by impact loading and their effects on low to high span to thickness ratios. Their work showed that impact damage in a low span to thickness ratio occurred through shear stresses whilst at the high span to thickness ratio, a large amount of kinetic energy supplied by the projectile was absorbed by elastic deformation (bending). Based on previous flexural modulus studies [13], pre-stressed samples in the current work could have been up to 50% stiffer than their control counterparts. Therefore, they may have absorbed more energy through elastic deflection.



**Figure 5-11.** Schematic illustration of the fracture processes at 24 and 60 mm Charpy span settings.

For 60 mm span ( $L$ ), the testing configuration was ISO-179 (Specimen Type-2). In contrast with shorter spans, the contribution to energy absorption from shear would have been comparatively small. Instead, following elastic deflection, samples would have exhibited simple transverse fracture, had they been as brittle as CFRP (this is discussed further in Section 5.3.6). Based on previous nylon fibre-based VPPMC bend test studies [13], Pang and Fancey estimated flexural modulus values for all samples were  $<10$  GPa, i.e. very low in comparison with, for example, GFRP (55 GPa) or CFRP (120 GPa) specimens used for Charpy tests [131, 132]. Thus although drag effects could have been negligible, samples deflecting elastically (prior to the onset of fracture mechanisms) will have been significant at the 60 mm span setting. A further concern with the 60 mm span setting was the frequent tendency for samples to be struck off-centre by the Charpy hammer. Vibrations and transient effects have been cited as complicating factors in pendulum-type impact tests [117] and dynamic analysis has demonstrated that a Charpy sample is not constrained as a simply supported three-point bend specimen [147]. Also, significant elastic deflection and limited support from the anvil base, coupled with uncertainty in the location of crack initiation (due to samples being un-notched), would have increased opportunities for unwanted lateral sample movement.

For the 40 mm span setting, the effect of  $V_f$  can be assessed without complications associated with the other two spans being significant. Analysis of the data (Figure 5-3) suggests only a statistically weak rise in energy absorbed by test samples (over their control counterparts) with  $V_f$ . A previous study [12] has shown there is an optimum  $V_f$  (~35-40%) at which VPPMCs provide the greatest improvement in tensile properties: this optimum was simply explained by the competing roles of fibres (which generate the available stress) and matrix (over which the stress can function). For Charpy (i.e. flexural) loading conditions, the situation is clearly much more complex. Three-point bend test studies [13] have indicated that the increase in flexural stiffness from viscoelastic pre-stress was insensitive to the limited  $V_f$  range studied (8-16%) and, although samples were not fractured in Ref [13], this insensitivity corresponds at least, with the current findings.

### 5.3.6 EFFECTS OF SPAN AND FIBRE VOLUME FRACTION ON ENERGY PER UNIT VOLUME

Referring to Equation 5-1 (Section 5.1.1), Figure 5-12 shows plots of energy/unit volume ( $u$ ) versus span to thickness ( $L/h$ ) for test and control samples at the highest and lowest  $V_f$  values investigated. In Figure 5-12, the contribution to energy absorption from shear stress-induced debonding is increases as  $L/h$  is reduced, which compares with Figure 5-10. Also shown for comparison are data from Ref [131] for unidirectional CFRP specimens over the same  $L/h$  range ( $L = 30-100$  mm;  $h = 3$  or 5 mm). Although  $V_f$  for the CFRP is unknown, it is suspected that it exceeded the  $V_f$  values investigated in this work.

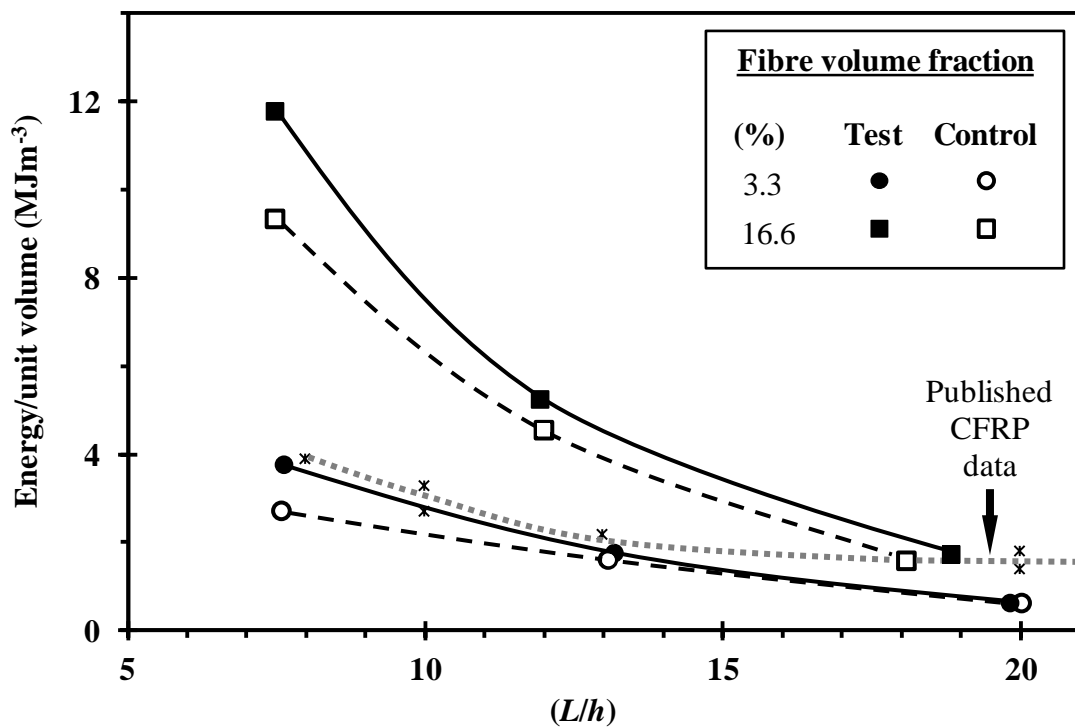


Figure 5-12. Dependence of impact energy/unit volume ( $u$ ), on span to thickness ratio ( $L/h$ ) for test (pre-stressed) and control (un-stressed) samples at 3.3% and 16.6%  $V_f$ . Also shown are CFRP data at comparable  $h$  values from Ref [131].

As  $L/h$  decreases, Figure 5-12 clearly shows that energy/unit volume ( $u$ ) for the 16.6%  $V_f$  (un-stressed) control samples increases faster than the CFRP data. This reflects the inherent toughness of the nylon fibre (even at relatively low  $V_f$ ), which demonstrates the energy absorbing capability of fibres being of great importance for low velocity impact resistance [15]. It is also apparent that at the lowest  $V_f$  (3.3%), brittle matrix characteristics become more significant as results lie close to the CFRP data. The (pre-stressed) test samples show higher ( $u$ ) values as ( $L/h$ ) decreases. This demonstrates the increasing effect of energy absorption from larger (shear stress-induced) debonding areas (Section 5.3.5).

As ( $L/h$ ) approaches 20, both test and control samples at 16.6%  $V_f$  show  $u$  values comparable to the CFRP data. In contrast with the multiple vertical cracking observed in samples tested at larger spans (Figure 5-4), however, Ref [131] reports the failure mode for their CFRP samples ( $h = 3$  mm) to be complete break into two separate pieces and this clearly reflects their brittle nature. For values of  $L/h > 20$ , the trends in Figure 5-12 indicated that if the nylon-fibre composites reach a constant (minimum) value for  $u$ , it will be lower than the corresponding CFRP data; this can be attributed to the relatively low  $V_f$  values used in this study.

### **5.3.7 EFFECTS OF DEBONDING AREA ON ENERGY**

In this study, the most widespread form of damage that occurs during impact testing appears to be debonding (shown in Figure 5-4). The energy absorption in a composite sample was not particularly helpful to characterise material behaviour. Therefore, damage regions in the samples were further investigated to find the link between energy absorption and impact damage i.e. the debonded region. Post-test analysis of composite materials have been conducted by other researchers [55, 117, 148]; in most cases, ultrasonic C-scan image analysis and visual inspection were performed to reveal the extent of the damage zone (delaminated region) for carbon and glass fibre composites. In the author's view, producing a 2D image of the delaminated regions through C-scan image analysis may not be a reliable method, because of the possibility of uncertainty in

the computational process. In this study, a profile projector was adopted for the inspection of debonded regions of impact tested samples. This enabled an estimate of debonding area over the sample face to be made. Figure 5-13 shows impact energy data, for all span settings, as a function of the product of estimated debonding area,  $A$  and fibre volume fraction ( $V_f$ ). The parameter  $AV_f$  provides a simple indication of a total debonding area through sample thickness for different  $V_f$  values [128]. Since this approach assumes similar debonded profile characteristics through the thickness ( $h$ ) of each sample,  $AV_f$  cannot be regarded as an accurate parameter. Nevertheless, Figure 5-13 shows that the test and control sample data form approximately linear trends for all spans, thus indicating some dependence of energy absorption on debonding area. These linear relationships can be compared with findings from impact tests on glass fibre/epoxy plate samples [149]. All test sample data points show higher  $AV_f$  values than corresponding control results, concurring with the larger debonding regions observed in Figure 5-4.

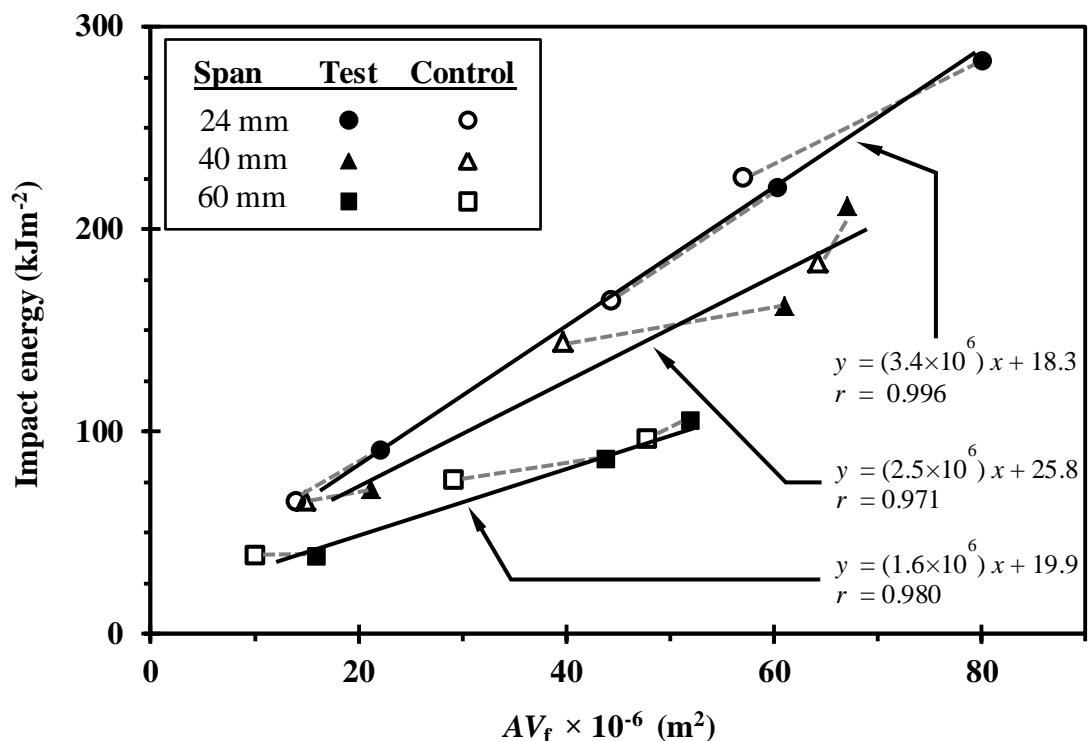


Figure 5-13. Mean impact energies (from Figure 5-10) at 24, 40 and 60 mm span setting plotted against the product of estimated debonding area ( $A$ ), and fibre volume fraction ( $V_f$ ). Solid lines and equations are from linear regression,  $r$  is the correlation of coefficient.

Of particular interest however, is the difference in gradients between the smallest and largest span settings ( $3.4 \times 10^6 \text{ kJm}^{-4}$  at  $L = 24 \text{ mm}$ ,  $1.6 \times 10^6 \text{ kJm}^{-4}$  at  $L = 60 \text{ mm}$ ). Data for 40 mm span follow an intermediate gradient value ( $2.5 \times 10^6 \text{ kJm}^{-4}$ ). The highest gradient value at 24 mm span indicates that energy absorption has a greater dependence on debonding than the 40 and 60 mm span settings. The more prominent role of debonding at the 24 mm span clearly concurs with greater contributions from shear stress effects, as considered in previous Sections 5.3.5 and 5.3.6.

### **5.3.8 INFLUENCE OF SHEAR STRESS ON IMPACT PERFORMANCE**

The most significant observation from the work in this chapter is that increased energy absorption arising from viscoelastically generated pre-stress depends principally on the presence of impact-induced shear stresses; these in turn activate residual (pre-stress-induced) shear stresses at the fibre-matrix interface to promote debonding during the impact process. In Charpy impact tests, the contribution from impact-induced shear stress and therefore, pre-stress-enhanced debonding, increases as span to thickness ratio ( $L/h$ ) are reduced, which supports the hypothesis in Section 5.1.2. Beam-shaped samples, having lower levels of transverse constraint, are more capable of absorbing energy than larger structures, such as circular plates [15]. Based on findings from the laboratory testing of samples with simple geometry and with fibre reinforcement being unidirectional, this study was effectively performed on composite samples representing one-dimensional behaviour. Nevertheless, it is still possible to make some inferences on the likely effectiveness of VPPMCs in real-world structures.

Since enhanced energy absorption from the pre-stress effect depends principally on shear stress, low velocity impact protection from structures where deflection is restricted may be further improved with VPPMC technology. Clearly, deflection-restricted structures are not uncommon, and these include composite panels or plates with stiffeners for aerospace and underwater structures [150] and thick laminates, e.g. glass fibre composites for marine applications [151].

Predicting the effects of VPPMC principles applied to high velocity low mass impact conditions may be considerably more speculative than those of low velocity impact scenarios. Damage is however much more localised, so that geometrical aspects become less important [15]. Previous studies on VPPMCs [10] have highlighted four Mechanisms which are briefly discussed in Chapter-2 (Section 2.6) and summarised below, that may contribute to VPPMC energy absorption capabilities and, by considering circumstantial evidence from published studies, all of these could contribute towards improved high velocity impact protection:

- |               |  |
|---------------|--|
| Mechanism-I   | Matrix compression impedes crack propagation.  |
| Mechanism-II  | Matrix compression attenuates dynamic overstress effects, thereby reducing the probability of fibre fracture outside the area of immediate impact. |
| Mechanism-III | Residual fibre tension causes the fibres to respond more collectively and thus more effectively to external loads.                                 |
| Mechanism-IV  | Residual shear stresses at the fibre-matrix interface regions promote energy absorbing fibre debonding over transverse fracture.                   |

From the work covered in this chapter, impact-induced shear is shown to encourage Mechanism-IV but in more general terms, this does not negate contributions from the other three mechanisms. The contribution from Mechanism-IV may however be significant under high velocity low mass impact conditions, because the highly localised deformation will cause large shear stresses. This deformation generally consists of dishing or cone formation within the localised damage zone, as observed in composites reinforced with carbon [152, 153], polymeric [154] and glass [155] fibres. Studies by Jevons on EPPMCs (glass fibre/epoxy) have shown that the local shear stresses from high velocity impact override pre-stressing benefits, so that no noticeable changes in delamination area or energy absorption were observed [67]. This suggests that brittle type fibres would provide no benefits either from EPPMC or VPPMC samples subjected to high velocity impact. These effects are further discussed in Chapter-8.

## 5.4 CONCLUSIONS

Charpy impact testing has been used to investigate the fracture and energy absorption characteristics of VPPMCs over a range of test span settings and  $V_f$  values. This chapter has highlighted some of the limitations of the Charpy impact test. Nevertheless, the improved understanding of energy-absorbing mechanisms from the findings could provide the basis for further, similar studies. By using fibre commingling techniques, investigating the effects of viscoelastic pre-stressing on the impact performance of relatively brittle composites (e.g. CFRP), would be of particular interest.

The main findings (based on observations and inferences) are as follows:

- (i) The improvement in impact energy absorption from viscoelastically generated pre-stress depends principally on shear stresses activating pre-stress-enhanced fibre-matrix debonding during the impact process. Thus a span setting of 24 mm shows greater increases in energy absorbed (25-40%) compared with 60 mm (0-13%).
- (ii) In contrast with relatively brittle composites such as CFRP, the mechanical properties (fracture characteristics, modulus) of the composite samples investigated in this study make the Charpy impact results much more sensitive to span setting.
- (iii) The benefits from shear stresses are demonstrated at 24 mm span setting; higher  $V_f$  samples tested at this setting are increasingly affected by drag, as the fractured (hinged break) samples are forced through the anvil supports following impact. Larger span settings, particularly at 60 mm, suggest there is an increasing contribution to energy absorption from elastic deflection, at the expense of energy being absorbed from fracture-based mechanisms: this causes lower energy absorption from all samples (i.e. both test and control groups) as well as reducing any improvements from pre-stress effects.

- (iv) Although higher  $V_f$  values may be expected to increase opportunities for energy absorption through pre-stress-enhanced fibre debonding, results at (the intermediate) 40 mm span show there is no more than a small, positive, but statistically weak trend between increased energy absorption (relative to control counterparts) and the  $V_f$  range studied (3.3-16.6%).
- (v) Visual evidence from impact-tested samples, that pre-stressing impedes crack propagation, is demonstrated. This validates previous proposed mechanisms, in which pre-stress effects are responsible for enhancing material properties by reducing crack propagation.

Based on these findings, it can be suggested that for structures where deflection is restricted, low velocity impact protection may be further improved with VPPMC technology. Structures subjected to high velocity impact from low mass projectiles may also benefit by commingling pre-stressing nylon fibre with other tough fibres in the same resin mix, since large shear stresses would be expected to occur from highly localised deformation.

# CHAPTER-6

## PERFORMANCE ENHANCEMENT OF HYBRID COMPOSITES (NYLON/KEVLAR FIBRE) THROUGH VISCOELASTICALLY GENERATED PRE-STRESS

---

### SUMMARY

The concept of intermingling two or more different types of fibre in the same resin mix (hybridisation) for the enhancement in material properties is well known concept. However, commingling nylon fibres for pre-stress with other tough fibres (such as Kevlar) in the same resin is a novel approach. Kevlar-29 fibres have high strength and stiffness and nylon 6,6 fibres have high ductility. Thus, by commingling these fibres prior to moulding in a resin, the resulting hybrid composite may be mechanically superior to the corresponding single fibre-type composites. The contribution made by viscoelastically generated pre-stress, via the commingled nylon should add further enhancement.

This chapter reports on the hybrid (commingled nylon and Kevlar fibre) composites in terms of impact toughness and stiffness performance. The main findings show that (i) hybrid composites with no pre-stress absorb more impact energy than Kevlar fibre composites, (ii) pre-stress further increases impact energy absorption and flexural modulus in the hybrid composites by up to 33% and 35% respectively.

An evaluation of the strength of hybrid composites based on their individual constituents is attempted. It was found that during impact loading, the composite is in a complex state of stress; this is discussed in relation to the fracture behaviour of both types of fibre. The evidence suggests that the Kevlar fibres have a predominant role in terms of absorbing impact energy through fibre breakage (brittle type fracture). Conversely, hybrid composite samples absorbed energy by debonding with few fibre fractures (ductile type fracture). The results suggest that fracture and failure behaviour of Kevlar fibre composites are significantly improved by commingling with nylon fibres and are further enhanced by pre-stressing.

## 6.1 INTRODUCTION

As demonstrated in chapter-5, investigation on nylon fibre-based VPPMC has shown improvement in impact energy absorption up to 40% in contrast with their un-stressed control counterparts. Similarly, Fancey's previous Charpy impact tests on VPPMC samples were found to absorb 25-30% more impact energy than their control counterparts, with some samples reaching increases of 50% [7-11]. Also, three-point bend tests [13] have shown flexural moduli to be ~50% greater than their corresponding control samples. All these findings [7-11, 13] were based on VPPMCs with pre-stress provided by nylon 6,6 fibres. Despite the potential benefits that VPPMC principles may offer, criticisms associated with the mechanical properties of fibres used for generating pre-stress could impede the development of VPPMC technology for practical composite applications. Clearly, a VPPMC requires fibres to possess appropriate viscoelastic characteristics, hence common structural PMC fibre materials (glass, carbon) must be ruled out. Similarly, some high performance polymeric fibres may be unsuitable for generating viscoelastic pre-stress. For example, aramid fibres will undergo tensile creep but the resulting strain is very low; moreover, creep strain-time curves appear to show significant Maxwell element behaviour (elastic spring in series with a viscous dashpot) [156, 157]. Both aspects reduce opportunities for appropriate long-term viscoelastic recovery, making aramid fibres impractical.

An alternative route to exploiting VPPMC technology for load-bearing composite applications would be to produce hybrid composites by commingling fibres for viscoelastically generated pre-stress with common structural fibres. This chapter reports on an evaluation (by Charpy and flexural testing) of hybrid VPPMCs consisting of commingled nylon and Kevlar fibres.

## 6.2 BACKGROUND

### 6.2.1 HYBRID COMPOSITES

Improving strength and stiffness of reinforced composites is particularly an important parameter. This can be done by hybridisation in which combining two or more reinforcing materials would result in a synergistic effect in respect to the composite performance. This can be achieved by combining different types of fibre in the same resin mix, so that strong, stiff fibres could be intermingled with tough fibres. A practical example is improving the low impact strength of carbon fibre reinforced composites by commingling with glass or aramid fibres [97]. Studies by Jang *et al* [158] on graphite fibres hybridised with tough (high strain-to-failure) fibres, have shown better resistance to impact loading. Therefore, the benefits from one type of fibre can complement those of another type, so that an optimum balance of performance can be achieved [159]. Clearly, the performance of hybrid composites mainly depends on the fibre types, fibre quantity and their orientation or intermingling characteristics.

The most common fibres used in a composite for structural applications are Kevlar, carbon and glass fibre. Although carbon and glass fibres are brittle in nature and have the lowest strain-to-failure value [43], they are widely used in the aircraft industry because of their high strength and stiffness properties. In comparison to glass and carbon fibres, the properties of Kevlar fibres are superior in terms of lower density, highest strength and stiffness [16]. Kevlar reinforced composites are used in many applications where stiffness, strength and damage resistance are important criteria, as well as weight saving. For example, a tough fibre reinforced composite in a racing car achieves a 35% weight reduction over aluminium [160].

A major advantage of composite materials is the potential to tailor the fracture process and the resulting fracture energy by means of constituent properties i.e. those of the matrix, fibres and the stacking sequence. Malik *et al* [161] found that hybrid composites

have superior impact characteristics based on Charpy impact and flexural tests. Impact studies performed by others on unidirectional Kevlar-29 fibres (3.4%  $V_f$ ) embedded with glass fibre/epoxy have shown 80% higher energy absorption than the equivalent pure glass fibre/epoxy composite has to offer [162]; in another study, commingling Kevlar or glass fibres to carbon fibre composites has also shown enhancement in impact performance [163]. Although composites with single fibre reinforcement behave as can be expected (based on their properties), damage and fracture mechanisms can be very complex in a hybrid case, as the arrangement of fibre volume fraction ( $V_f$ ), stacking sequence and properties of the individual fibres are key parameters to achieve better performance. Therefore, hybrid composite failure mechanisms can be more complicated than those encountered with single fibre types.

Important aspects that influence failure processes in hybrid composites are (i) strain-to-failure characteristics of the fibres, (ii) stiffness differences (which arise as a result of different fibre moduli and cross-sectional areas), (iii) fibre volume fractions and their ratios based on (i) and (ii). In Refs [26, 164], the authors have shown that the strain-to-failure of individual fibres in a hybrid composite plays an important role and it is suggested that maximum benefits can be achieved if one or both types of fibre offer high strain-to-failure properties.

Studies by Manders and Baders [165] have demonstrated that the failure strain of carbon fibres is enhanced by commingling with less stiff-higher elongation glass fibres. Hybrid effects investigated by others have shown improvements in the flexural modulus of graphite and glass fibre reinforced composites [166]. Enhancement in flexural strength [167] and fracture energy [161, 163, 168, 169] of Kevlar fibres intermingled with glass or carbon fibres are also reported. Another study has shown that the impact energy absorption of carbon fibre/epoxy composites was significantly increased by hybridising with high density polyethylene (HDPE) fibres [21, 107, 170, 171]; this positive effect was influenced by the rule of mixtures (ROM), in which the fibre volume fraction ratio of carbon and HDPE fibres and their adhesion with the epoxy matrix were considered.

The use of composites as structural materials to replace metals has become well established. However, impact damage in composite materials is still a major concern; such as transverse cracking, delamination, fibre/matrix debonding and fibre fractures. These are the potential failure modes in composite materials. The impact resistance of a material can be optimised with respect to (i) energy absorption and (ii) damage tolerance. However, both aspects are to some extent conflicting. For example, in Ref [100], these effects are highlighted such as the first approach is beneficial for crash and ballistic impact; often composites absorb energy by fibre breakage, debonding/delamination and fibre pull-out. Whilst, the second approach (damage tolerance) deals with structural composites, which includes post-impact properties, and is controlled by energy storage processes rather than damage (e.g. wind turbine blades). However, in a composite material, the freedom to enhance material properties in terms of energy absorption and damage tolerance can be done by combining two or more different types of fibre in the same resin mix to maximise strength.

The ability to withstand impact by foreign objects is an important characteristic of the material. High modulus fibres such as boron or graphite have relatively low strain-to-failure (less than 1%), which makes them relatively brittle materials, resulting in their susceptibility to impact damage [172]. Novak and De-Crescente [173] performed Charpy impact tests on hybrid unidirectional graphite and S-glass fibre/epoxy composites; they also investigated hybridisation effects of boron and glass fibre. It was found that the combination of boron or graphite fibres with glass fibre in a composite significantly increased impact energy absorption. Drop weight impact tests on thin hybrid graphite and Kevlar-49 fibre/epoxy laminates for aircraft fuselages performed by Beaumont *et al* [172], they have shown that the hybrid composites exhibited significantly better resistance to impact damage than thicker, heavier single fibre graphite laminates. In Ref [173], the authors reported that the fibre stress-strain behaviour plays an important role in the fracture mechanics of composite materials. Similar studies were undertaken by Chamis *et al* [174], on the impact fracture behaviour of unidirectional composites containing various combinations of graphite, glass, Kevlar-49 and boron fibres, reinforced in epoxy resin. It was found these hybrid composites had significantly greater impact energies than those containing individual fibre types.

The authors in Ref [174] suggested that using fibres with low interlaminar shear strength could improve impact energy absorption by promoting debonding (delamination) in composite materials. Similar effects were also reported by Moore [175] on his studies on boron and Kevlar-49 fibre composites, in which the impact energy absorption from the hybrid composites was significantly greater than boron fibre-only composites.

Studies by McColl and Morley [176] on crack growth in hybrid fibre composites have shown that the stability of transverse cracks in a brittle matrix could be improved by the addition of other fibres that can increase work of fracture. Many researchers have shown that the impact performance of carbon fibre reinforced composites can be improved by hybridisation with glass, graphite, aramid [161, 177, 178] and high density polyethylene fibres [179], in terms of resistance to impact damage and improvement in energy absorption [161, 177-179].

## **6.2.2 POTENTIAL BENEFITS FROM HYBRID VPPMCS**

Toughness (energy absorption) is generally associated with a combination of high ductility and high strength. Although Kevlar-29, as a polymer fibre, is well known for its high strength, the strain-to-failure is substantially less (at ~4%) than lower strength nylon 6,6 fibre (14-22%) [16, 17]. Thus by commingling these two fibres, the resulting hybrid composite may provide greater property improvement capabilities over the corresponding single fibre type composites. Graphite [158] and glass [180] fibres, when hybridised with ductile polymeric fibres, have produced composites demonstrating enhanced impact energy absorption. The contribution made by pre-stress, through commingled nylon fibres, should add a further benefit to impact performance. As reported in Chapter-2, Charpy impact studies have indicated that increased energy absorption in VPPMCs arises from residual shear stresses at the fibre-matrix interface regions promoting energy absorbing fibre debonding over transverse fracture [7-11]. Similar characteristics are observed from the nylon fibre-based VPPMC investigation

(reported in Chapter-5). Therefore, a nylon and Kevlar fibre hybrid VPPMC may also demonstrate improved impact toughness by the same means.

In flexural testing, stiffer fibres should be expected to produce stiffer composites, as the tensile region in bending will depend on Young's modulus  $E$  of the fibres. Although  $E$  for nylon 6,6 fibres is substantially lower (3.3 GPa) than Kevlar-29 (58 Gpa) [16, 17], the effect of pre-stress generated by nylon 6,6 fibres commingled with Kevlar-29 fibres may provide an increase in flexural modulus, by similar means reported in Chapter-2 (Section 2.4).

## **6.3 EXPERIMENTAL PROCEDURES**

### **6.3.1 PRODUCTION OF COMPOSITE SAMPLES**

Nylon fibre processing procedures (annealing, stretching) were followed as described in Chapter-3 (Section 3.2). However, the sample production and mechanical tests associated with this Chapter are summarised here. Batches of composite samples were required for Charpy impact testing and flexural stiffness evaluation. Hybrid composite samples were produced with continuous multi-filament nylon 6,6 and Kevlar-29 yarn embedded in polyester clear casting resin. In all cases, the nylon yarn was annealed in the fan-assisted oven (150°C, 0.5 hour); this was essential for long-term viscoelastic recovery [7-11], as reported in Chapter-3. Although annealing would have dehydrated the nylon fibres, it was found that equilibrium water content (by weight measurement) is restored within ~0.5 hour following removal from the oven; also, the annealing process has no significant effect on the mechanical strength of these fibres [12]. Since the Kevlar yarn had no role in viscoelastically generated pre-stress, this was used in as-received condition.

To produce hybrid samples, alternating (brushed) ribbons of nylon and Kevlar fibres were progressively combined by further brushing to form a randomly mixed bundle for subsequent moulding, schematically illustrated in Figure 6-1 below.

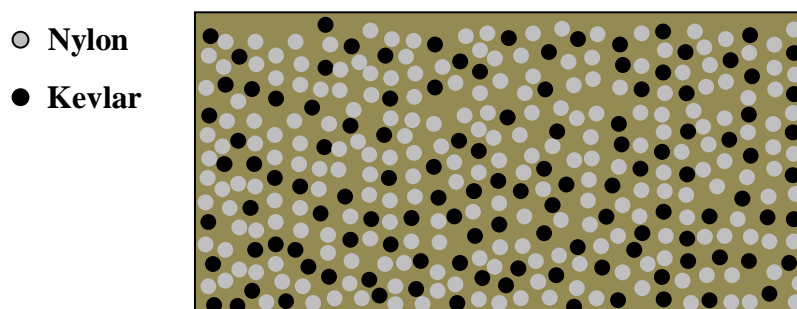


**Figure 6-1. Schematic illustration of hybrid (commingled nylon/Kevlar fibres) composite sample showing fibre dispersion.**

For all hybrid composite samples, nominal fibre volume fraction ( $V_f$ ) was 4.5%, consisting of 3.3% nylon with 1.2% Kevlar fibres. Each batch for Charpy impact testing comprises 5 test and 5 control samples, with dimensions being 80×10×3.1 mm. For flexural testing, just one test and one control sample was produced per batch, sample dimensions being 200×10×3.1 mm. Tolerance on sample thicknesses was  $\pm 0.1$  mm. All samples were stored in polythene bags at room temperature ( $20 \pm 2^\circ\text{C}$ ) prior to testing. To enable a more comprehensive analysis of results, additional composite samples with as-received Kevlar fibres only (3.6%  $V_f$ ) were produced for Charpy impact testing. Furthermore, resin-only samples were moulded and cut to appropriate dimensions for both Charpy impact and flexural testing.

### **6.3.2 MECHANICAL EVALUATION OF COMPOSITE SAMPLES**

The evaluation of composite samples was performed by low velocity Charpy impact testing and three-point bend tests, as described in Chapter-3 (Section 3.3). Since span to

thickness ratio is an important parameter in impact testing (discussed in Chapter-5), three batches (i.e. 15 test and 15 control samples) were each impact tested at span settings  $L$  of 60 and 24 mm. These  $L$  settings corresponded to BS EN ISO-179 Specimen Types 2 and 3 respectively. Similarly, the additional samples (15 Kevlar and 15 resin-only) were impact tested at both span settings. All samples were tested at 336 h (two weeks) after moulding.

Three-point bend tests with a freely suspended load were performed using a simple test rig (shown in Chapter-3, Figure 3.7). The set-up and procedures were identical to those performed with previous nylon 6,6 fibre-based VPPMCs [13], i.e. deflection reading was taken at 5 seconds after applying the load to obtain (as close as possible) the elasticity modulus and the same principle was adopted for this work. Although small deflections restricted measurement precision and accuracy, it was important to ensure that opportunities for specimen damage were minimized. For this study, a load of 4.2 N was adopted, i.e. similar to the load used for nylon 6,6 fibre-based VPPMCs in Ref [13]. Deflections were measured at  $20\pm 1^\circ\text{C}$  of each sample age (real time) ranging from 336 hours (2 weeks) to 12096 hours (~1.5 years). Equation 3-3 was then used to calculate flexural stiffness  $E(t)$ ; further details can be found in Chapter-3 (Section 3.3.2). To improve measurement accuracy, a video recording of each deflection in progress was made. For repeatability, three test and three control hybrid samples (i.e. three batches) and three resin-only samples were evaluated.

## 6.4 RESULTS AND DISCUSSIONS

### 6.4.1 FIBRE SPATIAL DISTRIBUTION IN COMPOSITE SAMPLES

As reported in Chapter-5 for nylon fibre-based VPPMC investigations on low to high  $V_f$ , as well as previous studies involving Charpy impact and flexural stiffness evaluation [7-11, 13], open casting offered the simplest composite sample production method. Also in common with previous work, mechanical evaluation necessitated the comparison of VPPMC ‘test’ samples with un-stressed ‘control’ counterparts. To ensure no differences between test and control samples, other than effects from pre-stress, each batch required simultaneous test and control sample production, followed by inspection of moulded cross-sections to compare fibre spatial distributions. Therefore, photographic evidence of effects that could adversely influence composite sample characteristics was required (by using optical microscopy). Ground and polished composite sample cross sections were taken from the moulded strips to observe fibre spatial distributions. Figure 6-2 shows representative cross-sections of the hybrid and Kevlar fibre-only composites. Of particular importance is that there appear to be no significant differences in fibre distributions between the test and control hybrid samples.

It can be seen from Figure 6-2, that both test and control samples (macroscopically) show similar fibre spatial distributions, the greatest concentration being in the lower half of the moulding, caused by fibres settling towards the bottom of the mould during casting. This demonstrates existence of two regions i.e. fibre-rich and matrix-rich regions. Microscopically, the (smaller) Kevlar fibres are randomly dispersed between the nylon fibres, with no observable differences between test and control samples. In Figure 6-2, the fibre spatial distribution in the Kevlar fibre-only sample is comparable to the hybrid samples. These distributions are also similar to those observed in Chapter-5 (Figure 5-2), on open-cast nylon 6,6 fibre composites produced from the same resin. This enables Charpy results from the hybrid VPPMCs to be compared with those from Chapter-5.

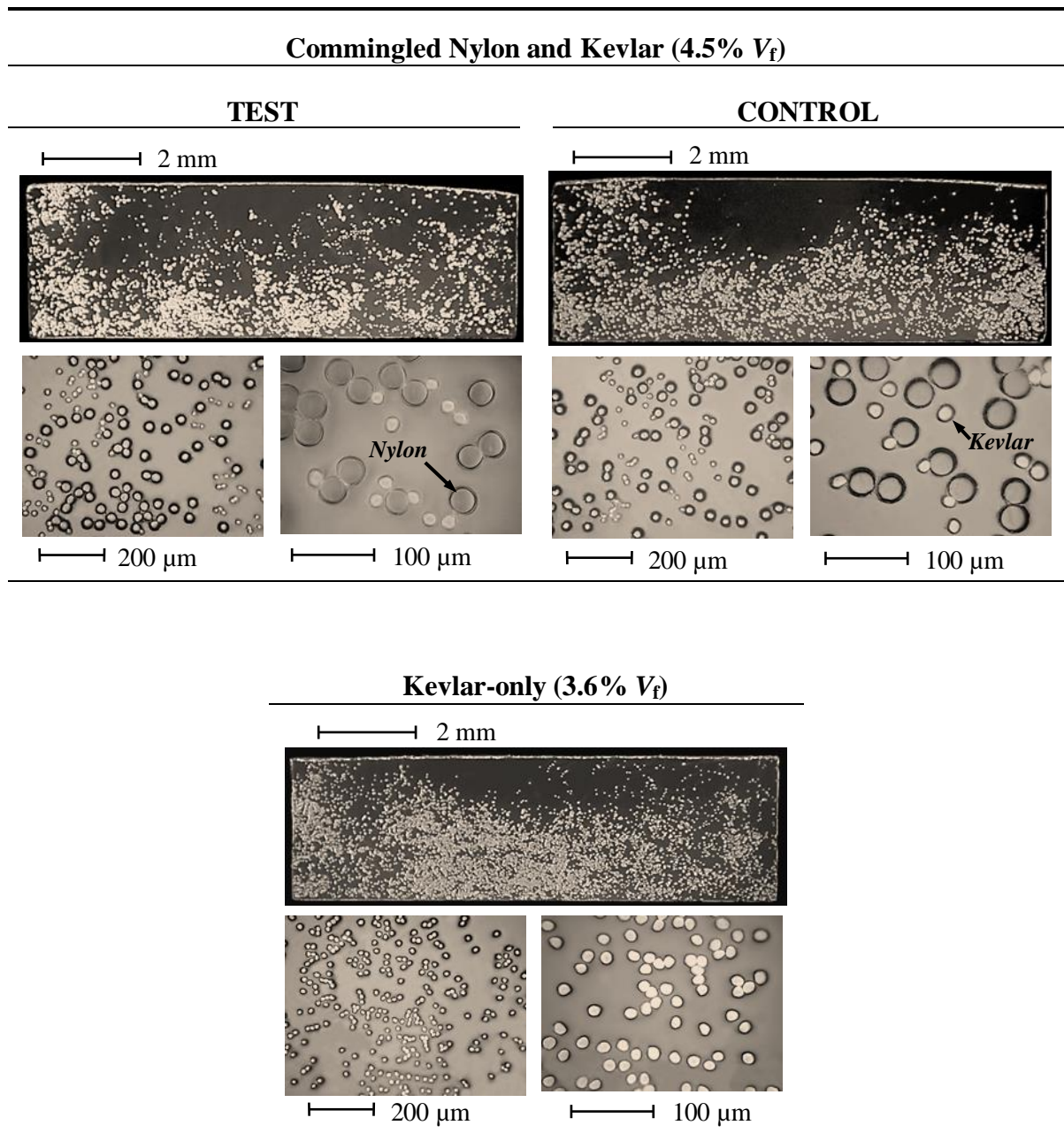


**Figure 6-2. Representative optical micrograph (polished) sections of the hybrid (nylon/Kevlar) and Kevlar fibre-only composite sample spatial distribution evaluated from open-casting with polyester resin. Note  $V_f$  values are nominal.**

## 6.4.2 CHARPY IMPACT TESTS

Table 6-1 shows impact energy data from the hybrid batches. Although both spans show the test samples absorbing more energy than their control counterparts, the pre-stress effect is clearly greater at the 24 mm span setting, an effect also observed with nylon 6,6 fibre VPPMCs (reported in Chapter-5). Table 6-2 shows data from the additional Kevlar fibre and resin-only samples. As expected, energy absorption for the resin-only samples is very low. Compared with the control samples in Table 6-1 however, the Kevlar fibre composite samples also exhibit poor results and these are relatively insensitive to span setting. Data from Table 6-1 and Table 6-2 are summarised in Figure 6-3. Also shown, for comparison, are impact energy results from Table 5-2 (Chapter-5), for nylon 6,6 fibre composites with 3.3%  $V_f$ , using the same resin, tested at 336 hours after moulding. At 24 mm span (Figure 6-3a), the nylon fibre-only composites absorb more energy than the hybrid case, though pre-stress-induced increases are comparable, i.e. 33% (Table 6-1) and 39% (Table 5-2). At 60 mm span (Figure 6-3b), however, the situation is reversed as energy absorption by the hybrid composites is less affected by the larger span setting. There is only a small increase in pre-stress-induced energy absorption from the hybrid composites (11.4% from Table 6-1), but this is an improvement over the nylon fibre-only case (~zero increase).

**Table 6-1. Charpy impact test data from hybrid (nylon and Kevlar commingled) fibre composite samples tested at 24 and 60 mm span. Each batch includes 5 test (pre-stressed) and 5 control (un-stressed) samples of nominal 4.5%  $V_f$  (3.3% nylon and 1.2% Kevlar). Data is normalised by dividing impact absorbed energy (J) by the sample cross-sectional area. S.E is the standard error of the mean. (Individual tested sample data are presented in Appendix-C).**

Charpy Span	Mean impact energy ( $\text{kJm}^{-2}$ )		Increase in energy (%)	Mean increase in energy (% $\pm$ S.E)
	Test $\pm$ S.E	Control $\pm$ S.E		
24 mm	$73.5 \pm 1.7$	$51.3 \pm 1.3$	43.2	$32.9 \pm 8.1$
	$65.2 \pm 3.1$	$55.8 \pm 1.4$	16.9	
	$71.4 \pm 2.6$	$51.5 \pm 0.6$	38.6	
60 mm	$53.5 \pm 1.9$	$47.3 \pm 2.0$	13.0	$11.4 \pm 1.1$
	$50.4 \pm 0.9$	$45.1 \pm 0.8$	11.9	
	$44.9 \pm 3.6$	$41.1 \pm 1.3$	9.2	

**Table 6-2. Charpy impact tests results from batches of Kevlar fibre-only composite (nominal 3.6%  $V_f$ ) and resin-only samples tested at 24 and 60 mm span (5 samples per batch). Data is normalised by dividing impact absorbed energy (J) by the sample cross-sectional area. S.E is the standard error of the mean. (Individual sample data are presented in Appendix-C).**

Charpy Span	Impact energy ( $\text{kJm}^{-2}$ )	
	Kevlar fibre	Resin-only
	Batch Mean $\pm$ S.E	Batch Mean $\pm$ S.E
24 mm	15.2 $\pm$ 0.4	5.4 $\pm$ 0.2
	17.4 $\pm$ 0.4	5.5 $\pm$ 0.8
	18.3 $\pm$ 0.8	4.4 $\pm$ 0.2
	<b>Mean <math>\pm</math> S.E</b> 17.0 $\pm$ 0.5	<b>5.1 <math>\pm</math> 0.4</b>
60 mm	18.8 $\pm$ 1.4	6.8 $\pm$ 0.7
	17.5 $\pm$ 0.4	6.6 $\pm$ 1.2
	23.0 $\pm$ 2.7	6.0 $\pm$ 0.5
	<b>Mean <math>\pm</math> S.E</b> 19.8 $\pm$ 1.5	<b>6.5 <math>\pm</math> 0.8</b>

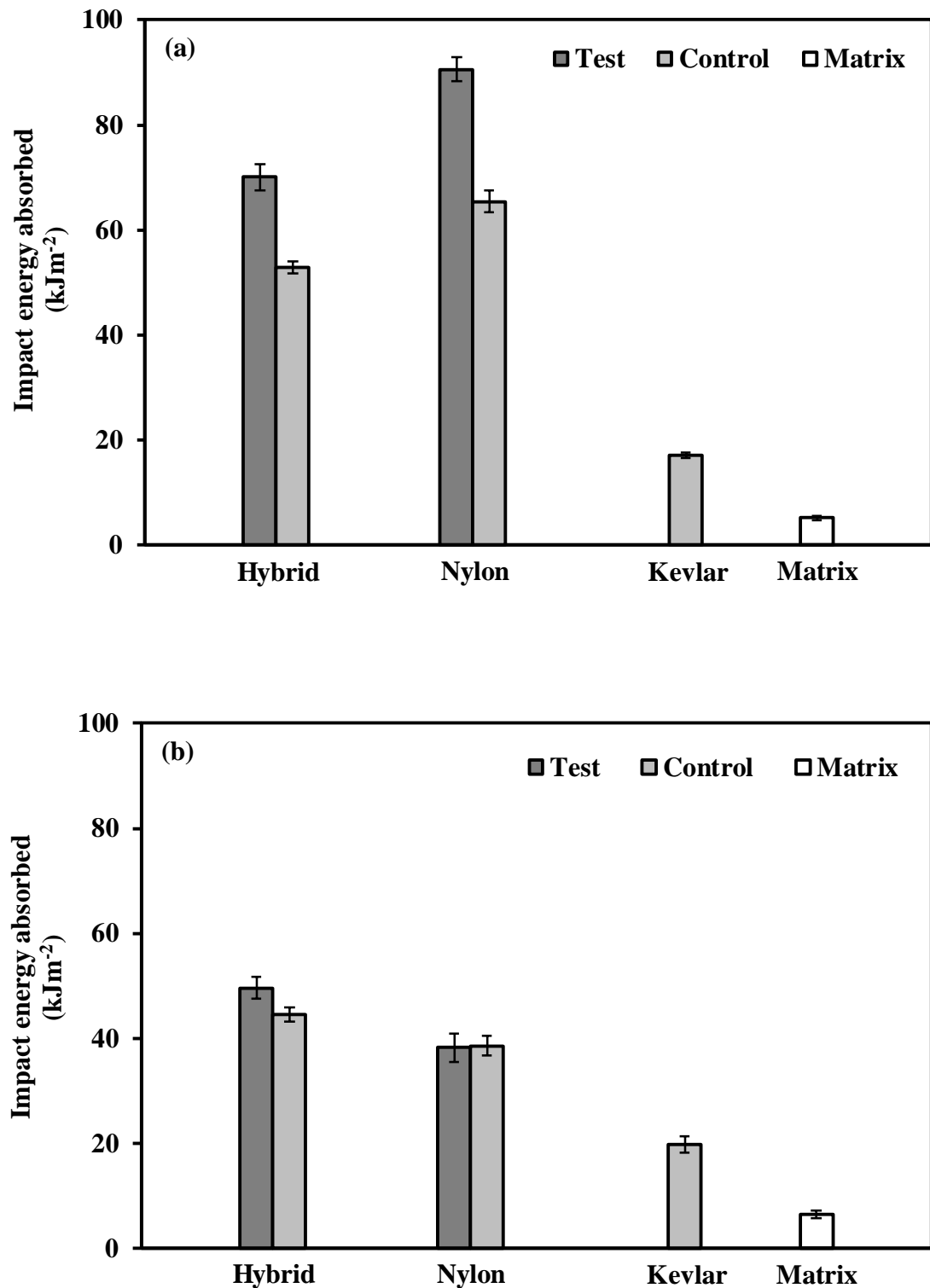
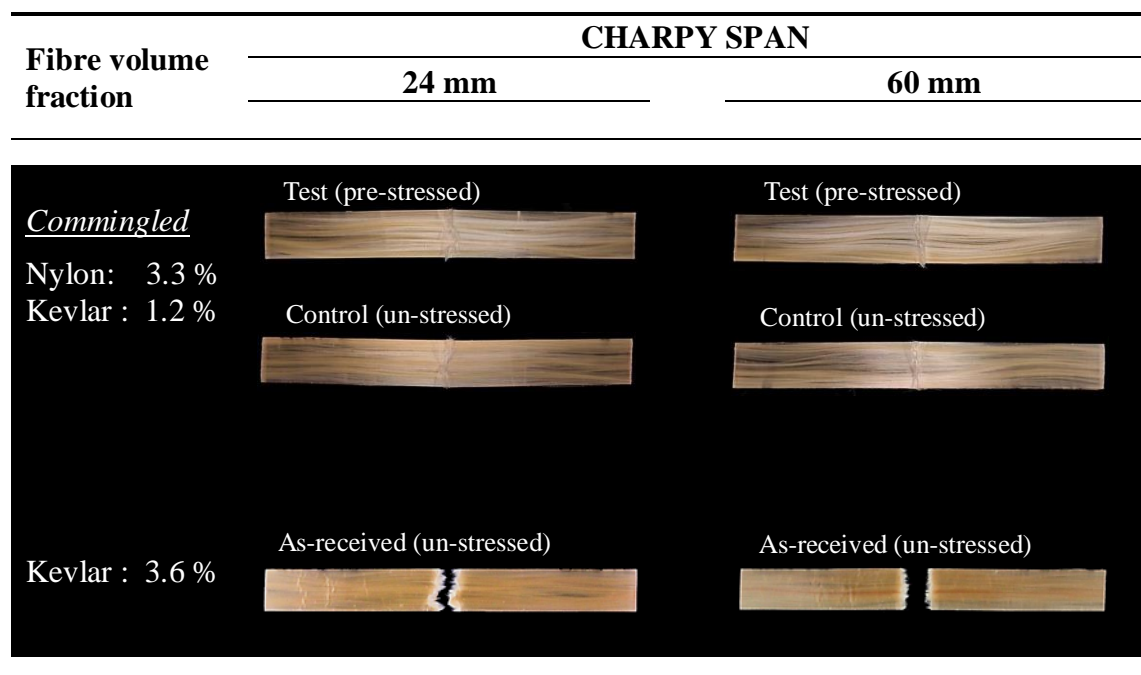


Figure 6-3. Mean impact energy data at (a) 24 mm and (b) 60 mm spans from test (pre-stressed) and control (un-stressed) hybrid composite batches of (3.3%  $V_f$  nylon and 1.2%  $V_f$  Kevlar commingled) from Table 6-1. Also shown for comparison are data from nylon fibre-only (3.3%  $V_f$ ) from Table 5-2, Kevlar fibre-only (3.6%  $V_f$ ) and matrix resin-only batches from Table 6-2. All samples were tested at 336 hours (2 weeks) after moulding.

Figure 6-4 shows typical hybrid and Kevlar fibre composite samples after impact testing. The Kevlar composites clearly indicate brittle fracture; in fact, all 15 samples at each span setting fractured into two pieces. The less wavy fracture profile at 60 mm span in Figure 6-4 may suggest a more pronounced brittle fracture at this span setting. In contrast, the hybrid composite shows fracture characteristics of a more ductile nature (hinged-break), where energy absorption through fibre-matrix debonding becomes more significant. The hybrid test samples show a greater debonded (lighter) region than their control counterparts. This is consistent with previous observations from nylon 6,6 fibre composites [7-11] and similar characteristics found in this study on nylon fibre-based VPPMC investigation (reported in Chapter-5, Figure 5-4); However, the presence of Kevlar fibres reduces the visibility of these regions in Figure 6-4 below.



**Figure 6-4.** Typical hybrid and Kevlar fibre composite samples after Charpy impact testing at 24 and 60 mm span settings. Note photos are taken from the fibre-rich side (away from the impact point).

### 6.4.3 IMPACT ENERGY ABSORPTION

As shown in Figure 6-4, there are clear differences in fracture characteristics between the Kevlar fibre-only and hybrid samples. The low  $V_f$  and unidirectional fibre lay-up used in this work may have exacerbated the brittle fracture characteristics of these Kevlar fibre samples. In other work [181], Charpy tests on woven aramid fibre un-notched composites with higher  $V_f$  (55%) showed only partial fracture, the pendulum hammer driving the damaged specimens between the anvil shoulders. As reported in Chapter-5 (Section 5.3), drag effects influence the measured impact energy and, although the  $V_f$  values used in this work may be criticised for being un-realistically low, the contribution from drag on hinged-break samples, especially at 24 mm span, is minimized.

The hinged-break fracture characteristics of the hybrid samples at 24 mm span in Figure 6-4 are similar to those observed with nylon 6,6 fibre-only composite samples shown in Figure 5-4 (Chapter-5). They show a main central crack (from direct contact with the Charpy hammer) and secondary cracks in the vicinity of the anvil shoulders (barely visible in Figure 6-4). However in Figure 6-3(a), there is less energy absorbed by the hybrid samples compared with those of only nylon fibre composite samples. Since this reduction occurs in both test and control groups, this suggests that the addition of (relatively stiff and brittle) Kevlar fibres may restrict energy-absorbing behaviour from the nylon fibres, possibly by (i) constraining their shear strain levels, hence less debonding during impact or (ii) shockwaves from fracturing Kevlar fibres promoting nylon fibre fractures over debonding. Nevertheless, as indicated by increased energy absorption from the hybrid test samples in Figure 6-3(a), the pre-stress-induced energy absorbing mechanism (i.e. residual shear stresses at the fibre-matrix interface regions promoting energy absorbing fibre debonding over transverse fracture) appears to remain effective. This occurs, even though the correspondingly greater debonded region in the test sample at 24 mm span in Figure 6-4 is less pronounced than that generally observed with nylon 6,6 fibre-only samples [7-11] and Figure 5-4 (Chapter-5).

As reported in Chapter-5, for nylon fibre composites tested at 60 mm span, energy absorption through elastic deflection (as the sample is forced through the anvil shoulders) was considered to be significant, with less contribution from fracture-inducing (plastic) deformation, especially from pre-stressed-induced debonding. This explains the lower energy absorption and zero increase from pre-stress effects observed in Figure 6-3(b) compared with the results in Figure 6-3(a) for these composites. Although the hybrid results in Figure 6-3(b) also show lower energy absorption compared with Figure 6-3(a), the reduction is smaller and there is still a positive pre-stress-induced energy increase. This suggests that the (stiff) Kevlar fibres will have suppressed elastic deflection to some extent, which in turn promotes more energy absorption from fracture and debonding.

#### **6.4.4 ANALYSIS ON FRACTURE BEHAVIOUR OF IMPACT TESTED SAMPLES**

Representative SEM micrographs of hybrid (nylon and Kevlar fibre) samples subjected to impact testing at 24 and 60 mm span setting are shown in Figures 6-5 and 6-6 . For comparison, Kevlar fibre-only composite samples are also shown in Figure 6-7. In, Figures 6-5 to 6-7, micrographs of the selected areas at higher magnification are indicated by arrows to highlight fracture morphologies. As reported in Section 6.4.2, Kevlar fibre-only composite samples fractured into two pieces (both sides of fracture surface are shown in Figure 6-7), suggesting at the event of impact, all Kevlar fibres progressively failed (brittle type failure). Conversely, nylon fibres in the hybrid composite maintain their integrity, and show ductile-type hinged-break failure. As a result, hybrid composite samples absorbed more impact energy mainly through debonding with a few fractured fibres showing ‘mushroom effects’ from short-term viscoelastic recovery at the fibre ends. Similar features are observed in all hybrid samples.

As reported in Chapter-5, nylon fibre-based composite samples tested at larger span (60 mm) slipped between the anvil supports; similar effects were also observed for hybrid

composite samples tested at 60 mm span setting. This indicates that the contribution to total impact energy absorption of the sample (before slippage) could possibly have occurred by (i) fibre breakage, mainly by Kevlar fibres at the tension side and (ii) through elastic deflection and the debonding mechanism provided by the nylon fibres. This validates findings from Table 6-1.

For Kevlar fibre-only composite samples, this would have occurred from the tensile stresses produced during impact. Initially, this results in matrix cracking and then as the impact load continues, the failure strength of the Kevlar fibres is exceeded, resulting in catastrophic failure of all fibres. The failure of Kevlar fibres indicates tensile type fracture at one side of the fracture surface, with a reduction in fibre cross-section and recoiling features on the opposite side, indicating these fibres are being stretched during the fracturing process. This suggests, during the impact process, total energy is absorbed by (i) fibre stretching (mainly plastic deformation), (ii) fibre fracture with no fibre pull-out or debonding mechanism and (iii) matrix cracking. Similar observations have been reported by Lin *et al* [182], in which tensile tests were performed to compare the properties of aramid and UHMWPE fibre composites. In Ref [182], authors reported that the elongation of aramid fibres in a composite subject to tensile load, in which the deformation of Kevlar fibres occurred in the form of fibre stretching with no indication of the fibre pull-out mechanism.

In this work, the catastrophic failure of Kevlar fibres is reduced by commingling with nylon fibres. However, Figures 6-5 and 6-6 suggest that Kevlar fibres have possibly caused dynamic overstress effects on the neighbouring nylon fibres, resulting in some nylon fibres also being fractured during the impact process. Interestingly, this effect is more pronounced in control samples, as it was expected that dynamic overstress effects would be less effective in pre-stressed composites. This supports the proposed Mechanism-II (discussed in Chapter-2, Section 2.6). Figures 6-5 and 6-6 clearly demonstrate this effect, in that impact damage and rapid crack growth were reduced by comingling nylon with Kevlar fibres, compared with Kevlar fibre-only composite samples (Figure 6-7). Moreover, impact energy absorption is further enhanced through

the debonding mechanism, promoted by the presence of pre-stress from nylon fibres in the hybrid samples.

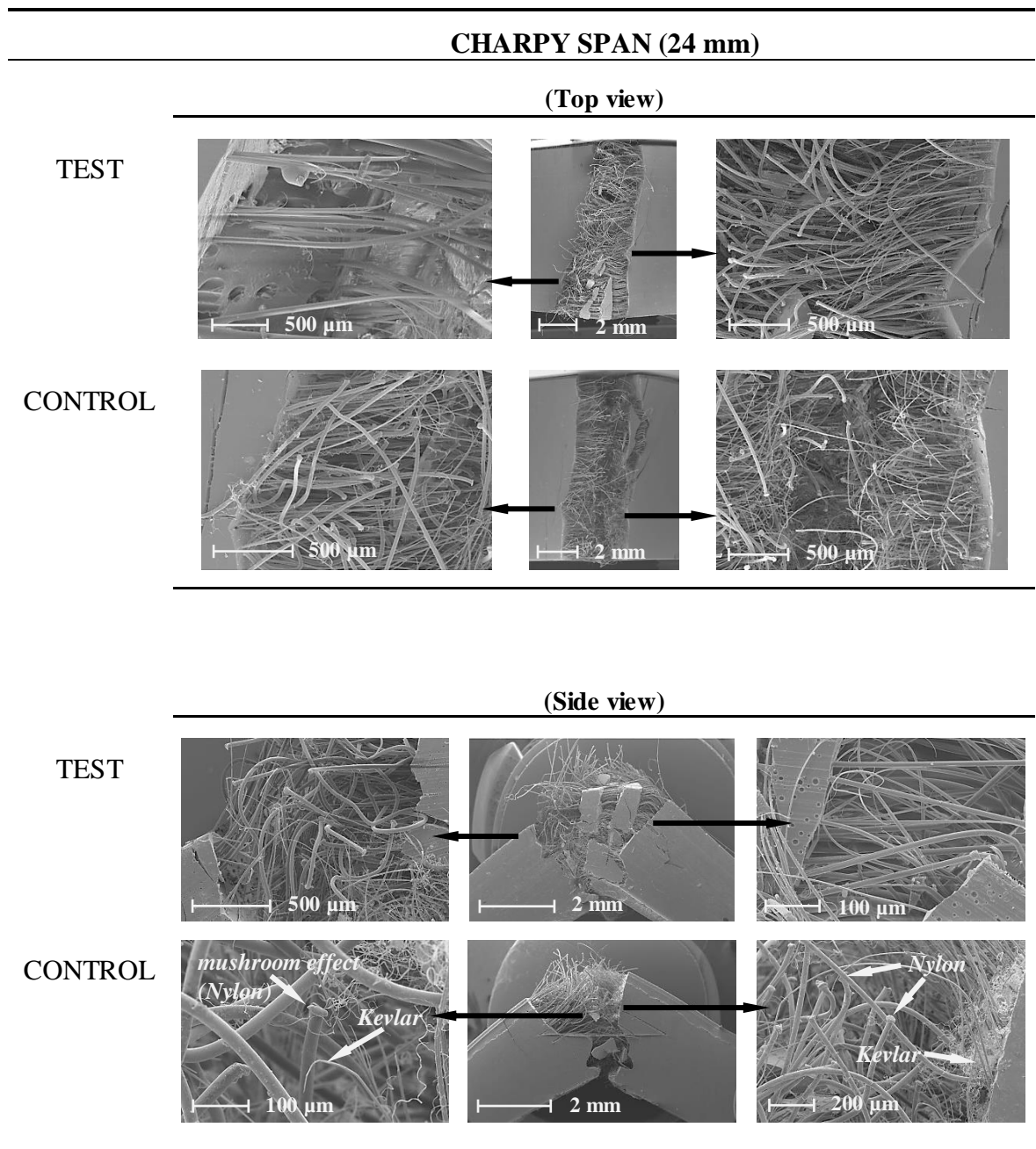


**Figure 6-5. Representative SEM micrograph cross-sections of commingled 4.5% nominal  $V_f$  (nylon 3.3%  $V_f$  and Kevlar 1.2%  $V_f$ ) samples tested by Charpy impact testing at 24 mm span (similar features are observed in all samples). Higher magnified images of selected areas are highlighted by arrows. Micrographs were taken at 4400 hours (~6 months) after impact testing; note differences in magnification.**

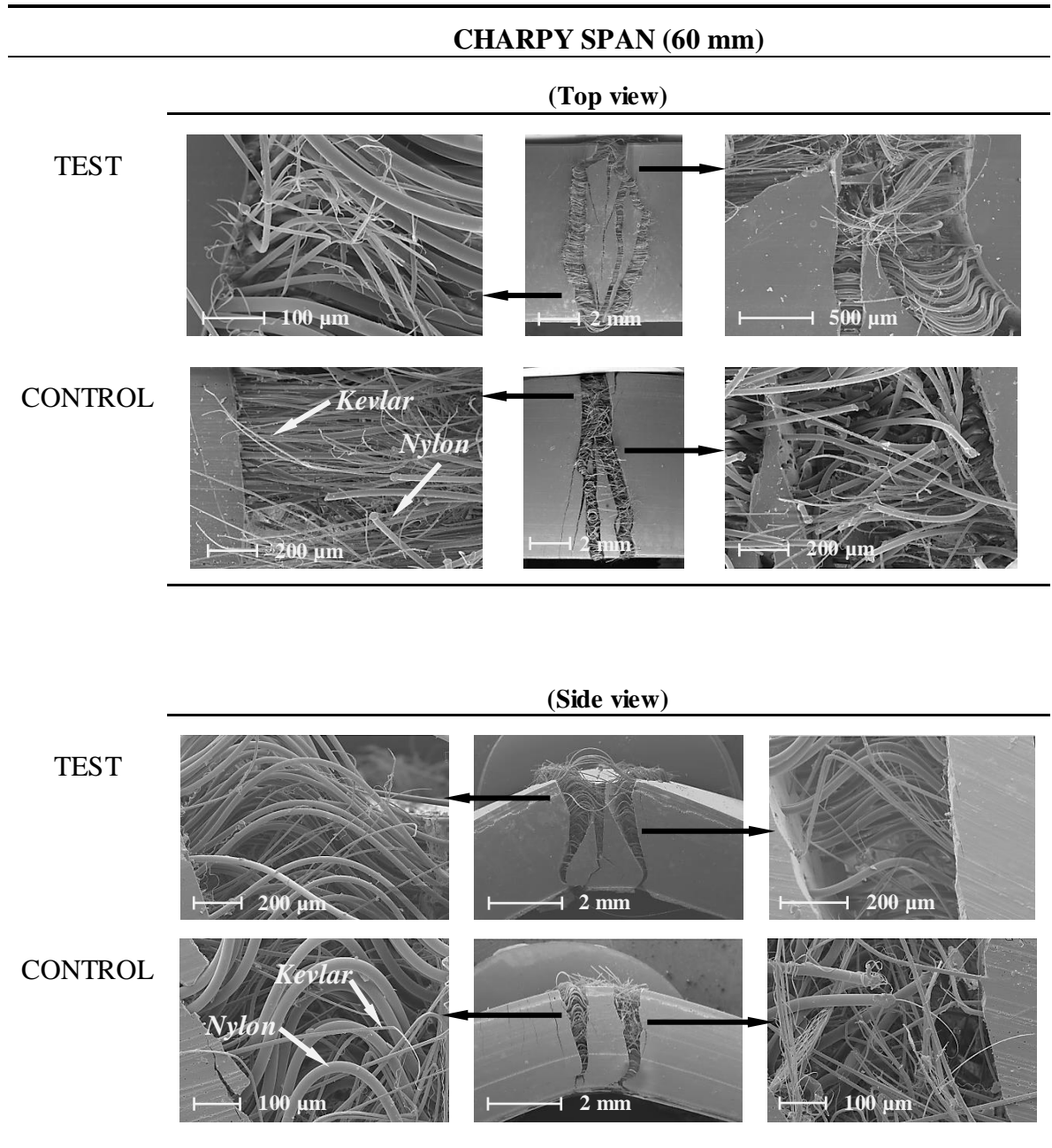


**Figure 6-6. Representative SEM micrograph cross-sections of commingled 4.5% nominal  $V_f$  (nylon 3.3%  $V_f$  and Kevlar 1.2%  $V_f$ ) samples tested by Charpy impact testing at 60 mm span (similar features are observed in all samples). Higher magnified images of selected areas are highlighted by arrows. Micrographs were taken at 4400 hours (~6 months) after impact testing; note differences in magnification.**

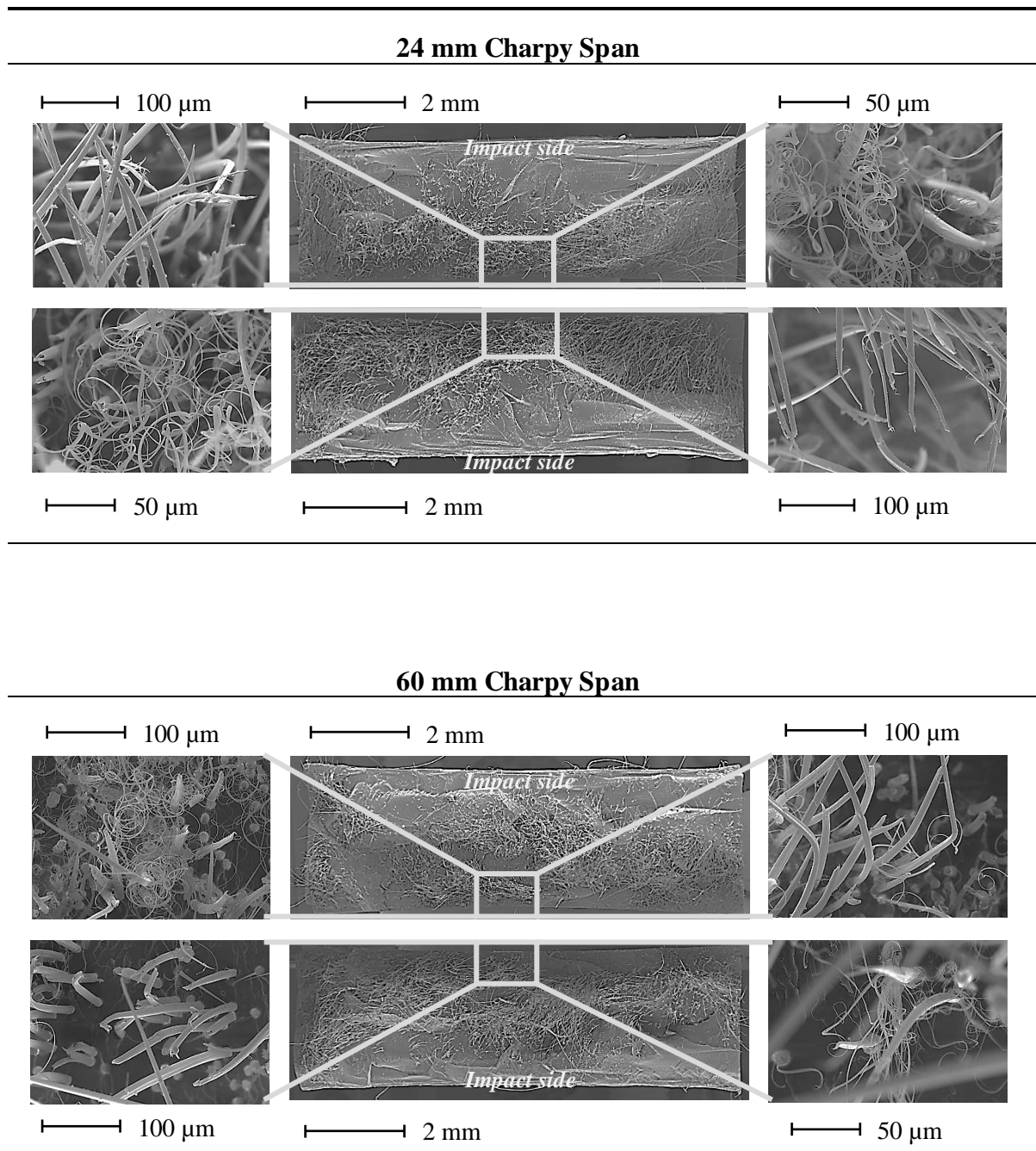


**Figure 6-7. Representative SEM micrograph cross-sections from both sides of the fracture surface of Kevlar fibre-only composite samples (3.6% nominal  $V_f$ ), subjected to Charpy impact tests at 24 and 60 mm spans. Area reduction at the fibre ends indicates tensile type failure, clearly visible in higher magnified micrographs. Composite samples were stored at room temperature for 336 hours (2 weeks) prior to testing. SEM micrographs were taken at 4400 hours (~6 months) after impact tests. Note difference in magnification; similar features are observed in all Kevlar fibre samples tested at 24 and 60 mm span settings.**

## 6.4.5 FLEXURAL STIFFNESS

Table 6-3 and Figure 6-8 summarise the flexural modulus results from the three test and three control hybrid samples and, for comparison, results from the resin-only samples is also shown. Clearly, there is no deterioration in modulus values (test or control) over the age range investigated (~1.5 year). Uncertainty in modulus values can be attributed to variations in measurement.

The increases in flexural modulus in Figure 6-8 are comparable to previous nylon fibre-based VPPMC studies [13], i.e. there are no indications that the addition of Kevlar fibres has detrimentally affected the viscoelastic pre-stress effect. The modulus increases may be attributed to the following three proposed mechanisms from Ref [13].

- (i) Deflection-dependent forces opposing the applied bending load.
- (ii) More collective response to bending forces from the pre-tensioned fibres.
- (iii) Pre-stress-induced shifting of the neutral axis in bending.

Nevertheless, the above mechanisms were originally speculated to explain pre-stress-induced increases in bending stiffness from composite cross-sections that had near-uniform fibre spatial distributions [13]. However, Figure 6-2 clearly shows non-uniform fibre spatial distributions, with the greatest fibre concentration lying close to the lower surface, i.e. the tensile region during three-point bend testing. For both test and control samples, the effect will clearly influence the contribution represented by second moment of area ( $I$ ) in Equation 3-3. For the test samples however, since compressive stresses from fibres are concentrated in the tensile region during bending, there is a direct contribution to increased flexural modulus.

**Table 6-3. Flexural modulus results from three-point bend tests on individual hybrid composite samples of 4.5% nominal  $V_f$  (commingled nylon 3.3%  $V_f$  and Kevlar 1.2%  $V_f$ ) and polyester resin-only samples. S.E is the standard error of the mean.**

<i>Flexural Modulus</i>				
Age (hours)	Hybrid composite sample			Resin-only sample
	(GPa)		Increase (%)	(GPa)
	Test	Control		
<b>336</b>	4.62	2.96	55.8	2.47
	4.55	3.59	26.9	2.44
	4.18	3.28	27.7	2.61
	<i>Mean ± S.E</i>	4.45 ± 0.14	3.28 ± 0.18	36.8 ± 9.5
<b>1008</b>	5.39	3.29	63.6	2.63
	4.55	3.59	26.9	2.44
	4.88	3.28	48.9	2.81
	<i>Mean ± S.E</i>	4.94 ± 0.24	3.39 ± 0.10	46.5 ± 10.7
<b>2016</b>	4.04	2.69	50.0	2.63
	3.54	2.94	20.6	2.44
	4.18	2.98	40.4	2.43
	<i>Mean ± S.E</i>	3.92 ± 0.19	2.87 ± 0.09	37.0 ± 8.7
<b>4032</b>	4.62	3.29	40.3	2.80
	3.54	2.94	20.6	3.05
	3.66	3.28	11.7	2.43
	<i>Mean ± S.E</i>	3.94 ± 0.34	3.17 ± 0.12	24.2 ± 8.4
<b>8064</b>	4.62	2.96	55.8	2.80
	3.98	3.23	23.4	3.33
	4.18	3.64	14.9	2.61
	<i>Mean ± S.E</i>	4.26 ± 0.19	3.28 ± 0.20	31.4 ± 12.5
<b>12096</b>	4.62	2.96	55.8	2.47
	3.54	2.94	20.6	2.82
	3.66	3.28	11.7	2.81
	<i>Mean ± S.E</i>	3.94 ± 0.34	3.06 ± 0.11	29.4 ± 13.5
<b>Grand Mean ± S.E</b>	<b>4.24 ± 0.24</b>	<b>3.18 ± 0.13</b>	<b>34.2 ± 10.5</b>	<b>2.67 ± 0.13</b>

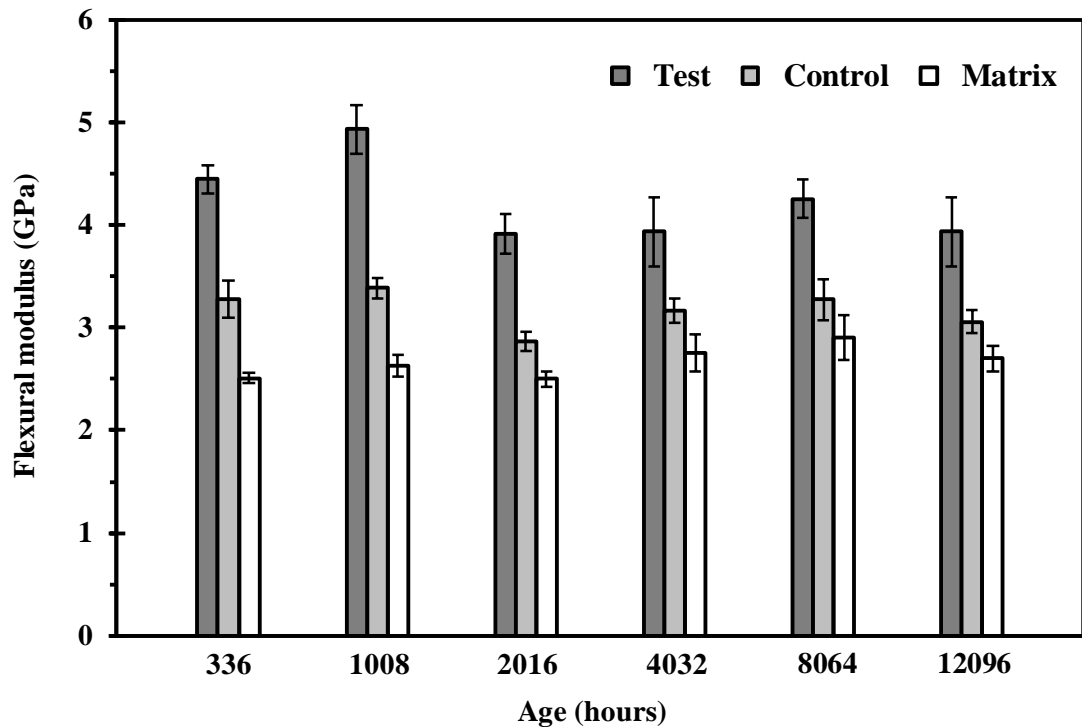


Figure 6-8. Flexural modulus values for test (pre-stressed) and control (un-stressed) hybrid composites determined from three-point bend tests; samples with 4.5% nominal  $V_f$  (commingled nylon 3.3%  $V_f$  and Kevlar 1.2%  $V_f$ ). Each value represents the mean of three samples with their corresponding standard error, from Table 6-3.

### **6.4.6 COMMINGLED HYBRID VPPMCS AS PRACTICAL COMPOSITE STRUCTURES**

In Chapter-5, one of the main findings from the nylon 6,6 fibre-only composites was that elastic deflection during impact would reduce improvements to energy absorption from pre-stress and similar effects are observed with the hybrid samples, as discussed in Section 6.4.2. Nevertheless, the addition of Kevlar fibres reduces concern over this effect. Clearly, for structures where deflection is limited, low velocity impact protection will be further improved by VPPMC technology and commingling the low modulus pre-stress generating nylon fibres with high modulus fibres, such as Kevlar, carbon or glass, may offer a practical solution to restricting deflection during impact.

This work has investigated commingled composites in which both types of fibre run parallel with each other. It may be suggested however that novel hybrid VPPMC structures could be created by running the pre-stress generating fibres in directions different to other fibres. One application might be morphing structures [128]. Non-symmetrical multilayer laminate composites can produce residual stresses (e.g. from thermal effects during moulding) and these can be exploited to create multi-stable deformations [183]. Elastic pre-stress generating fibres can be incorporated to create similar effects in symmetrical laminates [184]; thus alternatively, VPPMC techniques could be applied. Morphing aircraft wings, in which elastically pre-stressed carbon fibre composite strips are enclosed within a nylon fibre-reinforced skin [185], may benefit from VPPMC technology if it provides, for example, opportunities for simplified construction.

## 6.5 CONCLUSIONS

Charpy impact testing (24 mm and 60 mm spans) and three-point bend tests have been performed to investigate hybrid VPPMCs consisting of unidirectional commingled nylon 6,6 and Kevlar-29 fibres. A low  $V_f$  was used (3.3% nylon, 1.2% Kevlar), which minimised the contribution from drag effect during Charpy tests, from hinged-break samples. Where appropriate, results from these hybrid composites were compared with single fibre-type samples. The main findings (based on observations and inferences) are as follows:

- (i) All Kevlar fibre-only composite samples (3.6%  $V_f$ ) fractured into two pieces, with virtually no debonding, during impact testing at both spans investigated. Thus at least for the low  $V_f$  investigated in this work, energy absorption was comparatively low and occurred through brittle fracture.
- (ii) Hybridisation of nylon fibres with other types of tough fibres is an interesting approach to overcome the problems of low energy absorption through brittle failure.
- (iii) Charpy tests on the hybrid composites exhibited ductile fracture characteristics, producing hinged-break samples. Energy absorption through fibre-matrix debonding was significant, though the presence of Kevlar fibres made these debonded regions appear less pronounced compared with non-hybrid (nylon fibre-only) composites. The hybrid pre-stressed (test) samples absorbed more energy with larger debonded regions than their control counterparts, consistent with the view (from earlier work on pre-stressed composites) that residual shear stresses at the fibre-matrix interface regions promote energy absorbing debonding over transverse fracture.
- (iv) For Charpy testing at 24 mm span, the hybrid samples absorb slightly less impact energy than corresponding nylon fibre-only samples. This can be attributed to the Kevlar fibres reducing the energy-absorbing behaviour of the

nylon fibres in the commingled case; however, pre-stress-induced increases in energy absorption are comparable, i.e. 33% (hybrid) and 39% (nylon fibre-only sample).

- (v) At 60 mm Charpy span settings, the situation is reversed, in that the hybrid samples absorb slightly more energy. Moreover, there is a small increase in pre-stress-induced energy absorption (~11%), compared with ~zero increase in the nylon fibre-only samples. This suggests that the Kevlar fibres suppress elastic deflection at this wider span setting, thereby promoting more effective energy absorption from fracture and debonding.
- (vi) Flexural modulus data from three-point bend tests on hybrid composite samples have shown no deterioration in pre-stress effects over the age range investigated (up to 1.5 year).
- (vii) Bend tests on the hybrid composites demonstrated pre-stressing further enhances flexural modulus by ~35% (overall mean values), whilst some samples have shown improvements of up to ~60%. These differences can be attributed to variations in measurement rather than any time-dependency.
- (viii) In flexural stiffness, the addition of Kevlar fibres, at least for the low  $V_f$  investigated in this work, does not appear to be detrimental to the increased stiffness benefits provided by viscoelastic pre-stress.

These observations are derived from tests on simple composite samples with unidirectional fibre reinforcement, restricted to a single nylon and Kevlar fibre ratio at a low fibre volume fraction ( $V_f$ ). Although more extensive investigations would be required, the current results suggest that hybrid VPPMCs may provide a means to improve impact toughness and other mechanical characteristics for composite applications.

# CHAPTER-7

## VISCOELASTICALLY GENERATED PRE-STRESS FROM UHMWPE FIBRES AND THEIR PERFORMANCE ENHANCEMENT IN COMPOSITES

---

### SUMMARY

This chapter reports findings on the viscoelastic characteristics of ultra-high molecular weight polyethylene (UHMWPE) fibres. Investigation of creep-induced recovery strain and force output were performed to evaluate their potential for producing a continuous unidirectional UHMWPE fibre-based viscoelastically pre-stressed composite.

Polyethylene fibre processing procedures and composite sample production were followed as described in Chapter-3. The viability of UHMWPE fibre-based VPPMCs was demonstrated through low velocity Charpy impact and three-point bend tests. The findings were compared with their control (un-stressed) counterparts. From impact testing, the pre-stressed samples absorbed ~20% more energy than their control counterparts, with some batches reaching 30-40%; and increases in flexural stiffness of 25-35% were obtained with no deterioration over the time scale investigated (~2 years).

Generally, whether pre-stress is created through elastic or viscoelastic means, fibre-matrix debonding is known to be a major energy absorption mechanism in pre-stressed composites, but this was not evident in the polyethylene fibre-based samples. Instead, evidence of debonding at the skin-core interface within the UHMWPE fibres was found.

Investigation of the viscoelastic characteristics indicated that these fibres can release mechanical energy over a long timescale and the skin regions seem to possess lower stiffness and longer term viscoelastic activity. Fibre core-skin interactions and in particular, skin-core debonding, appears to have a significant energy absorbing role within the pre-stressed samples. This is believed to be previously unrecognised mechanism.

## 7.1 INTRODUCTION

In the last three decades, significant progress has been made in exploiting the fundamental properties of strong and tough polymer fibres. A good example of these fibres are aramid fibres, currently produced by DuPont under the trade name of Kevlar [18]. Aramid fibres can be manufactured with a high crystallinity due to their extremely stiff molecular structure (aromatic ring in the backbone), which offers Young's modulus and tensile strength values (in the fibre direction) of up to 450 GPa and 4.7 GPa respectively [30]. The most recent development in strong polymeric fibres are polyphenylene benzobisoxazole (PBO) fibres, produced by Toyobo under the trade name of Zylon [19].

As discussed previously in Chapter-6 (Section 6.1) and are summarised here, VPPMCs require fibres to possess appropriate viscoelastic characteristics; for this reason, common structural PMC fibre materials (e.g. glass, carbon) and some high performance polymeric fibres may be unsuitable for generating viscoelastic pre-stress. Therefore, an alternative route for exploiting VPPMC technology for load-bearing applications would be to investigate the viscoelastic properties of other semi-crystalline tough polymeric fibres. Low-density polyethylene (LDPE) possesses low crystallinity (about 45%) and contains polymer chains with weak intermolecular bonds. Therefore, LDPE has low tensile strength and Young's modulus. Nevertheless, polyethylene is a well suited material to form high strength fibres, because the high mobility of polymer chains in these fibres enables it to be easily drawn at high temperature (below the melting point) in the fibre direction [30]. Increasing the crystallinity to 75% produces high-density polyethylene (HDPE), where the properties significantly improve because the higher crystallinity increases the quantity and strength of intermolecular bonds. Moreover, ultra-high molecular weight polyethylene (UHMWPE) fibres can be produced by a special spinning method [30].

In late 70s, DSM invented a solution/gel spinning process that could produce UHMWPE fibres with outstanding mechanical properties. In 1979, Lemstra *et al* [186-

188] demonstrated the possibility of producing UHMWPE fibres by solution spinning from a non-oriented semi-dilute solution with strength and modulus values of over 3 GPa and 100 GPa respectively [189]. Nowadays, the production of high strength, high modulus UHMWPE fibres on a commercial scale follows the gel spinning method, these being produced by DSM, Toyobo and Allied Signal [113, 114]. Peterlin, Ward, Peijs, Govaert, Lemstra and their co-workers have made major contributions to these polyethylene fibres, they discovered the polymer composition and processing conditions to produce highly oriented polyethylene fibres with strength and modulus values of up to 1.5 GPa and 70 GPa respectively [106-115]. Jacobs reported in his studies on UHMWPE fibres that they can be produced on a commercial scale with a Young's modulus up to 150 GPa and a breaking-load of up to 4 GPa [20]. The gel spinning process of UHMWPE fibres is schematically shown in Figure 7-1 below. In the solution (gel) spinning method, a semi-dilute solution is used during spinning and the elongation of chains can be performed by drawing it in the semi-solid state. Traditionally, the chain orientation and extension in the spun fibres are generated by drawing these fibres during or immediately after spinning in the molten state at a high temperature but below the melting point [20].

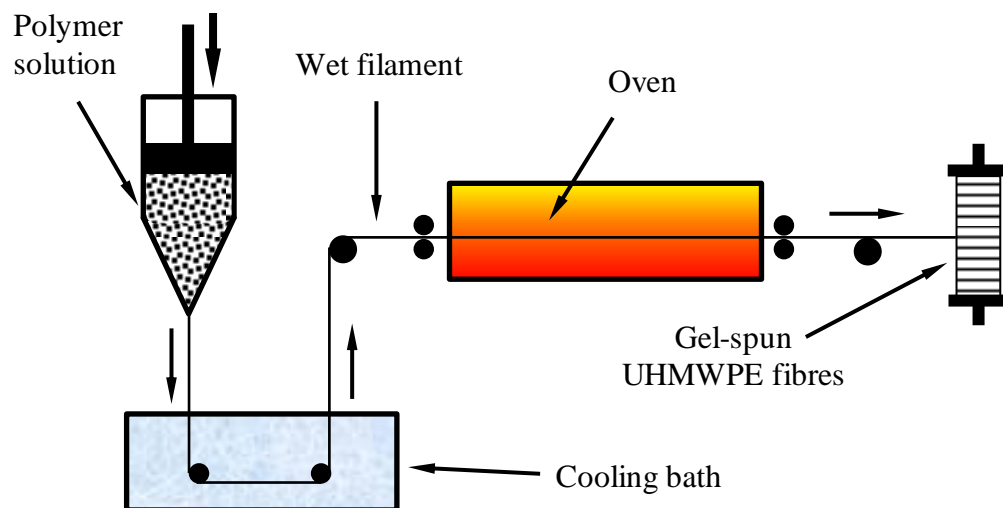


**Figure 7-1. Schematic illustration of the solution gel spinning process for producing UHMWPE fibres. After [20, 186] (re-drawn).**

Gel-spun polyethylene fibres possess fibrillar structures, which vary different in their sizes [124, 186, 190-192]. Typical gel spun UHMWPE fibres with fibrillar structures are shown in Figure 7-2. These fibril characteristics have been observed by many researchers and it is proposed that these fibrils consist of micro fibrils or weakly connected bundles of micro fibrils [190-193]. Their sizes range from macro to nano scale. The internal structure of micro fibrils is characterised by regular alternation of crystalline blocks separated by non-crystalline zones [20]. The morphology of gel-spun UHMWPE fibres is extremely complicated because of the numerous processing steps involved in production of the fibres. Studies by Jacobs [20], on gel spun polyethylene fibres have shown that plastic deformation in these fibres occurs by chain extension i.e. the applied load causes molecular chains to unfold. It seems that this could be due to elongation of the fibrils from the applied load; this also suggests that the fibrils play an important role in gel spun polyethylene fibres. The complexity of these fibrillar fibres are well defined in Refs [194, 195], in which authors state that it can be assumed that the “micro-fibril is one of the smallest elements of the fibre structure even though it is a very complicated system itself”.

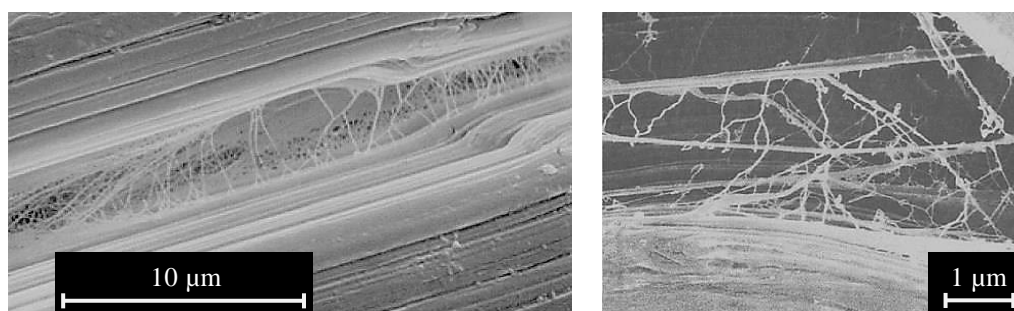


**Figure 7-2. Fibrillar structure of gel spun UHMWPE fibres, showing filaments are connected by bundles of very thin fibrils; also macro fibrillar structures on the surface of the filaments are clearly visible in both micrographs. After [20, 192].**

As previously reported, research into VPPMCs has been restricted to investigations with pre-stress provided by nylon 6,6 fibres [7-13]. Nevertheless, other researchers have successfully demonstrated VPPMCs based on bamboo, in which flexural moduli were increased by only 12% and flexural toughness was improved by 28% [14]. This chapter

reports on the first findings from UHMWPE fibre-based VPPMCs. The properties which motivate the use of highly oriented gel-spun UHMWPE fibres include high strength and stiffness (for all applications), high energy absorption capability for impact/blast protection (bullet proof vests, helmets, car panels, cut resistant gloves) and medical applications such as prosthetics and dental restoratives [20-23]. UHMWPE fibres with a tensile strength of 2.6 GPa and a modulus value of 87 GPa are ~4 times stronger and >20 times stiffer than nylon 6,6 fibres used in earlier VPPMC studies [17, 98]. Also, within the composites community, there is a significant interest in UHMWPE fibre reinforcement, especially for impact protection [196]. Thus the successful demonstration of enhanced impact performance from UHMWPE fibre VPPMCs could provide the basis for new directions in VPPMC technology.

To characterise the long-term behaviour of UHMWPE, an adequate method was needed for practical purposes, in the sense that it must be effective in performance and relatively simple in application for most engineering materials. Using short-term test data to predict the long-term behaviour of materials is clearly the most economic and appealing method. By using experimental data from the viscoelastic properties of UHMWPE fibres with respect to time and fitting it to a model makes it a possible tool for longer-term prediction of the material behaviour. This would allow fundamental questions to be addressed, such as (a) how long the viscoelastic recovery (creep induced strain recovery) can last in UHMWPE fibres, (b) how much force this can provide in pre-stressed composites and (c) do UHMWPE fibres exhibit viscoelastic characteristics that would provide significant mechanical property improvements in the form of a VPPMC. To address these questions, requires creep-recovery strain measurements for (a), recovery force monitoring for (b) and mechanical tests on UHMWPE fibre-based VPPMCs for (c), using Charpy impact tests and three-point bend tests. However, gel-spun UHMWPE fibres are structurally more complex than nylon 6,6 fibres, the former being considered to possess skin-core properties. The skin is suggested to consist of low molecular weight fragments and solvent excluded during crystallisation [126, 197] or as an unconstrained layer around a constrained core [198]. Thus, evidence of skin-core effects may be observable in fractured VPPMC samples following impact testing.

## **7.2 BACKGROUND**

### **7.2.1 UHMWPE FIBRE TREATMENT AND ANALYSIS OF VISCOELASTIC CHARACTERISTICS**

Viscoelastically generated pre-stress requires fibres to store mechanical energy so that it can be released over a very long timescale. Thus, after removing a tensile creep load and undergoing instantaneous (elastic) recovery, potentially suitable fibres should exhibit a significant proportion of long-term viscoelastic recovery strain followed by zero (or almost zero) steady-state strain from viscous flow effects. As reported in Chapter-2 (Section 2.5.2.2), Fancy's [8, 9] investigations on viscoelastic recovery have shown that annealed nylon 6,6 fibres produced significantly higher creep and residual recovery strain values in contrast with as-received fibres under the same loading conditions. Also, recovery strain from as-received fibres approached strain levels close to zero within 1000 hours after releasing the creep load [8-11]. In comparison, the viscoelastic recovery strain from annealed fibres was initially ~3%, dropping to ~2.5% after 2 hours and ~2% after 100 hours; i.e. the strain decreased very slowly with time and remained active beyond 1000 years at 20°C [10, 11].

Clearly, the treatment of UHMWPE fibres must be given similar consideration. For nylon 6,6 fibre-based VPPMCs, annealing conditions (150°C for 0.5 hour) were deduced from published sources [7-13]. For UHMWPE fibres, there is less certainty. Gupta [199] suggests that any meaningful heat-setting (to remove structural instabilities) of high-density polyethylene fibres would be performed at ~120°C; but it may be inferred from Ref [199] that the need to anneal UHMWPE fibres is more questionable, due to their high crystallinity. Thermal treatment (0.25 hour) of UHMWPE fibres shows that tensile strength is unaffected, though modulus decreases and strain-to-break increases progressively with increasing temperature up to 130°C [200]. Annealing at 100°C is found to relax some of the strain in the intermediate (oriented amorphous) phase between crystals, which results in a brittle to plastic

transition within these regions [201]. By considering these aspects, it was decided that the annealing conditions for this work should be set to 120°C for 0.5 hours.

The first practical requirement was to establish suitable load-time conditions for long-term viscoelastic energy storage. This is most easily achieved through strain-time measurements during recovery from an applied creep load. The resulting recovery strain data,  $\varepsilon_{rvis}(t)$ , as a function of time,  $t$ , may be fitted to Equation 2-1 below, previously used for nylon 6,6 fibre-based VPPMC investigations [89, 90]. This was discussed in Chapter-2 (Section 2.5.2.2) and is summarised here.

$$\varepsilon_{rvis}(t) = \varepsilon_r \left[ \exp \left( - \left( \frac{t}{\eta_r} \right)^{\beta_r} \right) \right] + \varepsilon_f \quad (2-1)$$

Equation 2-1 originated from the Weibull or Kohlrausch-Williams-Watts (KWW) relationship, where polymeric deformation can be represented by a model consisting of time-dependent mechanical latch elements [89, 90]. Viscoelastic strain recovery is represented by the  $(\varepsilon_r)$  function, which depends on the Weibull shape parameter  $(\beta_r)$  and characteristic life  $(\eta_r)$ . The permanent strain from viscous flow effects  $(\varepsilon_f)$  is the residual strain as time  $t$  approaches  $\infty$  and is ideally zero. Thus Equation 2-1 enables  $(\varepsilon_f)$  to be predicted from short-term recovery strain data. After establishing the most appropriate loading conditions, the viscoelastic recovery force from UHMWPE fibres was to be investigated using a bespoke force measurement rig originally used for nylon 6,6 fibre studies [91, 202]. Following creep and elastic recovery, the remaining time-dependent recovery force could be monitored. The required creep-recovery test cycle is represented by Figure 7-3.

Previous studies on nylon 6,6 fibre showed that the force grew to 3.4% of the applied creep load over a 2700 hours measured period  $t$ , and was predicted to approach a

maximum of 3.8% as  $t \rightarrow \infty$  [91]. This prediction was based on fitting recovery force data in Ref [91] to the following equation:

$$\sigma(t) = \sigma_v \left[ \exp\left(-\left(\frac{\Delta t}{\eta}\right)^\beta\right) - \exp\left(-\left(\frac{t}{\eta}\right)^\beta\right) \right] \quad (7-1)$$

Equation 7-1 shares the same origins as Equation 2-1. Here y-axis  $\sigma(t)$  represents the time dependent recovery stress (force across the fibre cross-sectional area) from the ( $\sigma_v$ ) function, as determined by the characteristic life ( $\eta$ ) and shape ( $\beta$ ) parameters. The time delay between releasing the creep load and establishing the onset of recovery force is represented by  $\Delta t$  in Equation 7-1 and Figure 7-3.

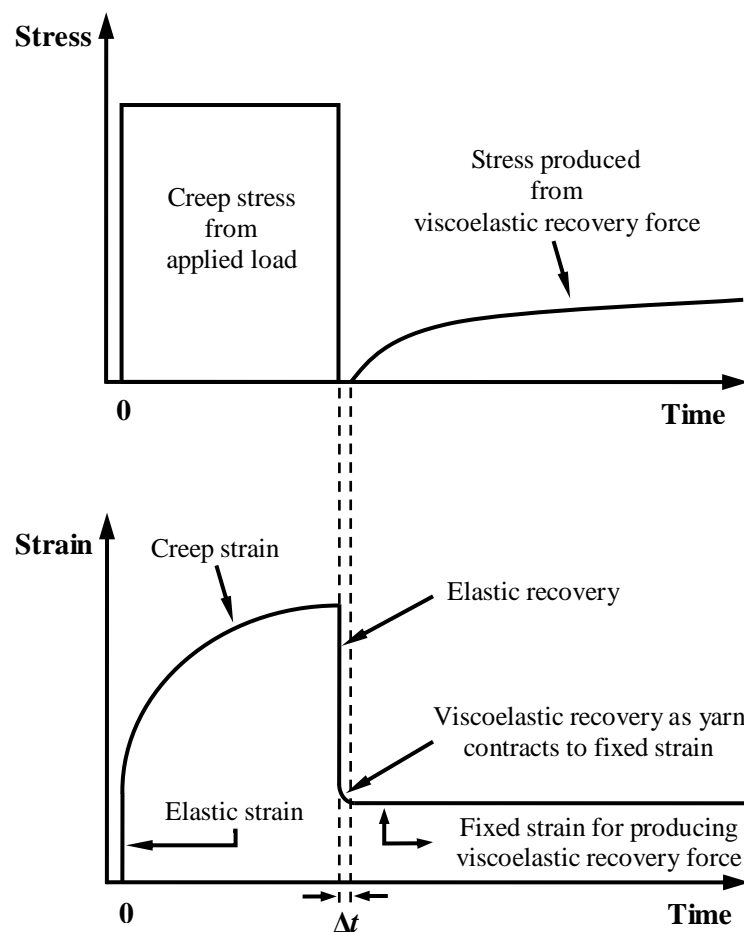


**Figure 7-3. Schematic diagram of the creep-recovery test cycle to investigate force-time characteristics of viscoelastically recovering UHMWPE fibres.**

## 7.2.2 COMPOSITE PRODUCTION AND EVALUATION

Although the long-term behaviour of UHMWPE fibres in terms of strain recovery and force measurement may show their capability for pre-stressed composite production, these data provide no information on possible composite performance. Therefore, mechanical evaluation of UHMWPE fibre-based VPPMCs becomes the preferred method for assessing composite performance. For this, open casting offers the simplest composite sample production method. The resulting beam-shaped samples enable the same mechanical evaluation procedures to be used as previous studies with nylon 6,6 fibre composites [7-9, 11, 13], so that comparative assessments can be made. As with previous studies, mechanical evaluation requires comparing the performance of VPPMC (test) samples with unstressed (control) counterparts. Clearly, this assumes no differences between test and control samples, other than the effects of pre-stress in the former case. To verify this necessitates (i) microscopic inspection of fibres and moulded composite cross-sections to look for any changes due to the stretching process and (ii) tensile testing of fibres to ensure that the stretching process does not cause work-hardening or any other unwanted mechanical changes.

Charpy impact testing has been the principal mechanical evaluation method for nylon fibre-based VPPMCs [7-11] and a similar approach is adopted in this work. However, further investigations on the flexural stiffness of polyethylene fibre-based VPPMCs were also undertaken. This was based on the fact that in the flexural tests, samples would not be destroyed during testing and thus could be repeatedly measured to correlate possible time-dependent changes with viscoelastic recovery data. In contrast, a substantial study would be required to provide opportunities for understanding the mechanisms associated with the observations made from impact testing. As reported in Chapter-3 (Section 3.3.2), flexural stiffness measurements for nylon fibre-based VPPMCs involved three-point bend tests on samples using a freely suspended load. To determine (as close as possible) the elasticity modulus, a deflection reading was taken at 5 seconds after applying the load [13] and the same principle was adopted for this work.

## **7.3 EXPERIMENTAL PROCEDURE**

### **7.3.1 ASSESSMENT OF CREEP AND RECOVERY STRAIN**

Fibre used for this study was a continuous multi-filament UHMWPE untwisted yarn (Dyneema SK60), supplied by Goodfellow Cambridge Ltd, UK. The yarn had 1600 filaments (fibres) with 12  $\mu\text{m}$  mean filament diameter (supplier specification) [98]. In common with nylon fibre-based VPPMC processing [7-13], the UHMWPE fibres required annealing to remove manufacturing-induced residual stresses and provide suitable viscoelastic creep-recovery characteristics. As reported in Chapter-3 (Section 3.2.1), for annealing, a suitable length of yarn was placed, unconstrained, in an aluminium tray and maintained at 120°C for 0.5 hours in a fan-assisted oven.

Creep-recovery procedures were similar to those previously used for nylon 6,6 fibre [7-9, 11], as discussed in Chapter-3 (Section 3.2.1), and are summarised here. For creep testing, the yarn was attached to loading Rig-(a) with counterbalanced platform to accommodate weights; a schematic diagram of the rig is shown in Chapter-3 (Figure 3-3). Creep and recovery strain measurements could be made in-situ by measuring the distance between two inked marks on the yarn, typically 300-400 mm apart, with a digital cursor ( $\pm 0.01$  mm precision). All strain measurements were made under ambient conditions of  $20 \pm 2^\circ\text{C}$  and  $40 \pm 10\%$  RH.

At least one sample of annealed yarn was loaded at one of four creep stress values (0.8 to 1.5 GPa) for 24 hours. Creep strain measurements were made and on releasing the load, measurements of recovery strain were subsequently taken. The high strain rates encountered during initial stages of measurement allowed only individual readings to be recorded for strain values during the first hour. Strain rates after 1 hour were considered to be sufficiently low to enable each strain value to be determined from the mean of three readings. To evaluate the effects of annealing, three further samples of yarn were subjected to the same creep-recovery conditions, with the annealing stage omitted.

As with earlier modelling studies [9, 11, 89, 90], Equation 2-1 was fitted to the recovery strain data using commercially available software (*CurveExpert-1.4*). In addition to providing equation parameters, the resulting correlation coefficient indicated the quality of fit between equation-predicted and measured strain-time values.

### 7.3.2 RECOVERY FORCE FROM POLYETHYLENE FIBRES

A knowledge of UHMWPE fibre recovery force magnitude and time dependency was required as this would provide some aid in understanding the fibre characteristics and resulting VPPMC behaviour. Here, annealed UHMWPE yarn was subjected to the creep-recovery test cycle, in which the creep stress was applied for 24 hours. On removal of the load stress (to allow elastic recovery), the yarn was transferred to the recovery force measurement rig (*FM*) and attached in a loose state, shown in Figure 7-4. Within a short time  $\Delta t$  (Figure 7-3), the initially loose loop of yarn progressively tightened through viscoelastic recovery, until a force output could begin to be monitored at a fixed strain. The force resulting from this state was monitored with a transducer built into the *FM* rig, as a function of time.

Full *FM* rig details are given in Ref [91], though essentially, the rig consisted of a frame with upper and lower bobbins to support a loop of viscoelastically recovery yarn. The upper bobbin was attached to a force sensor, as illustrated in Figure 7-4. All readings were recorded at  $20.9 \pm 1.0^\circ\text{C}$ . Subsequently, Equation 7-1 could be fitted to the resulting data, with the same software used for Equation 2-1. To apply the creep loading, stretching Rig-a (Figure 3-3) was utilised as it was compatible with the *FM* rig bobbin fixtures that enabled direct transfer of the recovering yarn. Owing to the high loading required for pre-stressing of UHMWPE fibres, combined with weight limitations for stretching Rig-(a), the yarn had to be separated out (before annealing) to reduce cross-sectional area by  $\sim 50\%$ . This was then attached to the *FM* upper and lower bobbins as a single loop (thus providing the approximate cross-sectional area of one single yarn) and fitted to Rig-(a) for the 24 hour creep loading.

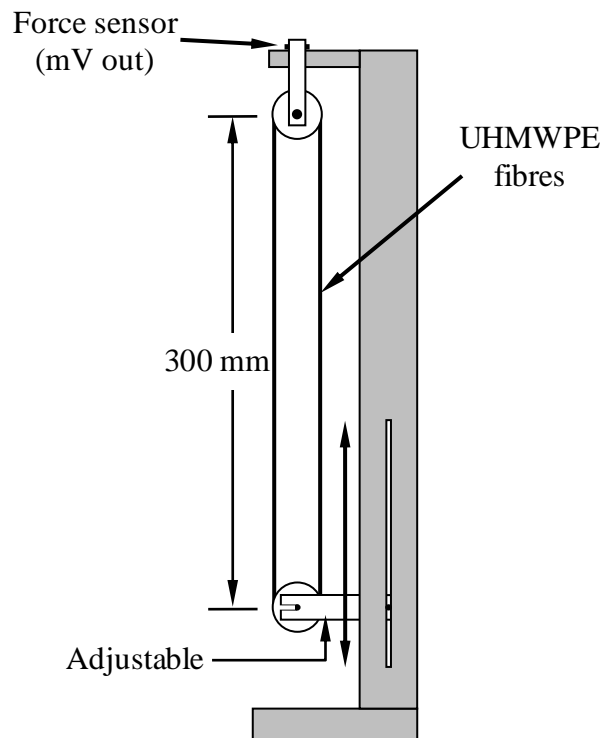


**Figure 7-4. Schematic diagram of the viscoelastic recovery force measurement rig. The adjustable lower bobbin allows the yarn (fibres) to contract to a fixed strain from a loose state. The cradle, suspending the upper bobbin, allows the contraction forces to exert compression on the sensor. After [91].**

### 7.3.3 MECHANICAL EVALUATION OF FIBRES

In addition to investigation fibre topography, as reported in Chapter-3 (Section 3.3.3), the tensile properties of UHMWPE fibres were evaluated to determine whether the stretching treatment (for creating pre-stress) affected the mechanical properties of the polyethylene fibres. If such changes, e.g. work hardening occur, then direct comparison between test and control composite samples would be inappropriate.

Nylon 6,6 fibre studies involved the tensile testing of individual test and control fibres to ensure no changes in the former [12]. As reported in Section 7.2.2, Fancy's previous studies on nylon fibres [7] have shown no significant changes in fibre diameter between

test and control fibres, which suggests that the stretching process does not affect fibre size. However, this was not possible with UHMWPE fibres, due to dimensional (cross-sectional) variations between individual filaments. These would cause difficulties in determining cross-sectional area; also test and control filament cross-sectional geometries would (ideally) need to be matched to enable direct comparison. Thus macroscopic tensile testing of test and control yarns (fibres bundles) had to be performed. According to Kromm *et al* [124] studies on UHMWPE single fibres show tensile and creep properties which are very close to those tested in bundles (yarn). In Ref [124], the authors suggested if the gauge length (tensile testing) is greater than 100 mm then it would give the rupture strength of the UHMWPE fibres. This suggests that gauge length plays an important role in tensile testing for the evaluation of these fibres. Compared with most materials, yarns are more sensitive to stress concentrations when clamped and stretched during tensile testing, though the capstan method can be an effective technique [125]. This principle was adopted and is shown in Figure 7-5 below, the capstan design and dimensions being comparable to those used elsewhere for UHMWPE fibre evaluation [126].

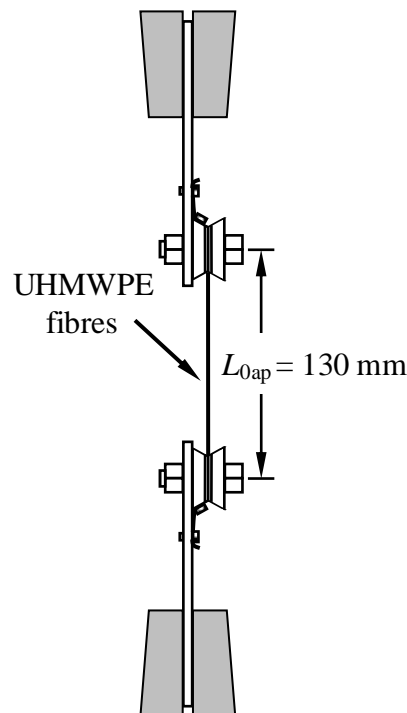


**Figure 7-5. Schematic diagram of the tensile testing setup and jig assembly for UHMWPE fibres.**

Although by using the testing setup illustrated in Figure 7-5, tensile strength ( $\sigma_f$ ) would be unaffected, a potential problem with this arrangement was the uncertainty in gauge length, which was required for determining the Young's modulus  $E$  and strain-to-failure ( $\epsilon_f$ ). During tensile testing, fibre movement around the capstans makes the effective gauge length ( $L_{0e}$ ) greater than the apparent gauge length ( $L_{0ap}$ ) as represented in Figure 7-5. For the evaluation of single UHMWPE filaments in Ref [126] however,  $L_{0e}$  was found to be equivalent to the total length, i.e.  $L_{0ap}$  plus length of material wound around the capstans. For the purposes of this work, in which the principal aim was to determine possible differences between yarns, the assumption that  $L_{0e}$  is equal to the total length was adopted. Individual lengths of yarn (4 test and 4 control) were tested in succession using the capstan jiggling in a Lloyd LR100K machine (with analysis software) at  $20\pm 1^\circ\text{C}$ . The total length for each yarn sample was 650 mm ( $L_{0ap} = 130$  mm) and the loading rate was 200 mm/min. The testing was performed 168 hours (1 week) following stretching procedures and the resulting stress-strain curves provided information on tensile strength ( $\sigma_f$ ), modulus  $E$  and strain-to-failure ( $\epsilon_f$ ).

### 7.3.4 COMPOSITE SAMPLE PRODUCTION

UHMWPE fibre composite sample processing and production procedures were followed as described in Chapter-3. However, additional processing and testing setups associated with this chapter are summarised here. As reported earlier, similar to nylon fibre-based VPPMC processing [7-13], UHMWPE fibres required annealing to remove manufacturing-induced residual stresses to provide suitable viscoelastic creep-recovery characteristics. To produce one batch, two lengths of yarn (designated test and control) were simultaneously annealed (unconstrained) at  $120^\circ\text{C}$  for 0.5 hours in a fan-assisted oven (shown in Chapter-3, Figure 3-2). Since larger quantities of yarn were required, stretching Rig-(b) was used (as shown in Chapter-3, Figure 3.3); this was previously employed by Fancy's for the production of higher  $V_f$  nylon fibre VPPMCs [12, 13]. The test yarn was subjected to a 24 hour creep load, whilst the control yarn was positioned close to the rig for exposure to the same ambient conditions. For Charpy impact testing, a total of 30 batches were produced all with a nominal fibre volume

fraction ( $V_f$ ) of 3.6% and tested at 24 and 60 mm span settings. For flexural tests, three batches of test and control samples (i.e. three samples each) with 3.6 and 7.2% nominal  $V_f$  were evaluated by three-point bend testing.

### **7.3.5 MECHANICAL EVALUATION OF COMPOSITE SAMPLES**

For impact testing, a Ceast Resil-25 Charpy machine with 7.5 J hammer was used for impact testing at  $3.8 \text{ ms}^{-1}$ , operating in accordance with BS EN ISO-179. Testing procedures were followed as described in Chapter-3 (Section 3.3). Three batches (15 test and 15 control samples) were each impact tested under ambient conditions ( $20 \pm 1^\circ\text{C}$ ) at a span setting ( $L$ ) of 24 and 60 mm. These  $L$  settings corresponded to BS EN ISO-179 Specimen Types 2 and 3 respectively. This testing procedure was performed over five periods (24-1008 hours) after moulding, to determine any short-term age-related effects. Following testing, fractured samples were selected for analysis, principally by scanning electron microscopy (SEM), to identify possible failure mechanisms.

Batches of composite samples for flexural stiffness evaluation were produced with two fibre volume fractions ( $V_f$ ) 3.6 and 7.2%. The higher  $V_f$  value (7.2%), was comparable to those used in previous nylon fibre-based VPPMC studies involving flexural stiffness [13], whilst the lower 3.6%  $V_f$  was similar to that used in impact investigation, such as the work reported in Chapters-5 and 6. At 7.2%  $V_f$ , the high loads required for stretching UHMWPE fibre limited production to just one test and one control sample per batch, each sample being  $200 \times 10 \times 3.1$  mm. Tolerance on sample thickness was  $\pm 0.1$  mm. Although this limitation did not apply to 3.6%  $V_f$ , the same methodology was adopted, to be consistent with production procedures.

Three-point bend tests were performed using a simple test rig with a freely suspended load, shown in Chapter-3 (Figure 3.7). The set-up and procedures were identical to those performed with nylon fibre-based VPPMC (long length) samples [13] and hybrid

VPPMCs (Chapter-6), i.e. each sample was mounted horizontally with the moulded bottom surface facing downwards and a deflection reading was taken at 5 seconds after applying the load. Although small deflections restricted measurement precision and accuracy, a low load was used in Ref [13] (~4 N) to minimise opportunities for specimen damage. As reported in Chapter-6, a similar approach has been followed, i.e. ~4.2 N load was applied to nylon fibre-based hybrid composite samples. However, to achieve comparable deflections from polyethylene fibre-based composite samples in this work, a load of 10 N was adopted. The measurement procedure was performed repeatedly over a period of 2 years after moulding, to determine any long-term age-related effects.

## **7.4 RESULTS AND DISCUSSIONS**

### **7.4.1 FIBRE-BASED MICROSCOPIC ANALYSIS**

Photographic evidence of effects that could adversely influence composite sample characteristics was required. This was to ensure that there would be no differences between test and control samples, other than mechanical effects from pre-stress. Scanning electron microscopy was used to assess potential changes in topography of the test yarn (filaments) following the applied creep stress. Figure 7-6 shows SEM micrographs of the annealed test and control yarn samples. It appears that there are no changes in fibre topography (no evidence of surface damage) or dimensions following the stretching treatment.

Although these filaments have a supplier-specified mean diameter (12  $\mu\text{m}$ ), these polyethylene fibres are not circular; instead, their cross-sectional geometries are bean or kidney-shaped, as described by others [122-124]. In Ref [124], it is suggested that this could be caused by the fibrous structure resulting from the manufacturing process,

which induces changes in the cross-section along filaments. Previous studies on nylon fibres [7] have shown no significant changes in fibre diameter in either test or control samples. This supports the view that the stretching process does not affect fibre size. However, this assessment was not possible with the UHMWPE fibres, due to dimensional (cross-sectional) variations between individual filaments.

It can be seen from Figure 7-6 below that the surface characteristics of both fibre samples (test and control) shows longitudinal features; these can be attributed to the manufacturing process i.e. they will have originated during spinning/drawing process. Most importantly, Figure 7-6 indicates that there is no difference in the surface features between the test and control fibres that could affect fibre-matrix bonding.

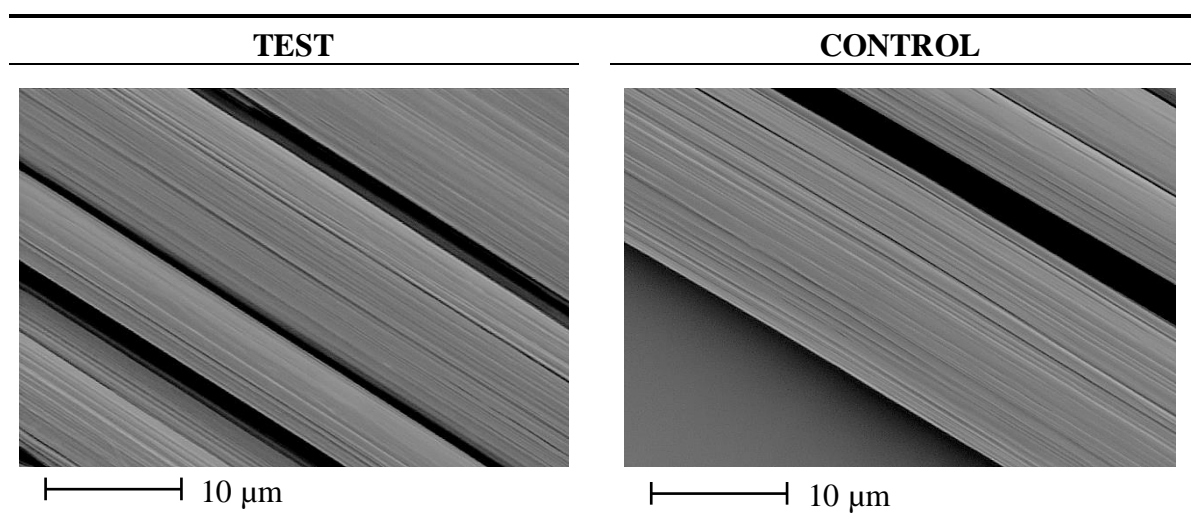


**Figure 7-6. Representative SEM micrograph of annealed test (previously loaded) and control (un-stressed) UHMWPE fibres. The test fibres were subjected to creep conditions adopted for composite samples. Both fibre groups were previously annealed at 120°C simultaneously. Micrograph for the test sample was taken 22 hours after releasing the 24 hour creep load.**

Although the annealing treatment at 120°C in oven was required to improve viscoelastic properties, oxidation could have been possible under these conditions [203, 204]. Oxygen is known to compete with the crosslinking reaction and causes chain scission [205]. Nevertheless, the short exposure time (0.5 hour) compared with published

findings at 120°C [23] suggest that oxidation should be negligible. Studies on polyethylene Spectra fibres and gel-cast tapes performed by others [20, 188] have shown that the presence of oxygen from the heat treatment does not necessarily result in strength loss in a highly oriented polyethylene.

To determine whether oxidation could result from annealing, Energy Dispersive X-ray analysis (EDX) was used to detect the possible presence of oxidation. In contrast with analysis using a conventional SEM outlined in (Chapter-3, Section 3.4), the EDX facility was fitted to a variable pressure SEM; this avoided the need for samples to be coated with an electrically conductive layer, which could have increased background oxygen levels. Samples of as-received and annealed fibres were mounted on graphite supports and scanned (mainly) for oxygen at 0.5249 keV ( $K\alpha$  radiation) at sites located remotely from the mounting area, to minimise possible detection of background oxygen. EDX samples are shown in Figure 7-7 below.

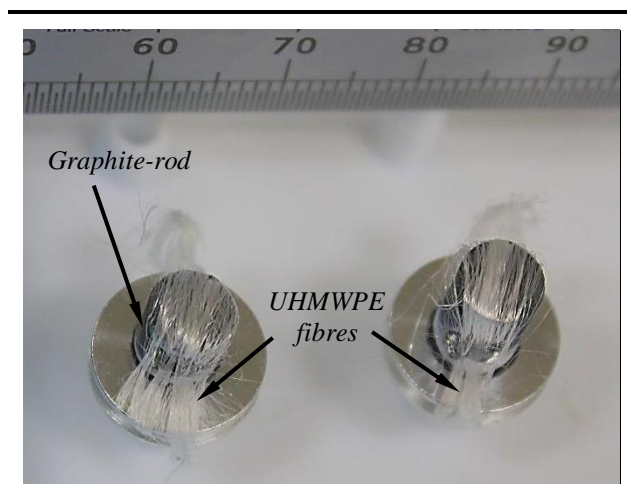


**Figure 7-7. UHMWPE annealed and as-received fibres are mounted on graphite rod sections, ready for EDX analysis.**

Result from the EDX analysis performed on the fibre samples are shown in Figure 7-8. No significant levels of oxygen within the annealed or as-received fibres could be found. Moreover, at the highest levels of sensitivity, there were no differences between

outputs from each sample that might indicate the smallest increase in oxygen from annealing. This suggests that there are no chemically-based changes to the fibres from the annealing process.

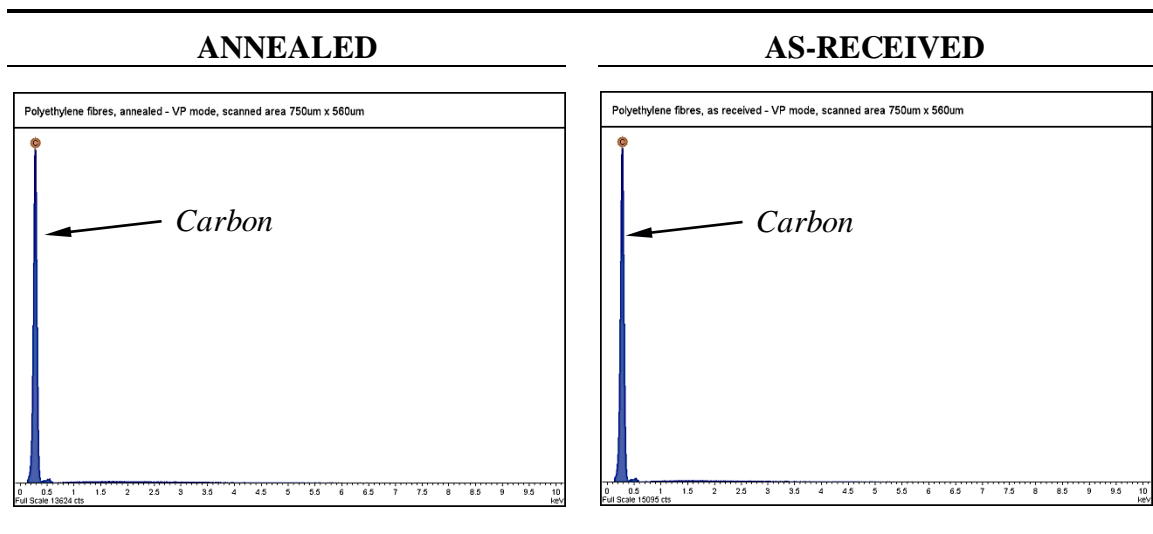


**Figure 7-8. EDX tests on UHMWPE fibres show no evidence of oxidation in the annealed fibres. Carbon is clearly visible in both samples with no indication of other elements, such as oxygen, from the annealing process.**

## 7.4.2 FEASIBILITY STUDY ON VISCOELASTIC BEHAVIOUR OF UHMWPE FIBRES

Figure 7-9 shows recovery strain of the annealed polyethylene fibres for the applied creep stress (24 hours) values ranging from 0.8 GPa to 1.5 GPa. The data points represent real time measurements up to ~3 years. It can be seen from Figure 7-9, that strain magnitude (after load removal) increases with higher creep stress. In general, polymeric fibres with highest recovery strain magnitude (those exhibiting viscoelastic properties) would be expected to be more beneficial for VPPMCs. In Figure 7-9(d), it can be observed that fibres subjected to 1.5 GPa creep stress show the highest creep strain; therefore, this stress value would be more favourable for UHMWPE fibre-based VPPMCs. However, after some unsuccessful attempts at 1.5 GPa, it was decided to reduce the risk of fibre breakage and a creep stress of 1.36 GPa was adopted instead. To validate recovery strain results of the fibres subjected to 1.36 GPa creep strain, further samples were prepared and processed to assess repeatability. These results are also shown in Figure 7-9(c) and they can be seen to follow a similar trend. In addition, three samples of non-annealed yarn subjected to the same creep conditions (1.3 GPa) were processed and the strain recovery results are also shown in Figure 7-9(c). For comparison, Figure 7-9(c) shows recovery strain data using annealed nylon 6,6 fibres from Ref [10]. The different behaviour of annealed and non-annealed fibres is discussed in Section 7.4.3.

Despite the scatter in Figure 7-9, the most important observation is that the yarn undergoes time-dependent strain recovery and remains active beyond 20,000 hours; also the strain-time magnitudes are greater with annealed yarn. The applied creep stress (1.36 GPa) for UHMWPE fibre was almost four times the value used in nylon 6,6 studies (i.e. 342 MPa), though the 24 hours creep strain for annealed UHMWPE in Figure 7-10(a), at 5.4%, is substantially lower than the 12.4% observed for annealed nylon 6,6 [8, 9]. Nevertheless, recovery strain-time levels are comparable; e.g. at 0.1 hour and 1000 hour respectively, UHMWPE gives 2.3% and 1.7% in Figure 7-9(c) compared with 2.8% and 1.6% for nylon 6,6 [10, 11].

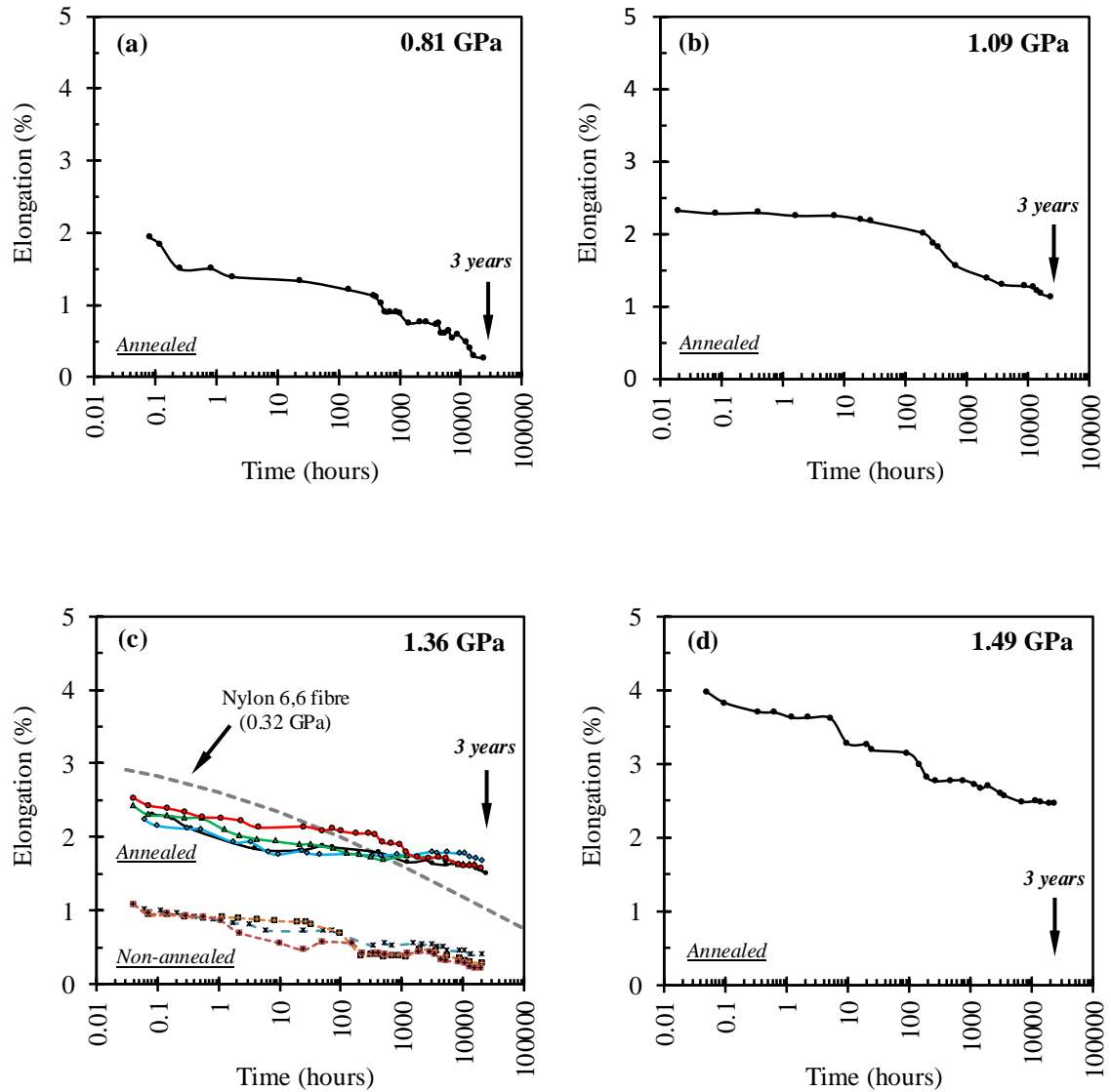


**Figure 7-9. Recovery strain behaviour of UHMWPE (Dyneema SK60) fibres subjected to various creep stress (real time ~3 years). Creep stress is determined from the applied load on a single yarn (24 hours) and unloaded yarn cross-sectional area. For comparison, data derived from Ref [10] is also shown for nylon 6,6 yarn. Note changes in Creep stress from (a) to (d).**

### 7.4.3 CREEP AND LONG-TERM RECOVERY STRAIN

The creep and recovery strain results as a function of the time are shown in Figure 7-10. Scatter in the data points can be attributed to uncertainty in locating ink mark edges on these multifilament yarns during strain measurement. This scatter was increased during strain recovery (Figure 7-10b), since data were also sensitive to ensuring that the yarn was maintained in a straight position during strain measurement. Comparing with results using nylon 6,6 yarns [8-11], there is greater data dispersion in recovery. This arises from the UHMWPE yarn characteristics, i.e. a high number of very fine filaments leading to their greater susceptibility to becoming separated from repeated handling. Filaments become readily separated in these yarns, as handling increases the presence of kink bands along the filaments, an effect also observed by others [206].

In Figure 7-10(a), the fibres exhibit a progressive increase in elongation from prolonged exposure to static loading; the creep stress (1.36 GPa) was determined from the applied load divided by the cross-sectional area of the fibres. It is also evident that annealing strongly increases the creep rate of the fibres and a slower recovery strain rate is also observed for the annealed fibres in Figure 7-10(b). For, recovery strain results corresponding to the creep load in Figure 7-10(b), the data points represent real time measurements up to ~3 years. The curve fitted to the data points (solid line) represents time dependent recovery strain  $\varepsilon_{rvis}(t)$  from Equation 2-1. This was fitted to the data with commercially available software (*CurveExpert-1.4*) and the resulting parameters are listed in the Figure 7-10.

By fitting Equation 2-1 to the recovery data in Figure 7-10(b), the indicative value for  $\varepsilon_f$  is  $9.44 \times 10^{-2}$  % (annealed) and  $1.77 \times 10^{-11}$  % (non-annealed); i.e. permanent strain from viscous flow effects is predicted to be negligible in both cases. Relevant published work is limited, though some comparison may be made with cyclic deformation studies on UHMWPE fibres [207]; here, complete viscoelastic recovery with no plastic deformation (viscous flow) was observed if the delay time between successive stress cycles (3.5 GPa) was ~3000 times longer than the stress cycle duration. Thus to some

extent, this lends support to the current findings i.e. very low  $\varepsilon_f$  predictions. Figure 7-10(b), indicates that the viscoelastic activity continues beyond the measured timescale. Extrapolating curve to 1100 years ( $10^7$  hours), it is useful to note that Equation 2-1 predicts the time dependent recovery strain  $\varepsilon_{rvis}(t)$  to be  $\sim 1.21\%$  for annealed and  $\sim 0.10\%$  for the non-annealed fibres; this suggests that viscoelastic activity (at least under these conditions) is a long term phenomenon.

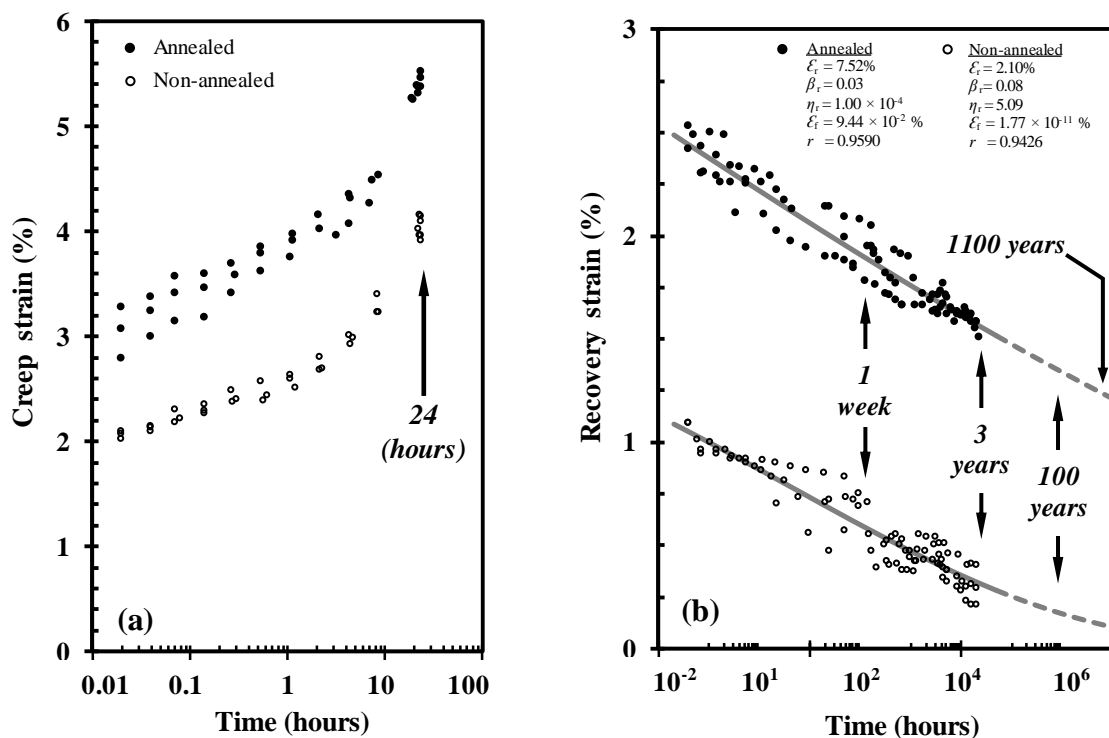


Figure 7-10. Creep and recovery strain results for annealed and non-annealed (as-received) UHMWPE (Dyneema SK60) fibres. (a) Strain from 24 hour, 1.36 GPa creep stress, in (b) recovery strain results corresponding to the creep data in (a). The solid curves represent the Weibull model fit using Equation 2-1, with listed parameters and coefficient of correlation.

Some comparison with other UHMWPE creep studies can be made. Berger *et al* [122] studied single filament creep at 1.5 GPa applied stress. This is close to the value used in this work (1.36 GPa), thus creep compliance at 24 hours from data in Ref [122], i.e.  $\sim 0.06 \text{ GPa}^{-1}$ , enables a comparison to be made with current results. From Figure 7-

10(a), the 24 hour creep compliance for annealed and non-annealed yarns are both lower, i.e. 0.040 and 0.030  $\text{GPa}^{-1}$  respectively. Some discrepancy may be expected, as the applied stress value in this work was determined from a yarn cross-sectional area derived from supplier information. Pre-treatment of the material used in Ref [122] is not stated, but a non-annealed condition would make the equivalent compliance from this study is only half their value. The non-annealed result (0.030  $\text{GPa}^{-1}$ ) in Figure 7-10(a) does however agree with the 24 hours (1.25 GPa) compliance value of Peijs *et al* [208] for (mechanically similar) Dyneema SK66 yarn in equivalent condition.

#### 7.4.4 RECOVERY FORCE

Figure 7-11 shows the viscoelastic recovery force data measured (in real time) over 14000 hours (~1.5 years) from UHMWPE yarn in terms of axial stress-time output. Here, the stress is from recovery force exerted by the fibres (yarn) over their cross-sectional area, and the curve fit comes from the Weibull/KWW Equation 7-1. Also shown for comparison is the output from nylon 6,6 yarn data, which grows towards a limiting value of 12 MPa [91]. In contrast with the nylon data, the UHMWPE output climbs to a maximum value at ~8 hours, followed by a gradual decline with time; however, from ~3000 hours, this levels off at 12-13 MPa.

From the Figure 7-11 results, two observations can be made. First, the UHMWPE output is notably higher (initially) than that of the nylon and this reflects the higher creep stress (>4fold) that could be applied to the former. The second observation is that although Equation 7-1 may be fitted to the first few hours of the UHMWPE plot, there is clearly a deviation from this characteristic at greater time values. This could suggest that a secondary (competing) mechanism working against the initial recovery force output becomes increasingly prominent. Fitting Equation 7-1 to the first 8 hours of data in Figure 7-11 shows that  $\beta < 1$ , i.e. as with nylon 6,6 yarn, the force growth rate decreases with time. Although output is predicted to increase progressively towards a limiting value (12 MPa) as  $t \rightarrow \infty$  for the nylon yarn [91], Equation. 7-1 for the UHMWPE predicts a limiting value of 21.5 MPa beyond the first 8 hours. However, in

practice, the output then decreases, until an apparent steady-state value of 12-13 MPa is reached, and this must be due to the increasing effects of the secondary mechanism.

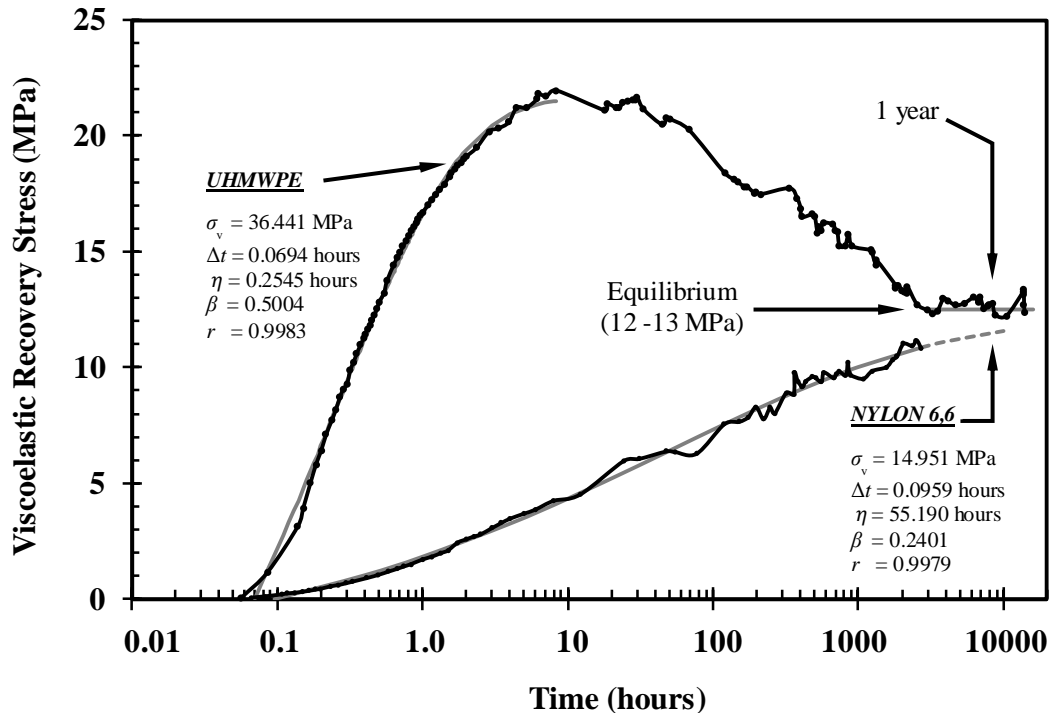


Figure 7-11. UHMWPE viscoelastic recovery force in terms of axial stress output (force relative to the total cross-sectional area of the fibres) for yarn subjected to a 24 hour creep stress of 1.36 GPa. For comparison, data derived from Ref [91] is also shown, in which nylon 6,6 yarn was subjected to a 24 hour creep stress of 0.32 GPa. Equation 7-1 is fitted to the first 8 hours for UHMWPE fibres; parameters are shown for both yarns.

#### 7.4.5 POLYETHYLENE FIBRES VISCOELASTIC RECOVERY FORCE AND TIME-DEPENDENT BEHAVIOUR

The possibility of two counteracting mechanisms causing the unexpected output characteristic for UHMWPE fibres in Figure 7-11 requires further consideration, especially since recovery strain data in Figure 7-10(b) shows no comparable trend, i.e. no counteracting mechanisms. The stretching stage, required the yarn to be wound (twice) around the lower bobbin to minimise stress concentration problems and this set-

up was maintained as the assembly was transferred to the *FM* rig (Figure 7-4). Thus at least some of the decreasing recovery in Figure 7-11 could be caused by gradual friction-affected slipping of the yarn around the lower bobbin, reducing force output from the main loop. Preliminary tests however, had been conducted where (following the stretching stage) the yarn was re-fitted to the lower bobbin after removing the wound material. Although unavoidable fibre damage affected force output, a similar trend in output with time was observed, suggesting that experimentally-induced yarn slippage was not the main cause.

This leads to the conclusion that the two mechanisms are structurally based and structural differences may originate from fibre heterogeneity. Researchers have referred to gel-spun UHMWPE fibres possessing skin-core properties, the skin most likely consisting of low molecular weight fragments and solvent excluded during crystallisation [126, 197], or as an unconstrained layer around a constrained core [198]. Etching experiments [123] have revealed long narrow density-deficient regions within the crystal structure of the core, resulting from contraction-induced stresses during crystallisation, an effect not occurring within the skin. Through micro-diffraction experiments with a single UHMWPE fibre, Riekel *et al* [209] have identified the possibility of a band of monoclinic phase material extending around the filament circumference, i.e. crystallographic differences between core and outer layers. Thus, although highly speculative, a variation in mechanical characteristics across each filament, in which the filament core is stiffer and time constants for viscoelastic mechanisms are shorter than for the outer skin, enables an explanation to be proposed, as follows.

Initially in Figure 7-11, the recovery force climbs within the first 8 hours due to the filament core regions causing a rapid build-up of force as they attempt viscoelastic retraction (at fixed strain). The rate of force build-up progressively decreases as sites that store energy within the cores become depleted through force generation and possibly by energy transfer to skin regions. At ~8 hours, longer term viscoelastic activity from the skin regions starts to become dominant. At this point, the force

magnitude cannot be maintained by the (less stiff) skin regions, and so the recovery force decreases. Initially, it was believed this decrease will lead to an output level that should result in a state of equilibrium existing between skin and core regions. Thus eventually, the UHMWPE force measurement data plotted in Figure 7-11 was expected to approach a constant (non-zero) value. Clearly, the most recent data shown in Figure 7-11 appears to confirm this hypothesis. Moreover, evidence of the proposed differences in mechanical characteristics between skin and core regions is presented in Section 7.4.7.3.

## **7.4.6 COMPARISON OF TEST AND CONTROL POLYETHYLENE FIBRES**

Stress-strain plots from tensile tests performed on the UHMWPE yarn are shown in Figure 7-12 and the data are summarised in Table 7-1. The linearity in Figure 7-12 enabled modulus  $E$  to be determined up to 3% strain; this provided more consistent run-to-run results than would have been obtained from initial gradient values. Mean values obtained from the as-received (non-annealed) samples in Table 7-1 are ~8% lower than the supplier-specified values for tensile strength  $\sigma_f$  (2.56 GPa) and strain-to-failure  $\epsilon_f$  (3.5%), and ~13% lower for  $E$  (87 GPa) [98], though this may be explained by differing test conditions. The almost linear deformation response and  $\epsilon_f$  values are similar to other non-annealed gel-spun UHMWPE fibre data [210].

In Ref [210], fibre annealing (24 hours at 149°C) caused  $\epsilon_f$  to increase by >100%, whereas  $\epsilon_f$  in this work increased by ~6%. Also, other parameters in Figure 7-12(a) and Table 7-1 show only small differences between as-received and annealed (control) samples, i.e. ~7% and ~15% reduction in strength and modulus. Of particular interest however, is that the data for test and control yarns are very similar in Figure 7-12(b) and Table 7-1. In fact, although statistical analysis (hypothesis testing, 5% significance level) for the mean values of  $\sigma_f$ ,  $\epsilon_f$  and  $E$  show differences between as-received and control yarns, there are no statistical differences between the test and control yarns for these parameters. This, together with evidence from Figure 7-6, demonstrates that the

stretching treatment applied to the test fibres cause no changes to their physical characteristics and tensile properties. Therefore, it may be concluded that any improvements in mechanical properties offered by the pre-stressed samples compared with their control (un-stressed) counterparts, must result from pre-stress effects alone.

**Table 7-1. Summary of the tensile test results of annealed test (previously stressed), control (un-stressed) and non-annealed (as-received) UHMWPE fibres. S.E is the standard error of the mean.**

	Test	Control	As-received
<b>Tensile strength, <math>\sigma_f</math> (GPa)</b>	2.21	2.10	2.27
	2.21	2.20	2.46
	2.20	2.21	2.36
	2.20	2.27	2.32
	<i>Mean <math>\pm</math> S.E</i>	$2.21 \pm 0.00$	$2.19 \pm 0.03$
<b>Modulus, <math>E</math> (GPa)</b>	63.36	64.44	76.67
	68.83	67.03	72.82
	65.15	64.14	74.17
	65.37	65.71	78.01
	<i>Mean <math>\pm</math> S.E</i>	$65.68 \pm 1.14$	$65.33 \pm 0.66$
<b>Strain to failure, <math>\epsilon_f</math> (%)</b>	3.50	3.40	3.10
	3.20	3.30	3.40
	3.30	3.50	3.40
	3.40	3.50	3.00
	<i>Mean <math>\pm</math> S.E</i>	$3.35 \pm 0.06$	$3.43 \pm 0.05$

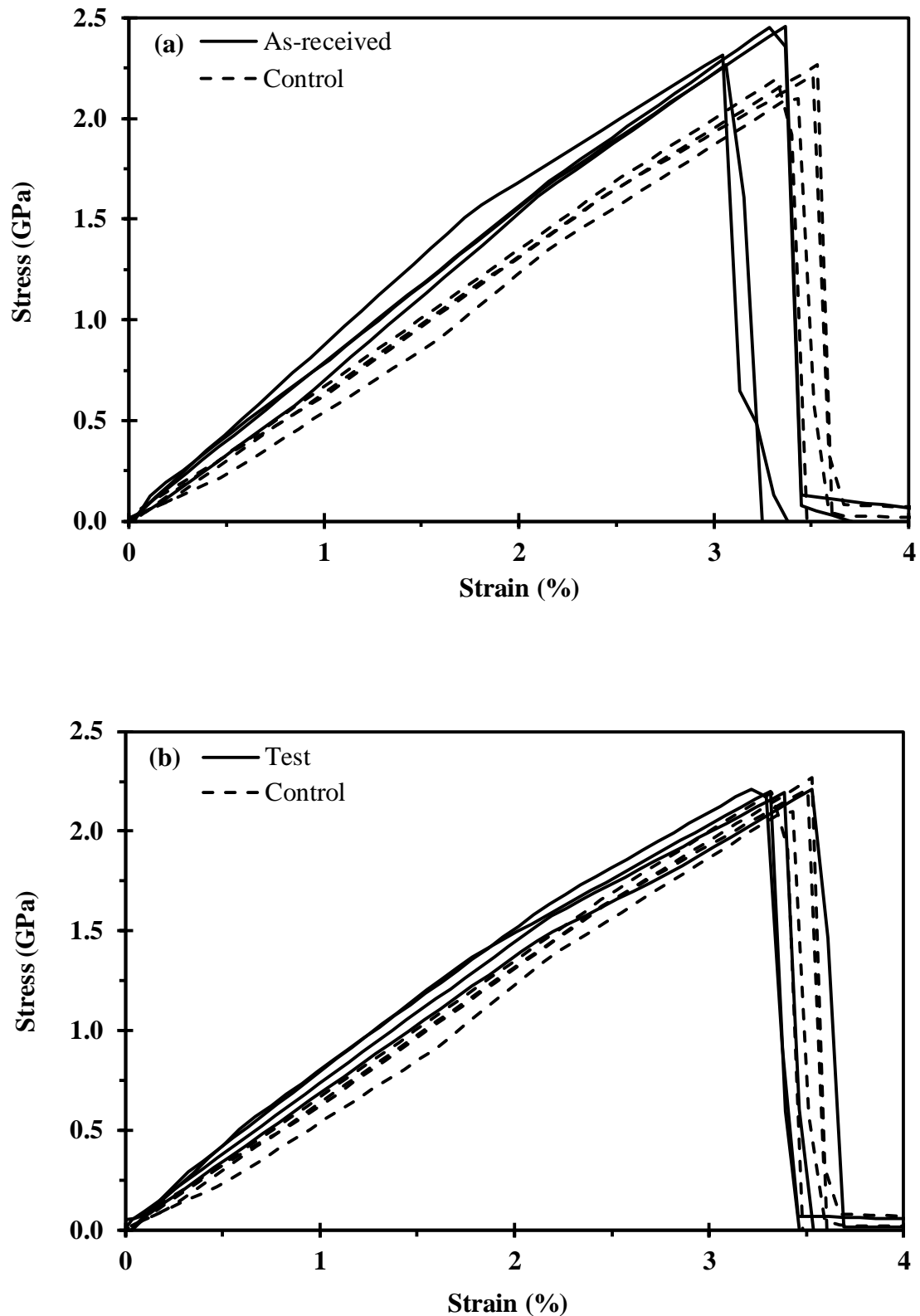
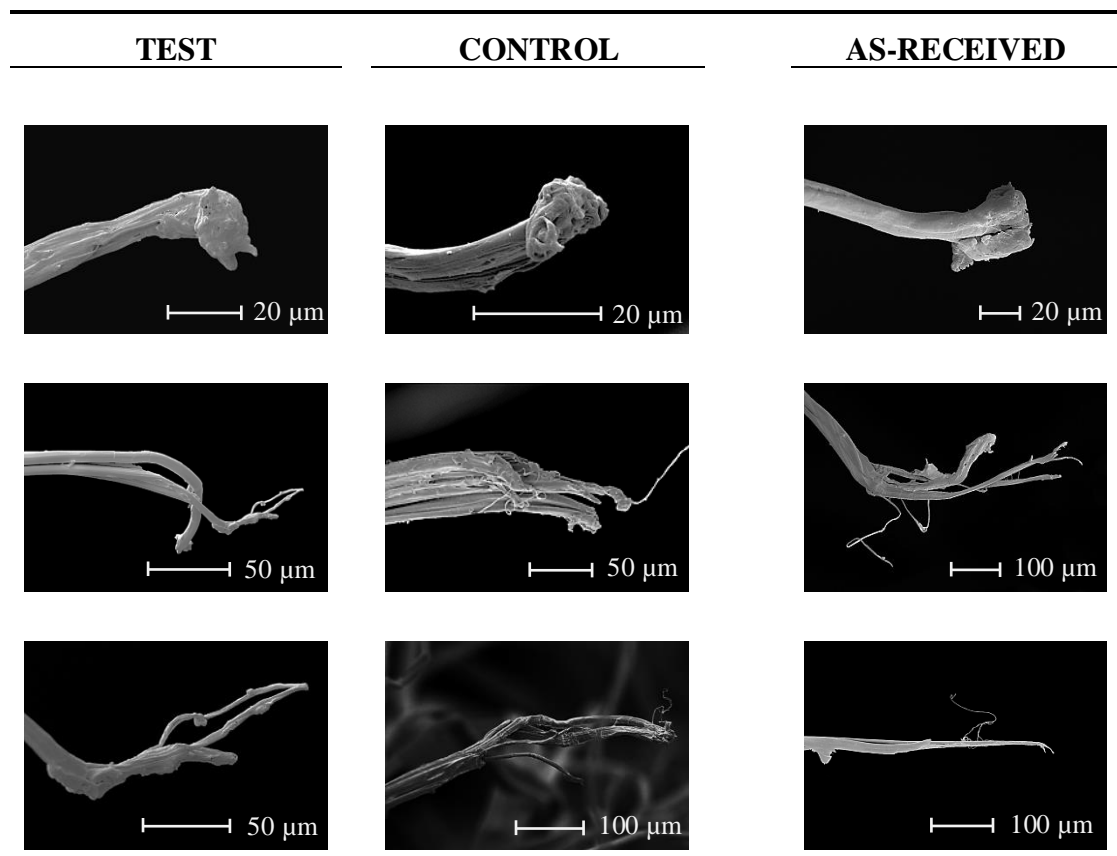


Figure 7-12. Stress-strain plots from tensile tests performed on UHMWPE yarn. (a) control (annealed) and as-received (non-annealed) fibres. (b) test (previously stressed) and control (un-stressed) fibres. The test yarn (fibres) in (b) was evaluated at 168 hours (1 week) after releasing the 24 hours creep stress of 1.3 GPa. (data from Table 7-1).

Typical fractured polyethylene filament ends from the tensile tests are shown in Figure 7-13 below. These fibres appear to be similar in appearance to those found in the literature [211, 212]. Figure 7-13 shows no visual evidence of differences in fracture characteristics between test and control fibres, which adds further support to the findings from Table 7-1 and Figure 7-6.



**Figure 7-13. Representative SEM micrographs of tensile tested UHMWPE fractured fibres. From left to right, annealed test (previously stressed), control (un-stressed) and non-annealed (as-received) samples show similar characteristics. Micrographs were taken at 1300 hours (~8 weeks) after testing. Note changes in magnification.**

## 7.4.7 CHARPY IMPACT TESTS

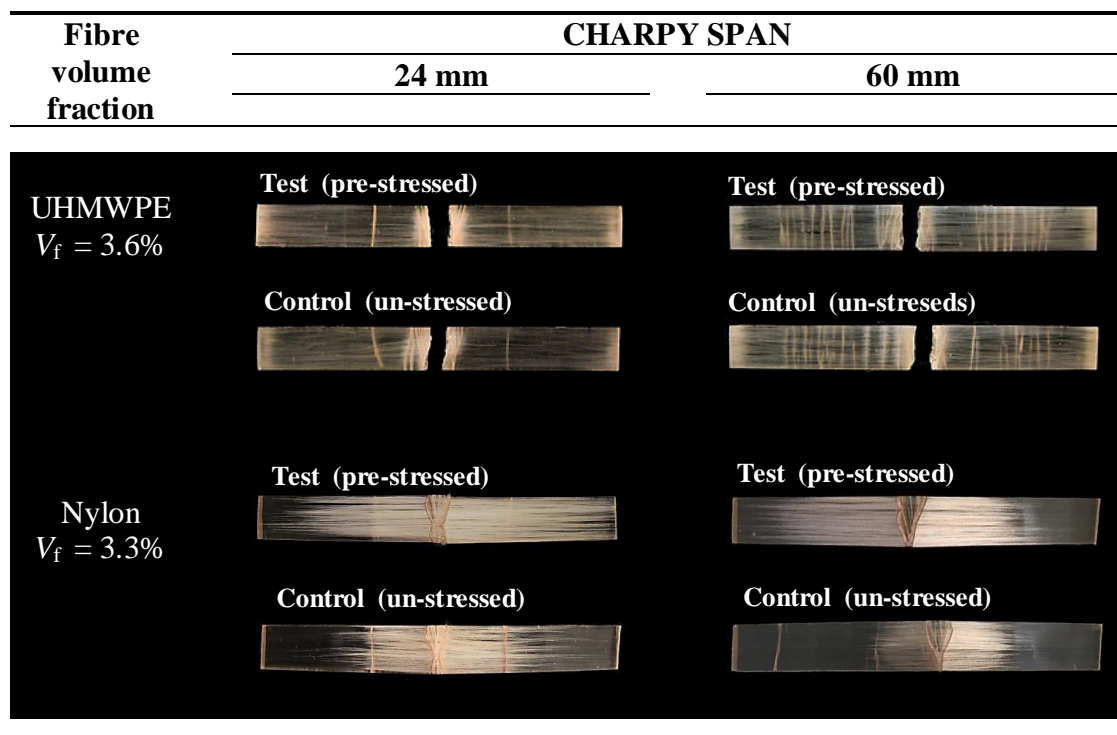
### 7.4.7.1 IMPACT DATA AND MACROSCOPIC EXAMINATION

Table 7-2 summarises the impact energy data. Some batches show the test samples absorbing 30-40% more energy than their control counterparts. For the two span settings, statistical hypothesis testing (5% significance level) shows no difference between overall mean increases in energy absorbed by the test samples, i.e. the average increase from both span settings is ~20%. In absolute terms, energy absorption is 30-40% higher for both test and control groups when the span is increased to 60 mm. These observations are not consistent with the 3.3%  $V_f$  nylon 6,6 fibre impact studies reported in Chapter-5, Table 5-2, where energy absorption in absolute terms dropped by 40-60% at 60 mm span, whilst the increase in energy absorption of the test samples was ~40% at 24 mm, but effectively zero at 60 mm span. These disparities between UHMWPE and nylon 6,6 fibre-based composites suggest significant differences in the role of energy absorption mechanisms.

Figure 7-14 shows typical impact-tested samples, and, for comparison, nylon 6,6 fibre-based samples from Figure 5-4. It can be seen from Figure 7-14, that the UHMWPE samples fractured into two pieces; in fact, all polyethylene fibre-based samples followed similar characteristics at both span settings. At 24 mm span, the vertical cracks away from the fracture site are similar for both UHMWPE and nylon fibre samples; these occur mainly at the anvil shoulder locations, as the Charpy hammer bends the sample into a 'V' shape during impact. For the UHMWPE samples at 60 mm span however, there is more opportunity for specimen deflection, resulting in a greater prominence of vertical cracks as the sample becomes 'U' shaped during impact. The nylon fibre samples show fewer vertical cracks at 60 mm span, as the relatively low modulus fibres allow sample fracture characteristics to be dominated by the (brittle) matrix. In Figure 5-4 (nylon fibre-based investigation), multiple vertical cracking was only observed with higher  $V_f$  values at this span. This suggests that the greater number of (energy absorbing) vertical cracks in the UHMWPE samples are responsible for the 30-40% increase in  $\text{kJm}^{-2}$  values from both test and control samples at the 60 mm span setting in

Table 7-2. These multiple cracks occur at a lower  $V_f$  than with the nylon case, as the much greater stiffness of UHMWPE fibres reduces the influence of the matrix characteristics. This fibre stiffness effect may also relate to the increase in energy absorption from pre-stress effects being maintained at 60 mm span in Table 7-2, an effect only observed from nylon fibre samples at higher  $V_f$  in Figure 5-4.

Of particular interest in Figure 7-14 is that in contrast with the nylon 6,6 samples, no significant fibre-matrix debonding can be observed in the UHMWPE samples. As reported in Chapter-5, pre-stress-induced residual shear stresses at the fibre-matrix interface regions promote energy absorbing fibre debonding over transverse fracture. This explains the greater debonded area in the nylon fibre test samples compared with control counterparts, but the corresponding UHMWPE fibre test and control samples show no differences in fracture characteristics. Here, this suggests that there is an equivalent mechanism, but the debonding is not visible in Figure 7-14 below, as it occurs (possibly) between skin and core regions within the UHMWPE fibres.



**Figure 7-14.** Typical UHMWPE fibre-based composites, showing test (pre-stressed) and control (un-stressed) samples after impact testing. For comparison, equivalent nylon 6,6 fibre-based samples are also shown from Figure 5-4. Note photos are taken from the fibre-rich side (away from the impact point).

**Table 7-2. Charpy impact tests data of UHMWPE fibre composite samples tested at 24 and 60 mm spans. For each span, a total of 15 batches were tested, each batch consisting of 5 test and 5 control samples. Data is normalised by dividing impact absorbed energy (J) by the sample cross-sectional area. S.E is the standard error of the mean. (Individual tested sample data are presented in Appendix-D).**

Age (hours)	24 mm span			Mean increase in energy (% ± S.E)
	Mean impact energy (kJm <sup>-2</sup> )		Increase in energy (%)	
	Test ± S.E	Control ± S.E		
24	43.34 ± 3.73	33.32 ± 1.43	30.09	24.14 ± 7.11
	30.35 ± 2.83	27.59 ± 1.75	9.97	
	37.35 ± 3.75	28.22 ± 1.45	32.35	
96	32.97 ± 1.21	28.18 ± 2.22	16.99	17.93 ± 6.81
	34.77 ± 1.97	32.60 ± 1.96	6.64	
	32.68 ± 1.92	25.11 ± 1.18	30.17	
168	32.98 ± 1.31	30.34 ± 0.48	08.73	14.47 ± 4.78
	30.19 ± 1.73	27.27 ± 1.47	10.72	
	30.17 ± 1.63	24.34 ± 0.83	23.96	
336	29.67 ± 1.29	23.75 ± 0.99	24.93	21.66 ± 1.64
	30.78 ± 1.68	25.66 ± 1.15	19.99	
	28.41 ± 0.58	23.67 ± 1.40	20.05	
1008	29.80 ± 2.20	23.36 ± 1.10	27.57	20.04 ± 3.78
	32.21 ± 1.12	27.57 ± 0.52	16.83	
	28.63 ± 0.85	24.74 ± 0.35	15.72	
<b>Mean ± S.E</b>	<b>32.29 ± 1.85</b>	<b>27.05 ± 1.22</b>	<b>19.37 ± 2.16</b>	
<b>60 mm span</b>				
24	41.75 ± 1.54	38.21 ± 3.10	9.27	21.25 ± 9.27
	42.57 ± 2.26	37.03 ± 3.09	14.98	
	46.83 ± 5.40	33.57 ± 3.13	39.49	
96	46.23 ± 5.24	39.89 ± 3.52	15.92	15.47 ± 5.72
	39.10 ± 3.47	37.11 ± 2.43	5.35	
	39.12 ± 3.59	31.26 ± 1.51	25.15	
168	46.25 ± 5.50	40.50 ± 4.20	14.21	23.97 ± 5.62
	44.22 ± 4.45	33.08 ± 2.20	33.69	
	39.34 ± 2.96	31.73 ± 2.39	24.01	
336	54.05 ± 6.69	46.87 ± 3.81	15.34	26.01 ± 8.04
	47.59 ± 4.61	39.35 ± 4.33	20.93	
	52.59 ± 4.07	37.10 ± 3.76	41.76	
1008	34.07 ± 4.49	31.81 ± 1.57	7.09	27.61 ± 10.73
	39.31 ± 3.29	29.69 ± 2.49	32.42	
	49.78 ± 4.46	34.71 ± 2.32	43.31	
<b>Mean ± S.E</b>	<b>44.19 ± 4.13</b>	<b>36.13 ± 2.92</b>	<b>22.31 ± 3.28</b>	

### 7.4.7.2 FIBRE SPATIAL DISTRIBUTION IN COMPOSITE SAMPLES

Figure 7-15 shows polyethylene fibre spatial distributions in the composite samples; these cross-sections were taken from the moulded strips and then ground and polished to enable observation by optical microscopy. As reported previously in Chapter-5 and Chapter-6, fibres tended to sink to the bottom of the mould during production of the composite samples (by open casting), resulting in greater fibre concentration at the lower mould face. Similar effects can be seen in the polyethylene fibre composite samples in Figure 7-15 below.

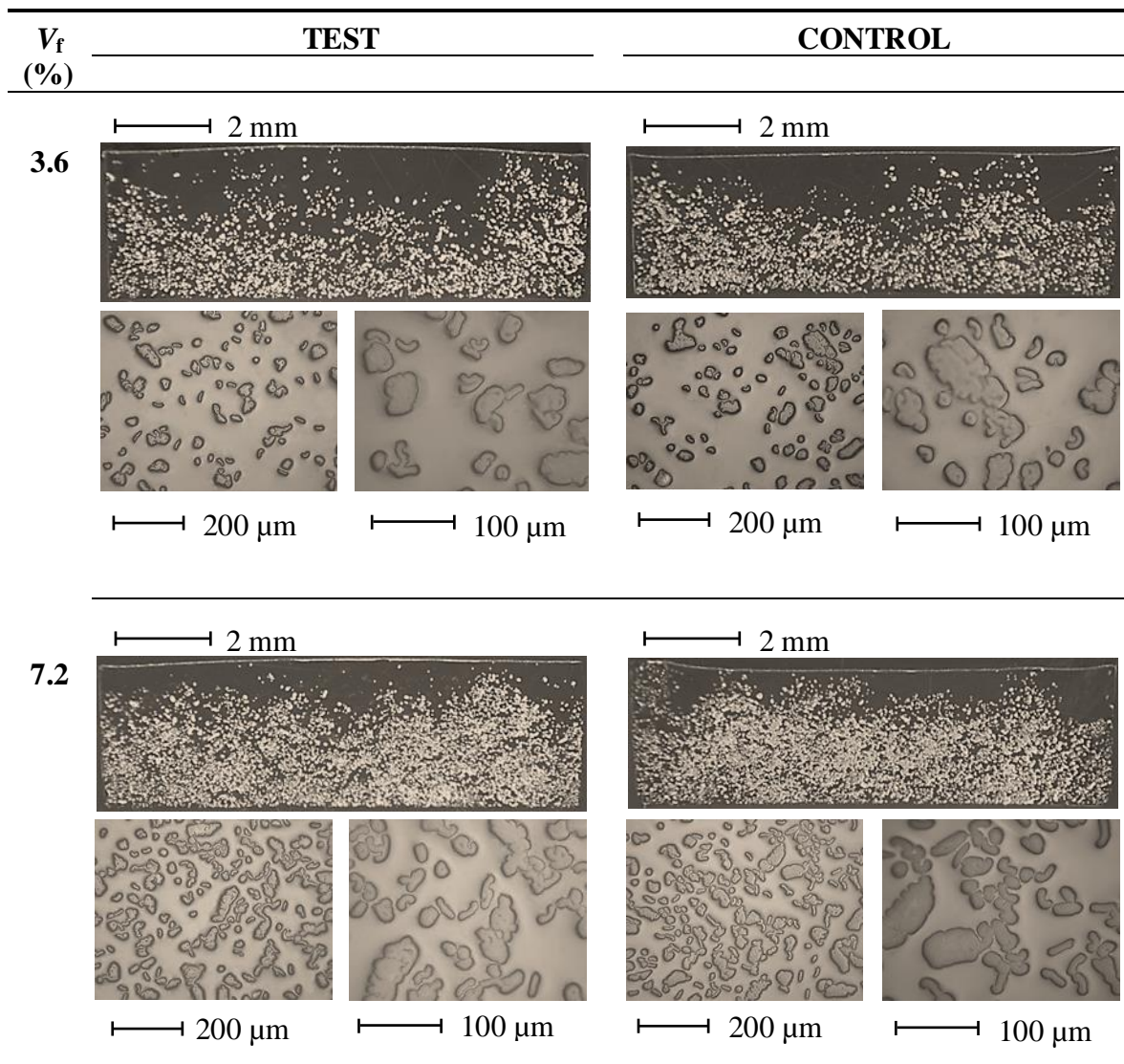


**Figure 7-15. Representative optical micrograph (polished) sections of UHMWPE fibre spatial distributions in composite samples produced by open-casting with polyester resin. Note  $V_f$  values are nominal.**

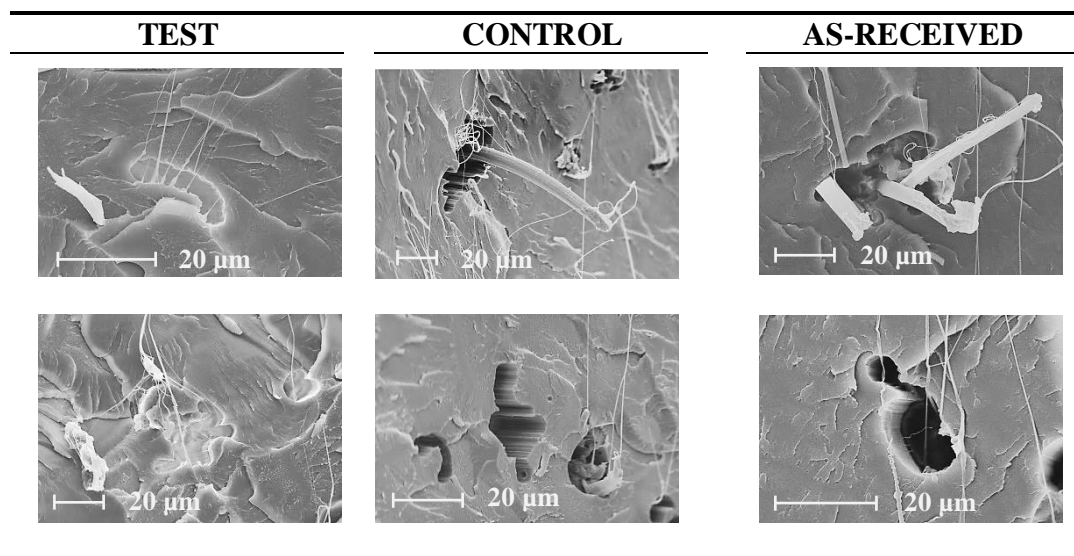
Figure 7-15 clearly show variations in fibre distribution, with a tendency for most fibres being in the lower half (3.6%  $V_f$ ) or 2/3 (7.2%  $V_f$ ) of the moulding. Even though the density of the fibres and resin (in liquid state) are very similar, this effect is also observed in the nylon fibre-based VPPMCs with polyester resin samples used for flexural studies [13] and Charpy impact testing [7-11]. Thus, as with previous work, all samples tested on Charpy and three-point bending were mounted with the fibre-rich side facing away from the impact or loading point. Of particular importance however, is that Figure 7-15 shows no discernible differences between cross-sections of the test and control samples. It should also be noted that there is a wide range of fibre sizes and shapes (some appearing to be bundles of filaments) dispersed within the matrix.

### 7.4.7.3 FIBRE INSPECTION AND ANALYSIS

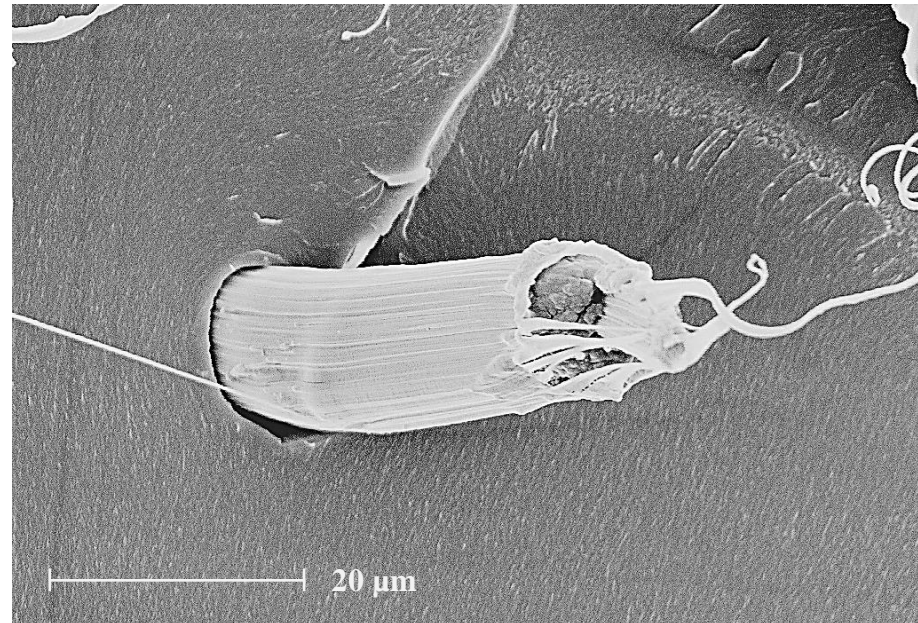
As reported in Section 7.4.7.1, all polyethylene fibre composite samples subjected to impact tests split into two pieces. This provided further opportunities to investigate the fracture characteristics of the test and control composite samples. Interestingly, various types of fracture mechanism were observed. The main fracture behaviour observed from SEM investigation included debonding between fibre skin/core regions, matrix cracking, fibre breakage, fibre pull-out, fibre fibril formation and tensile type fibre failure. These features are clearly visible in the SEM micrographs taken at macro and micro scale shown in Figures 7-16 to 7-21.

Figure 7-16 shows typical SEM fracture cross-sections. Although fibre pull-out with clear separation from the matrix can be seen in the control and as-received samples, there appears to be a layer of residual fibre material that has coated the pull-out cavities in the test samples, i.e. evidence of core-skin debonding (cohesive failure). Also, UHMWPE strands (fibrils) can be observed in Figure 7-16, these being more evident in the test samples, where they originate from the edges of the pull-out cavities. Therefore, these fibrils must originate from the fibre skin regions.

In Figure 7-16, the changing failure mode from total pull-out of fibres to fibril formation in the test sample appears to be promoted by pre-stressing, which may contribute to more energy absorption. Failure in the control and as-received samples shows rupturing within the fibre; and some fibre pull-out. Localised marks from drawn fibres can be seen as surface grooves replicated in the polyester matrix, which suggests forcible removal of the fibres during impact. The corresponding groove in the matrix indicates failure involves sliding at the interface region between fibre skin and matrix. The failure behaviour of UHMWPE fibres observed in Figure 7-16 for control and as-received samples has been previously reported by other researchers [109, 111, 197], while the skin/core debonding effect in test samples observed in this work is previously unrecognised. The SEM fracture section from a control sample in Figure 7-17 supports this view: here, this fractured (but otherwise intact) fibre clearly shows a core region surrounded by a more ductile skin from which fibrils are formed during the impact process.

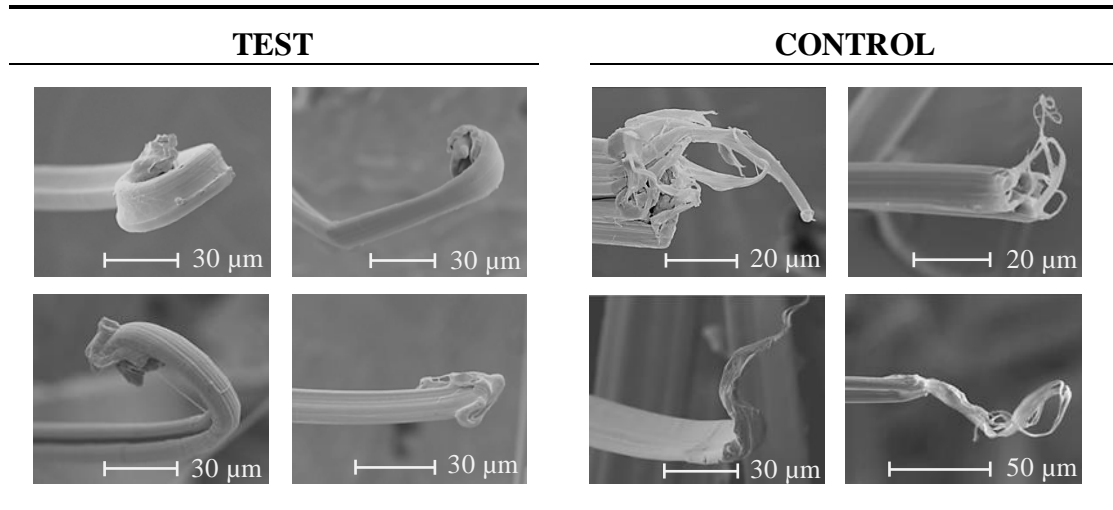


**Figure 7-16. Representative SEM micrographs of impact tested UHMWPE fibre composites showing typical fracture surfaces in test, control and as-received (non-annealed) samples. Similar features were observed across impact fracture surfaces of samples tested at both 24 and 60 mm span settings. Micrographs were taken at 1000 hours (~6 weeks) after impact tests. Note differences in magnification.**



**Figure 7-17. SEM image from the fracture surface of a control (un-stressed) sample, showing clear evidence of the skin-core structure in a UHMWPE fibre. Micrograph is taken at 1000 hours (~6 weeks) after impact tests.**

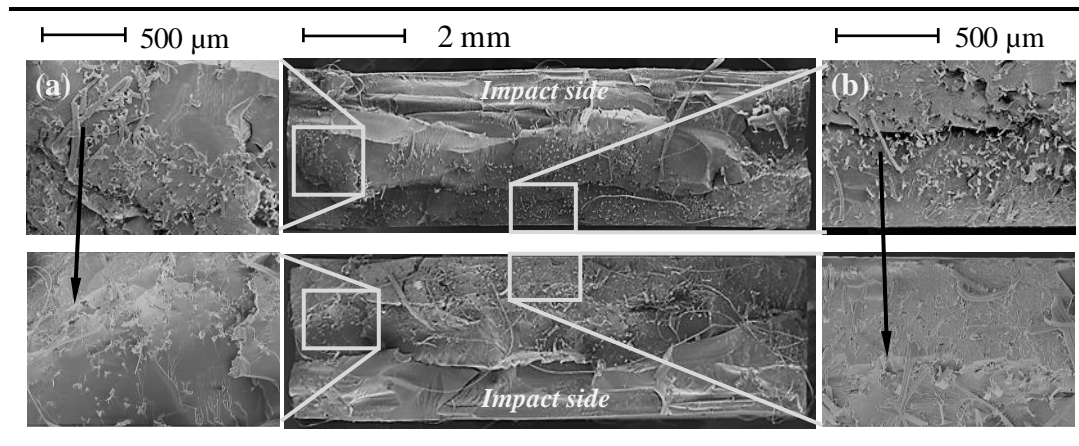
As reported in Section 7.2.1, the strain energy stored in the fibres from pre-stressing would be expected to remain active for a long-period of time. This may explain the different fracture behaviour between test and control UHMWPE fibres. Figure 7-18 shows examples of fibres (free of surrounding matrix material); it can be assumed that the surrounding matrix has fractured and been removed during impact penetration. Following fracture, the stored energy in the pre-stressing fibres causes the unconstrained fibres to be drawn back (recoil) in comparison with control samples, in which the fibres exhibit elongation features with tensile type fracture from plastic deformation.



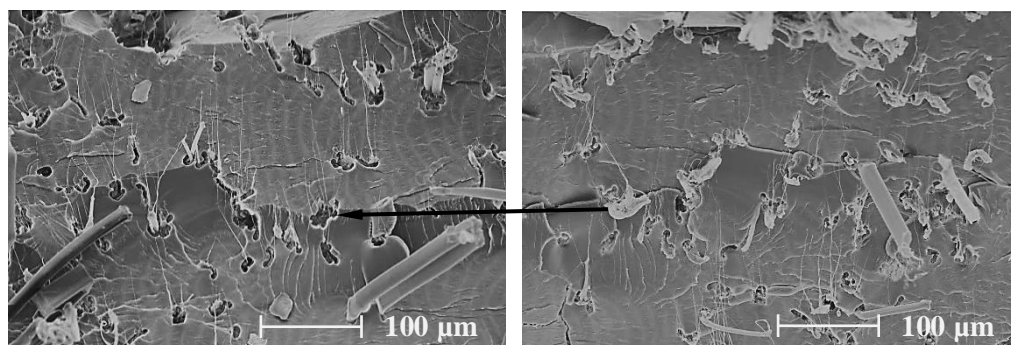
**Figure 7-18. Representative SEM micrographs of UHMWPE fibre-based composites subjected to Charpy impact tests. In the test (pre-stressed) samples, the stored energy from pre-stressing appears to be released in the form of fibre bending (recoiling) following fracture; in contrast with control (un-stressed) fibres which exhibit tensile type failure. Micrographs were taken at 1000 hours (~6 weeks) after impact tests. Note changes in magnification.**

Figure 7-19 shows representative SEM (macro) images of impact tested samples exhibiting brittle type fracture. The brittle behaviour of polyethylene fibres results in lower energy absorption (Table 7-2), in contrast with the nylon fibre-based composites, which shows ductile type failure (Chapter-5, Table 5-2). Jacobs's [20] investigation on polyethylene fibre composites has shown that the interlaminar shear strength of these fibres is limited because of the poor shear strength. Ref [20] reports that the low transverse and shear moduli of polyethylene fibres are due to the absence of specific interactions along the chains because of weak van-der-waals bonding.

From the SEM images shown in Figures 7-19 and 7-20, it can be observed that the fracturing process is a combination of matrix fracture and fibre pull-out. Fibre ends, protruding from the matrix, are clearly visible in Figure 7-20, and corresponding areas on the matching fracture surface show voids from vacated fibres.



**Figure 7-19.** Representative SEM micrographs of typical fractured cross-sections of a UHMWPE fibre-based composite sample from Charpy impact testing. All samples fractured into two halves. The two mating fracture surfaces show pull-out of fibres and corresponding cavities in (a) and (b). Similar features are observed in all samples tested at 24 and 60 mm Charpy span settings.



**Figure 7-20.** Representative SEM images of typical fractured cross-sections of a UHMWPE fibre-based composite sample from Charpy impact testing shows fibre pull out and their corresponding void formation in close detail. Arrow highlights the cavity from one fibre pulled out during the fracturing process.

Figure 7-21 below shows matrix cracking in an impact tested sample. The micrograph shows that the formation of river marks occurred before the vertical crack in the matrix, as these marks can be observed on both sides of the crack. This indicates progressive failure of the composite sample at the event of impact. These features are common to both test and control samples.

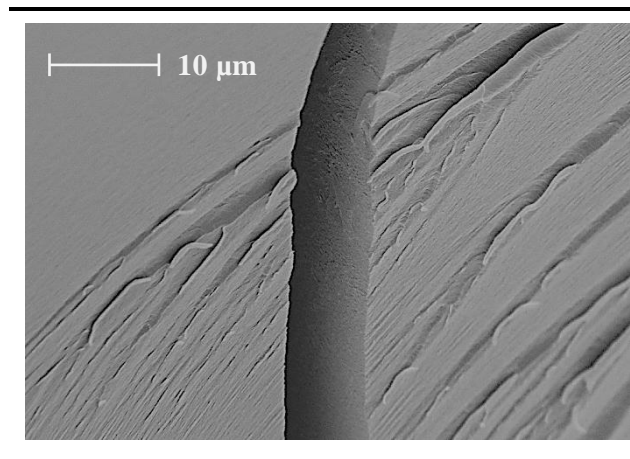


**Figure 7-21. Representative SEM micrograph of an impact tested UHMWPE fibre-based composite sample showing crack and river marks in the matrix.**

## 7.4.8 FLEXURAL TESTS

Figure 7-22, Tables 7-3 and Table 7-4 summarise the bend test results. The most significant observation is that the viscoelastic pre-stress effect increases flexural stiffness by typically 25-35%. As reported in Chapter-2 (Section 2.5.2), nylon fibre-based VPPMCs have showed no deterioration in predicted mechanical performance over a duration of  $\sim 20$  years at constant  $40^\circ\text{C}$  using time-temperature superposition principles [10]. However, such principles could not be used for UHMWPE fibres as the skin/core effects in these fibres might be expected to invalidate the time-temperature relationship value ( $\alpha_T$ ), required for accelerated ageing [213, 214]. Therefore, to support the longer-term recovery strain and force measurement findings of Figure 7-10(b) and Figure 7-11, the performance of polyethylene fibre-based VPPMC samples (nominal 3.6 and 7.2%  $V_f$ ) were evaluated by three-point bend tests over a period of  $\sim 2$  years. As seen in Figure 7-22, there appears to be no deterioration in test (or control) modulus values over the timescale investigated.

In Tables 7-3 and 7-4, the control samples show average modulus values increasing with  $V_f$ , from 3.6 GPa (3.6%  $V_f$ ) to 4.3 GPa (7.2%  $V_f$ ), i.e. the modulus is  $\sim 16\%$  higher. For the test samples, this is less, at  $\sim 10\%$  (4.8 GPa to 5.3 GPa). There is however, considerable variation in one of the 3.6%  $V_f$  batches at 336 hours in Table 7-3 (giving a 145% stiffness increase between test and control samples). Excluding this batch from the data reduces the flexural stiffness improvement from 35 to 29%. Thus, although differences between both  $V_f$  values are reduced, it is not negligible. During testing (and subsequent checking of video recordings), there appeared to be no assignable causes to the 145% increase at 336 hours, so there is no justification in excluding this batch. It is noteworthy, that repeated measurements data of the same batch recorded from 1000 to 16000 hours shows consistency.

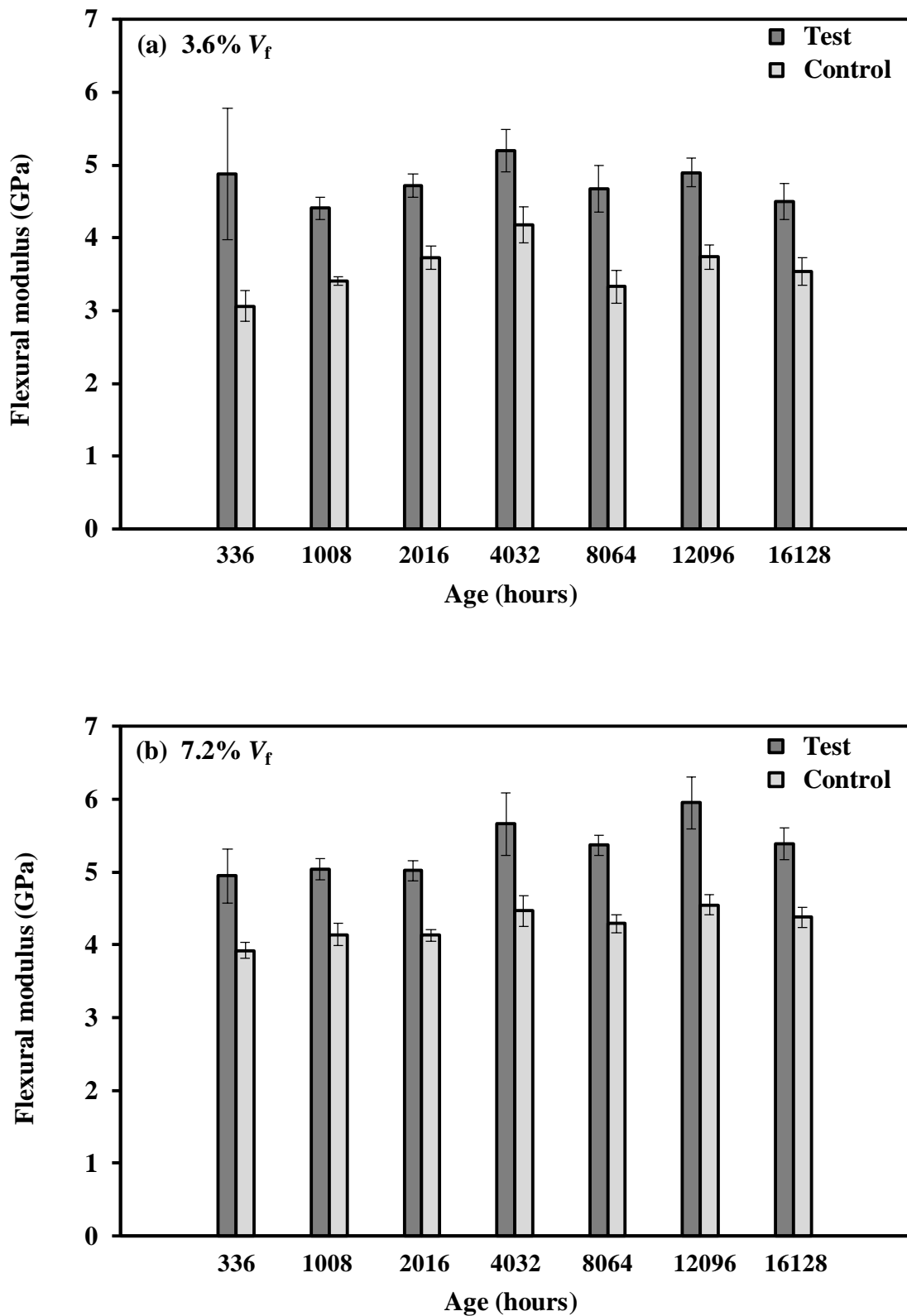


Figure 7-22. UHMWPE fibre-based composites: test (pre-stressed) and control (un-stressed) flexural modulus values, determined from the three-point bend tests. Each value represents the mean of three samples with corresponding standard error. (data from Tables 7-3 and 7-4).

**Table 7-3. UHMWPE fibre-based composites: flexural modulus results data from samples with nominal 3.6%  $V_f$  using the three-point bend tests. S.E is the standard error of the mean.**

<i>Nominal Fibre volume fraction (3.6%)</i>				
Age (hours)	Flexural modulus (GPa)		Increase (%)	Mean increase (% $\pm$ S.E)
	Test	Control		
<b>336</b>	3.74	3.03	23.7	64.0 $\pm$ 40.6
	4.24	3.44	23.2	
	6.65	2.71	145.2	
<b>1008</b>	4.28	3.49	22.5	29.3 $\pm$ 4.1
	4.71	3.44	36.8	
	4.23	3.30	28.5	
<b>2016</b>	4.73	3.95	19.8	26.9 $\pm$ 3.6
	4.99	3.81	31.1	
	4.44	3.42	29.8	
<b>4032</b>	5.29	4.32	22.2	24.5 $\pm$ 1.2
	5.66	4.52	25.1	
	4.66	3.69	26.2	
<b>8064</b>	4.28	3.49	22.5	41.0 $\pm$ 9.5
	5.30	3.62	46.6	
	4.44	2.88	53.9	
<b>12096</b>	4.73	3.78	25.0	31.1 $\pm$ 3.3
	5.30	4.02	31.9	
	4.66	3.42	36.3	
<b>16128</b>	4.28	3.63	17.8	27.3 $\pm$ 4.8
	4.99	3.81	31.1	
	4.23	3.18	33.1	
<b>Mean <math>\pm</math> S.E</b>	<b>4.75 <math>\pm</math> 0.14</b>	<b>3.57 <math>\pm</math> 0.10</b>	<b>34.9 <math>\pm</math> 5.8</b>	

**Table 7-4. UHMWPE fibre-based composites: flexural modulus results data from samples with nominal 7.2%  $V_f$  using the three-point bend tests. S.E is the standard error of the mean.**

<i>Nominal Fibre volume fraction (7.2%)</i>				
Age (hours)	Flexural modulus (GPa)		Increase (%)	Mean increase (% $\pm$ S.E)
	Test	Control		
<b>336</b>	5.65	4.05	39.5	25.9 $\pm$ 6.8
	4.81	4.01	19.9	
	4.38	3.70	18.2	
<b>1008</b>	4.99	3.85	29.6	22.0 $\pm$ 4.7
	4.81	4.25	13.3	
	5.31	4.32	23.1	
<b>2016</b>	5.30	4.28	23.9	21.7 $\pm$ 1.2
	4.81	4.01	19.9	
	4.96	4.09	21.2	
<b>4032</b>	6.52	4.81	35.6	26.6 $\pm$ 6.4
	5.16	4.51	14.2	
	5.31	4.09	29.9	
<b>8064</b>	5.65	4.05	39.5	25.6 $\pm$ 7.4
	5.16	4.51	14.2	
	5.31	4.32	23.1	
<b>12096</b>	6.52	4.81	35.6	30.6 $\pm$ 3.8
	6.01	4.51	33.2	
	5.31	4.32	23.1	
<b>16128</b>	5.65	4.53	24.8	22.8 $\pm$ 1.1
	5.55	4.51	22.3	
	4.96	4.09	21.2	
<b>Mean <math>\pm</math> S.E</b>	<b>5.34 <math>\pm</math> 0.12</b>	<b>4.27 <math>\pm</math> 0.06</b>	<b>25.0 <math>\pm</math> 1.7</b>	

## 7.4.9 INFLUENCE OF PRE-STRESS MECHANISMS ON FLEXURAL MODULUS

Various mechanisms have been speculated to explain how pre-stress could increase flexural modulus [13] but the current findings may facilitate further understanding. As reported in the previous section, the results in Figure 7-22 suggest that the contribution to flexural stiffness from pre-stress does not increase as fast as the actual fibre contribution when  $V_f$  is increased from 3.6% to 7.2%. Thus although flexural modulus is ~35% higher at 3.6%  $V_f$ , this drops to ~25% at 7.2%  $V_f$ . Reasons for this reduction as  $V_f$  increases could include effects of (i) deflection-dependent forces, (ii) an optimum  $V_f$  value and (iii) changes in fibre spatial distribution. These effects are summarised as follows:

- (i) Flexural modulus may be increased by a mechanism proposed for elastically pre-stressed (glass fibre-epoxy resin) composites [70]. Here, the applied (downwards) bending force is opposed by residual tension in the fibres which creates a vertical (upwards) force component, the latter increasing as bending angle (deflection) increases. Thus there will be less deflection in bending (at a given load) for a stiffer material. Therefore, as  $V_f$  is increased (which in itself produces a stiffer beam), this pre-stress-induced stiffening mechanism would be expected to become less effective.
- (ii) Tensile testing of nylon fibre-based VPPMC samples [12] showed that maximum improvements in mechanical properties occurred at ~35-40%  $V_f$ . This was explained by the competing effects of fibres: too few fibres create less compressive stress within the matrix, whereas too many fibres reduce the cross-sectional area over which compressive stresses can operate. Therefore, an optimum  $V_f$  may also apply to flexural tests, but the mechanisms influencing its value will be more complex than the situation observed with tensile testing. For example, external loading imposes a combination of tensile and compressive stresses in bending, so an optimum  $V_f$  value may depend on flexural deflection conditions. Also, the effects of non-uniform fibre spatial distribution (Figure 7-

15) will influence  $I$  in Equation 3-3: if most fibres lie close to the lower surface (subjected to tension during bending), the optimum (whole sample)  $V_f$  value for maximising bending stiffness from pre-stress may be significantly lower than the case for axially applied tensile loads.

- (iii) In addition to the effects of non-uniform fibre spatial distribution on (ii), any changes in this distribution over composite cross-sectional area as  $V_f$  is increased will also affect pre-stress contributions. As stated earlier in Section 7.4.7.2, Figure 7-15 shows the fibres at 3.6%  $V_f$  being mainly confined to the lower half of the sample, but this increases to  $2/3$  at 7.2%  $V_f$ . Thus effectiveness of the pre-stress contribution to bending stiffness is reduced in the latter case, as the fibre distribution extends further from the lower surface. To some extent this view may also be supported by the observation that previous three-point bend tests on nylon fibre-based VPPMC samples with 8-16%  $V_f$  produced from epoxy resin [13], had relatively uniform fibre spatial distributions; these showed no significant pre-stress related dependency on fibre volume fraction.

#### **7.4.10 VISCOELASTIC RECOVERY FORCE FROM UHMWPE FIBRES**

It should be noted that the impact energy data in Table 7-2 show no evidence of deterioration with sample age (24-1008 hours), but in Figure 7-11 there is a decline in recovery force output of ~30% over the same period. Since recovery strain characteristics (Figure 7-10b) are derived from the free movement of fibres and values are determined by measurements confined to the skin regions, the resulting data are insensitive to the competing effects from the core-skin interactions. This apparent discrepancy can be explained by considering that Figure 7-11 shows the fibre axial force output, whereas pre-stress mechanisms within a VPPMC depend on shear stress transfer between fibres and matrix. Clearly, pre-stress effects in a polyethylene fibre-based VPPMC is determined by the viscoelastic recovery characteristics of the fibre

skin regions. Although no deterioration in pre-stress effects within the VPPMC samples evaluated by three-point bend tests was observed over the timescale (up to 2 years) investigated, Figure 7-11 shows a drop in output of ~40% over a period of ~2 years. However, consistency in the non-zero value between 3000 and 16000 hours indicates a state of equilibrium in the polyethylene fibre skin/core effect. This supports the view that the skin regions have the dominant role in longer term viscoelastic activity.

In terms of force output characteristics, other aspects may require further consideration, e.g. the effects of (i) annealing, (ii) filament geometry and sub-structure. For (i), despite only small changes in short-term mechanical properties (Table 7-1, Figure 7-12a), the annealing treatment has a major effect on viscoelastic activity, as demonstrated in Figure 7-10. Thus recovery force must also be affected and perhaps skin-core effects. X-ray diffraction results for Dyneema UHMWPE fibres annealed at 120°C [198] indicate some crystalline re-arrangement may occur during the annealing cycle and strain relaxation within the amorphous regions can also be expected [201, 215]. Optimum annealing conditions for recovery force output would require further investigation. For (ii), as indicated in Figures 7-6, 7-15 and 7-16, the filament cross-sections are not circular; also they have a sub-structure of typically 150 macro-fibrils, a macro-fibril being 0.5-2 µm in diameter [122]. Thus filaments and their macro-fibrils have variations in section area. Therefore, for smaller section areas, it is possible that skin-related effects may be more significant.

#### **7.4.11 IMPLICATIONS FOR POLYETHYLENE FIBRE-BASED VPPMCS**

Although this work highlights the significance of skin-core interactions within UHMWPE fibres, further investigations would be required to understand the implications for long-term viscoelastic activity (over many years) and how this might affect subsequent VPPMC performance. In contrast with the uniform size and shape of nylon 6,6 fibres [12], gel-spun UHMWPE fibre cross-sections have no such uniformity, as evident from Figure 7-15. The fibres have varying cross-sectional areas, with

filaments having sub-structures of microfibrils, these also possessing varying sizes, being typically 0.5-2  $\mu\text{m}$  diameter [105, 122].

Although there appears to be little relevant information published on skin-core behaviour, skin-related effects might be expected to be more significant for fibre structures and sub-structures with smaller section areas. Thus, it can be speculated that long-term viscoelastic mechanisms within a UHMWPE fibre-based VPPMC might be influenced by the typical size and size distribution of the fibres under consideration.

In addition, the long-term behaviour of UHMWPE fibre-based VPPMCs obtained from accelerated ageing (time-temperature superposition) may not be possible because of the skin/core effects, as it may invalidate the  $\alpha_T$  (shift factor) value needed for accelerated ageing. As reported in Chapter-2 (Section 2.5.2), Fancey has successfully demonstrated the longer-term behaviour of nylon 6,6 fibre-based VPPMCs by using accelerated ageing, in which he has shown no deterioration in impact performance over a duration equivalent to 1000 years at a constant 20°C [10]. It is interesting to note that there appears to be a contradiction in  $\alpha_T$  values from the literature for UHMWPE fibres [213, 214]. Since the skin-core characteristics from other gel-spun UHMWPE fibre grades may differ from the material studied in this work (Dyneema SK60), their possible effects on VPPMC performance would require further investigation.

## 7.5 CONCLUSIONS

This chapter reports on investigations into the potential of UHMWPE fibres for providing viscoelastically generated pre-stress within a composite material. The main findings (based on observations and inferences) are as follows:

- (i) No chemically-based changes were observed in the Dyneema SK60 UHMWPE fibres subjected to annealing condition at 120°C for 30 minutes.
- (ii) By using appropriate annealing and creep conditions, long-term viscoelastic recovery strain can be achieved, which suggests that these fibres can release mechanical energy over a very long timescale.
- (iii) The adopted annealing conditions (120°C for 30 minutes) have only a minor effect on short-term (tensile) mechanical properties of the UHMWPE fibres. However, future investigations could include determining the optimum annealing conditions for maximising VPPMC performance.
- (iv) It was found that the stretching process for pre-stressing had no effect on UHMWPE fibre topography or tensile properties (such as work hardening). Also, no differences in fibre spatial distributions could be observed between the resulting test (pre-stressed) and control (un-stressed) composite samples.
- (v) Viscoelastically generated recovery force has been successfully demonstrated; however, the force output–time characteristic indicates that two competing mechanisms could be occurring. The findings suggest that this may arise from skin-core interactions occurring within the fibres, caused by differences in viscoelastic properties between fibre skin and core regions. Although axially measured viscoelastic recovery force from the UHMWPE fibres shows an initial rise and fall in output with time, equilibrium is reached after ~3000 hours. These observations are attributed to the fibre skin regions possessing

lower stiffness and longer term viscoelastic activity than the cores. Evidence from impact tests provides further support for these inferences.

- (vi) Viscoelastically generated pre-stress increased impact energy absorption by typically 20%, with some batches reaching 30-40%. Although fibre-matrix debonding is known to be a major energy absorption mechanism in EPPMCs and VPPMCs, this was not evident in this work. There is, instead, evidence of debonding at the skin-core interface within the UHMWPE fibres during impact and this appears to have a significant energy absorbing role in the pre-stressed composite samples. This is believed to be a previously unrecognised energy absorption mechanism.
- (vii) In contrast with nylon 6,6 fibre-based VPPMCs (Chapter-5), the increase in energy absorption from equivalent UHMWPE composites was maintained at the larger (60 mm) Charpy span setting; also energy absorption in absolute terms was 30-40% higher for all (test and control) samples. It is suggested, that these effects emanate from the much greater stiffness of the UHMWPE fibres reducing the influence of the (brittle) matrix on fracture behaviour.
- (viii) The longer term viability of VPPMCs using UHMWPE fibres has been demonstrated through three-point bend tests. Compared with control (un-stressed) counterparts, VPPMC samples show mean increases in flexural stiffness of 35% and 25% at 3.6 and 7.2%  $V_f$ , respectively, with no deterioration in modulus values over the timescale (~2 years) investigated.
- (ix) A lower than expected increase in flexural moduli at 7.2%  $V_f$  was observed, which may arise from effects relating to deflection-dependent forces, optimum fibre-matrix ratio and changes in fibre spatial distribution within the composite as  $V_f$  is increased.

Current observations are derived from tests on simple composite samples with unidirectional fibre reinforcement, restricted to low  $V_f$  values (3.6 to 7.2%  $V_f$ ). Although

more extensive investigations are required, the results in this Chapter suggest that the use of viscoelastically generated pre-stress in UHMWPE fibre-based composites may provide a means to improve impact toughness for various composite applications. A potentially important aspect of this study is the evidence of energy absorption via the UHMWPE fibre skin-core interface and whether this has wider implications for applications using such fibres.

Some of the findings raise issues concerning the fundamental properties of UHMWPE fibres and the proposed explanations are speculative. Nevertheless, this work provides sufficient evidence to demonstrate that these fibres should have an important role in the future development of VPPMC technology.

# CHAPTER-8

## GENERAL SUMMARY, POTENTIAL APPLICATIONS AND DIRECTIONS FOR FUTURE WORK

---

### SUMMARY

The work presented in this thesis covers research studies on viscoelastically pre-stressed composites based on nylon 6,6 and UHMWPE fibres. Mechanical tests on the composite samples were performed by low velocity impact and three-point bend tests. This study contributes to a further understanding of the viscoelastic properties of these fibres. However, the main contributions of this work include demonstrating the viability of UHMWPE fibres and commingling high strain-to-failure nylon 6,6 fibres with strong, stiff Kevlar fibres for VPPMC technology.

VPPMC technology offers the means to produce composite materials with enhanced mechanical properties without the need to increase mass or section size. The fibre stretching (pre-stressing) and moulding operations are decoupled; therefore flexibility in composite production and the opportunities to produce complex components should be comparable to conventional polymeric composites. Although this work has provided a valuable insight into VPPMCs, the technology remains limited to the research field and some distance away from the commercialisation. Nevertheless, this work may eventually bring VPPMC technology closer to industrial exploitation.

In this chapter, a detailed summary based on the findings of this work are presented, which leads to highlighting some potential applications for future exploitation. Also, suggestions for the direction of future work in the field of VPPMCs are discussed.

## 8.1 OVERALL FINDINGS

### 8.1.1 MATERIAL PROCESSING

Preliminary investigations (Chapter-4) on the processing of materials have been performed to acquire information needed for this research work. These include (a) selection of the matrix material and (b) the effects of ovens used for fibre annealing. For these aspects, composite samples were produced, tested on the Charpy impact tester and the results were compared with previously published nylon fibre-based VPPMCs. The main observations and findings are summarised below:

- (i) From the two resins selected for evaluation, i.e. a polyester general purpose (GP) and a clear casting (CC) resin, the CC resin has been adopted. From Charpy impact testing, nylon fibre-based VPPMC samples showed a mean increase in energy absorption of at least 40% compared with control counterparts, using the CC resin. However, there was no equivalent increase in energy absorption using the GP resin. This may be due to fibre-matrix adhesion effects. The GP resin investigated in this work was the only resin found (to date), that was unsuccessful in demonstrating improved performance from viscoelastically generated pre-stressing. To address this issue, further investigations would be required, e.g. fibre pull-out tests to evaluate fibre-matrix adhesion. However, it was beyond the scope of this thesis to investigate.
- (ii) By performing X-ray diffraction analysis on annealed nylon 6,6 fibres and Charpy impact testing of associated composite samples, no differences were detected between annealing fibres in the fan-assisted oven (used for this work) and the muffle furnace (used in previous nylon fibre-based VPPMC studies).

## 8.1.2 NYLON FIBRE-BASED VPPMCS

In Chapter-5, Charpy impact testing has been used to investigate the fracture and energy absorption characteristics of VPPMC samples over a range of test span settings and  $V_f$  values. This work has highlighted some of the limitations of the Charpy impact test. Nevertheless, the improved understanding of energy-absorbing mechanisms from these findings could provide the basis for further, similar studies. In Chapter-6, impact toughness and bending stiffness of hybrid VPPMCs consisting of unidirectional commingled nylon 6,6 and Kevlar-29 fibres have been evaluated through Charpy impact testing and three-point bend tests. Where appropriate, results of the hybrid composites were compared with single fibre-type samples. The main observations and findings from Chapter-5 and Chapter-6 are as follows:

- (i) The improvement in impact energy absorption from viscoelastically generated pre-stress depends principally on shear stresses activating pre-stress-enhanced fibre-matrix debonding (delamination) during the impact process. Thus a span setting of 24 mm shows greater increases in energy absorbed (25-40%) compared with 60 mm (0-13%) for nylon fibre-based VPPMCs. In contrast with relatively brittle fibre-based composites, the mechanical properties (fracture characteristics, modulus) of nylon fibre-only composite samples investigated in this study make the Charpy impact results much more sensitive to span setting.
- (ii) The benefits from shear stresses are demonstrated at the 24 mm Charpy span setting; higher  $V_f$  samples tested at this span setting are increasingly affected by drag, as the fractured (hinged break) samples are forced through the anvil supports following impact. Larger span settings, particularly at 60 mm, suggest there is an increasing contribution to energy absorption from elastic deflection, at the expense of energy being absorbed from fracture-based mechanisms: this causes lower energy absorption from all samples (i.e. both test and control groups) as well as reducing any improvements from pre-stress effects.

- (iii) Although higher  $V_f$  values may be expected to increase opportunities for energy absorption through pre-stress-enhanced fibre debonding, results at (the intermediate) 40 mm Charpy span setting show there is no more than a small, positive, but statistically weak trend between increased energy absorption (relative to control counterparts) and the  $V_f$  range studied (3.3-16.6%).
- (iv) Visual evidence (using SEM analysis) from impact-tested samples, that pre-stressing impedes crack propagation, is demonstrated. This validates previous proposed mechanisms, in which pre-stress effects are responsible for enhancing material properties by reducing crack propagation.
- (v) All Kevlar fibre-only composite samples (3.6%  $V_f$ ) fractured into two pieces, with virtually no debonding, during impact testing at both spans (24 and 60 mm) investigated. Thus at least for the low  $V_f$  investigated in this work, energy absorption was comparatively low and occurred through brittle fracture.
- (vi) Hybridisation of nylon fibres with other types of tough fibre provides an interesting approach to overcome the problems of low energy absorption through brittle fracture. Charpy tests on nylon/Kevlar fibre hybrid composites exhibited ductile fracture characteristics, producing hinged-break samples. Energy absorption through fibre-matrix debonding was significant, though the presence of Kevlar fibres made these debonded regions appear less pronounced compared with nylon fibre-only composite samples. The pre-stressed (test) samples absorbed more energy with larger debonded regions than their control counterparts, consistent with the view (from earlier work on pre-stressed composites) that residual shear stresses at the fibre-matrix interface regions promote energy absorbing debonding over transverse fracture.
- (vii) For Charpy testing at 24 mm span, the nylon/Kevlar fibre hybrid samples absorb slightly less impact energy than corresponding nylon fibre-only samples. This can be attributed to the Kevlar fibres reducing the energy-absorbing behaviour of the nylon fibres in the commingled case; however, pre-stress-induced increases in energy absorption are comparable, i.e. 33% (hybrid)

and 39% (nylon fibre-only composites). At 60 mm Charpy span settings, the situation is reversed, in that the hybrid samples absorb slightly more energy. Moreover, there is a small increase in pre-stress-induced energy absorption (~11%), compared with ~zero increase in the nylon fibre-only composite samples. This suggests that the Kevlar fibres suppress elastic deflection at this wider span setting, thereby promoting more effective energy absorption from fracture and debonding.

- (viii) Flexural modulus data from three-point bend tests on the nylon/Kevlar fibre hybrid composite samples have shown no deterioration in pre-stress effects over the age range investigated (up to 1.5 years).
- (ix) Bend tests on the nylon/Kevlar fibre hybrid composites demonstrated pre-stressing further enhances flexural modulus by ~35% (overall mean values), whilst some samples showed improvements of up to 60%. These differences can be attributed to variations in measurement rather than any time-dependency.
- (x) In flexural stiffness, the addition of Kevlar fibres, at least for the low  $V_f$  composites investigated in this work, does not appear to be detrimental to the increased stiffness benefits provided by viscoelastic pre-stress.

Based on these findings, it can be suggested that for structures where deflection is restricted, low velocity impact protection may be further improved with VPPMC technology using nylon 6,6 fibre reinforcement. Structures subjected to high velocity impact from low mass projectiles may also benefit, since large shear stresses would be expected to occur from highly localised deformation. Elastic deflection can also be suppressed by the addition of Kevlar fibres to produce nylon/Kevlar fibre hybrid VPPMCs. These findings are derived from tests on simple composite samples with unidirectional fibre reinforcement. Nevertheless, the findings indicate that VPPMCs may provide a means to improve impact toughness and other mechanical characteristics for composite applications.

### 8.1.3 POLYETHYLENE FIBRE-BASED VPPMCS

In Chapter-7, investigations into the potential of UHMWPE fibres (Dyneema SK60) for providing viscoelastically generated pre-stress within a composite material were investigated. This indicated the longer term measurements of UHMWPE fibre viscoelastic recovery strain and force output to determine their capability for producing UHMWPE fibre reinforced VPPMCS. The main observations and findings from Chapter-7 are as follows:

- (i) No chemically-based changes were observed in the UHMWPE fibres subjected to annealing at 120°C for 0.5 hours by using the fan-assisted oven.
- (ii) By using appropriate annealing and creep conditions, long-term viscoelastic recovery strain can be achieved, which suggests that these fibres can release mechanical energy over a very long timescale. However, future investigations could include determining the optimum annealing conditions for maximising VPPMC performance.
- (iii) The adopted annealing conditions (120°C for 0.5 hours) have only a minor effect on the short-term (tensile) mechanical properties of the UHMWPE fibres.
- (iv) It was found that the stretching process for pre-stressing had no effect on UHMWPE fibre topography or tensile properties (such as work hardening). Also, no differences in fibre spatial distributions could be observed between the resulting test (pre-stressed) and control (un-stressed) composite samples.
- (v) Viscoelastically generated recovery force has been successfully demonstrated; however, the force output–time characteristic indicates that two competing mechanisms could be occurring. The findings suggest this may be arising from skin-core interactions occurring within the fibres, caused by differences in viscoelastic properties between fibre skin and core regions. Although axially

measured viscoelastic recovery force from the UHMWPE fibres shows an initial rise and fall in output with time, an equilibrium is reached after ~3000 hours so that a steady state output is reached. These observations are attributed to the fibre skin regions possessing lower stiffness and longer term viscoelastic activity than the cores. Evidence from impact tests provides further support for these inferences.

- (vi) Viscoelastically generated pre-stress increased Charpy impact energy absorption by typically 20%, with some batches reaching 30-40%. Although fibre-matrix debonding is known to be a major energy absorption mechanism in EPPMCs and nylon fibre-based VPPMCs, this was not evident in polyethylene fibre-based VPPMCs. There is, instead, evidence of debonding at the skin-core interface within the UHMWPE fibres during impact and this appears to have a significant energy absorbing role in the pre-stressed composite samples. This is believed to be a previously unrecognised energy absorption mechanism.
- (vii) In contrast with the findings on nylon 6,6 fibre-based VPPMCs, the increase in energy absorption from equivalent UHMWPE composites was maintained at the larger (60 mm) Charpy span setting; also energy absorption in absolute terms was 30-40% higher for all (test and control) samples. It is suggested that these effects come from the much greater stiffness of the UHMWPE fibres, reducing the influence of the (brittle) matrix on fracture behaviour.
- (viii) The longer term viability of VPPMCs using UHMWPE fibres has been demonstrated through three-point bend tests. Comparing with control (un-stressed) counterparts, polyethylene fibre-based VPPMC samples show mean increases in flexural stiffness of 35% and 25% at 3.6 and 7.2%  $V_f$ , respectively, with no deterioration in modulus values over the timescale (~2 years) investigated.
- (ix) A lower than expected increase in flexural modulus at 7.2%  $V_f$  was observed, which may arise from effects relating to deflection-dependent forces, optimum

fibre-matrix ratio and changes in fibre spatial distribution within the composite as  $V_f$  is increased.

Current findings on UHMWPE fibre-based VPPMCs are derived from tests on simple composite samples with unidirectional fibre reinforcement, restricted to low  $V_f$  values. Although more extensive investigations are required, these observations suggest that the use of viscoelastically generated pre-stress in UHMWPE fibre-based composites may provide a means to improve impact toughness for various composite applications. An interesting aspect of this study is the evidence of energy absorption from the UHMWPE fibre skin-core interface and whether this has wider implications for applications using these fibres. Some of the findings raise issues concerning the fundamental properties of UHMWPE fibres and the proposed explanations are speculative. Nevertheless, this work provides sufficient evidence to demonstrate that these fibres should have an important role in the future development of VPPMC technology.

## 8.2 POTENTIAL APPLICATIONS

The potential applications for VPPMCs have been reported in Refs [10, 85] and are further discussed and updated here.

### 8.2.1 BALLISTIC PROTECTION

In contrast with low velocity impact tests, high velocity impact (e.g. from blast fragments) is usually associated with low mass projectiles striking material structures. In general, high performance fibres such as aramid (Kevlar), ultra-high molecular weight polyethylene (Dyneema/Spectra), carbon and glass fibres or the combination of two or three different types of these fibres are used in composites for ballistic protection. Studies by others on the ballistic impact behaviour of composite materials have described that the energy absorption and resulting damage in a composite from high velocity impact occurs by a moving cone causing tension in the primary yarns, deformation in the secondary yarns, debonding (delamination) and matrix cracking [216].

Nylon 6,6 woven mesh-based polymer matrix composites are amongst the materials used for ballistic protection [154, 217]. It is well known (as stated above) that for material subjected to a high velocity impact, the kinetic energy from the cone of deformation surrounding the projectile is the dominant energy absorption effect. This has been observed for composite materials reinforced with nylon [154] and woven glass fibre [216] subjected to ballistic impact. For materials with woven glass fibre that showed incomplete perforation, secondary yarn deformation was found to be the most significant effect [216]. For woven nylon 6,6 composites, impact by fragment-simulating projectiles indicated significant energy absorbing processes involving delamination and tensile failure of the fibres. Therefore, although the dominant energy absorbing effects may vary with impact conditions, they seem to depend mainly on fibre/matrix deformation, tensile type fibre failure and debonding (delamination).

Work in this thesis includes investigation into the fracture and energy absorbing characteristics of VPPMC samples subjected to low velocity impact. Clearly, the possible benefits from VPPMCs subjected to high velocity impact are still unknown. However, studies by Jevons [67] on elastically pre-stressed composites (glass fibre/epoxy) are of particular interest, since he has shown that the local shear stresses from high velocity impact override any pre-stressing benefits and this resulted in no noticeable changes in delamination area or energy absorption. For high velocity impacts, the findings from Ref [67] may indicate that composite materials produced from brittle type fibres would provide no benefits either as EPPMCs or VPPMCs. However, in this work (Chapter-6, Section 6.4), hybridisation (using commingled nylon and Kevlar fibres) has improved impact toughness of the composite samples. Although current investigations have been restricted to low velocity impact studies, it was observed that the energy absorption and performance of Kevlar fibre-only composite samples were improved by the addition of nylon 6,6 to Kevlar fibres and this changed the fracture mechanism from brittle to ductile type (hinged-break) failure. Since nylon 6,6 fibre is already used for high velocity impact applications, it may be possible that viscoelastically generated pre-stress from these ductile fibres makes a more positive contribution to energy absorption under high velocity impact conditions, compared with pre-stress generated from brittle fibres (as in EPPMCs). It is envisaged that the effect of pre-stressing would depend on how the shockwave is influenced by the fibre ductility.

## **8.2.2 CRASHWORTHY STRUCTURES**

In general, vehicular structures are required to be crashworthy with minimum mass for maximum fuel efficiency. The principal parameter for the materials used in crashworthy structures is the specific energy absorption (energy absorbed per unit mass). In comparison with steel or aluminium, the specific energy absorption of polymer matrix composites is higher [218]. Crashworthiness of polymer matrix composites usually involves axial compression, and there are several progressive crushing modes. In ductile fibre reinforced thermoset composites (Kevlar or Dyneema-Polyethylene), failure involves progressive folding (local buckling) [218-220]. Here, the local buckling occurs

from plastic deformation with interlaminar cracks and delamination at buckle sites [220]. VPPMCs have not been investigated for axial crush-loading conditions. However, since the crushing mode involves localised bending and matrix cracking, more energy may be absorbed through viscoelastically generated pre-stressing. In particular, this could occur through the need to work against matrix compressive stresses generated from pre-stressing and the more collective response from taut fibres i.e. Mechanisms-I and III (discussed in Chapter-2, Section 2.6).

It is well known that impact failure involves bending of material from the applied load. In Ref [221], it is suggested that structures subjected to impact loading can fail through crushing associated with bending. For example, fibre reinforced polymer matrix composites have been investigated in automotive applications such as beam [222] and grid-stiffened panels [223] for car doors to provide side impact protection in transverse loading. Thus, in bend-related impact failures, viscoelastic pre-stressing could make contributions to enhancing energy absorption through a combination of Mechanisms-I to IV as discussed in Chapter-2, Section 2.6.

In addition to the potential for high velocity (blast fragment) and crash protection, viscoelastically generated pre-stress technology may generally offer resistance to crack propagation through Mechanism-I (matrix compression impeding crack propagation) and Mechanism-III (more collective response from fibres). This could also be particularly useful for wind turbine blades for power generation. As known from the literature, carbon fibre reinforced composite materials offer better fatigue performance than glass fibre; the former are stiffer and lighter but more brittle than glass fibre [224]. Therefore, the addition of viscoelastically strained fibres such as UHMWPE or commingled nylon structures could reduce brittleness of the carbon reinforced composites and may offer improved fatigue resistance. This could be particularly important for larger wind turbine blades developed for off-shore structures.

### **8.2.3 FIBRE REINFORCEMENT TO ENHANCE CRACK RESISTANCE IN CONCRETE STRUCTURES**

The development of fibre reinforced concrete (FRC) has been progressing since the early 1960s [225]. This provides another opportunity for the potential application of VPPMC technology, to improve crack resistance in concrete structures [85]. As discussed in Ref [85], in FRC structures, the use of randomly oriented fibres has been shown to prevent cracks [225-227]. The most common polymeric fibres are polypropylene and nylon, though nylon has been found to sustain higher flexural stress [226]. Therefore, if these polymeric fibres were also used for providing pre-stress, they would offer further opportunities to improve resistance to crack propagation.

### **8.2.4 BIAXIAL MORPHING STRUCTURES**

As reported in Chapter-6 (Section 6.4.6), hybrid VPPMC composites for structures could be created by running the pre-stress generating fibres in directions different to other reinforcing fibres. One application might be morphing structures [128]. Non-symmetrical multilayer laminate composites can produce residual stresses (e.g. from thermal effects during moulding) and these can be exploited to create multi-stable deformations [183]. Elastic pre-stress generating fibres can be incorporated to create similar effects in symmetrical laminates [184]; thus alternatively, VPPMC techniques could be applied. Morphing aircraft wings, in which elastically pre-stressed carbon fibre composite strips are enclosed within a nylon fibre-reinforced skin [185, 228], may benefit from VPPMC technology, if it provides, for example, opportunities for simplified construction.

## 8.3 DIRECTIONS FOR FUTURE WORK

The following are suggestions for continuing this research to provide further understanding and to expand on the findings from the current work.

- To improve the processing methods for the production of VPPMC samples, especially fibre separation within the yarns (i.e. brushing techniques).
- UHMWPE fibre-based hybrid VPPMCs commingled with other commercially available strong and stiff fibres such as glass or carbon would be particularly interesting.
- Hybrid sandwich VPPMC plates for impact protection i.e. producing prepreg laminates of pre-stressed nylon with other strong fibres such as Kevlar, glass and carbon. Composite sandwich structures are being increasingly considered for vehicle front-end structures. The high energy absorbing capability of sandwich structures makes them an attractive solution for crashworthiness. Their energy absorption capability may be further enhanced by using a combination of other conventional strong fibres within hybrid VPPMC sandwich laminates. This study has demonstrated the benefits of hybrid (commingled nylon/Kevlar) fibres, as the nylon fibre has high strain-to-failure values and toughness; therefore a greater concentration of pre-stressing nylon fibres could be positioned on the tension side.
- The excellent ballistic properties of UHMWPE fibres are exploited in the literature; for example, protective clothing and armour to shield against fragments and debris from explosions etc. This study has demonstrated improvements in the impact toughness of UHMWPE fibre-based composites through pre-stressing. It is possible that high velocity impact protection may benefit from UHMWPE-based VPPMC technology.
- Over the last few decades, polymers and polymer composites have attracted wide attention for their use in medical and biomedical devices (e.g. orthopaedic

applications). For medical applications, UHMWPE is a preferred material because of its biocompatibility, low density, superior mechanical toughness and wear resistance. Based on the findings from this work, UHMWPE fibre-based VPPMCs for medical applications may further improve material properties and provide further benefits.

- The VPPMC production process is simpler in comparison with that of EPPMCs. Therefore, it may be beneficial for this technology to be exploited for complex structures. The creation of morphing structures is a particularly interesting example, since the polymeric fibres for generating pre-stress can be positioned in different orientations to fibres used for structural support.

# CHAPTER-9

## CONCLUSIONS

---

### SUMMARY

In this work, a comprehensive experimental research investigation has been performed on VPPMCs. The composite samples were evaluated by mechanical testing using low velocity Charpy impact testing and three-point bend tests.

Following the detailed summary presented in Chapter-8, this chapter highlights the main findings of this work, which were unknown before the research was undertaken. The main contribution includes demonstrating the viability of UHMWPE fibres for VPPMC technology. In analytical terms, useful knowledge on crack propagation has been uncovered in this work. It is believed that pre-stressing generated from strong polymeric fibres, e.g. UHMWPE, or less stiff high strain-to-failure nylon 6,6 fibres commingled with strong Kevlar fibres offer potential benefits for composite structures.

## 9.1 MATERIALS-RELATED FINDINGS

The annealing process, using different heating environment, does not affect fibre properties. This finding was based on X-ray diffraction analysis in which no differences were observed between annealing fibres in a fan-assisted oven or a muffle furnace. These findings were further confirmed from Charpy impact testing of the associated composite samples. In addition, no chemically-based changes were observed from the annealing process, in the Dyneema SK60 UHMWPE fibres subjected to 120°C for 0.5 hours by using the fan-assisted oven. Moreover, the fibre stretching process for pre-stressing had no effect on UHMWPE fibre topography or tensile properties (such as work hardening).

## 9.2 NYLON FIBRE-BASED VPPMCS

The Charpy impact fracture characteristics of nylon fibre-based VPPMC samples were very sensitive to the Charpy span setting. The benefits from pre-stressing are demonstrated at a short span setting (24 mm). However, for samples tested at a larger span (60 mm), the results suggest that there is an increasing contribution to energy absorption from elastic deflection, at the expense of energy being absorbed from fracture-based mechanisms: this causes lower energy absorption from all samples (i.e. both test and control groups) as well as reducing any improvements from pre-stress effects. Interestingly, this effect was suppressed by the addition of Kevlar fibres (to produce commingled nylon/Kevlar fibre hybrid VPPMCs), suggesting that the stiffer Kevlar fibres suppress elastic deflection at wider span setting, thereby promoting more effective energy absorption from fracture and debonding.

The benefits of hybridisation (commingled nylon/Kevlar fibres) in a composite are demonstrated. The hybrid composites exhibited ductile fracture characteristics, producing hinged-break samples, in contrast with Kevlar fibre-only composite samples, which fractured into two pieces (brittle type failure). In addition, impact energy absorption was further enhanced through the pre-stressing technique to produce hybrid

VPPMCs; these absorbed more energy mainly through larger debonded regions. Moreover, flexural modulus data from three-point bend tests on hybrid composite samples have shown no deterioration in pre-stress effects over the age range investigated (up to 1.5 years).

### **9.3 UHMWPE FIBRE-BASED VPPMCS**

By using appropriate annealing and creep conditions, long-term viscoelastic recovery strain can be achieved, which suggests that UHMWPE fibres can release mechanical energy over a very long timescale. This is confirmed by viscoelastically generated recovery force measurements.

The viability of UHMWPE fibre-based VPPMCS is demonstrated through Charpy impact and three-point bend tests. Fibre-matrix debonding, which is known to be a major impact energy absorption mechanism in EPPMCs and nylon fibre-based VPPMCs, was not evident in this work for the UHMWPE fibre-based VPPMCs. There is, instead, evidence of debonding at the skin-core interface within the UHMWPE fibres and this appears to have a significant energy absorbing role in the pre-stressed composite samples. This is believed to be a previously unrecognised energy absorption mechanism. In addition, the longer term performance of these VPPMCs has been demonstrated, in which increases in flexural stiffness were observed with no deterioration in modulus values over timescale of two years.

### **9.4 PRE-STRESS EFFECTS ON CRACK PROPAGATION**

Visual evidence from impact tested samples using SEM analysis has demonstrated that viscoelastically generated pre-stressing impedes crack propagation. This validates previous proposed mechanisms, in which pre-stress effects are responsible for enhancing material properties by reducing crack propagation.

## REFERENCES

---

1. Hargitai, H. and Racz, I., *Applications of macro and microfiller-reinforced polymer composites*, in *Polymer Composites*, Thomas, S., et al., Editors., 2012, Wiley-VCH: Singapore. p. 749-790.
2. Greszczuk, L. B., *Foreign object impact damage to composites*. ASTM STP 568. Vol. STP 568. 1973, Philadelphia: American Society for Testing and Materials.
3. Zhigun.I.G, *Experimental evaluation of the effect of prestressing the fibers in two directions on certain elastic characteristic of woven-glass reinforced plastics*. *Polymer Mechanics* 1968. **4**(4-6): p. 691-695.
4. Manders, P. W. and Chou, T.-W., *Enhancement of strength in composites reinforced with previously stressed fibers*. *Journal of Composite Materials* 1983. **17**(1): p. 26-44.
5. Tuttle.M.E, *A mechanical/thermal analysis of prestressed composite laminates*. *Journal of Composite Materials* 1988. **22**(8): p. 780-792.
6. Fancey, K. S., *Composite fibre-containing materials*, 1997: UK (Patent Number: 2281299B).
7. Fancey, K. S., *Investigation into the feasibility of viscoelastically generated pre-stress in polymeric matrix composites*. *Materials Science and Engineering A*, 2000. **279**(1-2): p. 36-41.
8. Fancey, K. S., *Prestressed polymeric composites produced by viscoelastically strained nylon 6,6 fibre reinforcement*. *Journal of Reinforced Plastics and Composites*, 2000. **19**(15): p. 1251-1266.
9. Fancey, K. S., *Fiber-reinforced polymeric composites with viscoelastically induced prestress*. *Journal of Advanced Materials*, 2005. **37**(2): p. 21-29.
10. Fancey, K. S., *Viscoelastically prestressed polymeric matrix composites – Potential for useful life and impact protection*. *Composites: Part B*, 2010. **41**: p. 454-461.

11. Pang, J. W. C. and Fancey, K. S., *An investigation into the long-term viscoelastic recovery of Nylon 6,6 fibres through accelerated ageing*. Materials Science and Engineering A, 2006. **431**(1-2): p. 100-105.
12. Pang, J. W. C. and Fancey, K. S., *Analysis of the tensile behaviour of viscoelastically prestressed polymeric matrix composites*. Composites Science and Technology, 2008. **68**(7-8): p. 1903-1910.
13. Pang, J. W. C. and Fancey, K. S., *The flexural stiffness characteristics of viscoelastically prestressed polymeric matrix composites*. Composites: Part A, 2009. **40**(6-7): p. 784-790.
14. Cui, H., Guan, M., *et al.*, *The flexural characteristics of prestressed bamboo slivers reinforced parallel strand lumber (PSL)*. Key Engineering Materials, 2012. **517**: p. 96-100.
15. Cantwell, W., J and Morton, J., *The impact resistance of composite materials-a review*. Composites, 1991. **22**(5): p. 347-362.
16. Goodfellow. *Catalogue, Polyaramid fibre-AR305744 (Kevlar-29 properties)*. 2013 [Accessed 14 October 2013]; Available from: <http://www.goodfellow.com/E/Polyaramid-Fibre.html>.
17. Goodfellow. *Catalogue, Polyamide fibre-AM325790 (Nylon 6, 6 properties)*. 2013 [Accessed 14 October 2013]; Available from: <http://www.goodfellow.com/E/Polyamide-Nylon-6-6.html>.
18. DuPont. *Technical guide: Kevlar aramid fiber*. 2014 [Accessed 28 January 2014]; Available from: [www.kevlar.com](http://www.kevlar.com).
19. Termonia, Y. and Smith, P., *Kinetic model for tensile deformation of polymers. 5. Effect of temperature on orientation efficiency*. Macromolecules, 1993. **26**(15): p. 3738-3741.
20. Jacobs, M. J. N., *Creep of gel-spun polyethylene fibres: Improvements by impregnation and crosslinking*, 1999, Eindhoven University of Technology: The Netherlands (PhD Thesis).
21. Peijs, A. A. J. M., Catsman, P., *et al.*, *Impact resistant and damage tolerant hybrid composite structures based on carbon and polyethylene fibres*. Composite Structures, 1991: p. 585-598.
22. Carr, D. J., *Failure mechanisms of yarns subjected to ballistic impact*. Journal of Materials Science Letters, 1999. **18**(7): p. 585-588.

23. Wu, Y., Zhong, W., *et al.*, *Behavior of aramid fiber/ultrahigh molecular weight polyethylene fiber hybrid composites under Charpy impact and ballistic impact*. *Journal of Materials Science and Technology*, 2002. **18**(4): p. 357-360.
24. Seymour, R. B., *Reinforced plastics: Properties and applications*, 1991, Richmond, TX, U.S.A: ASM International.
25. Hejazi, S. M., Abtahi, S. M., *et al.*, *Introducing two simple models for predicting fiber-reinforced asphalt concrete behavior during longitudinal loads*. *Journal of Applied Polymer Science*, 2008. **109**(5): p. 2872-2881.
26. Sivasubramanian, P., Pothan, L. A., *et al.*, *Hybrid textile polymer composites*, in *Polymer Composites*, Thomas, S., *et al.*, Editors., 2012, Wiley-VCH: Singapore. p. 469-482.
27. Agrawal, S., Singh, K. K., *et al.*, *Impact damage on fibre-reinforced polymer matrix composite – A review*. *Journal of Composite Materials*, 2014. **48**(3): p. 317-332.
28. Park, S.-J. and Seo, M.-K., *Carbon fiber-reinforced polymer composites: preparation, properties and applications*, in *Polymer Composites*, Thomas, S., *et al.*, Editors., 2012, Wiley-VCH: Singapore. p. 135-184.
29. Jose, J. P., Malhotra, S. K., *et al.*, *Advances in polymer composites: Macro and microcomposites - state of art, new challenges and opportunities*, in *Polymer Composites*, Thomas, S., *et al.*, Editors., 2012, Wiley-VCH: Singapore. p. 3-16.
30. Rosler, J., Harders, H., *et al.*, *Mechanical behaviour of engineering materials* 2007, Berlin: Springer.
31. Czigan, T. and Deak, T., *Preparation and manufacturing techniques for macro and microcomposites*, in *Polymer Composites*, Thomas, S., *et al.*, Editors., 2012, Wiley-VCH: Singapore. p. 111-134.
32. Sugita, Y., Winkelmann, C., *et al.*, *Environmental and chemical degradation of carbon/epoxy lap joints for aerospace applications, and effects on their mechanical performance*. *Composites Science and Technology*, 2010. **70**(5): p. 829-839.
33. KPMG. *The impact of composites on the aerospace and defense industry (Report)*. 2008 [Accessed 19 March 2014]; Available from: [http://www.kpmgcorporatefinance.com/engine/rad/files/library/Sector/Aerospace\\_Defense\\_Summer08.pdf](http://www.kpmgcorporatefinance.com/engine/rad/files/library/Sector/Aerospace_Defense_Summer08.pdf).
34. Lu, B. and Wang, N., *The Boeing 787 dreamliner designing an aircraft for the future*. *Journal of Young Investigators*, 2010. **19**(24).

35. Bor, Z. J., *Advanced polymer composites (Report)*, 1994, USA: ASM International.
36. Lee, S.-Y. and George, S. S., *Effects of cure on the mechanical properties of composites*. Journal of Composites Materials, 1988. **22**: p. 15-29.
37. Campbell, D., Pethrick, R., A, *et al.*, *Polymer characterization*. Second ed, 2000, Cheltenham: Stanley Thornes.
38. Campbell, F., *Manufacturing processes for advanced composites*, 2003, Oxford: Elsevier Advanced Technology.
39. Lawrence, J. B. and Rotam, A., *Impact strength and toughness of fiber composite materials*. Foreign Object Impact Damage to Composite Material-(ASTM), 1975. **568**: p. 114-133.
40. Piggott, M. R., *Theoretical estimation of fracture toughness of fibrous composites*. Journal of Materials Science, 1970. **5**(8): p. 669-675.
41. Tetelman, A. S., *Fracture processes in fiber composite materials*, in *Testing and Design*, 1969, American Society for Testing and Materials: Philadelphia, Pennsylvania p. 473-502.
42. Talreja, R., *Fatigue of composite materials: damage mechanisms and fatigue-life diagrams*. Proceedings Royal Society A, 1981. **378**(1775): p. 461-475.
43. Richardson, M. O. W. and Wisheart, M. J., *Review of low-velocity impact properties of composite materials*. Composites Part A: Applied Science and Manufacturing, 1996. **27**(12): p. 1123-1131.
44. Fuwa, M., Bunsell, A., R, *et al.*, *Tensile failure mechanisms in carbon fibre reinforced plastics* Journal of Materials Science, 1975. **10**(12): p. 2062-2070.
45. Wu, H.-Y. T. and Springer, G. S., *Measurements of matrix cracking and delamination caused by impact on composite plates*. Journal of Composite Materials, 1988. **22**(6): p. 518-532.
46. Jayaraman, K. and Reifsnider, K. L., *The interphase in unidirectional fiber-reinforced epoxies: Effect on residual thermal stresses*. Composites Science and Technology, 1993. **47**(2): p. 119-129.
47. Asp, L. E., Berglund, L. A., *et al.*, *Effects of fiber and interphase on matrix-initiated transverse failure in polymer composites*. Composites Science and Technology, 1996. **56**(6): p. 657-665.

48. Reifsnider, K. L., Jayaraman, K., *et al.*, *The interphase in unidirectional fiber-reinforced epoxies: Effect on local stress fields*. Journal of Composites Technology and Research, 1994. **16**(1): p. 21-31.
49. Schultz, J., Lavielle, L., *et al.*, *The role of the interface in carbon fibre-epoxy composites*. The Journal of Adhesion, 1987. **23**(1): p. 45-60.
50. Hoecker, F. and Karger-Kocsis, J., *Effects of the interface on the mechanical response of CF/EP microcomposites and macrocomposites*. Composites, 1994. **25**(7): p. 729-738.
51. Ageorges, C., Friedrich, K., *et al.*, *Single-fibre Broutman test: fibre-matrix interface transverse debonding*. Composites Part A: Applied Science and Manufacturing, 1999. **30**(12): p. 1423-1434.
52. Zhandarov, S. and Mäder, E., *Characterization of fiber/matrix interface strength: applicability of different tests, approaches and parameters*. Composites Science and Technology, 2005. **65**(1): p. 149-160.
53. Lee, S. M., *Influence of fiber/matrix interfacial adhesion on composite fracture behavior*. Composites Science and Technology, 1992. **43**(4): p. 317-327.
54. Lu, X., Zhang, Y., *et al.*, *Influence of fiber morphology in pull-out process of chain-shaped fiber reinforced polymer composites*. Scripta Materialia, 2006. **54**(9): p. 1617-1621.
55. Krishnamurthy, S., *Prestressed advanced fibre reinforced composites: Fabrication and mechanical performance*, in *Defence College of Management and Technology-Engineering System Department*, , 2006, Cranfield University: UK (PhD Thesis).
56. Cook, J., Gordon, J. E., *et al.*, *A mechanism for the control of crack propagation in all-brittle systems*. Proceedings of the Royal Society of London. Series A. Mathematical and Physical Sciences, 1964. **282**(1391): p. 508-520.
57. William D, C., Jr, *Materials science and engineering: An introduction*. 7th ed, 2007, USA: John Wiley & Sons.
58. Soudki, K. A., Green, M. F., *et al.*, *Transfer length of carbon fiber rods in precast pretensioned concrete beams*. Precast/Prestressed Concrete Institute (PCI), 1997. **42**(5): p. 78-87.
59. Sen, R., Spillett, K., *et al.*, *Fabrication of aramid and carbon fiber reinforced plastic pretensioned beams*. Concrete International 1994. **16**(6): p. 45-47.

- 
60. Stoll, F., Saliba, J., E, *et al.*, *Experimental study of CFRP-prestressed high-strength concrete bridge beams*. *Composite Structures*, 2000. **49**(2): p. 191-200.
  61. Jorge, L. D. A., Marques, A. T., *et al.*, *The influence of prestressing on the mechanical behaviour of uni-directional composites*. *Applied Science*, 1990: p. 897-902.
  62. Schulte, K. and Marissen, R., *Influence of artificial pre-stressing during curing of CFRP laminates on interfibre transverse cracking*. *Composites Science and Technology*, 1992. **44**(4): p. 361-367.
  63. Sui, G. X., Yao, G., *et al.*, *Influence of artificial pre-stressing during the curing of VIRALL on its mechanical properties*. *Composites Science and Technology*, 1995. **53**(4): p. 361-364.
  64. Tuttle, M. E., Koehler, R., T, *et al.*, *Controlled thermal stresses in composites by means of fibre prestress*. *Composites Materials*, 1996. **30**(4): p. 486-502.
  65. Zhao, J. and Cameron, J., *Polypropylene matrix composites reinforced with pre-stressed glass fibers*. *Polymer Composites*, 1998. **19**(3): p. 218-224.
  66. Hadi, A. S. and Ashton, J., N, *On the influence of pre-stress on the mechanical properties of a unidirectional GRE composite*. *Composite Structures*, 1998. **40**(3-4): p. 305-311.
  67. Jevons, M. P., *The effects of fibre pre-stressing on the impact performance of composite laminates in College of Defence Technology Engineering System Department*, 2004, Cranfield University: UK (PhD Thesis).
  68. Motahhari, S. and Cameron, J., *Impact strength of fiber pre-stressed composites*. *Reinforced Plastics and Composites*, 1998. **17**(2): p. 123-130.
  69. Jevons, M. P., Fernando, G. F., *et al.*, *Effect of pre-tensioning on the low velocity impact performance of glass fibre composites*, in *10th European conference on composite materials*, 2002: Brugge (Belgium).
  70. Motahhari, S. and Cameron, J., *Fibre prestressed composites: Improvement of flexural properties through fibre prestressing*. *Reinforced Plastics and Composites*, 1999. **18**(3): p. 279-288.
  71. Schlichting, L. H., de Andrada, M. A. C., *et al.*, *Composite resin reinforced with pre-tensioned glass fibers. Influence of prestressing on flexural properties*. *Dental Materials*, 2010. **26**(2): p. 118-125.

- 
72. Cao, Y. and Cameron, J., *Flexural and shear properties of silica particle modified glass fiber reinforced epoxy composite*. Journal of Reinforced Plastics and Composites, 2006. **25**(4): p. 347-359.
73. Hine, P. J., Duckett, R., A, *et al.*, *The effect of hydrostatic pressure on the mechanical properties of glass fibre/epoxy unidirectional composites*. Composites Part A: Applied Science and Manufacturing, 2005. **36**(2): p. 279-289.
74. Shokrieh, M. M., *Residual stresses in composite materials*, 2013, Cambridge UK: Woodhead Publishing Ltd
75. Chapman, T. J., Gillespie, J. W., *et al.*, *Prediction of process-induced residual stresses in thermoplastic composites*. Journal of Composite Materials, 1990. **24**(6): p. 616-643.
76. Sonmez, F. O., Hahn, H. T., *et al.*, *Analysis of process-induced residual stresses in tape placement*. Journal of Thermoplastic Composite Materials, 2002. **15**(6): p. 525-544.
77. Jeronimidis, G. and Parkyn, A. T., *Residual stresses in carbon fibre-thermoplastic matrix laminates*. Journal of Composite Materials, 1988. **22**(5): p. 401-415.
78. Cowley, K. D. and Beaumont, P. W. R., *The measurement and prediction of residual stresses in carbon-fibre/polymer composites*. Composites Science and Technology, 1997. **57**(11): p. 1445-1455.
79. Hahn, H. T. and Pagano, N. J., *Curing stresses in composite laminates*. Journal of Composite Materials, 1975. **9**(1): p. 91-106.
80. Dvorak, G., J and Alexander, P., Suvorov, *The effect of fiber pre-stress on residual stresses and the onset of damage in symmetric laminates*. Composites Science and Technology, 2000. **60**(8): p. 1129-1139.
81. Motahhari, S. and Cameron, J., *Measurement of micro-residual stresses in fiber-prestressed composites*. Journal of Reinforced Plastics and Composites, 1997. **16**(12): p. 1129-1137.
82. Nishi, Y., Okada, T., *et al.*, *Effects of tensile prestress level on impact value of 50 vol% continuous unidirectional 0 degree oriented carbon fiber reinforced epoxy polymer (CFRP)*. Materials Transactions, 2014. **55**(2): p. 318-322.
83. Daynes, S., Potter, K. D., *et al.*, *Bistable prestressed buckled laminates*. Composites Science and Technology, 2008. **68**(15-16): p. 3431-3437.

84. Motahhari, S., *Fibre prestressed composites*, in *Department of Materials & Metallurgical Engineering*, 1998, Queen's University: Kingston, Ontario, Canada (PhD Thesis).
85. Fancey, K. S., *Viscoelastically prestressed polymer matrix composites*, in *Polymer Composites*, Thomas, S., *et al.*, Editors., 2012, Wiley-VCH: Singapore. p. 715-746.
86. Fancey, K. S. and Fazal, A., *Prestressed polymeric matrix composites: longevity aspects*. *Polymer Composites*, 2014 (In press).
87. Crawford, R. J., *Plastics engineering*. 3rd ed, 1998, Oxford: Butterworth-Heinemann.
88. Liu, X., Zhang, S., *et al.*, *Study on the creep and recovery behaviors of UHMWPE/CNTs composite fiber*. *Fibers and Polymers*, 2013. **14**(10): p. 1635-1640.
89. Fancey, K. S., *A Latch-based Weibull model for polymeric creep and recovery*. *Journal of Polymer Engineering*, 2001. **21**(6): p. 489-509.
90. Fancey, K. S., *A mechanical model for creep, recovery and stress relaxation in polymeric materials*. *Journal of Materials Science*, 2005. **40**: p. 4827-4831.
91. Pang, J. W. C., Lamin, B. M., *et al.*, *Force measurement from viscoelastically recovering nylon 6,6 fibres*. *Materials Letters*, 2008. **62**: p. 1693-1696.
92. Murayama, T., Dumbleton, J. H., *et al.*, *The viscoelastic properties of oriented nylon 66 fibers. Part III: Stress relaxation and dynamic mechanical properties*. *Journal of Macromolecular Science, Part B*, 1967. **1**(1): p. 1-14.
93. Carter, A. D. S., *Mechanical reliability*. 2nd ed, 1986, London: Macmillan.
94. Dobрева, A., Gutzow, I., *et al.*, *Stress and time dependence of relaxation and the Kohlrausch stretched exponent formula*. *Journal of Non-Crystalline Solids*, 1997. **209**(3): p. 257-263.
95. Gálvez, V. S. and Paradela, L. S., *Analysis of failure of add-on armour for vehicle protection against ballistic impact*. *Engineering Failure Analysis*, 2009. **16**(6): p. 1837-1845.
96. Rose, D. H. and Whitney, J., M. *Effect of prestressed fibres upon the response of composite materials*. in *8th Technical conference on composites*. 1993. Lancaster PA: Proceedings of American Society of Composites.

97. Verbeek, J. and Christopher, M., *Mica-reinforced polymer composites*, in *Polymer Composites*, Thomas, S., et al., Editors., 2012, Wiley-VCH: Singapore. p. 673-713.
98. Goodfellow. *Catalogue, Polyethylene fibre-ET305710 (UHMWPE properties)*. 2013 [Accessed 14 October 2013]; Available from: <http://www.goodfellow.com/E/Polyethylene-UHMW.html>.
99. Goodfellow. *Catalogue, Carbon fibre HM (properties)*. 2013 [Accessed 25 December 2013]; Available from: <http://www.goodfellow.com/A/Carbon-Fiber.html>.
100. Peijs, A. A. J. M., *High-performance polyethylene fibres in structural composites?*, 1993, Eindhoven University of Technology: The Netherlands (PhD Thesis).
101. Clegg, D. W. and Collyer, A. A., *Mechanical properties of reinforced thermoplastics*, 1986: Elsevier Applied Science Publishers.
102. Causin, V., *Nylon fiber-reinforced polymer composites*, in *Polymer Composites*, Thomas, S., et al., Editors., 2012, Wiley-VCH: Singapore. p. 293-314.
103. Baley, C., Perrot, Y., et al., *Mechanical properties of composites based on low styrene emission polyester resins for marine applications*. *Applied Composite Materials*, 2006. **13**(1): p. 1-22.
104. Das, C. K., Nayak, G. C., et al., *Kevlar fiber-reinforced polymer composites*, in *Polymer Composites*, Thomas, S., et al., Editors., 2012, Wiley-VCH: Singapore. p. 209-274.
105. Karger-Kocsis, J. and Barany, T., *Polyolefin fiber and tape-reinforced polymeric composites*, in *Polymer Composites*, Thomas, S., et al., Editors., 2012, Wiley-VCH: Singapore. p. 315-337.
106. Peterlin, A., *Annealing of drawn crystalline polymers*. *Polymer Engineering & Science*, 1978. **18**(6): p. 488-495.
107. Peijs, T., Rijdsdijk, H., A, et al., *The role of interface and fibre anisotropy in controlling the performance of polyethylene-fibre-reinforced composites*. *Composites Science and Technology*, 1994. **52**(3): p. 449-466.
108. Govaert, L. E. and Peijs, T., *Tensile strength and work of fracture of oriented polyethylene fibre*. *Polymer*, 1995. **36**(23): p. 4425-4431.

- 
109. Mercx, F. P. M., Benzina, A., *et al.*, *Improved adhesive properties of high-modulus polyethylene structures*. *Journal of Materials Science*, 1993. **28**(3): p. 753-759.
110. Dijkstra, D. J., Torfs, J. C. M., *et al.*, *Temperature-dependent fracture mechanisms in ultra-high strength polyethylene fibers*. *Colloid and Polymer Science*, 1989. **267**(10): p. 866-875.
111. Ladizesky, N. H. and Ward, I. M., *A study of the adhesion of drawn polyethylene fibre/polymeric resin systems*. *Journal of Materials Science*, 1983. **18**(2): p. 533-544.
112. Ladizesky, N. H. and Ward, I. M., *Ultra-high-modulus polyethylene fibre composites: I—The preparation and properties of conventional epoxy resin composites*. *Composites Science and Technology*, 1986. **26**(2): p. 129-164.
113. Hoogsteen, W., Hooft, R. J., *et al.*, *Gel-spun polyethylene fibres Part I Influence of spinning temperature and spinline stretching on morphology and properties*. *Journal of Materials Science*, 1988. **23**(10): p. 3459-3466.
114. Hoogsteen, W., Kormelink, H., *et al.*, *Gel-spun polyethylene fibres*. *Journal of Materials Science*, 1988. **23**(10): p. 3467-3474.
115. Zwijnenburg, A., Hutten, V. P. F., *et al.*, *Longitudinal growth of polymer crystals from flowing solutions V.: Structure and morphology of fibrillar polyethylene crystals*. *Colloid and Polymer Science*, 1978. **256**(8): p. 729-740.
116. Prevorsek, D. C., *Structural aspects of the damage tolerance of spectra fibres and composites*, in *Oriented Polymer Materials*, 2008, Wiley-VCH Verlag GmbH. p. 444-466.
117. Hogg, P. J. and Bibo, G., A, *Impact and damage tolerance*, in *Mechanical testing of advanced fibre composites*, Hodgkinson, J. M., Editor, 2000, Woodhead Publishing Ltd: Cambridge, England. p. 211-247.
118. BSI. *Plastics-Determination of Charpy impact properties BS EN ISO 179-1 (Part1: Non-instrumented impact test)*. 2010.
119. Hodgkinson, J. M., *Flexure*, in *Mechanical testing of advanced composites*, Hodgkinson, J. M., Editor, 2000, Woodhead Publishing Ltd: Cambridge, England. p. 124-142.
120. Timoshenko, S., *Strength of materials. Part I. Elementary theory and problems*. 3rd ed, 1955, New York: Krieger.

121. Turner, S., *General principles and perspectives*, in *Mechanical testing of advanced fibre composites*, 2000, Woodhead Publishing Ltd: Cambridge, England. p. 4-35.
122. Berger, L., Kausch, H., H, *et al.*, *Structure and deformation mechanisms in UHMWPE-fibres*. *Polymer*, 2003. **44**(19): p. 5877–5884.
123. El-Maaty, M. I. A., Olley, R., H, *et al.*, *On the internal morphologies of high-modulus polyethylene and polypropylene fibres*. *Journal of Materials Science*, 1999. **34**(9): p. 1975-1989.
124. Kromm, F. X., Lorriot, T., *et al.*, *Tensile and creep properties of ultra high molecular weight PE fibres*. *Polymer Testing*, 2003. **22**(4): p. 463-470.
125. Tan, V. B. C., Zeng, X. S., *et al.*, *Characterization and constitutive modeling of aramid fibers at high strain rates*. *International Journal of Impact Engineering*, 2008. **35**(11): p. 1303–1313.
126. Silverstein, M. S. and Breuer, O., *Mechanical properties and failure of etched UHMW-PE fibres*. *Journal of Materials Science*, 1993. **28**(15): p. 4153-4158.
127. Hull, A. W., *A new method of chemical analysis*. *Journal of the American Chemical Society*, 1919. **41**(8): p. 1168-1175.
128. Fancey, K. S., *Private discussion*, 2014: School of Engineering, University of Hull, UK.
129. Pang, J. W. C. and Fancey, K. S. *An evaluation of viscoelastically prestressed polymeric matrix composite materials*. in *28th SAMPE Europe International Conference*. 2007. Paris: SEICO 07.
130. Adams, D. F. and A, K., Miller, *The influence of transverse shear on the static flexure and Charpy impact response of hybrid composite materials*. *Journal of Materials Science*, 1976. **11**: p. 1697-1710.
131. Nagai, M. and Miyairi, H., *The study on Charpy impact testing method of CFRP*. *Advanced Composite Materials*, 1994. **3**(3): p. 177-190.
132. Tillie, M. N., Lam, T., M, *et al.*, *Insertion of an interphase synthesised from a functionalised silicone into glass-fibre/epoxy composites*. *Composites Science and Technology*, 1998. **58**: p. 659-663.
133. Hufenbach, W., Marques, I., F, *et al.*, *Charpy impact tests on composite structures – An experimental and numerical investigation*. *Composites Science and Technology*, 2008. **68**: p. 2391-2400.

- 
134. Pegoretti, A., Cristelli, I., *et al.*, *Experimental optimization of the impact energy absorption of epoxy-carbon laminates through controlled delamination*. *Composites Science and Technology*, 2008. **68**: p. 2653-2662.
135. Khan, M. A., Ganster, J., *et al.*, *Hybrid composites of jute and man-made cellulose fibers with polypropylene by injection moulding*. *Composites: Part A*, 2009. **40**: p. 846-851.
136. Ghasemnejad, H., Furquan, A. S. M., *et al.*, *Charpy impact damage behaviour of single and multi-delaminated hybrid composite beam structures*. *Materials and Design*, 2010. **31**: p. 3653-3660.
137. Golzar, M. and Poorzeinolabedin, M., *Prototype fabrication of a composite automobile body based on integrated structure*. *International Journal of Advanced Manufacturing Technology*, 2010. **49**(9-12): p. 1037-1045.
138. Guo, J., Tang, Y., *et al.*, *Wood Plastic Composite Produced by Nonmetals from Pulverized Waste Printed Circuit Boards*. *Environmental Science & Technology*, 2010. **44**(1): p. 463-468.
139. Thomason, J. L., Ali, J. Z., *et al.*, *The thermo-mechanical performance of glass-fibre reinforced polyamide 66 during glycol-water hydrolysis conditioning*. *Composites: Part A*, 2010. **41**: p. 820-826.
140. Butylina, S., Hyvarinen, M., *et al.*, *Accelerated weathering of wood-polypropylene composites containing minerals*. *Composites Part A: Applied Science and Manufacturing*, 2012. **43**(11): p. 2087-2094.
141. Mehrjerdi, A. K., Adl-Zarrabi, B., *et al.*, *Mechanical and thermo-physical properties of high-density polyethylene modified with talc*. *Journal of Applied Polymer Science*, 2013. **129**(4): p. 2128-2138.
142. Huber, T., Bickerton, S., *et al.*, *Flexural and impact properties of all-cellulose composite laminates*. *Composites Science and Technology*, 2013. **88**: p. 92-98.
143. Amaro, A. M., Reis, P. N. B., *et al.*, *Delamination effect on bending behaviour in carbon-epoxy composites*. *Strain*, 2011. **47**: p. 203-208.
144. Cantwell, W. J. and Morton, J., *Detection of impact damage in CFRP laminates*. *Composite Structures*, 1985. **3**(3-4): p. 241-257.
145. Cantwell, W. J. and Morton, J., *Geometrical effects in the low velocity impact response of CFRP*. *Composite Structures*, 1989. **12**(1): p. 39-59.
146. Cantwell, W. J. and Morton, J., *Comparison of the low and high velocity impact response of CFRP*. *Composites*, 1989. **20**(6): p. 545-551.

- 
147. Marur, P. R., *Charpy specimen-a simply supported beam or a constrained free-free beam?* Engineering Fracture Mechanics, 1998. **61**: p. 369-386.
  148. Dunn, C., Babic, L., *et al.*, *Damage Development and its significance in GRP subjected to impact.* Plastics and Rubber Processing and Applications, 1989. **12**: p. 199-207.
  149. Hong, S. and Liu, D., *On the relationship between impact energy and delamination area.* Experimental Mechanics, 1989. **29**(2): p. 115-120.
  150. Gong, S. W. and Lam, K., Y, *Transient response of stiffened composite plates subjected to low velocity impact.* Composites: Part B, 1999. **30**: p. 473-484.
  151. Sutherland, L. S. and Guedes, S., C, *Impact characterisation of low fibre-volume glass reinforced polyester circular laminated plates.* International Journal of Impact Engineering, 2005. **31**: p. 1-23.
  152. Cantwell, W., J and Morton, J., *Impact perforation of carbon fibre reinforced plastic.* Composites Science and Technology, 1990. **38**(2): p. 119-141.
  153. Hazell, P. J. and Thomas, G. A., *A study on the energy dissipation of several different CFRP-based targets completely penetrated by a high velocity projectile.* Composite Structures, 2009. **91**: p. 103-109.
  154. Morye, S. S., Hine, P. J., *et al.*, *Modelling of the energy absorption by polymer composites upon ballistic impact.* Composites Science and Technology, 2000. **60**: p. 2631-2642.
  155. Sabet, A., Fagih, N., *et al.*, *Effect of reinforcement type on high velocity impact response of GRP plates using a sharp tip projectile.* International Journal of Impact Engineering, 2011. **38**: p. 715-722.
  156. Lafitte, M. H. and Bunsell, A. R., *The creep of Kevlar-29 fibers.* Polymer Engineering & Science, 1985. **25**(3): p. 182-187.
  157. Knoester, H., Decker, P. d., *et al.*, *Creep and failure time of aramid yarns subjected to constant load.* Macromolecular Materials and Engineering, 2012. **297**(6): p. 559-575.
  158. Jang, B., Z, Chen, L., C, *et al.*, *Impact resistance and energy absorption mechanisms in hybrid composites.* Composites Science and Technology, 1989. **34**(4): p. 305-335.
  159. Thwe, M. M. and Liao, K., *Durability of bamboo-glass fiber reinforced polymer matrix hybrid composites.* Composites Science and Technology, 2003. **63**(3-4): p. 375-387.

- 
160. Theodore J, R., *Engineered materials handbook: Composites*. Vol. 1. 1987, USA: ASM International.
161. Mallick, P. K. and Broutman, L. J., *Static and impact properties of laminated hybrid composites*. Journal of Testing and Evaluation, 1977. **5**(3): p. 190-200.
162. Cheon, S. S., Lim, T. S., *et al.*, *Impact energy absorption characteristics of glass fiber hybrid composites*. Composite Structures, 1999. **46**(3): p. 267-278.
163. Dorey, G., Sidey, G. R., *et al.*, *Impact properties of carbon fibre/Kevlar 49 fibre hybrid composites*. Composites, 1978. **9**(1): p. 25-32.
164. Sreekala, M. S., George, J., *et al.*, *The mechanical performance of hybrid phenol-formaldehyde-based composites reinforced with glass and oil palm fibres*. Composites Science and Technology, 2002. **62**(3): p. 339-353.
165. Manders, P. W. and Bader, M. G., *The strength of hybrid glass/carbon fibre composites*. Journal of Materials Science, 1981. **16**(8): p. 2246-2256.
166. Wagner, H. D., Roman, I., *et al.*, *Hybrid effects in the bending stiffness of graphite/glass-reinforced composites*. Journal of Materials Science, 1982. **17**(5): p. 1359-1363.
167. Fischer, S. and Marom, G., *The flexural behaviour of aramid fibre hybrid composite materials*. Composites Science and Technology, 1987. **28**(4): p. 291-314.
168. Marom, G., Fischer, S., *et al.*, *Hybrid effects in composites: conditions for positive or negative effects versus rule-of-mixtures behaviour*. Journal of Materials Science, 1978. **13**(7): p. 1419-1426.
169. Marom, G., Drukker, E., *et al.*, *Impact behaviour of carbon/Kevlar hybrid composites*. Composites, 1986. **17**(2): p. 150-153.
170. Peijs, A. A. J. M. and Venderbosch, R. W., *Hybrid composites based on polyethylene and carbon fibres Part IV Influence of hybrid design on impact strength*. Journal of Materials Science Letters, 1991. **10**(19): p. 1122-1124.
171. Peijs, A. A. J. M., Catsman, P., *et al.*, *Hybrid composites based on polyethylene and carbon fibres Part 2: influence of composition and adhesion level of polyethylene fibres on mechanical properties*. Composites, 1990. **21**(6): p. 513-521.
172. Beaumont, P. W. R., Riewald, P. G., *et al.*, *Methods for improving the impact resistance of composite materials*, in *Foreign Object Impact Damage to Composites*, Greszczuk, L. B., Editor, 1974, American Society for Testing and Materials: Philadelphia, Pennsylvania. p. 134-158.

173. Novak, R. C. and De Crescente, M. A., *Impact behavior of unidirectional resin matrix composites tested in the fiber direction*, in *Composite Materials: Testing And Design (Second Conference)*, H T, C., Editor, 1972, American Society for Testing and Materials: Philadelphia, Pennsylvania p. 311-323.
174. Chamis, C. C., Hanson, M. P., *et al.*, *Impact resistance of unidirectional fiber composites*, in *Composite Materials: Testing and Design (Second Conference)*, H T, C., Editor, 1972, American Society for Testing and Materials: Philadelphia. p. 324-349.
175. Moore, J. W. and Smith, W. S., *A new organic high modulus reinforcing fiber*, in *Unsaturated Polyester Technology*, Paul F, B., Editor, 1976, Gordon and Breach: New York.
176. McColl, I. R. and Morley, J. G., *Crack growth in hybrid fibrous composites*. *Journal of Materials Science*, 1977. **12**(6): p. 1165-1175.
177. Harris, B. and Bunsell, A. R., *Impact properties of glass fibre/carbon fibre hybrid composites*. *Composites*, 1975. **6**(5): p. 197-201.
178. Perry, J. L. and Adams, D. F., *Charpy impact experiments on graphite/epoxy hybrid composites*. *Composites*, 1975. **6**(4): p. 166-172.
179. Ladizesky, N. H. and Ward, I. M., *Ultra-high-modulus polyethylene composites: III—An exploratory study of hybrid composites*. *Composites Science and Technology*, 1986. **26**(3): p. 199-224.
180. Thanomsilp, C. and Hogg, P., J., *Penetration impact resistance of hybrid composites based on commingled yarn fabrics*. *Composites Science and Technology*, 2003. **63**(3-4): p. 467-482.
181. Faur-Csukat, G., *A study on the ballistic performance of composites*. *Macromolecular Symposia*, 2006. **239**(1): p. 217-226.
182. Lin, S. P., Han, J. L., *et al.*, *Composites of UHMWPE fiber reinforced PU/epoxy grafted interpenetrating polymer networks*. *European Polymer Journal*, 2007. **43**(3): p. 996-1008.
183. Hufenbach, W. and Gude, M., *Analysis and optimisation of multistable composites under residual stresses*. *Composite Structures*, 2002. **55**(3): p. 319-327.
184. Daynes, S., Potter, K. D., *et al.*, *Bistable prestressed buckled laminates*. *Composites Science and Technology*, 2008. **68**(15-16): p. 3431-3437.

- 
185. Daynes, S., Lachenal, X., *et al.* *Twisting structures with tailored stability and their application to morphing wings.* in *23rd International Conference on Adaptive Structures and Technologies (ICAST)*. 2012. Nanjing, China.
186. Smith, P. and Lemstra, P. J., *Ultra-high-strength polyethylene filaments by solution spinning/drawing.* *Journal of Materials Science*, 1980. **15**(2): p. 505-514.
187. Smith, P., Lemstra, P. J., *et al.*, *Ultradrawing of high-molecular-weight polyethylene cast from solution. II. Influence of initial polymer concentration.* *Journal of Polymer Science: Polymer Physics Edition*, 1981. **19**(5): p. 877-888.
188. Van Aerle, N. A. J. M. and Lemstra, P. J., *Drawing of ultra-high-molecular-weight polyethylene in the melt. Influence of crystallization history.* *Die Makromolekulare Chemie*, 1988. **189**(6): p. 1253-1266.
189. Van Aerle, N. A. J. M. and Braam, A. W. M., *A structural study on solid state drawing of solution-crystallized ultra-high molecular weight polyethylene.* *Journal of Materials Science*, 1988. **23**(12): p. 4429-4436.
190. Marikhin, V. A., *Structural aspects of mechanical destruction of oriented polymers.* *Die Makromolekulare Chemie*, 1984. **7**(S19841): p. 147-169.
191. Marikhin, V. A. and Myasnikova, L. P., *Heterogeneity of structure and mechanical properties of polymers.* *Makromolekulare Chemie. Macromolecular Symposia*, 1991. **41**(1): p. 209-227.
192. Wong, W. F. and Young, R. J., *Analysis of the deformation of gel-spun polyethylene fibres using Raman spectroscopy.* *Journal of Materials Science*, 1994. **29**(2): p. 510-519.
193. Marikhin, V. A. and Myasnikova, L. P., *Structural basis of high-strength high-modulus polymers*, in *Orientational Phenomena in Polymers*, Myasnikova, L., *et al.*, Editors., 1993, Steinkopff. p. 39-51.
194. Mark, H. F., Atlas, S. M., *et al.*, *Man-made fibers: science and technology.* Vol. 1. 1967, New York: Interscience Publishers.
195. Tucker, P. and George, W., *Microfibers within fibers: A review.* *Polymer Engineering & Science*, 1972. **12**(5): p. 364-377.
196. Andreia, L. D. S. A., Cassiano, N. L. F., *et al.*, *Influence of weathering and gamma irradiation on the mechanical and ballistic behavior of UHMWPE composite armor.* *Polymer Testing*, 2005. **24**(1): p. 104-113.

- 
197. Tissington, B., Pollard, G., *et al.*, *A study of the influence of fibre/resin adhesion on the mechanical behaviour of ultra-high-modulus polyethylene fibre composites*. *Journal of Materials Science*, 1991. **26**(1): p. 82-92.
198. Kakiage, M., Tamura, T., *et al.*, *Hierarchical constraint distribution of ultra-high molecular weight polyethylene fibers with different preparation methods*. *Journal of Materials Science*, 2010. **45**(10): p. 2574-2579.
199. Gupta, V. B., *Heat setting*. *Journal of Applied Polymer Science*, 2002. **83**: p. 586-609.
200. Devaux, E. and Caze, C., *Composites of UHMW polyethylene fibres in a LD polyethylene matrix. I. Processing conditions*. *Composites Science and Technology*, 1999. **59**(3): p. 459-466.
201. Hu, W., Buzin, A., *et al.*, *Annealing behavior of gel-spun polyethylene fibers at temperatures lower than needed for significant shrinkage*. *Journal of Polymer Science: Part B: Polymer Physics*, 2003. **41**: p. 403-417.
202. Lamin, B. M., *Visco-elastic Force Measuring Apparatus*, in *Department of Engineering*, 2005, University of Hull: UK (BEng Thesis).
203. Costa, L., Luda, M., P, *et al.*, *Ultra high molecular weight polyethylene—II. Thermal- and photo-oxidation*. *Polymer Degradation and Stability*, 1997. **58**(1-2): p. 41-54.
204. Jacobson, K., *Oxidation of ultra high molecular weight polyethylene (UHMWPE) part 1: Interpretation of the chemiluminescence curve recorded during thermal oxidation*. *Polymer Degradation and Stability*, 2006. **91**(9): p. 2126-2132.
205. Smook, J. and Pennings, J., *Influence of draw ratio on morphological and structural changes in hot-drawing of UHMW polyethylene fibres as revealed by DSC*. *Colloid and Polymer Science*, 1984. **262**(9): p. 712-722.
206. Grubb, D. T. and Li, Z. F., *Single-fibre polymer composites Part II Residual stresses and their effects in high-modulus polyethylene fibre composites*. *Journal of Materials Science*, 1994. **29**(1): p. 203-212.
207. Werff, H. v. d. and Pennings, A. J., *Tensile deformation of high strength and high modulus polyethylene fibers*. *Colloid and Polymer Science*, 1991. **269**(8): p. 747-763.
208. Peijs, T., Smets, E., A, M, *et al.*, *Strain rate and temperature effects on energy absorption of polyethylene fibres and composites*. *Applied Composite Materials*, 1994. **1**: p. 35-54.

- 
209. Riekkel, C., Cedola, A., *et al.*, *Microdiffraction experiments on single polymeric fibers by synchrotron radiation*. *Macromolecules*, 1997. **30**: p. 1033-1037.
210. Dijkstra, D., J and Pennings, A., J, *Annealing of gel-spun hot-drawn ultra-high molecular weight polyethylene fibres*. *Polymer Bulletin*, 1988. **19**(5): p. 481-486.
211. Smook, J., Hamersma, W., *et al.*, *The fracture process of ultra-high strength polyethylene fibres*. *Journal of Materials Science*, 1984. **19**(4): p. 1359-1373.
212. Languerand, D. L., Zhang, H., *et al.*, *Inelastic behavior and fracture of high modulus polymeric fiber bundles at high strain-rates*. *Materials Science and Engineering: A*, 2009. **500**(1-2): p. 216–224.
213. Deng, M., Latour, R. A., *et al.*, *Study of creep behavior of ultra-high-molecular-weight polyethylene systems*. *Journal of Biomedical Materials Research*, 1998. **40**(2): p. 214-223.
214. Kanagaraj, S., Fonseca, A., *et al.*, *Thermo-mechanical behaviour of ultrahigh molecular weight polyethylene-carbon nanotubes composites under different cooling techniques*. *Defect and Diffusion Forum*, 2011. **312-315**: p. 331-340.
215. Peterlin, A., *Drawing and annealing of fibrous material*. *Journal of Applied Physics*, 1977. **48**(10): p. 4099-4108.
216. Naik, N. K., Shrirao, P., *et al.*, *Ballistic impact behaviour of woven fabric composites: Formulation*. *International Journal of Impact Engineering*, 2006. **32**(9): p. 1521-1552.
217. Iremonger, M. J. and Went, A. C., *Ballistic impact of fibre composite armours by fragment-simulating projectiles*. *Composites Part A: Applied Science and Manufacturing*, 1996. **27**(7): p. 575-581.
218. Ramakrishna, S., *Microstructural design of composite materials for crashworthy structural applications*. *Materials & Design*, 1997. **18**(3): p. 167-173.
219. Jacob, G. C., Fellers, J. F., *et al.*, *Energy absorption in polymer composites for automotive crashworthiness*. *Journal of Composite Materials*, 2002. **36**(7): p. 813-850.
220. Farley, G. L. and Jones, R. M., *Crushing characteristics of continuous fiber-reinforced composite tubes*. *Journal of Composite Materials*, 1992. **26**(1): p. 37-50.
221. Mamalis, A. G., Robinson, M., *et al.*, *Crashworthy capability of composite material structures*. *Composite Structures*, 1997. **37**(2): p. 109-134.

- 
222. Lim, T. S. and Lee, D. G., *Mechanically fastened composite side-door impact beams for passenger cars designed for shear-out failure modes*. Composite Structures, 2002. **56**(2): p. 211-221.
223. Prakash, J., Mantena, P. R., *et al.*, *Energy absorption and damage evaluation of grid stiffened composite panels under transverse loading*. Composites Part B: Engineering, 2005. **37**(2–3): p. 191-199.
224. Kensche, C. W., *Fatigue of composites for wind turbines*. International Journal of Fatigue, 2006. **28**(10): p. 1363-1374.
225. Zollo, R. F., *Fiber-reinforced concrete: an overview after 30 years of development*. Cement and Concrete Composites, 1997. **19**(2): p. 107-122.
226. Kurtz, S. and Balaguru, P., *Postcrack creep of polymeric fiber-reinforced concrete in flexure*. Cement and Concrete Research, 2000. **30**(2): p. 183-190.
227. Carpinteri, A. and Brighenti, R., *Fracture behaviour of plain and fiber-reinforced concrete with different water content under mixed mode loading*. Materials & Design, 2010. **31**(4): p. 2032-2042.
228. Daynes, S. and Weaver, P. M., *Stiffness tailoring using prestress in adaptive composite structures*. Composite Structures, 2013. **106**: p. 282-287.

# APPENDICES

---

## SUMMARY

Four appendices are included, particularly showing impact test data from individual batches related to Chapter-4 (preliminary work), Chapter-5 (nylon fibre-based VPPMCs), Chapter-6 (hybrid VPPMCs) and Chapter-7 (polyethylene fibre-based VPPMCs). In addition, stretching rig calibration data are also presented.

## **APPENDIX-A**

### **CHAPTER – 4 (EXPERIMENTAL DATA)**

- This appendix presents stretching rig calibration data.
- Impact energy data of the individual samples tested at 24 mm Charpy span settings are shown.

Table A-1. Stretching rig calibration data (shown in Figure 4-2a, Chapter-4). S.E is the standard error.

	<i>A</i>	<i>B</i>	<i>C</i>	<i>D</i>	<i>E</i>
<i>Applied load (N)</i>	<i>49.05</i>	<i>98.10</i>	<i>196.20</i>	<i>225.63</i>	<i>235.44</i>
<b>Reading from digital scale (N)</b>	53.96	102.51	201.60	231.52	241.82
	53.46	105.46	202.09	233.48	241.33
	53.96	105.46	201.11	233.48	242.80
	54.45	104.48	204.54	232.50	244.27
	54.45	104.48	205.03	234.46	243.78
	54.94	103.50	205.03	232.50	243.78
	54.94	105.95	203.56	232.50	241.33
	54.45	105.46	203.56	233.97	241.33
<i>Mean ± S.E</i>	<b>54.32 ± 0.18</b>	<b>104.46 ± 0.41</b>	<b>203.31 ± 0.55</b>	<b>233.05 ± 0.34</b>	<b>242.55 ± 0.44</b>

Table A-2. Stretching rig calibration data (shown in Figure 4-2b, Chapter-4). S.E is the standard error.

	<i>A</i>	<i>B</i>	<i>C</i>	<i>D</i>	<i>E</i>	<i>F</i>	<i>G</i>
<i>Applied load (N)</i>	<b>0.00</b>	<b>9.81</b>	<b>19.62</b>	<b>29.43</b>	<b>39.24</b>	<b>49.05</b>	<b>58.86</b>
<b>Reading from digital scale (N)</b>	27.96	94.67	170.69	247.21	320.30	385.53	464.99
	35.81	103.50	175.11	248.68	321.77	388.48	462.54
	37.28	105.46	180.99	259.97	321.28	388.97	464.50
	33.84	103.01	182.47	253.59	322.26	389.46	464.50
	36.79	103.01	185.41	250.16	326.18	389.95	465.48
	33.84	101.53	184.43	251.63	340.90	390.44	465.98
	32.37	105.46	186.88	256.04	322.75	390.93	466.96
	32.86	99.97	179.03	258.49	323.73	391.42	467.45
<i>Mean ± S.E</i>	<b>33.84 ± 1.05</b>	<b>102.02 ± 1.25</b>	<b>180.62 ± 1.94</b>	<b>253.22 ± 1.64</b>	<b>324.89 ± 2.37</b>	<b>389.40 ± 0.65</b>	<b>465.30 ± 0.55</b>

**Table A-3. Charpy impact data from nylon fibre composites (2-4%  $V_f$ ) produced from clear-casting (CC) and general purpose (GP) polyester resins (data are shown in Figure 4-6, Chapter-4). Batches of test (pre-stressed) and control (un-stressed) samples tested at 24 mm span setting. Data are normalised by dividing impact energy (J) by the cross-sectional area of the sample. S.E is the standard error of the mean.**

Resin	Impact energy absorbed ( $\text{kJm}^{-2}$ )												Mean increase Energy (%)	
	TEST						CONTROL							
	Mean $\pm$ S.E						Mean $\pm$ S.E							
CC	55.98	59.60	55.27	54.08	59.62	56.51 $\pm$ 1.29	39.37	47.11	42.18	41.91	47.19	43.55 $\pm$ 1.55	29.75	
	65.69	59.61	53.43	54.80	61.65	59.04 $\pm$ 2.25	41.12	39.85	45.36	41.68	34.30	40.46 $\pm$ 1.79	45.90	
	75.80	75.88	72.05	75.03	66.46	73.04 $\pm$ 1.79	46.17	52.51	45.43	42.95	44.68	46.35 $\pm$ 1.63	57.60	
	<b><i>Mean <math>\pm</math> S.E</i></b>						<b>62.86 <math>\pm</math> 1.77</b>							<b>43.45 <math>\pm</math> 1.66</b>
GP	48.21	48.39	48.03	36.48	40.06	44.23 $\pm$ 2.50	47.56	54.53	46.48	58.17	55.48	52.44 $\pm$ 2.30	-15.65	
	48.40	57.65	56.84	64.30	53.15	56.07 $\pm$ 2.63	54.24	61.80	53.73	59.89	56.87	57.31 $\pm$ 1.57	-2.16	
	48.63	58.89	59.25	59.80	57.24	56.76 $\pm$ 2.08	57.05	58.95	56.64	58.70	51.21	56.51 $\pm$ 1.40	-0.45	
	<b><i>Mean <math>\pm</math> S.E</i></b>						<b>52.35 <math>\pm</math> 2.40</b>							<b>55.42 <math>\pm</math> 1.76</b>

**Table A-4. Charpy impact data from nylon fibre composites (2-4%  $V_f$ ) produced from fibre annealed in fan-assisted oven (data are shown in Figure 4-8, Chapter-4). Batches of test (pre-stressed) and control (un-stressed) samples tested at 24 mm span setting. Data are normalised by dividing impact energy (J) by the cross-sectional area of the sample. S.E is the standard error of the mean.**

FAN-ASSISTED OVEN														
Span (mm)	Impact energy absorbed ( $\text{kJm}^{-2}$ )												Mean increase Energy (%)	
	TEST						CONTROL							
						Mean $\pm$ S.E							Mean $\pm$ S.E	
24	54.75	72.10	68.04	59.43	71.10	65.08 $\pm$ 3.41	40.19	41.95	45.78	47.73	49.39	45.01 $\pm$ 1.73	44.61	
	59.62	71.88	47.91	67.96	81.21	65.72 $\pm$ 5.64	55.03	53.85	54.08	47.67	46.31	51.39 $\pm$ 1.82	27.88	
	58.42	56.25	54.05	55.74	55.74	56.04 $\pm$ 0.70	50.50	44.23	50.15	45.71	42.55	46.63 $\pm$ 1.59	20.19	
	73.46	63.24	65.03	64.31	60.06	65.22 $\pm$ 2.23	48.03	56.65	42.02	41.03	43.31	45.01 $\pm$ 1.85	44.91	
	53.96	62.46	63.64	61.41	55.63	59.42 $\pm$ 1.94	37.27	39.33	51.86	41.48	46.67	43.32 $\pm$ 2.65	37.16	
	65.47	68.83	64.38	51.96	61.56	62.44 $\pm$ 2.87	45.54	41.38	42.81	45.00	47.35	44.42 $\pm$ 1.05	40.58	
	61.59	44.00	74.92	60.43	72.61	62.71 $\pm$ 5.49	38.32	37.27	32.82	36.70	41.90	37.40 $\pm$ 1.46	67.66	
	54.21	71.76	62.79	54.67	53.74	59.43 $\pm$ 3.50	46.23	37.77	34.66	41.90	50.00	42.11 $\pm$ 2.77	41.13	
	<b>Mean <math>\pm</math> S.E</b>					<b>62.01 <math>\pm</math> 3.22</b>						<b>44.41 <math>\pm</math> 1.86</b>	<b>40.51 <math>\pm</math> 4.92</b>	

**Table A-5. Charpy impact data from nylon fibre composites (2-4%  $V_f$ ) produced from fibre annealed in muffle oven (data are shown in Figure 4-8, Chapter-4). Batches of test (pre-stressed) and control (un-stressed) samples tested at 24 mm span setting. Data are normalised by dividing impact energy (J) by the cross-sectional area of the sample. S.E is the standard error of the mean.**

MUFFLE OVEN														
Span (mm)	Impact energy absorbed ( $\text{kJm}^{-2}$ )												Mean increase Energy (%)	
	TEST						CONTROL							
						Mean $\pm$ S.E							Mean $\pm$ S.E	
24	44.14	45.02	47.83	49.16	38.38	44.91 $\pm$ 1.87	42.31	35.26	36.16	33.00	39.80	37.31 $\pm$ 1.66	20.37	
	53.23	59.69	54.75	52.94	59.86	56.09 $\pm$ 1.53	44.49	50.91	44.52	43.45	50.54	46.78 $\pm$ 1.62	19.91	
	64.31	59.32	54.49	56.81	65.32	60.05 $\pm$ 2.10	40.06	39.26	44.44	41.39	34.11	39.85 $\pm$ 1.68	50.68	
	75.37	74.48	70.39	73.54	65.59	71.87 $\pm$ 1.78	46.06	52.52	45.34	42.59	44.04	46.11 $\pm$ 1.71	55.88	
	60.28	63.14	56.42	60.27	45.33	57.09 $\pm$ 3.13	40.82	41.14	44.70	41.81	55.40	44.77 $\pm$ 2.74	27.50	
	65.42	57.45	66.77	66.77	70.09	65.30 $\pm$ 2.11	45.54	53.94	55.10	38.44	43.09	47.22 $\pm$ 3.20	38.28	
	70.59	68.14	58.22	67.47	67.60	66.40 $\pm$ 2.12	43.73	44.41	42.23	37.88	37.50	41.15 $\pm$ 1.46	61.37	
	61.78	60.75	73.17	66.26	60.44	64.48 $\pm$ 2.41	39.14	45.15	40.37	38.99	38.99	40.53 $\pm$ 1.18	59.10	
	<b>Mean <math>\pm</math> S.E</b>					<b>60.77 <math>\pm</math> 2.13</b>						<b>42.97 <math>\pm</math> 1.91</b>	<b>41.64 <math>\pm</math> 6.14</b>	

## **APPENDIX-B**

### **CHAPTER – 5 (EXPERIMENTAL DATA)**

- This appendix presents individual sample data (low to high  $V_f$ ).
- Impact energy data of samples tested at 24, 40 and 60 mm Charpy span settings are shown.

**Table B-1. Charpy impact data from nylon fibre composites (data are shown in Figure 5-3, Chapter-5). Batches of test (pre-stressed) and control (un-stressed) samples (3.3%  $V_f$ ) tested at 24, 40 and 60 mm span settings. Data are normalised by dividing impact energy (J) by the cross-sectional area of the sample. S.E is the standard error of the mean.**

3.3% Fibre Volume Fraction														
Span (mm)	Impact energy absorbed ( $\text{kJm}^{-2}$ )												Mean increase Energy (%)	
	TEST						CONTROL							
	Mean $\pm$ S.E						Mean $\pm$ S.E							
<b>24</b>	94.10	92.64	88.69	90.24	90.06	91.15 $\pm$ 0.97	72.59	62.96	53.50	57.10	62.92	61.81 $\pm$ 3.24	47.45	
	94.06	89.30	98.67	87.91	89.87	94.96 $\pm$ 1.97	71.84	70.66	68.05	72.94	64.50	69.60 $\pm$ 1.51	32.13	
	84.64	82.77	79.94	100.94	95.31	88.72 $\pm$ 4.01	61.04	68.79	62.73	67.52	63.58	64.73 $\pm$ 1.47	37.06	
	<b>Mean <math>\pm</math> S.E</b>						<b>90.61 <math>\pm</math> 2.32</b>							<b>65.38 <math>\pm</math> 2.07</b>
<b>40</b>	65.40	70.95	71.57	79.93	67.67	71.10 $\pm$ 2.47	57.24	66.67	68.87	63.75	68.04	64.91 $\pm$ 2.11	9.54	
	69.68	67.09	83.49	77.35	69.54	73.43 $\pm$ 3.05	62.37	65.86	61.26	71.10	58.12	63.74 $\pm$ 2.22	15.20	
	66.56	69.21	74.50	61.81	65.66	67.55 $\pm$ 2.10	68.92	80.52	56.05	69.45	58.63	66.71 $\pm$ 4.37	1.25	
	<b>Mean <math>\pm</math> S.E</b>						<b>70.69 <math>\pm</math> 2.54</b>							<b>65.12 <math>\pm</math> 2.90</b>
<b>60</b>	37.80	33.68	37.93	24.32	35.99	33.94 $\pm$ 2.53	40.14	41.41	27.67	40.07	27.71	35.40 $\pm$ 3.16	-4.11	
	27.84	46.20	49.05	44.86	41.32	41.85 $\pm$ 3.72	40.85	39.53	37.67	40.13	42.42	40.12 $\pm$ 0.78	4.32	
	35.79	41.67	33.44	43.53	39.81	38.85 $\pm$ 1.86	40.13	39.00	46.58	36.54	38.14	40.08 $\pm$ 1.73	-3.07	
	<b>Mean <math>\pm</math> S.E</b>						<b>38.22 <math>\pm</math> 2.70</b>							<b>38.53 <math>\pm</math> 1.89</b>

## Nylon fibre-based VPPMCs: Impact characteristics on fibre volume fraction and their effects on Charpy span settings

**Table B-2. Charpy impact data from nylon fibre composites (data are shown in Figure 5-3, Chapter-5). Batches of test (pre-stressed) and control (un-stressed) samples (10%  $V_f$ ) tested at 24, 40 and 60 mm span settings. Data are normalised by dividing impact energy (J) by the cross-sectional area of the sample. S.E is the standard error of the mean.**

10% Fibre Volume Fraction													
Span (mm)	Impact energy absorbed ( $\text{kJm}^{-2}$ )												Mean increase Energy (%)
	TEST						CONTROL						
	Mean $\pm$ S.E						Mean $\pm$ S.E						
24	234.58	269.37	255.18	254.41	240.19	250.75 $\pm$ 6.13	133.23	160.38	191.25	175.24	167.92	165.60 $\pm$ 9.57	51.41
	228.08	234.15	180.00	169.37	212.76	204.87 $\pm$ 12.92	136.71	171.56	159.46	170.29	144.14	156.43 $\pm$ 6.96	30.97
	259.56	197.65	184.15	196.52	191.15	205.81 $\pm$ 13.65	165.25	196.85	179.21	196.26	121.65	171.84 $\pm$ 13.85	19.76
	<b>Mean <math>\pm</math> S.E</b>						<b>220.47 <math>\pm</math> 10.90</b>	<b>164.63 <math>\pm</math> 10.13</b>					
40	158.03	164.92	164.29	157.47	156.39	160.22 $\pm$ 1.81	140.00	141.99	153.48	156.07	153.78	149.06 $\pm$ 3.34	7.48
	178.13	176.26	188.43	181.27	174.71	179.76 $\pm$ 2.43	160.57	142.42	163.17	151.06	146.11	152.67 $\pm$ 4.02	17.75
	152.17	141.64	137.86	147.34	138.95	143.59 $\pm$ 2.70	130.43	129.48	129.31	129.94	123.44	128.52 $\pm$ 1.28	11.73
	<b>Mean <math>\pm</math> S.E</b>						<b>161.19 <math>\pm</math> 2.31</b>	<b>143.42 <math>\pm</math> 2.88</b>					
60	90.37	86.62	81.82	82.35	96.33	87.50 $\pm$ 2.70	78.50	70.90	65.19	81.94	93.85	78.08 $\pm$ 4.91	12.07
	85.96	75.72	87.86	84.78	93.56	85.58 $\pm$ 2.89	61.94	81.31	69.21	90.42	80.24	76.62 $\pm$ 4.98	11.68
	88.25	91.10	92.35	86.24	70.59	85.71 $\pm$ 3.93	65.95	78.44	80.38	71.99	71.29	73.61 $\pm$ 2.61	16.43
	<b>Mean <math>\pm</math> S.E</b>						<b>86.26 <math>\pm</math> 3.17</b>	<b>76.10 <math>\pm</math> 4.16</b>					

**Table B-3. Charpy impact data from nylon fibre composites (data are shown in Figure 5-3, Chapter 5). Batches of test (pre-stressed) and control (un-stressed) samples (16.6 %  $V_f$ ) tested at 24, 40 and 60 mm span settings. Data are normalised by dividing impact energy (J) by the cross-sectional area of the sample. S.E is the standard error of the mean.**

16.6% Fibre Volume Fraction													
Span (mm)	Impact energy absorbed ( $\text{kJm}^{-2}$ )												Mean increase Energy (%)
	TEST						CONTROL						
	Mean $\pm$ S.E						Mean $\pm$ S.E						
24	272.81	240.90	290.65	273.83	250.76	265.75 $\pm$ 8.88	212.17	224.27	243.15	204.33	187.29	214.24 $\pm$ 9.39	24.06
	303.02	320.24	316.92	280.65	282.86	300.74 $\pm$ 8.28	202.11	240.37	234.08	263.81	231.82	234.44 $\pm$ 9.87	28.28
	277.96	282.67	291.67	278.64	282.69	282.73 $\pm$ 2.44	215.51	215.22	263.19	223.58	219.58	227.42 $\pm$ 9.07	24.32
	<b>Mean <math>\pm</math> S.E</b>						<b>283.08 <math>\pm</math> 6.53</b>	<b>225.37 <math>\pm</math> 9.45</b>					
40	206.97	200.90	194.79	206.06	203.59	202.46 $\pm$ 2.19	189.51	186.67	171.94	162.76	165.47	175.27 $\pm$ 5.46	15.51
	219.63	212.95	208.36	224.09	197.58	212.52 $\pm$ 4.61	168.22	174.11	173.19	194.08	195.37	180.99 $\pm$ 5.70	17.42
	231.99	211.61	215.90	221.01	206.91	217.48 $\pm$ 4.31	203.11	196.05	180.97	202.69	179.82	192.53 $\pm$ 5.11	12.96
	<b>Mean <math>\pm</math> S.E</b>						<b>210.82 <math>\pm</math> 3.70</b>	<b>182.93 <math>\pm</math> 5.42</b>					
60	110.90	96.71	105.02	99.66	107.03	103.86 $\pm$ 2.55	109.58	116.21	91.18	96.18	105.59	103.75 $\pm$ 4.52	0.11
	93.11	98.03	100.33	102.56	102.94	99.39 $\pm$ 1.80	103.31	83.95	72.91	82.27	96.40	87.77 $\pm$ 5.39	13.25
	116.15	111.25	110.27	112.98	106.96	111.52 $\pm$ 1.52	93.10	99.72	93.73	98.89	101.39	97.37 $\pm$ 1.67	14.54
	<b>Mean <math>\pm</math> S.E</b>						<b>104.93 <math>\pm</math> 1.95</b>	<b>96.29 <math>\pm</math> 3.86</b>					

## **APPENDIX-C**

### **CHAPTER – 6 (EXPERIMENTAL DATA)**

- This appendix presents individual sample data of hybrid (nylon/Kevlar) and Kevlar fibre-only composites.
- Impact energy data of the samples tested at 24 and 60 mm Charpy span settings are shown.

**Table C-1. Charpy impact data from hybrid (nylon and Kevlar commingled) fibre composite samples tested at 24 and 60 mm span (data are shown in Figure 6-3, Chapter-6). Each batch comprises 5 test (pre-stressed) and 5 control (un-stressed) samples of 4.5%  $V_f$  (3.3% nylon and 1.2% Kevlar). Data are normalised by dividing impact energy (J) by the sample cross-sectional area. S.E is the standard error of the mean.**

HYBRID VPPMC														
Span (mm)	Impact energy absorbed ( $\text{kJm}^{-2}$ )												Mean increase Energy (%)	
	TEST						CONTROL							
						Mean $\pm$ S.E							Mean $\pm$ S.E	
<b>24</b>	69.93	79.49	69.85	74.00	74.05	$73.46 \pm 1.77$	51.04	47.88	51.98	55.51	50.13	$51.31 \pm 1.25$	43.18	
	55.77	71.94	72.27	62.24	63.97	$65.24 \pm 3.12$	54.00	53.58	60.92	54.34	56.32	$55.83 \pm 1.36$	16.85	
	75.34	64.27	66.08	75.83	75.31	$71.37 \pm 2.55$	52.50	52.97	51.48	51.09	49.33	$51.47 \pm 0.63$	38.64	
	<b><i>Mean <math>\pm</math> S.E</i></b>						<b><math>70.02 \pm 2.48</math></b>							<b><math>52.87 \pm 1.08</math></b>
<b>60</b>	51.24	59.72	56.30	50.58	49.63	$53.49 \pm 1.94$	43.09	50.83	42.77	52.50	47.46	$47.33 \pm 1.97$	13.02	
	47.39	52.76	50.67	50.42	50.79	$50.41 \pm 0.86$	42.74	44.32	46.86	47.00	44.37	$45.06 \pm 0.82$	11.87	
	40.97	52.37	51.32	33.02	46.74	$44.88 \pm 3.58$	37.35	40.37	44.71	43.44	39.65	$41.10 \pm 1.33$	9.20	
	<b><i>Mean <math>\pm</math> S.E</i></b>						<b><math>49.59 \pm 2.13</math></b>							<b><math>44.50 \pm 1.37</math></b>

**Table C-2. Charpy impact tests results from batches of Kevlar fibre-only composites (3.6%  $V_f$ ) and resin-only samples tested at 24 and 60 mm span (data are shown in Figure 6-3, Chapter-6). Data are normalised by dividing impact energy (J) by the sample cross-sectional area. S.E is the standard error of the mean.**

Span (mm)	Impact energy absorbed ( $\text{kJm}^{-2}$ )																
	Kevlar fibre-only composite (3.6% $V_f$ )						Resin-only samples										
	Mean $\pm$ S.E						Mean $\pm$ S.E										
<b>24</b>	14.50	14.38	16.25	15.61	15.38	15.22 $\pm$ 0.35	4.73	5.39	5.51	5.70	5.82	5.43 $\pm$ 0.19					
	17.76	16.64	17.69	18.64	16.38	17.42 $\pm$ 0.41	7.52	3.52	5.70	5.40	5.40	5.51 $\pm$ 0.63					
	18.05	18.93	20.63	15.56	18.49	18.33 $\pm$ 0.82	4.22	5.14	3.70	4.70	4.47	4.44 $\pm$ 0.24					
	<b>Mean <math>\pm</math> S.E</b>						<b>16.99 <math>\pm</math> 0.53</b>						<b>5.13 <math>\pm</math> 0.35</b>				
<b>60</b>	13.79	20.29	18.87	18.71	22.45	18.82 $\pm$ 1.43	7.74	5.69	8.21	7.67	4.89	6.84 $\pm$ 0.65					
	15.97	17.94	17.92	17.82	17.84	17.50 $\pm$ 0.38	5.00	4.66	7.64	10.78	5.15	6.65 $\pm$ 1.16					
	21.18	31.83	15.12	22.13	24.55	22.96 $\pm$ 2.71	8.04	4.93	5.74	5.39	5.77	6.03 $\pm$ 0.54					
	<b>Mean <math>\pm</math> S.E</b>						<b>20.89 <math>\pm</math> 2.07</b>						<b>6.51 <math>\pm</math> 0.78</b>				

## **APPENDIX-D**

### **CHAPTER – 7 (EXPERIMENTAL DATA)**

- This appendix presents individual sample data of polyethylene fibre composites (ageing from 24 to 1008 hours).
- Impact absorbed energy data of the samples tested at 24 and 60 mm Charpy span settings are shown.

**Table D-1. Charpy impact data of UHMWPE fibre composite samples (3.6%  $V_f$ ) tested (24 hours after moulding) at 24 and 60 mm span. Each batch comprises 5 test (pre-stressed) and 5 control (un-stressed) samples. Data are normalised by dividing impact energy (J) by the sample cross-sectional area. S.E is the standard error of the mean.**

(AGE = 24 HOURS)														
Span (mm)	Impact energy absorbed ( $\text{kJm}^{-2}$ )												Mean increase Energy (%)	
	TEST						CONTROL							
						Mean $\pm$ S.E							Mean $\pm$ S.E	
<b>24</b>	48.85	52.52	35.67	46.18	33.49	43.34 $\pm$ 3.73	33.98	31.89	37.49	34.36	28.87	33.32 $\pm$ 1.43	30.09	
	40.69	31.14	29.43	25.26	25.21	30.35 $\pm$ 2.83	25.12	24.35	33.03	30.50	24.97	27.59 $\pm$ 1.75	9.97	
	28.90	42.05	33.76	49.60	32.42	37.35 $\pm$ 3.75	23.45	30.57	29.94	30.85	26.28	28.22 $\pm$ 1.45	32.35	
	<i>Mean <math>\pm</math> S.E</i>						<b>37.01 <math>\pm</math> 3.44</b>							<b>29.71 <math>\pm</math> 1.54</b>
<b>60</b>	47.17	39.58	42.22	41.62	38.15	41.75 $\pm$ 1.54	28.96	32.66	43.16	44.27	41.99	38.21 $\pm$ 3.10	9.27	
	40.07	35.91	48.79	41.95	46.15	42.57 $\pm$ 2.26	37.08	35.15	32.56	31.60	48.75	37.03 $\pm$ 3.09	14.98	
	41.19	68.01	44.72	42.03	38.20	46.83 $\pm$ 5.40	44.70	27.47	35.45	28.26	31.98	33.57 $\pm$ 3.13	39.49	
	<i>Mean <math>\pm</math> S.E</i>						<b>43.72 <math>\pm</math> 3.07</b>							<b>36.27 <math>\pm</math> 3.10</b>

**Table D-2. Charpy impact data of UHMWPE fibre composite samples (3.6%  $V_f$ ) tested (96 hours after moulding) at 24 and 60 mm span. Each batch comprises 5 test (pre-stressed) and 5 control (un-stressed) samples. Data are normalised by dividing impact energy (J) by the sample cross-sectional area. S.E is the standard error of the mean.**

(AGE = 96 HOURS)														
Span (mm)	Impact energy absorbed ( $\text{kJm}^{-2}$ )												Mean increase Energy (%)	
	TEST						CONTROL							
						Mean $\pm$ S.E							Mean $\pm$ S.E	
<b>24</b>	31.35	32.75	34.45	29.68	36.63	$32.97 \pm 1.21$	24.27	29.80	35.16	29.12	22.57	28.18	$28.18 \pm 2.22$	16.99
	31.86	42.25	34.81	31.32	33.61	$34.77 \pm 1.97$	39.41	33.90	31.98	28.54	29.19	32.60	$32.60 \pm 1.96$	6.64
	40.01	31.37	32.58	29.20	30.24	$32.68 \pm 1.92$	22.14	23.13	28.61	24.86	26.79	25.11	$25.11 \pm 1.18$	30.17
	<b><i>Mean <math>\pm</math> S.E</i></b>					<b><math>32.83 \pm 1.56</math></b>							<b><math>26.65 \pm 1.70</math></b>	<b><math>23.58 \pm 6.81</math></b>
<b>60</b>	58.85	35.44	47.13	33.27	56.48	$46.23 \pm 5.24$	38.91	28.04	43.19	39.64	49.65	39.89	$39.89 \pm 3.52$	15.92
	47.38	29.80	46.32	38.73	33.27	$39.10 \pm 3.47$	36.26	37.43	40.24	28.62	43.02	37.11	$37.11 \pm 2.43$	5.35
	30.04	42.11	50.49	33.12	39.84	$39.12 \pm 3.59$	31.71	28.87	31.68	27.65	36.38	31.26	$31.26 \pm 1.51$	25.15
	<b><i>Mean <math>\pm</math> S.E</i></b>					<b><math>41.48 \pm 4.10</math></b>							<b><math>36.09 \pm 2.48</math></b>	<b><math>15.47 \pm 5.72</math></b>

**Table D-3. Charpy impact data of UHMWPE fibre composite samples (3.6%  $V_f$ ) tested (168 hours after moulding) at 24 and 60 mm span. Each batch comprises 5 test (pre-stressed) and 5 control (un-stressed) samples. Data are normalised by dividing impact energy (J) by the sample cross-sectional area. S.E is the standard error of the mean.**

(AGE = 168 HOURS)														
Span (mm)	Impact energy absorbed ( $\text{kJm}^{-2}$ )												Mean increase Energy (%)	
	TEST						CONTROL							
	Mean $\pm$ S.E						Mean $\pm$ S.E							
<b>24</b>	36.12	34.24	29.22	30.61	34.73	32.98 $\pm$ 1.31	32.04	29.57	29.31	30.63	30.13	30.34 $\pm$ 0.48	8.73	
	34.88	25.20	27.57	30.76	32.56	30.19 $\pm$ 1.73	23.98	32.36	26.96	24.94	28.11	27.27 $\pm$ 1.47	10.72	
	27.03	34.04	27.84	34.25	27.70	30.17 $\pm$ 1.63	25.90	23.43	25.28	25.61	21.48	24.34 $\pm$ 0.83	23.96	
	<i>Mean <math>\pm</math> S.E</i>						<b>31.12 <math>\pm</math> 1.55</b>							<b>27.32 <math>\pm</math> 0.93</b>
<b>60</b>	66.36	39.47	47.10	45.19	33.13	46.25 $\pm$ 5.59	50.73	49.86	32.20	38.56	31.13	40.50 $\pm$ 4.20	14.21	
	50.93	28.29	40.70	51.80	49.38	44.22 $\pm$ 4.45	28.59	34.37	27.63	39.41	35.38	33.08 $\pm$ 2.20	33.69	
	43.26	48.18	30.96	38.03	36.29	39.34 $\pm$ 2.96	27.20	28.49	39.19	28.18	35.37	31.73 $\pm$ 2.39	24.01	
	<i>Mean <math>\pm</math> S.E</i>						<b>43.27 <math>\pm</math> 4.33</b>							<b>35.10 <math>\pm</math> 2.93</b>

**Table D-4. Charpy impact data of UHMWPE fibre composite samples (3.6%  $V_f$ ) tested (336 hours after moulding) at 24 and 60 mm span. Each batch comprises 5 test (pre-stressed) and 5 control (un-stressed) samples. Data are normalised by dividing impact energy (J) by the sample cross-sectional area. S.E is the standard error of the mean.**

(AGE = 336 HOURS)														
Span (mm)	Impact energy absorbed ( $\text{kJm}^{-2}$ )												Mean increase Energy (%)	
	TEST						CONTROL							
	Mean $\pm$ S.E						Mean $\pm$ S.E							
<b>24</b>	28.49	25.58	29.43	32.59	32.25	29.67 $\pm$ 1.29	20.44	23.88	23.26	24.68	26.48	23.75 $\pm$ 0.99	24.93	
	29.18	30.19	36.28	32.11	26.16	30.78 $\pm$ 1.68	27.23	24.77	27.61	21.50	27.17	25.66 $\pm$ 1.15	19.99	
	26.84	27398	29.08	27.92	30.25	28.41 $\pm$ 0.58	20.39	23.31	28.82	23.45	22.37	23.67 $\pm$ 1.40	20.05	
	<i>Mean <math>\pm</math> S.E</i>						<b>29.62 <math>\pm</math> 1.18</b>	<i>Mean <math>\pm</math> S.E</i>						<b>24.36 <math>\pm</math> 1.18</b>
<b>60</b>	68.95	36.78	39.21	64.51	60.82	54.05 $\pm$ 6.69	48.54	48.13	34.23	45.40	58.03	46.87 $\pm$ 3.81	15.34	
	47.78	55.17	49.47	30.15	55.36	47.59 $\pm$ 4.61	35.20	36.24	29.03	41.57	54.71	39.35 $\pm$ 4.33	20.93	
	48.56	42.79	49.62	55.12	66.88	52.59 $\pm$ 4.07	47.02	27.82	29.42	37.96	43.28	37.10 $\pm$ 3.76	41.76	
	<i>Mean <math>\pm</math> S.E</i>						<b>51.41 <math>\pm</math> 5.13</b>	<i>Mean <math>\pm</math> S.E</i>						<b>41.11 <math>\pm</math> 3.97</b>

**Table D-5. Charpy impact data of UHMWPE fibre composite samples (3.6%  $V_f$ ) tested (1008 hours after moulding) at 24 and 60 mm span. Each batch comprises 5 test (pre-stressed) and 5 control (un-stressed) samples. Data are normalised by dividing impact energy (J) by the sample cross-sectional area. S.E is the standard error of the mean.**

(AGE = 1008 HOURS)														
Span (mm)	Impact energy absorbed ( $\text{kJm}^{-2}$ )												Mean increase Energy (%)	
	TEST						CONTROL							
						Mean $\pm$ S.E							Mean $\pm$ S.E)	
<b>24</b>	27.07	38.25	28.90	29.03	25.77	29.80 $\pm$ 2.20	24.56	21.41	22.78	21.06	27.00	23.36 $\pm$ 1.10	27.57	
	33.34	35.19	31.62	32.53	28.38	32.21 $\pm$ 1.12	28.36	27.96	28.83	26.47	26.24	27.57 $\pm$ 0.52	16.83	
	29.99	28.31	26.21	30.98	27.64	28.63 $\pm$ 0.85	24.08	24.36	24.63	24.54	26.08	24.74 $\pm$ 0.35	15.72	
	<b><i>Mean <math>\pm</math> S.E</i></b>						<b>30.21 <math>\pm</math> 1.39</b>							<b>25.22 <math>\pm</math> 0.65</b>
<b>60</b>	39.24	28.14	48.84	23.49	30.63	34.07 $\pm$ 4.49	27.83	34.55	36.01	31.70	28.97	31.81 $\pm$ 1.57	7.09	
	45.53	31.93	31.71	39.97	47.41	39.31 $\pm$ 3.29	33.92	23.33	26.05	28.33	36.80	29.69 $\pm$ 2.49	32.42	
	57.98	54.15	58.31	36.42	42.04	49.78 $\pm$ 4.46	33.59	42.19	32.86	28.21	36.83	34.74 $\pm$ 2.32	43.31	
	<b><i>Mean <math>\pm</math> S.E</i></b>						<b>41.05 <math>\pm</math> 4.08</b>							<b>32.08 <math>\pm</math> 2.12</b>